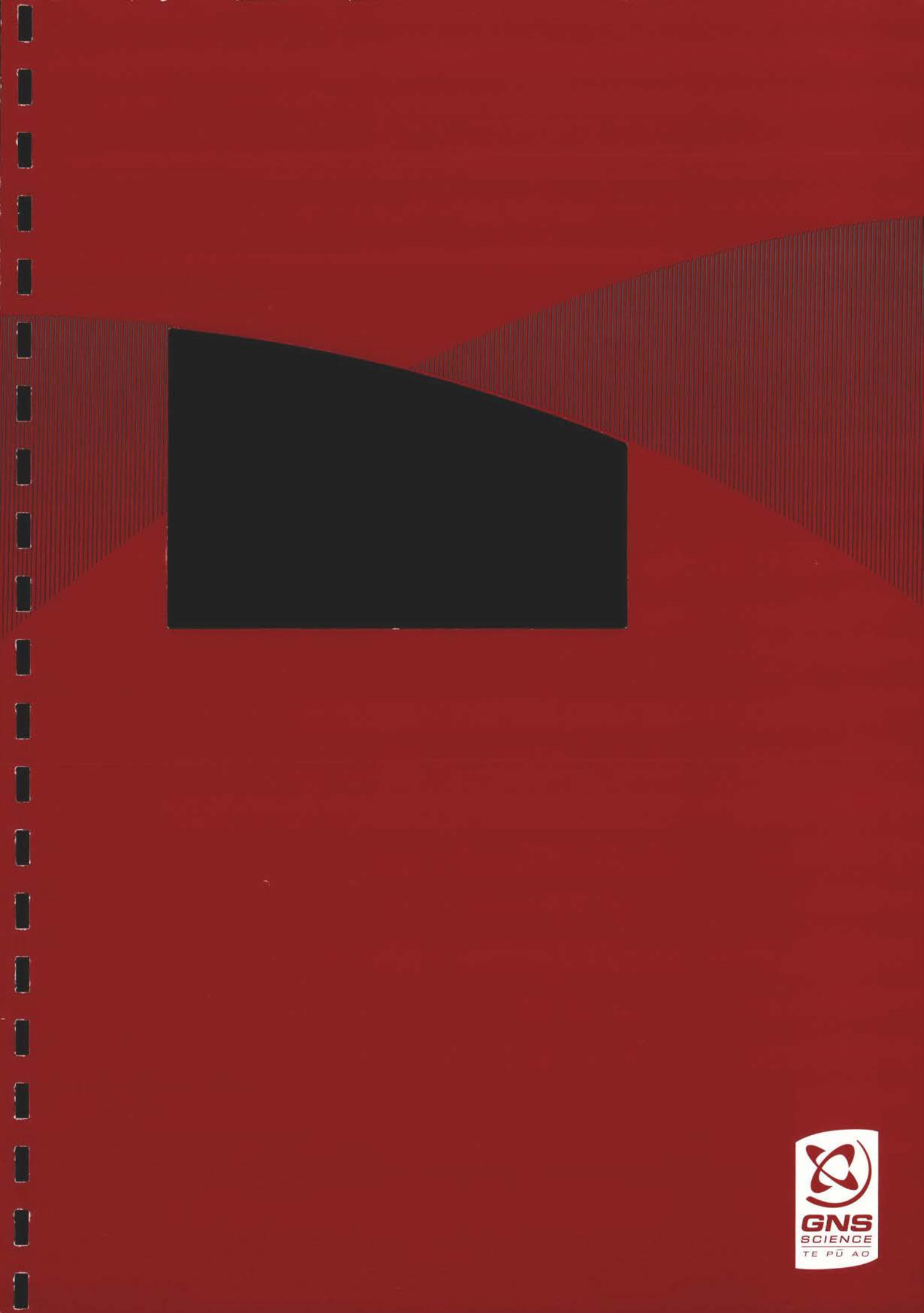


S&G 3732

S&G 3732



**Indicators of recent paleoseismic  
activity along the western Hope Fault**

R. Langridge	GNS Science, Avalon
R. Duncan	Landcare, Lincoln
P. Almond	Lincoln University, Lincoln
R. Robinson	GNS Science, Avalon

**GNS Science Consultancy Report 2006/151  
October 2007**

**CONFIDENTIAL**

This report has been prepared by the Institute of Geological and Nuclear Sciences Limited (GNS Science) exclusively for and under contract to the Earthquake Commission (EQC). Unless otherwise agreed in writing, all liability of GNS Science to any other party other than EQC in respect of the report is expressly excluded.

The data presented in this Report are  
available to GNS Science for other use from  
October 2007

To: r.langridge@gns.cri.nz  
From: Graham Hancox <gthancox@paradise.net.nz>  
Subject: Review of Western Hope Fault Report-Summary comments  
Cc: g.hancox@gns.cri.nz  
Bcc:  
Attached:

Hi Rob,

I've finished my review of the EQC Report on the Western Hope Fault, and will bring it in tomorrow morning after I've been to physio (for a bad back and neck after a fall in the field!).

Re the report, I have made comments (in red pen) on the text, which should all be self explanatory, and hopefully helpful. We may need to discuss some points, mainly to help my understanding of the issues so that my comments make sense. My overall comments may be summarised as follows:

- (1) The report is very long and presents a lot of data on the tree core plots, ages, and uncertainties. I agree with KRB's comment that it is fine as a data report, but thought that the paleoseismicity conclusions needed to be brought out more strongly in the text.
- (2) Some of the data, and especially the treatment of uncertainty, might have been better placed in an Appendix as it tends to unbalance the report.
- (3) The new (shorter) Technical Summary brings out the main conclusions quite well, but I have made lots of editorial comments, hopefully to improve it and make the writing clearer. Also, you do need to refer to the synthetic seismicity modelling in the new summary (it was in the old version). It seems that if an Alpine Fault event terminates at a certain point it creates more CFS on the WHF - so this may make a WHF event more likely - but does not prove it (?). If that is correct, perhaps this needs to be spelt out in those terms.
- (4) If fault movements occurred on the Western Hope Fault in 1717 (?), 1765, and 1832..., I don't recall reading why it is necessary to rely on forest damage to prove these fault ruptures events occurred. Why is there no fault trace that can be dated (with traditional c14 methods) to confirm that those movements occurred? - perhaps we can discuss this tomorrow.
- (5) It also occurred to me that it would be good to have a Table that matches your study objectives against the results (as answers to the questions posed in Section 1.2) - see my suggestion on page 2. This table could perhaps be included in the summary, as it would then leave no doubt as to what was planned - and what the study actually achieved.
- (6) I agree with KRB that the report ends rather abruptly. Perhaps you need a short section wrapping the issues up in terms of (and clearly stating) : (a) did you achieve what was intended; (b) if not, why not; (c) was this important to the overall outcome of the study; and (d) now that this work has been done, where to now for the WHF issue, forest damage studies along the fault zone, and clusters of landslides as indicators of large prehistoric earthquakes on major faults - a big future in NZ because the issue has not really been properly looked at yet.

That's about it for now. I'll talk to you about these and some other points tomorrow.

Regards

Graham

---

*Graham T Hancox  
Senior Engineering Geologist  
GNS Science  
Phone: (04) 570 4742 (GNS)  
Home: (04) 904 9678; Mobile: (029) 904 9678  
email: g.hancox@gns.cri.nz (GNS)*

## CONTENTS

<b>FIGURES ARE ANNOTATED FOR EACH CHAPTER</b>	<b>TECHNICAL SUMMARY .....</b>	<b>II</b>
<b>TECHNICAL SUMMARY .....</b>	<b>.....</b>	<b>III</b>
<b>1.0 INTRODUCTION .....</b>	<b>.....</b>	<b>1</b>
1.1 Pre-amble .....	.....	1
1.2 Project Objectives .....	.....	2
1.3 Relevance of research topic .....	.....	3
1.4 Background .....	.....	4
1.5 Scope and Outline of Report .....	.....	6
<b>2.0 LANDSCAPE AND PALEOSEISMIC DATA .....</b>	<b>.....</b>	<b>7</b>
2.1 Landscape Observations .....	.....	7
2.2 Late Holocene Relative Soil Chronology .....	.....	8
2.3 Radiocarbon dates .....	.....	9
2.4 The Matagouri Flat Paleoseismic Trench .....	.....	13
2.4.1 Background .....	.....	13
2.4.2 The trench and its stratigraphy .....	.....	14
2.4.3 Radiocarbon Dating of Trench Deposits .....	.....	15
2.4.4 Faulting .....	.....	16
<b>3.0 METHODOLOGY OF TREE RESEARCH .....</b>	<b>.....</b>	<b>18</b>
3.1 Site Strategy .....	.....	18
3.2 Tree coring methodology .....	.....	19
3.3 Tree core sampling and preparation .....	.....	20
3.4 Fault scarp plots .....	.....	20
3.5 Alluvial plots .....	.....	21
3.6 Summary of tree core data .....	.....	22
<b>4.0 RESULTS OF INDIVIDUAL TREE CORE PLOTS .....</b>	<b>.....</b>	<b>25</b>
4.1 Plots 1-10 .....	.....	25
4.1.1 Plot 1 .....	.....	25
4.1.2 Plot 2 .....	.....	28
4.1.3 Plot 3 .....	.....	29
4.1.4 Plot 4 .....	.....	31
4.1.5 Plot 5 .....	.....	33
4.1.6 Plot 6 .....	.....	36
4.1.7 Plot 7 .....	.....	39
4.1.8 Plot 8 .....	.....	42
4.1.9 Plot 9 .....	.....	44
4.1.10 Plot 10 .....	.....	46
4.2 Plots 11-14 .....	.....	48
4.2.1 Plot 11 .....	.....	49
4.2.2 Plot 12 .....	.....	51
4.2.3 Plot 13 .....	.....	53
4.2.4 Plot 14 .....	.....	55
4.3 Summary of the un-treated tree age dataset .....	.....	57
<b>5.0 UNCERTAINTY &amp; INTERPRETATION OF TREE PLOTS .....</b>	<b>.....</b>	<b>58</b>
5.1 Uncertainty of tree ages .....	.....	58
5.2 Summary of tree core data incorporating uncertainty .....	.....	60
5.3 Incorporating uncertainty at the Plot level .....	.....	62
5.3.1 Uncertainty-treated Plots 1-3 .....	.....	62
5.3.2 Uncertainty-treated Plots 4-6 .....	.....	64
5.3.3 Uncertainty-treated Plots 7-10 .....	.....	65
5.3.3 Uncertainty-treated Plots 11-14 .....	.....	68
5.4 Summary of the uncertainty-treated dataset .....	.....	70
5.5 Summary of the Uncertainty Treatment .....	.....	71
5.6 Similarity and Cluster Diagrams .....	.....	72

5.6.1	The Similarity Cluster Diagram.....	72
5.6.2	The Plot Cluster Diagram .....	73
5.7	Individual Age Offset Features at Plots .....	74
5.7.1	The significance of Plot 3 .....	74
5.7.2	The Significance of Plot 7 .....	75
5.7.3	The Significance of Plot 12.....	76
5.7.4	The Significance of Plot 11.....	77
5.7.5	The Significance of Troughs vs. Peaks in the Dataset.....	78
5.8	Summary of Age Offset, Plot Similarity and Clustering Features.....	81
<b>6.0</b>	<b>INTEGRATION OF LANDSCAPE, PALEOSEISMIC &amp; TREE DATASETS .....</b>	<b>83</b>
6.1	The penultimate faulting event .....	83
6.2	The most recent faulting event .....	83
6.3	Integration of Landscape, Paleoseismic and Tree data .....	85
6.5	The likelihood and frequency of strong shaking .....	88
<b>7.0</b>	<b>USING SYNTHETIC SEISMICITY TO MODEL FAULT INTERACTIONS .....</b>	<b>90</b>
7.1	The Fault Network .....	90
7.2	The Synthetic Seismicity Model.....	91
7.3	Alpine – Hope Fault Interaction .....	92
7.4	Summary .....	94
<b>8.0</b>	<b>SUMMARY &amp; CONCLUSIONS.....</b>	<b>95</b>
<b>9.0</b>	<b>REFERENCES.....</b>	<b>99</b>
<b>10.0</b>	<b>ACKNOWLEDGEMENTS .....</b>	<b>104</b>
<b>APPENDICES .....</b>		<b>105</b>
	APPENDIX 1 – Soil Profile Descriptions .....	105
	APPENDIX 2 – Trench Unit Descriptions and Radiocarbon samples .....	115
	APPENDIX 3 – Tree site data .....	115

**FIGURES ARE ANNOTATED FOR EACH CHAPTER**

## TECHNICAL SUMMARY

The report presents the results of a comprehensive study of paleoseismic, landscape features, and dendrochronologic data to assess the timing of the most recent faulting events along the Hurunui section of the Hope Fault, South Island. Geomorphic observations supported by radiocarbon dates and relative soil age estimates show that the investigated sites along the fault in the upper Hurunui and Hope areas are all late Holocene in age.

Several radiocarbon ages are used to define the age of events in the landscape. Data from a hand-dug trench at Matagouri Flat showed evidence for at least 2 faulting events. The most recent faulting event there is dated from a colluvial wedge developed across a fresh fault scarp, and probably occurred since AD 1458-1655. The age of this event is supported by other radiocarbon ages on buried or fallen trees. This wedge appears to be weakly re-organised, perhaps suggesting some minor, sympathetic re-faulting since the most recent faulting event. The penultimate faulting event is recognised by warped sand and paleosol units toward the base of the trench, and probably occurred before AD 1297-1425.

One of the main objectives of the research was to determine the timing and history of forest change along the fault, as a test of the fault rupture data. Approximately 250 Red, Silver and Mountain Beech (*Nothofagus*) trees were cored at 14 tree plots at selected alluvial and fault scarp sites. Ten of the plots were located in the west close to data from our paleoseismic and slip rate sites at Matagouri Flat and McKenzie Stream. The other 4 plots were located farther east near the western end of the AD 1888 North Canterbury earthquake rupture.

In general, we observed that the forest had an even (sized?) appearance comprising trees ranging in size from 20-70 cm in diameter, giving core ages of 90-280 yr. Three main peaks of tree colonisation are indicated by the tree dataset. The youngest peak occurred near the turn of the 20<sup>th</sup> Century, and is interpreted to be related to damage from rupture of the Hope River segment of the Hope Fault in the 1888 earthquake. At one site in particular (Plot 3), we were able to demonstrate that it took c.  $21 \pm 4$  yr time to re-colonise this open canopy site. Five of the plots show a strong signal of this event. An older peak in the tree ring data occurred at c. 150 yr ago. Based on the 21 yr colonisation offset, this second peak has been attributed to an earthquake of age c. AD  $1830 \pm 5$  yr. Eight of the tree plots show evidence of this event. The oldest peak occurs at c. 230-240 rings (yr) ago and is attributed to an earthquake at c. AD  $1760 \pm 5$  yr. Similarity diagrams of the tree plots show that each of the three peaks is observed at specific plots that have clustered age data. Another minor tree age peak may precede this one. We infer that such a peak is evidence of shaking from the AD 1717 rupture of the Alpine Fault in at Plot 4 in our study area.

One of the clearest results from the dendrochronologic data is that the forest has not undergone wholesale change through damage since at least the time of the 1888 earthquake. It appears that the 1929 Arthur's Pass earthquake had little or no impact at the plots we investigated. However, before this there are up to 4 instances (1888, c. 1830, c. 1760 and c. 1717) where the forest underwent significant change through tree loss and re-colonisation. The trench and landscape records indicate 2 and possibly 3 earthquake ruptures between c. AD 1460-1888, while the forest change record indicates 3 and possibly 4 major forest damaging events during the period AD 1717-1888 (171 yr). These give simple recurrence ranges of 214-428 yr and 57-85 yr, respectively.

The difference between these two recurrence ranges is related to the recurrence of surface faulting earthquakes along the Hurunui section of the Hope Fault, compared to the return time for Intensity VIII or greater shaking throughout the study area. In other words, the forest

plots we investigated have been subject to strong shaking and other agents of forest change besides simply the single 'Hurunui' fault source. The short recurrence period exhibited by the forest change data is indicative of repeated, high intensity damage by earthquakes in this very active part of the South Island plate boundary.

There is a considerable level of uncertainty about the results of this study, mainly because it is difficult to inter-relate the two types of data produced by this study, i.e. imprecisely aged but accurate (paleoseismic) results from trenching and landscape modification, versus, precisely aged but less easily interpretable data from forest change. We infer that large earthquakes are the strongest agents of forest change at the sites we studied and other agents such as storm, windthrow, and fire were of much lower importance.

A new model of synthetic seismicity was developed to test the effects of rupture probability in the western Marlborough Fault System following an Alpine Fault rupture. The elastic Coulomb Failure Stress models give low probabilities of triggered ruptures along the western Hope Fault within 3 years of an Alpine Fault rupture. This is in agreement with our forest damage results that indicate there are (several years to) decades between strong shaking and/or surface faulting, large earthquake events.

This project has been instrumental in demonstrating the value of dendrochronological studies along the very active faults of the Marlborough Fault System. In future, larger, more comprehensive datasets need to be collected to provide more robust interpretations of tree data that are discussed in this report. In addition, studies of tree growth suppression may be a useful means to determine the age of damaging events in these areas.

## 1.0 INTRODUCTION

### 1.1 Pre-amble

**Did the western Hope Fault fail between AD 1717 (Alpine Fault) and 1888 (central Hope Fault),** as part of a series of plate boundary-scale earthquake events? That was the original title and hypothesis of this EQC-funded research project. Or, was the 1888 earthquake a throughgoing rupture that progressed to the west beyond where that rupture was mapped by Alexander McKay (1890). What impact would this knowledge have on our view of fault rupture segmentation and thereby risk reduction? This project aims to determine the age and significance of the most recent surface faulting earthquake for the Hurunui section of the Hope Fault (Fig. 1.1; Langridge & Berryman 2005), using a four-pronged approach of geomorphologic, paleoseismic, and dendro-chronological field studies, and failure stress modelling.

The major carriers of plate boundary slip through central New Zealand, with slip rates of  $\geq 10$  mm/yr, are the Alpine, Hope, Kekerengu, Booboo and Wairarapa Faults, and the Hikurangi Subduction Zone (Fig. 1.1) (e.g. Berryman et al. 1992; Langridge et al. 2003; Holt & Haines 1995). These faults are capable of generating large ( $M \geq 7$ ) to great ( $M \geq 8$ ) surface-rupturing earthquakes every few hundred years. However, during New Zealand's short historical period (post-1840) only two of these "fastest-slipping" faults have produced faulting events, i.e. the 1855 Wairarapa and 1888 North Canterbury earthquakes (Grapes & Downes 2000; Cowan 1991). However, research into the paleoearthquake record of the Alpine Fault has identified a number of dateable large to great earthquakes, of which the last two occurred as recently as c. AD  $1615 \pm 10$  and c.  $1717 \pm 5$  (Yetton et al. 1998; Wells et al. 1999; 2001). If plate boundary stresses are transferred from one major fault, e.g., the AD 1717 Alpine Fault event, to another in an "end-on" fashion (Robinson 2004), then a significant geographic and temporal gap exists between the prehistoric 1717 Alpine Fault event, and the historic 1888 event along the Hope River section of the Hope Fault (Cowan & McGlone 1991).

Reconnaissance level mapping was recently conducted as part of a FRST Post-Doctoral Fellowship in this "gap" along the Hurunui section of the Hope Fault (Langridge 2004). The results of that reconnaissance show this section of the fault carries a high slip rate (c. 12 mm/yr) with the capability of generating  $M 7+$  earthquakes (Langridge & Berryman 2005). Geomorphic indicators suggest that a young prehistoric event may have occurred on this segment of the fault. In this present study, the age of the most recent surface faulting event will be evaluated by analysis and dating of geomorphic evidence and trench exposures, and also through studies of the age of stands of Beech (*Nothofagus*) trees along or near the fault trace.

In addition to the paleoseismic studies, simulations of synthetic seismicity have been undertaken on the Alpine-Hope earthquake sequence to determine whether the western part of the Marlborough Fault Zone could be elevated toward rupture following an Alpine Fault earthquake (c.f. Robinson 2004). Testing the concept of fault segmentation and failure stress through central New Zealand is important in developing a model for assessing and better understanding New Zealand's future seismic risk – should we also be prepared for one event at a time, or a cascading series of earthquakes along the South Island plate boundary?, e.g. Langridge (2006).

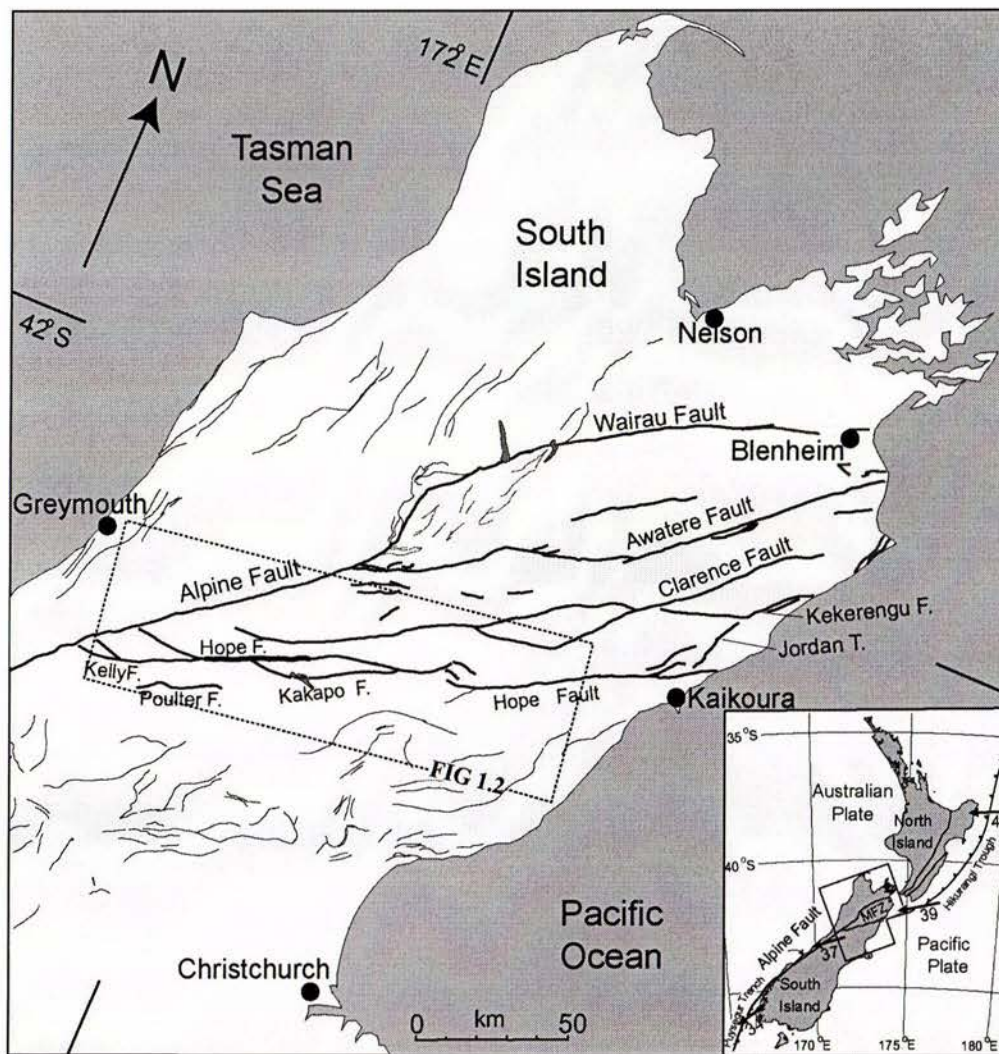


**Figure 1.1.** Location of the Hope Fault in the Marlborough Fault Zone (MFZ), northern South Island. Faults modified from the GNS Active Faults Database. Major faults of the MFZ and Alpine Fault are highlighted. The Hurunui section of the Hope Fault is emboldened. *Inset:* New Zealand plate boundary including the Alpine Fault, MFZ and Hikurangi subduction margin. Arrows show the Nuvel-1 plate motions (in mm/yr) and directions (after DeMets et al. 1994).

## 1.2 Project Objectives

The primary objectives of this study are to determine the age of the most recent, large, surface rupturing earthquake (MRE) for the Hurunui section of the Hope Fault and to put this result in a framework of fault segmentation and failure stress in that region, i.e. along the Alpine-Hope fault system in the northern South Island (Fig. 1). We wanted to answer questions such as: i) did the western part of the Hope Fault fail, time-wise, between the last events on the central Hope Fault (AD 1888; Cowan 1991) and the Alpine Fault (AD  $1717 \pm 5$ ; Yetton et al. 1998) (Fig. 1.2); ii) could such a "Hurunui" rupture event have been triggered by some of the large to great events nearby; iii) could a Hurunui event have triggered the historical 1888 earthquake; (iv) conversely, did the Hurunui section of the fault rupture during the 1888 event; and v) was a Hurunui event and those others from AD 1717 through 1888 related to a more complete failure of the fastest moving portions of the New Zealand plate boundary

through South Island, including the Conway segment of the Hope Fault (c. AD 1780 ± 60; Langridge et al. 2003).

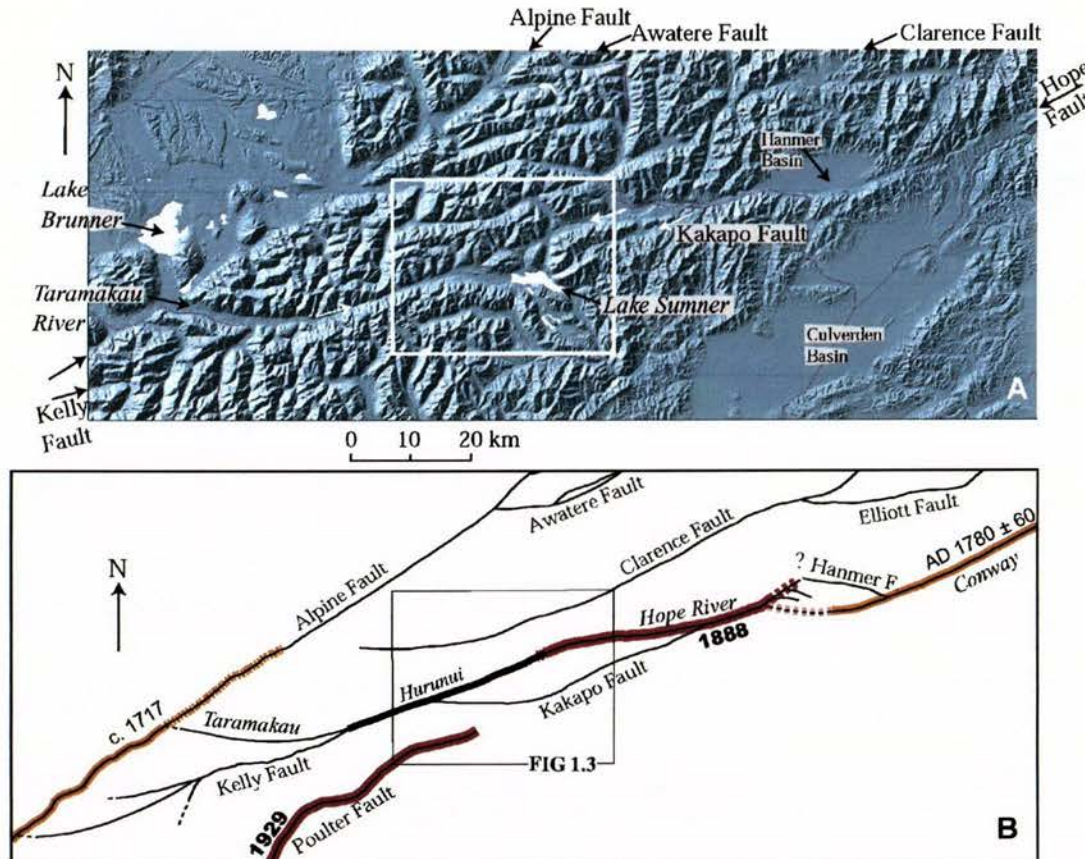


**Figure 1.2.** Digital elevation model and active fault map of the southwestern Marlborough Fault Zone, showing: **A.** topographic relief and geographic features. **B.** active faults, historic and paleoseismic surface faulting events in the region, e.g. AD 1888. The Hope Fault system (including Kelly Fault) consists of ENE-trending strike-slip segments/ sections separated by extensional (Hanmer Basin) and compressional rhombs (with Kakapo Fault). The Hurunui section of the Hope Fault is emboldened in black.

### 1.3 Relevance of research topic

The proposed research can contribute both to fundamental and applied earthquake geology. The concept of fault segmentation and rupture progression through a fault system has not been seriously addressed in New Zealand, although this phenomenon has been very evident in Turkey during historical times. The North Anatolian Fault is a classic example of a plate boundary fault system that has ruptured progressively, segment by segment, through the 20<sup>th</sup> Century (Barka 1992), most recently culminating in the Izmit and Düzce earthquakes of 1999 (Barka et al. 2002; Langridge et al, 2002; Stein et al, 1997).

Understanding the role of fault segmentation is an important and logical next step in earthquake geology studies in New Zealand (see Schwartz & Coppersmith 1984). This project addresses one of the most important fault interaction zones in New Zealand – the Alpine to Hope Fault transition - in terms of the contribution of slip rate, short recurrence time, magnitude of earthquake, slip, and seismic risk posed to

infrastructure (Langridge et al. 2003; 2005). While the western part of the Hope Fault is distant from population centres, the entire Alpine-Hope system impinges on towns and cities from the West Coast to Kaikoura. In addition, each fault segment is individually a strong source of seismic shaking to distances that will affect the urban centre of Christchurch (Fig. 1.1; Pettinga et al. 2001).

New Zealand has been in a state of relative seismic quiescence since 1942 when the last major cycle of earthquakes occurred in eastern North Island (Downes et al. 2001). During the second half of the 19<sup>th</sup> Century and first half of the 20<sup>th</sup> Century there were many large ( $M > 7$ ) events through central New Zealand. The middle part of the last plate boundary "uNZip" progressed through the northern South Island in the early historic period in New Zealand (Fig. 1.2), e.g. AD 1830's? (eastern Hope Fault; Bull, 1998; Langridge et al. 2003) 1848 (Grapes et al. 1998), 1888 (Cowan 1991), and 1929 (Poulter Fault) (Berryman & Villamor 2004). We need to understand events of the first half of this failure process (1717-1840), to be able to piece together a more complete picture of plate boundary failure. Did the whole length of the high-slip rate Hope Fault fail over a period of decades straddling the colonisation period in NZ? Can we expect that this type of failure process will occur in the future? From this work and its outputs we will be more able to consider time-dependent models for future seismic hazard in New Zealand, not only for the Alpine-Hope Fault system, but also for the Hikurangi subduction margin and North Island Shear Belt faults.

#### 1.4 Background

Alexander McKay's (1890) observations of fault rupture and tree disturbance form the backdrop for this project. Notwithstanding the advances made by his recognition of strike-slip surface displacements at the time, or the recent studies of forest age and recolonisation along the Alpine Fault (e.g. Wells et al, 1999; 2001), McKay's insights into forest damage remain immensely useful to this day. Perhaps the best combined example of observation and location is the following:

*A mile below the junction of the Kiwi we crossed from the south to the north side of the middle Hope Valley...noting that very many of the dry birch-trees [Beech] in the bush had been broken and thrown down by the earthquakes, and these were generally broken off 10 ft. to 15 ft. from the ground, the timber, though dry, being sound for the most part, and the roots holding firm in the ground. Some of the trees thus broken were at least 1 ft. in diameter, and some I should estimate were larger than that....*

from McKay (1890).

We can recognise a number of important points from this statement:

1. the location described is a marked distance downstream of the Hope-Kiwi confluence (Fig. 1.3);
2. the predominant bush cover is indeed beech (*Nothofagus*) in much of this country to this day;
3. At heights of c. 3-5 m above the ground, many of the trees were whipped and snapped by strong ground motions caused by the 1888 earthquake.
4. the trees that were broken were large, with diameters of c. 30 cm or more.

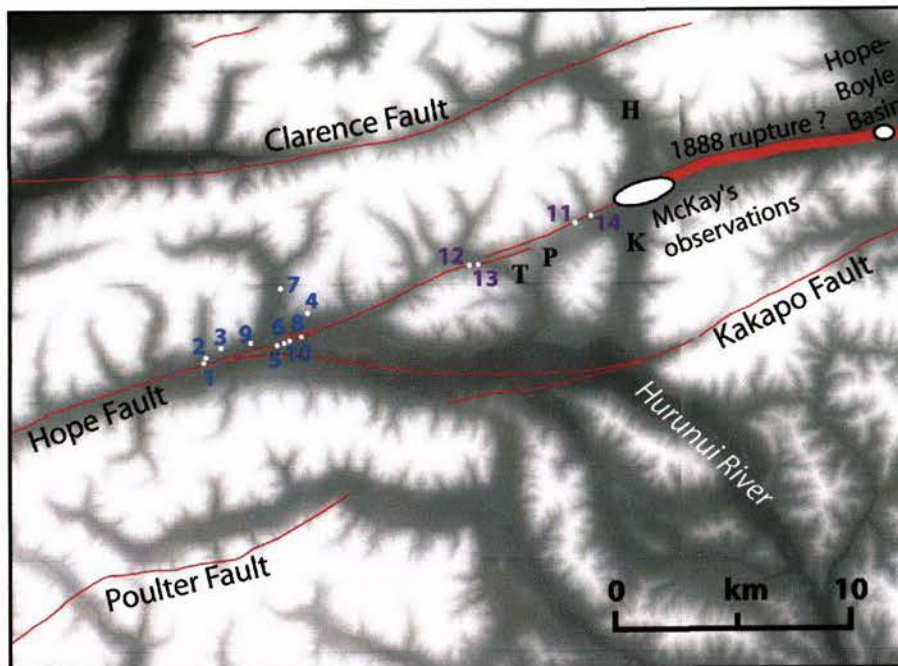


**Figure 1.3.** DEM showing the western end of the Hope Fault from the Hope-Boyle Basin in the east to near Harper Pass. Dendrochronology plots are numbered 1 through 14 (in blue or purple) along and near the trace of the Hope Fault. Alexander McKay's most westerly observations of the 1888 earthquake zone were made near the Hope-Kiwi river confluence. Labelled rivers and streams are: H, Hope; K, Kiwi; P, Parakeet; and T, Three Mile.

From a basic understanding of tree age vs. size (see Fig. 3.4), we can infer that these trees were at least 100 yr old and had probably damaged by the 1888 earthquake.

The quotation above is possibly the westernmost reference to tree damage by McKay (1890). No observations were made to the west of this area, though it appears likely that the rupture trace extended to at least the Hope-Kiwi confluence (Hancox et al. 1997), rather than the Hope-Boyle Basin area as described by Cowan (1991).

Another extract from McKay (1890), for example:

*...we returned to the junction of the Kiwi Creek with the Hope. We might have followed the earth-fractures, old and new, about a mile farther, to the edge of the bush on the east side of the low saddle mentioned; but the day was passing...*

A significant question remains concerning the rupture length of the 1888 event: did it continue farther to the west beyond the saddle (of Parakeet Stream) toward the North Branch of the Hurunui River. This was discounted by Langridge & Berryman (2004) on the basis of a lack of fresh rupture traces in that area. Dendrochronology and trenching provide independent tests of the likelihood of this occurrence.

## 1.5 Scope and Outline of Report

This report presents the results and conclusions reached from studies of three independent paleoseismic indicators along the Hurunui section of the Hope Fault in North Canterbury. These are:

- a) Radiocarbon ages and interpretation from a hand-dug paleoseismic trench across the Hope Fault at Matagouri Flat.
- b) Radiocarbon ages from a swamp, downed or buried trees, aggradation surfaces and mass movement deposits that date moments of punctuated landscape change.
- c) Forest stand ages which indicate periods of synchronous local forest disturbance and re-establishment.

The structure of the report is as follows. Both a) and b) above are discussed in Section 2. Section 3 of the report describes the methodology used for studies of tree age, and Section 4 discusses the results of that work. Section 5 brings together the results from all three paleoseismic studies. Section 6 briefly describes the Synthetic Seismicity modelling of Alpine Fault ruptures and how those ruptures may trigger events in the Marlborough Fault Zone. The overall conclusions of the study are presented in Section 7.

The scope of this project has evolved as time has progressed, though the main hypotheses and goals of this work are as outlined above. As many as 267 trees were cored in this project, in order to date faulting and/or landscape change events. This has led to a better understanding of why the tree damage record may have more events in it, than are accounted for by radiocarbon dates from the landscape or from a trench. It has also become apparent that prehistoric landslides are an important foil to support our landscape-, tree- and trench-based analysis of the paleo-earthquake record along the Hope Fault.

For example, McKay (1890) also discusses a landslip that we have recognised as part of our study and called McKay's slip.

*...The mountain-range lying between the low saddle mentioned and the source of the Hope River and Hope Saddle had on its eastern spur one notably large slip and some of lesser size....Mr. Rutherford, not having noted it previously, was of opinion that it not only was caused by the earthquakes, but also that it appeared right in the line of greater dislocation...*

These types of observations are critical to our understanding of the 1888 earthquake in relation to other, preceding events.

## 2.0 LANDSCAPE AND PALEOSEISMIC DATA

This project relies on three main methods of identifying the age of large earthquake signals along the Hurunui section of the Hope Fault. These are: (i) traditional paleoseismic methods, e.g. trenching; (ii) observations and dates on young landscape features and soil ages on geomorphic surfaces; and (iii) dendro-chronological studies. This chapter deals with (i) and (ii) to set a framework for the tree age work. We will first discuss geomorphic indicators of large earthquakes described in this study; followed by a presentation of the organic material that was dated in this study; and, finally we will describe the results from a paleoseismic trench at Matagouri Flat.

### 2.1 Landscape Observations

Large ( $M > 7$ ) earthquakes cause strong, long-duration shaking and can do considerable damage in the landscape. The effects of large earthquakes in the mountainous Southern Alps region are well documented, and include very large rockfalls, landslides and rock avalanches, and forest damage (e.g., Hancox et al. 1997; 2002; Berryman & Villamor 2004; Yetton et al. 1998). The results of this damage include rockfall and landslide deposits, landslide dammed lakes (Adams 1981; Perrin & Hancox, 1992) and disrupted forest (Duncan et al. 1998). These products of accelerated erosion (mass wasting) rapidly find their way into streams and rivers and end up as fan deposits, river gravel and terrace deposits, and as recently discovered, they can form dateable successions of dune deposits at the west coast of South Island (Wells & Goff, 2006).

While the effects of historic events such as both the 1929 Arthur's Pass and Murchison earthquakes are well known and can still be investigated (Hancox et al. 2002; Berryman & Villamor 2004), it should also be possible to recognise the effects of pre-historic events. Some attempts to date pre-historic earthquakes in the Southern Alps have focused on each of the possible sources of debris material or forest damage listed above. These include: landslide-dammed lakes (Adams 1981; Perrin & Hancox, 1992); landslide distribution and age (Whitehouse & Griffiths 1983), the age of rockfall deposits using lichen (Bull & Brandon 1998; Bull, 2003), terrace chronologies and alluvial surface ages using dendrochronology (Wells et al. 1998; 2001; Duncan 1989; Yetton et al. 1998).

In this study we have relied on a sparse number of surface ages previously published by Langridge & Berryman (2005). We have built up a thorough understanding of the ages of surfaces in the stretch of landscape that includes the Landslip Stream (fan), Matagouri Flat, McKenzie Fan, McKenzie Stream and The Park (Figs. 2.1, 2.2). This is an important step toward undertaking forest ecology studies. For example, it is important to appreciate whether a colony of 280 yr old trees is living on a 300 yr old surface or a 1500 yr old surface. Observations and dates on surfaces are supported by comparing them with relative age dating of soil exposures.

For the tree-covered McKenzie Fan, a radiocarbon date based on material dated in the upstream reach of McKenzie Stream provides an age of  $2331 \pm 55$  radiocarbon

yr BP (2179-2467 cal yr BP) (Table 1). This is the accepted age for the fan and was used in concert with a series of displaced streams to estimate a slip rate of  $9.6 \pm 1.5$

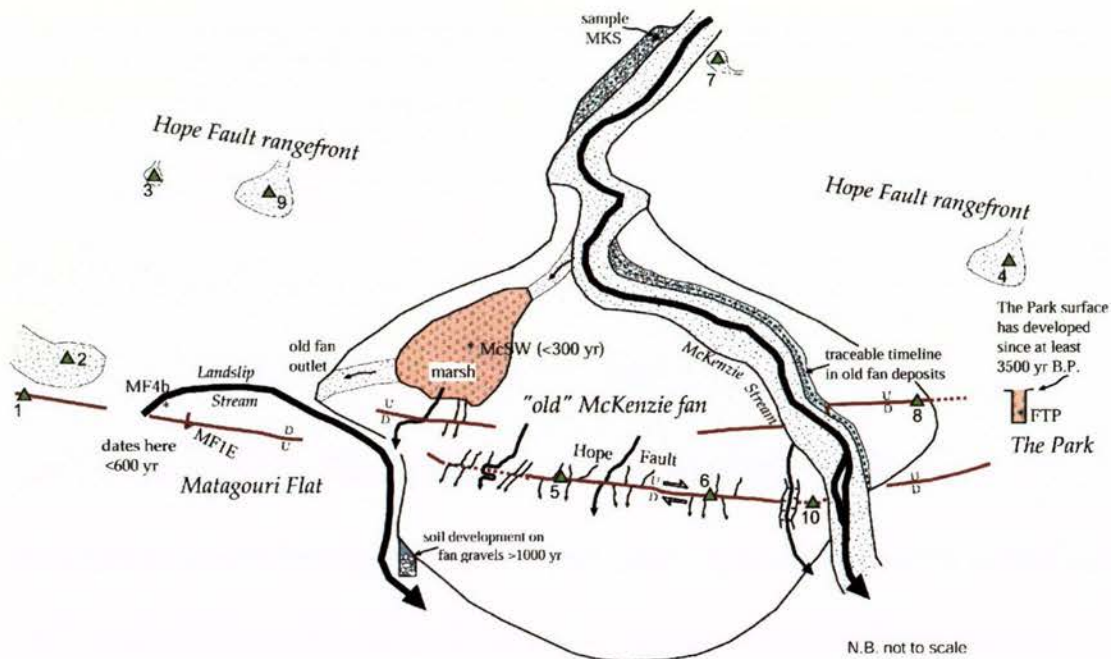


**Figure 2.1** Geomorphic map of the Hope Fault from Matagouri Flat in the west to McKenzie Fan and on to The Park. The formation of these major geomorphic elements generally youngs to the west. Ages come from radiocarbon dates and relative ages supplied by soil chronology. Numbered dendro plots are marked by green triangles. The trench site on Matagouri Flat is marked by a red bar.

mm/yr for the Hope Fault at McKenzie fan (Langridge & Berryman 2005). N.B. The slip rate calculated farther east near Three Mile Stream Hut was  $13 \pm 1.5$  mm/yr.

The McKenzie fan grades to the surface of 'The Park' and terraces of the Hurunui River (Fig. 2.1). An age from peat exposed in a rupture (fissure) trace at The Park gave an age of  $3400 \pm 55$  radiocarbon yr BP (3476-3826 cal yr BP). The peat was sampled at a depth of 1.2 m below the surface of the open fissure there. This corresponds to an average peat accumulation rate of c. 0.3 mm/yr.

## 2.2 Late Holocene Relative Soil Chronology

We have two good soil exposures on the old McKenzie fan complex. The first is an erosional exposure at the western edge of the fan complex (see Appendix 1). This soil is a composite Brown Soil representing something in the order of a few thousand years of soil development. The estimate of accumulated time to develop this soil is roughly equivalent to the radiocarbon date for the age of the fan described in the previous section, i.e. c. 2179-2467 cal yr. It is logical that the fan has grown in different areas at different times and that the western edge of the fan could represent an older part of the fan complex than in other parts.

At the opposite end of McKenzie fan at Plot 6 (Fig 2.1) a pit was excavated to analyse the relative age of the soil and to sample the substrate material for OSL dating. In the pit, surrounded by Beech trees of Plot 6, a weakly developed forest soil is formed on 0.8 m of alluvial fine sand and silt deposited over cobbly alluvial gravel

(Fig. 4.12a). The subsequent OSL age from a sample in this pit yielded an age of c.  $17.7 \pm 2.2$  kyr BP. This age is not believable as it requires that the fan and overbank deposits were emplaced during the last glacial period. At this location, a valley glacier filled the Upper Hurunui catchment at this time (Suggate 1965; Clayton 1968). It is likely that the material we sampled had not been reset by exposure to the sun. The level of soil development seen in the forest soil in this pit is considered to represent at least 1600 yr, and possibly 2000-5000 yr of soil development (see Appendix 1). This is of similar age to the soil exposure at the western end of the fan.

### 2.3 Radiocarbon dates

A list of samples submitted for radiocarbon dating is presented in Table 1. Most of these samples were described in either Langridge & Berryman (2005) or Langridge (2004). The latter report included some samples derived from the early phases of this EQC project. They come from: i) a hand-dug trench at the west end of Matagouri Flat and adjacent outcrop exposure (grid ref. L32/302345); ii) a drowned Matagouri bush and peat from a drowned offset channel adjacent to the trench; and iii) samples of wood from buried or fallen trees in the vicinity of the Hope Fault. These dated samples were intended to provide a background to the age results of very young geomorphic and/or burial events, and to our dendro-chronological work nearby.

The location of samples from (i) and (ii) are shown on Figure 2.2. Those samples related to (i) will be discussed in Section 3.4. Other samples described below that are not on Figure 2.2 can be located by their grid reference (Table 1).

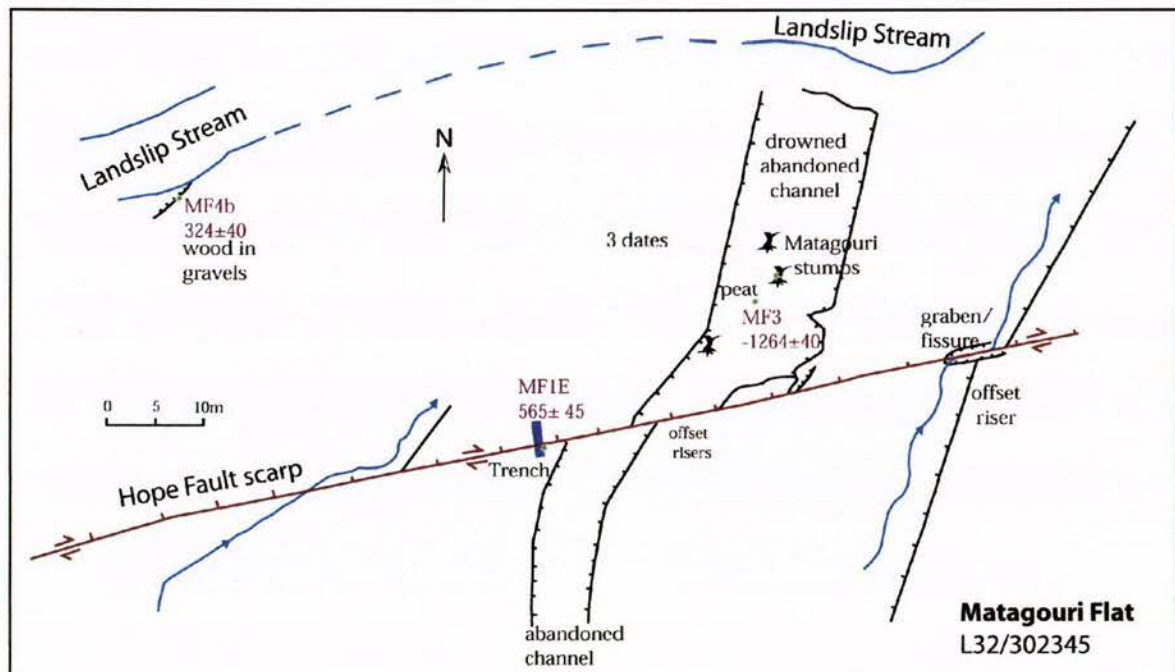


**Figure 2.2** Sketch map of trench site area at west end of Matagouri Flat, North Branch Hurunui River. The trench was hand-dug across a small scarp of the Hope Fault (ticks on downthrown side). One radiocarbon date came from this trench. Wood from the gravel bank of Landslip Stream was also sampled and dated. Several dates came from a Matagouri bush and peat within the drowned channel near the trench (see Table 1).

Three AMS radiocarbon dates were attempted on the trunk of a Matagouri bush that was drowned in a channel adjacent to the hand-dug trench. The hypothesis for this drowning event was that it was related to the displacement of the channel (c. 5 m horizontal; c. 0.3 m vertical). Flooding of the channel (and drowning of the bush) was consistent with displacement in a down-to-the-north sense of motion across the fault at this location.

Sample Mat1 comes from the exterior part of the Matagouri bush drowned in the channel shown on Fig. 2.3, i.e. an AMS date on the outside ring (Ring 1) of the Matagouri bush. Its radiocarbon age of  $-2855 \pm 40$  is clearly modern. Mat 83 (i.e. ring 83) was sampled from the rings in the core of the Matagouri bush cutting in the hope that the technique of "wobble-matching" could be applied to the age structure of this bush. Mat83 also yielded a modern age ( $-19.3 \pm 4.6$  radiocarbon yr B.P.). A re-check of these two dates was made to rule out laboratory error in the dating of these two samples. Mat789 represents a date of rings 7-9 from near the outside of the bush. This sample also yielded a modern age of  $-3482 \pm 35$  yr B.P. An additional date on material growing in the buried peaty soil (MF3) above the roots of the Matagouri bush also yielded a modern radiocarbon age ( $-1264 \pm 40$  yr B.P.). These four results clearly show that the Matagouri bush that was sampled from the water-filled channel grew and died within the modern period. It could be possible to calibrate the 3 Matagouri dates on the "bomb curve" (modern post-atomic bomb era) to get a precise measure of when the Matagouri began growing and ended its lifespan (R. Sparks, personal communication 2004).

It seems clear that it lived during the 20<sup>th</sup> century. As there are no large seismic events that could have conceivably caused this drowning event, it is more likely that the drowning was caused by a fluvial or landslide-damming event in Landslip Stream or a human impact such as back filling of the channel edge. A preliminary attempt to match these dates to the bomb curve suggested that the drowning event, marked by the death of the Matagouri bush, could have happened around AD 1972-73. This date is consistent with a flooding event in the Hurunui valley around that time. Based on the ring count, the Matagouri bush was c. 83 yr old. Therefore, it began growing at around AD 1890, which may be related to forest clearance of lowland areas by early miners or farmers.

Sample McSWMP3 was collected from a modern peat bog that occurs on the upthrown side of the Hope Fault on "McKenzie fan", north of Plot 5 (L32/314353; Fig. 2.1). The piece of Red Beech (*Nothofagus fusca*) wood sampled by auger bit from a depth of c. 1.2 m beneath the bog, yielded a radiocarbon age of  $269 \pm 40$  yr B.P. (282-434 cal. yr B.P.). This age is interesting for two reasons. First, Red Beech would typically not grow in such a wet footing as the bog indicates. Second, that since the burial of this wood, in the last few hundred years only, there has been an accumulation of >1 m of fresh, fluid peat in 'McKenzie swamp' (i.e. at an uncompacted rate of c.  $\leq 4.3$  mm/yr).

Sample LSW comes from the outside of a buried log within a stream cut exposure through a small fan that extends along the fault trace at Lodge Stream near tree Plot 14 (L32/455405; Fig. 1.3). The log has an age of  $26 \pm 30$  yr B.P. (AD 1690-1950) and occurs in deposits that are believed to be faulted. This implies that there has been at

least one faulting since 1690 at this site.

Sample DB1 (Langridge, 2004) comes from the outside of a fallen tree in a drainage just to the west of Three Mile Stream Hut at tree Plot 12 (Fig. 1.3). DB1 yielded a radiocarbon age of  $50 \pm 30$  yr B.P (also 1690-1950 A.D.). This tree is hypothesised to have fallen down as a result of strong shaking and displacement during the last large earthquake event (as opposed to wind or other factors). It lies perpendicular to the fault and has been backfilled by a debris flow deposit that has emanated from the neighbouring small catchment. In addition, the backfilling by the debris flow has kept the tree wet and free from rot. Following this, the debris flow was colonised by tree seedlings. The current size of these trees implies that at least 200 yr but not likely 400 yr has passed since the tree fell, which is consistent with the radiocarbon date on the outside of the fallen tree. This site has potential in determining the timing of the most recent event, which was possibly c. 200-320 yr ago. The cored ages of the colonising trees will better constrain the timing of the debris flow and other related events (see Section 5.5.3).

**Table 1.** Radiocarbon dates from the western Hope Fault region.

Location – sample ID (NZMS 260 grid ref.)	Lab No.		Radiocarbon age (yr BP)	Calibrated age cal BP		Material & significance
				1 $\sigma$ range	2 $\sigma$ range	
McKenzie Stream, MKS (L32/319369)	NZA 13360	-26.07	2331 $\pm$ 55	2330-2358	2179-2467	Woody twigs collected from sandy layer within aggradation gravels in McKenzie stream catchment, 2 km upstream of fault.
The Park, FP (L32/332355)	NZA 13358	-29.59	3400 $\pm$ 55	3576-3697	3476-3826	Fresh peat collected from open fissure on The Park. Grab sample of peat taken from a depth of ~1.2 m within fissure
McMillan Stream, MMS (L32/383379)	NZA 13361	-29.29	12,897 $\pm$ 65	15,052- 15,742	14,489- 15,979	Compressed peat sampled in section above glacial outwash gravel in bank in side catchment above McMillan Stream
3-Mile Stream, .3MS (L32/393382)	NZA 13362	-29.51	6052 $\pm$ 55	6795-6981	6738-7149	Faulted compressed peat sampled in exposure of fault zone adjacent to shutter ridge in catchment above Three Mile Stream
Hope-Kiwi Lodge, HKL (L32/476413)	NZA 13357	-28.19	10,782 $\pm$ 60	12,659- 12,941	12,634- 13,060	Compressed peat formed between two fine glacial outwash gravels in exposure near Hope-Kiwi Lodge
Matagouri Flat, MF1E (L32/302345)	NZA 18592	-25.56	565 $\pm$ 45	531-630	515-653	Delicate plant remains sampled from fine-grained unit w
Matagouri Flat, MF4b (L32/302345)	NZA 18951	-25.29	324 $\pm$ 40	308-463	295-492	
Matagouri Flat, MF3 (L32/302345)	NZA 18593	-28.39	-1264 $\pm$ 40	modern	modern	Peaty soil above the buried soil that the Matagouri are rooted in
Matagouri Flat, Mat1 (L32/302345)	NZA 18763	-27.28	-2855 $\pm$ 40	modern	modern	The outermost rings of a drowned Matagouri bush in the channel near the Matagouri Flat trench dated by AMS
Matagouri Flat, Mat83 (L32/302345)	NZA 18764	-24.45	-19.3 $\pm$ 4.6	modern	modern	The innermost rings (c. yr 83) of a drowned Matagouri bush in the channel near the Matagouri Flat trench dated by AMS
Matagouri Flat, Mat789 (L32/302345)	NZA 19966	-26.44	-3482 $\pm$ 35	modern	modern	Rings 7, 8 and 9 from near the outside of a drowned Matagouri bush in the channel near the Matagouri Flat trench (AMS)
McKenzie fan, Mcswp3 (L32/315353)	NZA 19720	-24.79	269 $\pm$ 35	292-314	282-434	
Lodge stream, LSW (L32/455405)	NZA 20803	-23.7	26 $\pm$ 30	0-260	0-260	Wood from the outside of a log found in a deposit along the Hope Fault at Lodge Stream, this stream is shown in paper
Three Mile Stream, DB1 (L32/403385)	NZA 20804	-23.96	50 $\pm$ 30	0-250	0-260	Wood from the outside of a

Radiocarbon age: Conventional radiocarbon age before present (AD 1950) calculated using Libby half-life of 5568 years, and corrected to  $\delta^{13}\text{C}$  of  $-25\text{‰}$ .

Calibrated age: Calendar years before present (AD 1950) and calendar years AD/BC using C-14 calibration programme CALIB 4.3 (Stuiver, Reimer & Reimer: <http://depts.washington.edu/qil/calib>). A Southern Hemisphere offset of  $-27$  radiocarbon years has been applied to all samples prior to calibration (McCormac et al., 1998). A lab error multiplier of 1.0 has been applied to NZA samples. Age ranges listed are minimum and maximum values of the calibrated age range based on a radiocarbon age error of either  $1\sigma$  or  $2\sigma$ .

## 2.4 The Matagouri Flat Paleoseismic Trench

### 2.4.1 Background

One goal of this project was to open a paleoseismic trench across the western part of the Hope Fault within the study area to develop an on-fault record of fault rupture timing. This record of fault movements could both stand alone and be compared to estimates of earthquake timing from dendrochronologic and landscape change arguments.

A clear, uphill-facing scarp was recognised across Matagouri Flat during reconnaissance mapping of the fault (Langridge 2004; Langridge & Berryman 2005). Several stream channels that crossed Matagouri Flat were shown to be deflected in a dextral sense in aerial photographs and from the air during a helicopter reconnaissance. On the ground, the channels and risers at the west end of Matagouri Flat were displaced dextrally by up to 12-14 m, with smaller estimates of 5-6 m on individual channel edges (Langridge 2004). A trench site was chosen next to a displaced channel (Fig. 2.2). At this location the scarp was north-facing with a down-to-the-north sense of movement that created a c. 0.6 m high scarp. This sense of movement is reflected in the nearby channel; the downthrown side is waterlogged by the higher relative groundwater level, while the upthrown side of the channel is dryer and abandoned (Fig 2.3). The vertical scarp across the offset channel is perhaps 1/3 to 1/2 the size of the scarp at the trench. The implications of this result are that we expect that the dextral and vertical movements to be the result of perhaps at least two fault movements.

The North Branch of the Hurunui River is extremely isolated and has limited access due to its dual control between private and Dept. of Conservation landowners. This meant that we did not consider using a mechanical digger to excavate a trench, but rather that we dug the trench by hand.



**Figure 2.3** The Matagouri Flat trench site. The trench was hand-dug through the fault scarp here. Offset channel and riser pair are shown beyond the trench. Matagouri bushes at this site date to c. AD 1890. The trace of the Hope Fault, shown by the yellow tape measure, trends towards the McKenzie fan (far midground) and notch on the skyline near Three Mile Stream Hut.

## 2.4.2 The trench and its stratigraphy

The Matagouri Flat trench was c. 3.5 m long and c. 1 m deep. The water table occurred at a depth of c. 70 cm on the lower side of the trench. The trench crossed the scarp and showed displaced, but matchable stratigraphy from the downthrown to upthrown sides of the trench. Both trench walls are presented for ease of comparison in Fig. 2.5. Unit descriptions are presented in the Appendix 2.

On the upthrown block, the trench was floored by a pebble to cobble gravel (Unit 6). This was a coarse, angular channel gravel that we believe can be correlated with the broader construction of Matagouri Flat when the Hurunui River extended across this part of its plain. Unit 6 gravel is overlain by a package of well sorted sands (Unit 5), ranging from coarse sand to silty medium to fine sand and sandy silt. Unit 5a had a light brown colour and was interpreted as a weak paleosol. Units 5 and 6 were not exposed in the trench on the downthrown side.

Unit 4a is a thick, light coloured, massive, fine sand to sandy silt. Unit 4b consists of lenses of coarse sand intercalated within the finer unit 4a (Fig. 2.4). Correlatives of Unit 4 deposits were recognised in a pit below the water table near metre-4 on the downthrown block. Unit 4 deposits are cut into and overlain by deposits of Unit 3. These are fine (pebble to cobble) gravels to gravelly sand. Unit 3 varies from matrix- to clast-supported. We suspect that, from their character, that these deposits are local to Landslip Stream, rather than being Hurunui River gravels.



**Figure 2.4.** Exposure of the scarp of the Hope Fault and East wall of the Matagouri Flat trench. The light coloured units (middle right) are of Unit 4a sandy silts (see Fig. 2.5). Unit 4a is truncated by fault F1. Gravelly units 3a and 2a and a topsoil overly Unit 4a.

Unit 2a is a rounded pebble gravel with a dirty sand matrix. This unit is quite similar to Unit 3 gravels, and may be the C or BC horizon of the modern soil that is forming on gravels of Landslip Stream. Unit 2a is separated across the steepest part of the scarp by Unit 2b which is interpreted as a colluvial unit. It contains more sand and soil than the adjacent gravel units.

The trench stratigraphy is capped by a medium brown topsoil with, in places, a darker organic sandy subsoil.

### 2.4.3 Radiocarbon Dating of Trench Deposits

Only two small samples of root-like grass were extracted from the Matagouri Flat trench. Sample MF1E comes from the east wall of the trench. This sample comes from near the top of the weak paleosol unit (5a) on the upthrown side of the trench. The age of the root-like grass is  $565 \pm 45$  radiocarbon yr BP ( $525-653$  cal. yr B.P.). We are not certain if this material and age represents the depositional age of the silty fine sand on which the soil developed, or is rooty material that is more akin to the development of the soil itself. Sample MF2W had a very similar appearance to MF1E but came from Unit 4a immediately above the weak paleosol. This material was not considered for dating at this time.

Sample M4b comes from a low gravel bank exposure in Landslip Stream immediately adjacent to the trench site (Fig. 2.2). It is discussed here because the gravel exposure in that bank is essentially the same height above the modern stream as the trench, and the

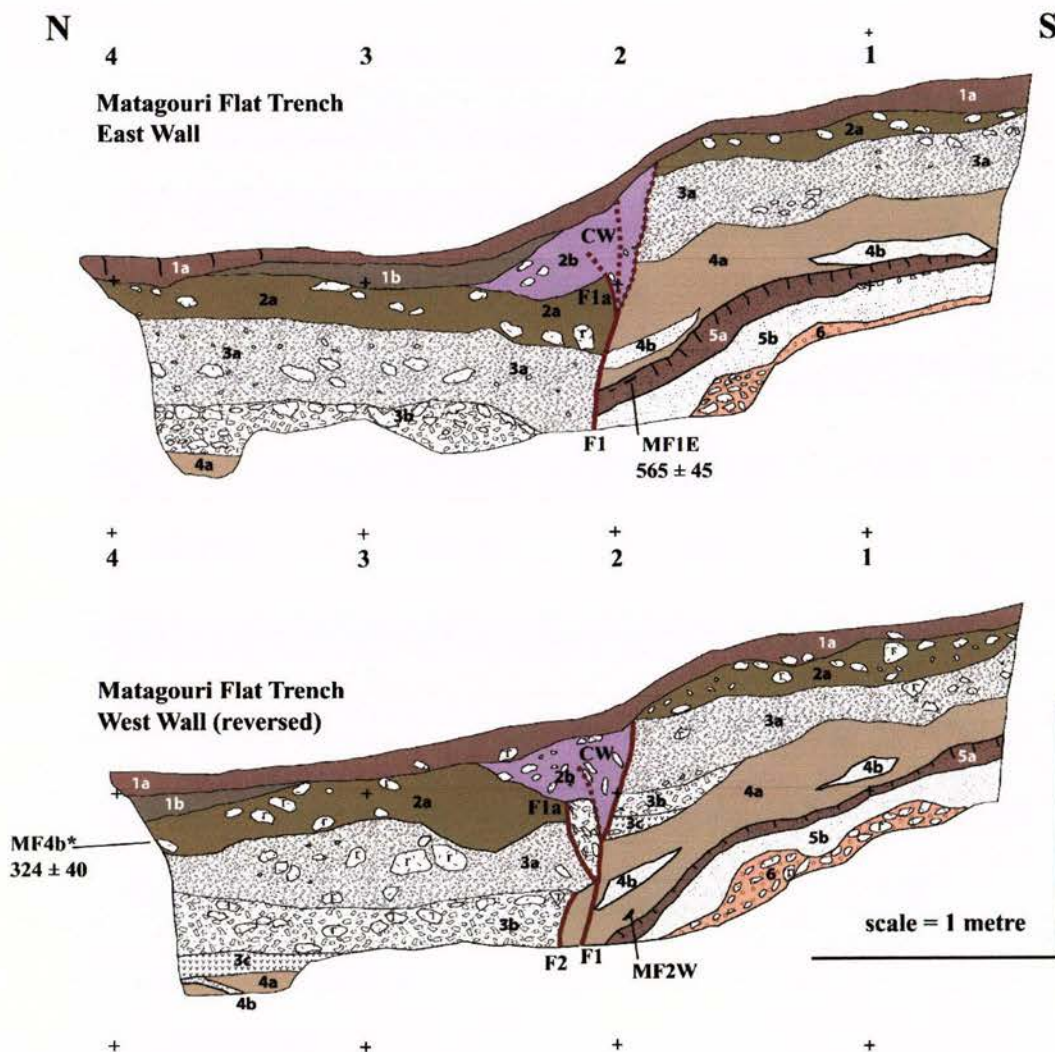


**Figure 2.5** Logs of the Matagouri Flat trench. The west wall of the trench has been reversed for ease of comparison. Faults are drawn in red, e.g. F2. The trench provides evidence for at least 2 surface faulting events.

sediment itself is similar to Unit 2a or 3a in the trench. Sample MF4b wood yielded an age of  $324 \pm 40$  radiocarbon yr B.P. (295-492 cal. yr B.P.). Therefore, this date not only tells us about the age of recent gravel sedimentation along this drainage, but can also be correlated to units in the trench. We believe that the gravel dated in the bank of Landslip Stream is equivalent to Unit 2a, or possibly the underlying Unit 3a.

#### 2.4.4 Faulting

We carefully considered whether the feature we had dug through in such a shallow exposure could not have been a low fluvial terrace riser of Landslip Stream, but were convinced that it was a fault for the following reasons:

- (i) it is associated with deflected channels;
- (ii) those channels have vertical steps across the lineament;
- (iii) the scarp continues to be uphill-facing to the west for some distance, creating a small waterfall across a creek and continuing into the bush toward Plot 1.
- (iv) The units are vertically stepped (faulted) across the wall of the trench
- (v) There is a pattern of cumulative deformation toward the base of the trench

We expand on the story of recent faulting below:

The fault zone in the trench is quite narrow and typically consists of a single strand (F1) that branches in the upper half of the trench (Figs 2.4, 2.5). On the west wall a second minor fault (F2) juxtaposes Unit 3b against Unit 4a, forming a sliver next to F1. The stratigraphic position of faulting in the trench is equivocal. The most recent event is defined by the formation of a colluvium (Unit 2b; CW) that covers the scarp. Unit 2a is vertically separated across F1 by 0.45-0.75 m. This unit also shows thickness change across the fault zone in the trench. Considering the scarp height (0.6 m) and variability of strike-slipped units, this separation could account for the entire scarp in one displacement event.

The surficial soil in the trench is not faulted. Beneath this, it is clear that gravel 2a and gravel 3a are faulted. We observe that fault 1A terminates on the base of unit 2b on the west wall. Therefore, the most recent event horizon happened after the deposition of Unit 2a and is marked by the deposition of Unit 2b. Based on the date of these gravels from the nearby stream bank ( $324 \pm 40$  yr BP), the most recent event faulting occurred since 295-492 cal yr BP (i.e. since AD 1458-1695).

A weak vertical fabric within Unit 2b perhaps suggests that some later shearing of the colluvium reorganised some of the pebbly grains. We do not infer that this represents a full 'rupture' of the fault. It is more likely to be 'sympathetic' shear formed during a nearby fault movement that did not disrupt the ground surface at Matagouri Flat. However, a very young faulting event that shears the colluvial wedge 2b cannot be ruled out.

Unit 5a is clearly deformed to a greater extent than those above it. This weak sandy soil is buckled and folded, vertically offset an unknown amount from the upthrown to downthrown side of the trench. Units 5 and 6 have a greater dip on the upthrown block than is visible in Units 4 through 1, though it is possible that Unit 4 is equivalently deformed as Unit 5. If the event horizon for the penultimate faulting event is the top of unit 5a (a weakly developed soil horizon) then the date from MF1E ( $565 \pm 45$  yr BP) should provide a date for the timing of that event. Therefore, it is possible that the penultimate event was at or after 515-653 cal yr BP (AD 1297-1435).

The age and event data is combined in Figure 2.6. Based on this small amount of data, the time between the penultimate event and the most recent event is c. 23-398 yr. Two rupture events in the last 572-710 yr equates to an approximate recurrence time (to today) of 286-355 yr. If we consider that the colluvial wedge has in fact been re-faulted by a third, young event, then the recurrence interval range is c. 191-355 yr. Finally, the recurrence time based on 2-3 events between AD 1297 and 1840 (the beginning of the European period) is c. 272-543 yr.

The average recurrence interval for the western Hope Fault based on slip rate (8.1-11 mm/yr) and single-event displacement (3.2-3.8 m) arguments in this area is 291-469 yr. This is essentially the same range as for the whole of the Hurunui section of the Hope Fault (310-490 yr) published by Langridge & Berryman (2005).

Although there is both considerable uncertainty in the stratigraphic position, timing and interpretation of events in the trench, we believe that we have neither under- or over-interpreted the record from such a shallow exposure. All of the measures of recurrence time listed above overlap and are compatible with each other. With only a few radiocarbon dates and even fewer exposures it is difficult to determine the exact number of, or precise ages of paleoseismic events along the Hope Fault here.

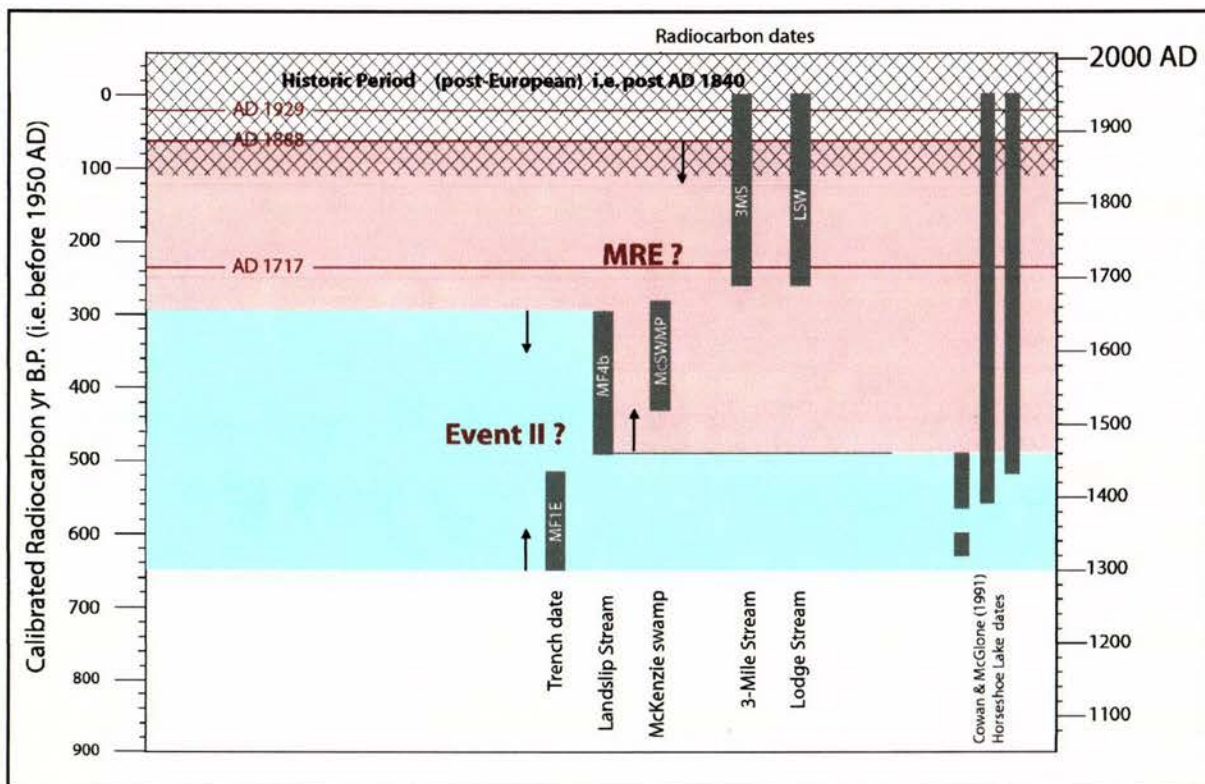


**Figure 2.6** Possible event history for the western Hope Fault between Matagouri Flat and McKenzie fan based on dated geomorphic and trench data. Radiocarbon ages from Table 1 are shown as dark vertical bars. Revised calibrated ages from Cowan & McGlone (1991) are also shown for comparison. Not enough age control exists to precisely date the most recent event (MRE) or Event II.

### 3.0 METHODOLOGY OF TREE RESEARCH

#### 3.1 Site Strategy

An initial reconnaissance trip to the North Branch Hurunui River in February 2002 realised the potential for dendro-chronologic (tree age) studies along the western end of the Hope Fault. Following funding of the project, in February 2004 a pilot study at the future Plot 1 site was undertaken to test the viability of the dendrochronologic study. Subsequently, in the summer of 2005, a total of 14 plots were chosen to investigate forest age along and adjacent to the western end of the Hope Fault (Fig. 1.3). Plots were chosen on the basis of their location relative to the fault and to the youthful landforms in the study area.

N.B. An additional site (called Plot Ø) consists of extra trees that were cored during a pre-pilot reconnaissance study along the fault in 2002 to the west of Hope-Kiwi Lodge .

Of the 14 complete plots, five were effectively on or adjacent to the mapped fault trace, i.e. all of the trees were within c. 10 m of the fault scarp. Three of the plots were specifically chosen because they were on young fluvial sites or surfaces, while another six sites were located on young fan or debris deposits adjacent to the range front.

At each plot a number of site variables were recorded such as general location and geomorphic status of plot (scarp, terrace, fan etc). A layout sketch map of the plot was drawn showing the relative positions of each tree in the plot. An example of these plot maps is shown in Fig. 3.1, while the remainder appear in Section 4.

Three species of native New Zealand trees were prevalent in the study area: Red Beech (*Nothofagus fusca*); Silver Beech (*N. menziesii*) and Mountain Beech (*N. solandri*). For each tree a number of variables were recorded. These variables included the species of tree, the circumference of the tree at the borer height, and a number which was assigned to it (e.g. RB7) to locate it within the plot and data stream. Each tree was tagged and could (theoretically) be relocated at a later time using the map and tag. The data for each plot and tree are presented in Appendix 3. In each of the plot maps, we have shown the distribution of trees relative to landforms and each other, and shown their tag and relative size, i.e. circumference measured at the borer height (Fig. 3.2).

Finally, some comments were made about each tree that relate to its growing conditions and health. Such observations about the condition of the roots, e.g. buried by sediment, straightness of the trunk, e.g. tilted trunk or dual trunks, evidence of damage in the canopy, e.g. snapped crown or nursery root growth, were all noted. At each plot we randomly selected a plot centre which was usually tree #1. From this point almost all trees in a radius of c. 10 m were sampled. This strategy meant that we should have a complete, unbiased forest age distribution for any given plot.

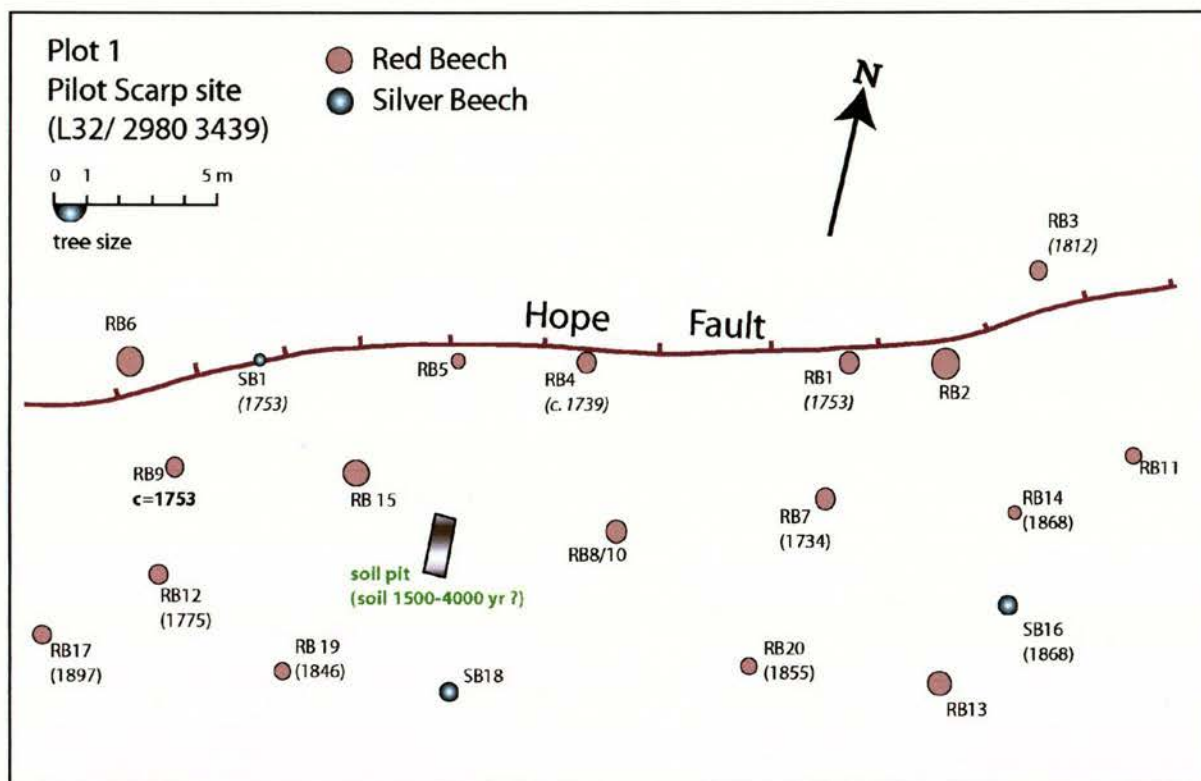


**Figure 3.1.** Sketch map of Plot 1 (drawn to scale). Trees are mapped according to their size, species and location. AD calendar ages when trees reached borer height are shown below the tree I.D.'s, e.g. c=1753 is a core that intercepted the tree centre, while ages in parentheses are 'good Arc' ages. Other minimum ages from Short cores are not shown here (see Appendix 3).

### 3.2 Tree coring methodology

For each tree that was sampled, the tree borer is placed against the tree at about the sternum height of the person who cored it. The borer height reflects the time at which a tree seedling reaches the sternum height of the sampler. As this is dependent on the overall height of the sampler, there is a potential uncertainty in the age of tree dates cored by one sampler vs. another.

Tree cores were taken by Marshall Smith (c. 96 trees; 1.40 m borer height), Vicente Perez (101; c. 1.28 m), Richard Duncan (29; c. 1.30 m), Robert Langridge (18; 1.35 m), Peter Almond (13; 1.28 m); and Vasso Mouslopoulou (7; 1.23 m).

The average borer height is therefore c. 1.35 m. We consider that once a seedling reaches a height of c. 1.2 m, it is likely to quickly 'shoot up' past 1.4 m. Thus we believe that the error related to different borer heights (operators) is potentially negligible with respect to this study, therefore, we have ignored an assessment of this issue in this study.

However, we recognise that there is an offset in time between a major event in the landscape that created a new landform, e.g. rejuvenated fan, fire, or a displacement/shaking event that knocked down parts of the forest along the fault trace, and the age of trees re-populating the landform. This offset includes:

- (i) the time it takes for Beech seeds to land in a new open piece of ground;
- (ii) the growth rate of seedlings to borer height, which may be species dependent;
- (iii) the growth rate based on environmental conditions, e.g. underlying soil substrate, altitude, aspect, rainfall; and

(iv) the ability to “shoot up”, i.e. how much of the previous canopy has been removed at pre-existing tree plot sites.

Later, in Chapter 5, we discuss several tree plots that allow us to make estimates of colonisation rates on new or pre-existing surfaces, and of Beech tree growth rates.

### 3.3 Tree core sampling and preparation

Trees were cored with a standard 45 cm tree borer. Each core was sampled at the indicated borer (sternum) height of that particular sampler. The cores were extracted, placed in plastic ‘AI’ tubes and labelled. On return to the Forest Ecology Lab at Lincoln, the cores were prepared and analysed by Marshall Smith. Each core was mounted on a long, thin-guttered wooden mount and sanded down to near its cross-section. The core was then ready for ring counting under a microscope.

The quality of each core, with respect to its ability to date the age of the tree, was assessed in both the field and lab environments. In the field, it was useful to view each core to see whether it had passed through or near the centre of the tree. If it passed through the centre, the sample was stored in an AI tube for analysis. If the core showed an arcuate pattern of rings (Arcs), suggesting that the borer had passed near the centre of the tree, then the quality of those arcs was assessed, i.e. good Arcs meant that there was a tight set of arcs that would give a low uncertainty on the estimated age of the tree (see Appendix 3). Broad arcs meant that the borer had passed several cm from the tree's centre and the uncertainty was probably too large. In these cases, the core was often rejected and a second attempt was made to core the tree. In some cases the core length was short or the tree had a rotten interior. These cores were often kept, to provide a minimum age for the sampled tree.

In the lab, the polished core mounts were counted for tree rings and estimates of the uncertainty were made on tree age based on the proximity of the core to the tree centre. Reliable tree ages were claimed for c. 80 % of the trees (207 of 250 trees). The remaining ages were rejected due to inaccuracy. In this study, the tree ages were binned into 20 year intervals for plotting on histograms. The results of each plot are discussed in Section 4.

### 3.4 Fault scarp plots

Six of the tree plots were chosen along or adjacent to the scarp of the fault; in plots 1, 5, 6, 8, 11, 14 and also trees in ‘Plot Ø’. The fault scarp is essentially the sloping panel between the upthrown and downthrown surfaces of the fault, where the fault has displaced a planar alluvial surface. The scarp in these situations is generally 3-5 m wide and thus, a single large tree is likely to grow on or adjacent to the scarp panel. This is important when considering co-seismic effects on trees. The fault scarp is the area that is expected to undergo surface rupture, with horizontal and vertical displacements, during a large M7+ earthquake. In addition, the fault scarp and the upthrown and downthrown sides of the fault (within 20 m) are likely to experience secondary fault displacements and deformation and very strong ground motions of MM Intensity IX or greater. Due to the rupture fissures and vertical separation, the fault scarp itself could be considered as a new or disrupted geomorphic surface after a large, surface-rupturing earthquake. Therefore, it is likely that trees growing in this location will be tipped over or tilted due to long period shaking and disruption of the substrate by surface rupture and displacement (e.g. Fig. 3.2).



**Figure 3.2.** Photo of Plot 1 viewed from the east. Large trees are growing on the upthrown side (e.g. RB15) and panel of the fault scarp (e.g. RB5, SB1, RB6) there.

### 3.5 Alluvial plots

About half of the plots investigated in this study fall into the category of new or reactivated depositional features that are here simply called “alluvial plots”. The alluvial plots are plots 2, 3, 4, 7, 9, 10, 12, 13 and 14 (Appendix 3). Trees cored on these plots give a minimum age for the genesis or rejuvenation of the alluvial site. Plots 2, 10 and 14 are related to relatively flat, fluvial terrace surfaces. In these cases, material has been deposited by a stream forming a new fluvial terrace surface. Subsequent to this, trees colonise the surface, grow to the canopy height and are involved in developing a soil on that new land surface.

Plots 2, 4, 7, 9, 12 and 13 have formed on new or rejuvenated surfaces related to alluvial fan deposition and debris slides. Several of these plots are on the steeper apron slopes of the range front of the Hope Fault. At or near these plots it is expected that very strong shaking will generate landslips and rockfalls in the steeper upper parts of catchments. The sediment released from higher in the landscape is transported through the catchment and deposited on the lower gradient and elevated parts of alluvial fans and floodplains. The transport distance may vary from 10-1000 m or more. In some cases, completely new fan surfaces are created, whereby the former land surface is covered, along with the previous forest. In other cases, a fan surface may be rejuvenated whereby a smaller amount of deposited sediment only partially affects (buries/levels) the previous stands of trees, i.e. the effects are partial rather than catastrophic. In either case, the recolonisation of trees onto these fan or debris lobe plots will provide a minimum age for significant landscape events on that alluvial

surface.

### 3.6 Summary of tree core data

The strength and validity of the data in this study are in the number, distribution and relevance of the tree plots and trees sampled. Whether the plots were on or near fault scarps, fluvial surfaces, fan or debris deposits, all trees sampled (excluding plot 7) were growing within 500 m (Plot 4) or less from the active traces of the Hope Fault.

We sampled c. 250 (261 including Plot Ø) trees along a c. 17 km section of the fault between Lodge Stream near the Hope-Kiwi Lodge and Landslip Stream (Fig. 1.3). From these 250 cored trees, we were able to date 207 Beech trees. Figure 3.4 shows the relationship between tree diameter at borer (sample) height (Dbh) in cm versus age for these 207 dated trees. The data has been subdivided into the three Beech species: Red (*N. fusca*), Silver (*N. menziesii*) and Mountain (*N. solandri*) Beech.

The general feature of Figure 3.4 is that tree diameter is positively correlated with age, so that young trees are generally smaller/thinner than older ones. The second observation concerns the age distribution. We have not dated any trees less than 50 yr in age, whilst the oldest reliable tree age from any plot is 402 yr. For the lower age limit, we believe that our strategy was sound in that we attempted to sample all trees with a diameter of > c. 15 cm. Even though we overlooked smaller trees, they were generally less common in any plot due to the establishment of a dense canopy that prevented a full forest floor covering.

For the upper age limit, it is difficult to get the maximum age of very large old trees due to:

- (i) the general mortality of older trees;
- (ii) rotten centres of old trees;
- (iii) missed tree centres, i.e. off-centre borer execution or asymmetric tree shape; and
- (iv) the sheer size of the biggest trees that does not allow full extraction of the record with a standard borer.

The oldest tree (402 yr) had a diameter of c. 93 cm. We sampled a number of larger trees that were probably older than this, but perhaps the main feature of Figure 3.4 is the overall size and distribution, and antiquity of the forest along the study area. The figure shows that there is a large cluster of tree data between c. 15-90 cm diameter, and in age structure from 70-330 rings (years). About 2/3 of the tree data occurs in a range of 20-70 cm diameter and from 80-280 yr in age. This result is consistent with our assessment of the forest in the field, being of relatively even size and age structure. The largest tree diameters measured in the study area were c. 120 cm.

This age structure is borne out in histograms of the complete data set (e.g. Figure 3.4). Figure 3.4a shows the age structure of all 207 dated trees. The data show a predominance for trees to be in the 80-260 year range with a median tree age of c. 170 yr, with modes around 100-120, 140-160 and 200-240 yr. The age structure is mirrored by the size structure data. We observe that the sampled median tree diameter is c. 50 cm with modes at 30-40 and 50-60 cm diameter (Fig 3.4b).

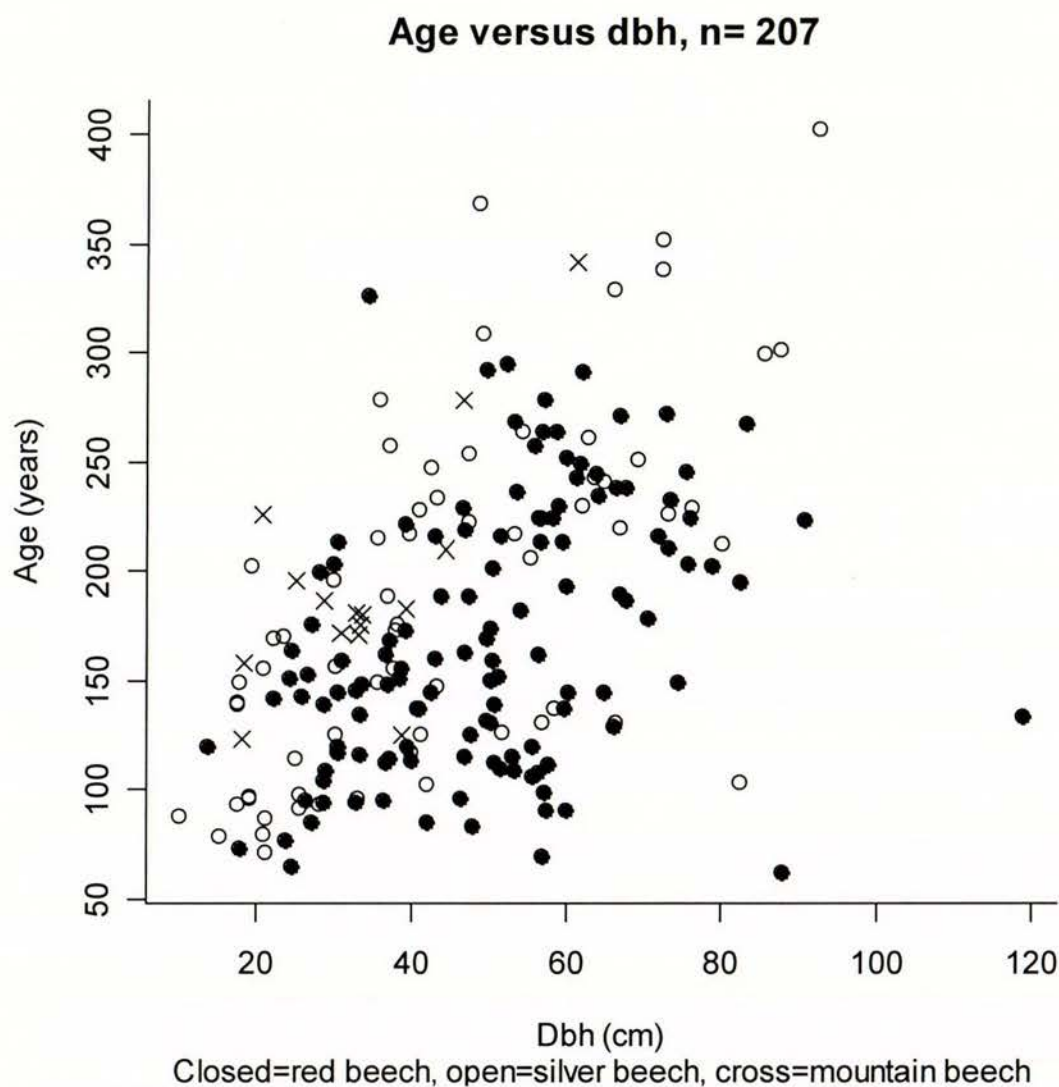


**Figure 3.3.** Age vs. tree size for all 207 dated trees in the study. Dbh = tree diameter at borer height. Red Beech have a higher average growth rate than Silver or Mountain Beech. Mountain Beech were almost exclusively sampled at Plot 11.

In a normal healthy forest the median tree size and age will depend on the environmental conditions of that forest and the time since major tree establishments. In general, large old trees will succumb to windthrow and other events, and young trees will re-establish and flourish into parts of the canopy where older trees have been removed.

One interesting facet of the overall dataset, which we will discuss later (Section 5) is that there are multiple large peaks (and consequent troughs) in both the age and size structure of the forest along the Hurunui section of the Hope Fault. In other words, though we might have expected a generally unimodal distribution of tree ages in the forest, this was not the case.

From Fig. 3.3 it should be possible to determine the average growth rates for Red, Silver and Mountain Beech trees in this study area. We recognise average rates of diameter increase of 3.0, 2.5 and 2.2 mm/yr for the three species, respectively. From this we can quickly estimate the age of trees that McKay recognised in 1890 (Section 1, *quotation*) as being at least c.110 ( $\pm 20$ ) years old when they were snapped off by the 1888 earthquake.

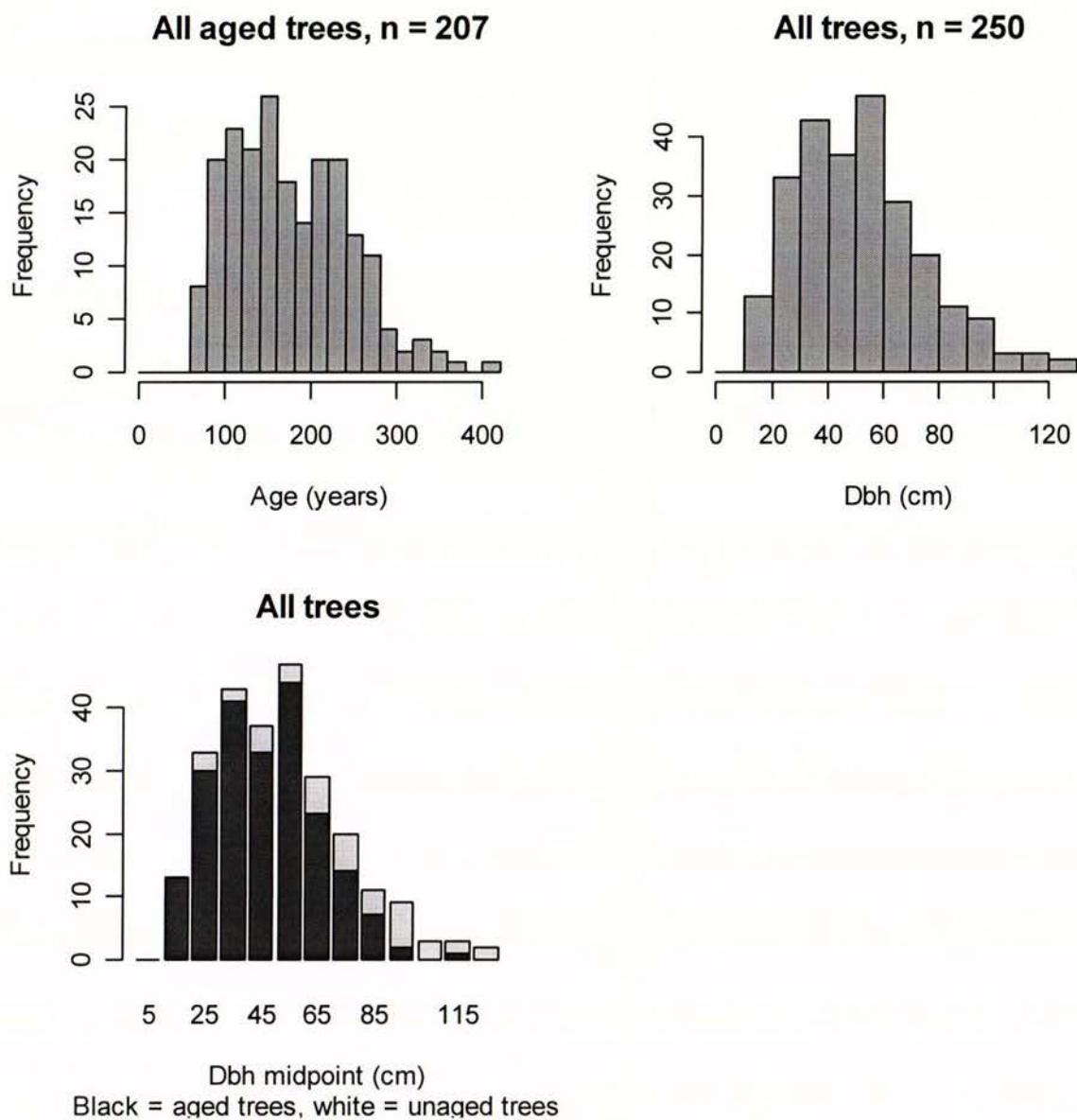


**Figure 3.4.** Histograms of age and size structure for all trees in the study. **A.** Age structure in 20 yr bins for all dated trees. **B.** Size structure of all trees cored in the study; Dbh = diameter at borer height. **C.** size structure of aged vs. undated trees in the study

## 4.0 RESULTS OF INDIVIDUAL TREE CORE PLOTS

### 4.1 Plots 1-10

Tree plots 1 through 10 were accessed via the Lake Sumner Road. Beyond Lakes Station a 4-wheel drive road and farm tracks allows access up the North Branch of the Hurunui River to the McKenzie Stream area and beyond to No.3 Hut.

Plots 1 through 10 were all sited within c. 2 km of the Hope Fault, on the north side of the Hurunui River (Fig. 1.3). These plots were also all located within 2 km of McKenzie Stream and its fan complex north of the Hurunui River (Fig. 2.1).

Plots 1-3 and 9 were situated together between the Hope Fault trace and its range front adjacent to Matagouri Flat and Landslip Stream (Fig. 4.1). Plots 4 and 9 were situated on range front alluvial fans to the east of McKenzie fan above The Park, and to the west of McKenzie fan above Matagouri Flat, respectively. Plot 7 was situated c. 2 km upstream of McKenzie fan and was sited on a side valley fan adjacent to McKenzie Stream. Plots 5, 6, 8 and 10 were sited on or adjacent to scarps of the Hope Fault across McKenzie fan (Figs. 2.1, 4.6).

The general philosophy of the study in the North Branch of the Hurunui River area was to:

- (i) test the collective age of the Beech forest on and around the Hope Fault to look for signals of forest damage and re-colonisation in its age structure;
- (ii) test a range of sites and environments adjacent to the fault to examine individual plot age structures; and
- (iii) develop a robust argument for surface faulting ages along the Hope Fault, based on forest damage and re-colonisation derived from (i) and (ii).

In the following sections we try to discuss the results of the tree coring at each individual plot without placing too much interpretation on what the data mean in terms of earthquakes or other events.

#### 4.1.1 Plot 1

Plot 1 is located at grid reference L32/298344 and was initially targeted as a pilot site in 2004. The plot is sited on a small (c. 1 m high) north facing scarp between Landslip Stream and Matagouri Flat (Figure 3.1). The site was revisited in 2005 and called Plot 1. Ten trees were cored in 2004 and a further 11 trees were cored in 2005 to complete a sufficient plot count (Fig. 4.2). One of the 2004 trees (RB8) was re-cored as RB10. All of the trees were either Red Beech (*N. Fusca*) or Silver Beech (*N. Menziesii*). From the 2004 dataset, five good tree dates were determined, i.e. in the trees that were cored, a set of arcs near the centre, or the centre itself, were recognised in the cores. The other five trees gave minimum ages as the trees had rotten centres. All 11 of the trees sampled in 2005 gave reliable tree ages.

A soil pit of c. 1 m depth was excavated at the site in 2004. The pit exposed a soil formed on Hurunui River gravels that exhibited incipient podzolisation (see Appendix 1). An estimate of the relative age of the soil based on the condition of the stony silt forming the soil and of the gravel itself was c. 1500-4000 yr in age (Fig. 11). The range depends on the exact rainfall conditions at the site, the rate of physical and chemical weathering and biological activity. Annual rainfall at the site is probably close to 2000 mm (NIWA data), which is considerably

less than the West Coast of the South Island, where one author (PA) has greater experience in the relative dating of late Holocene soils and landscapes. However, this age is quite consistent with the development and abandonment of alluvial terraces in the upper Hurunui River catchment.

The oldest tree at Plot 1 had 292 rings (in 2005). This age could be considered as the minimum age of the upthrown side of the fault scarp. However, based on the soil profile development, this soil was more likely the product of multiple cycles of forest establishment and growth. About two-thirds of the trees sampled at Plot 1 came from the upthrown side of the fault on the flat upper surface of the scarp, while the other third came from the edge of the scarp and scarp itself. In this location a tree may experience surface faulting at the scarp during a large M7+ event on the Hope Fault, in addition to the very high ground motions experienced elsewhere. Some of the trees were growing on small elevated mounds that were considered to be the site of former tree falls. This is known as a 'nursery' situation, whereby a new tree takes advantage of the open canopy space, elevation and nutrition provided by an older fallen tree and disturbed substrate. Two large trees growing on the fault

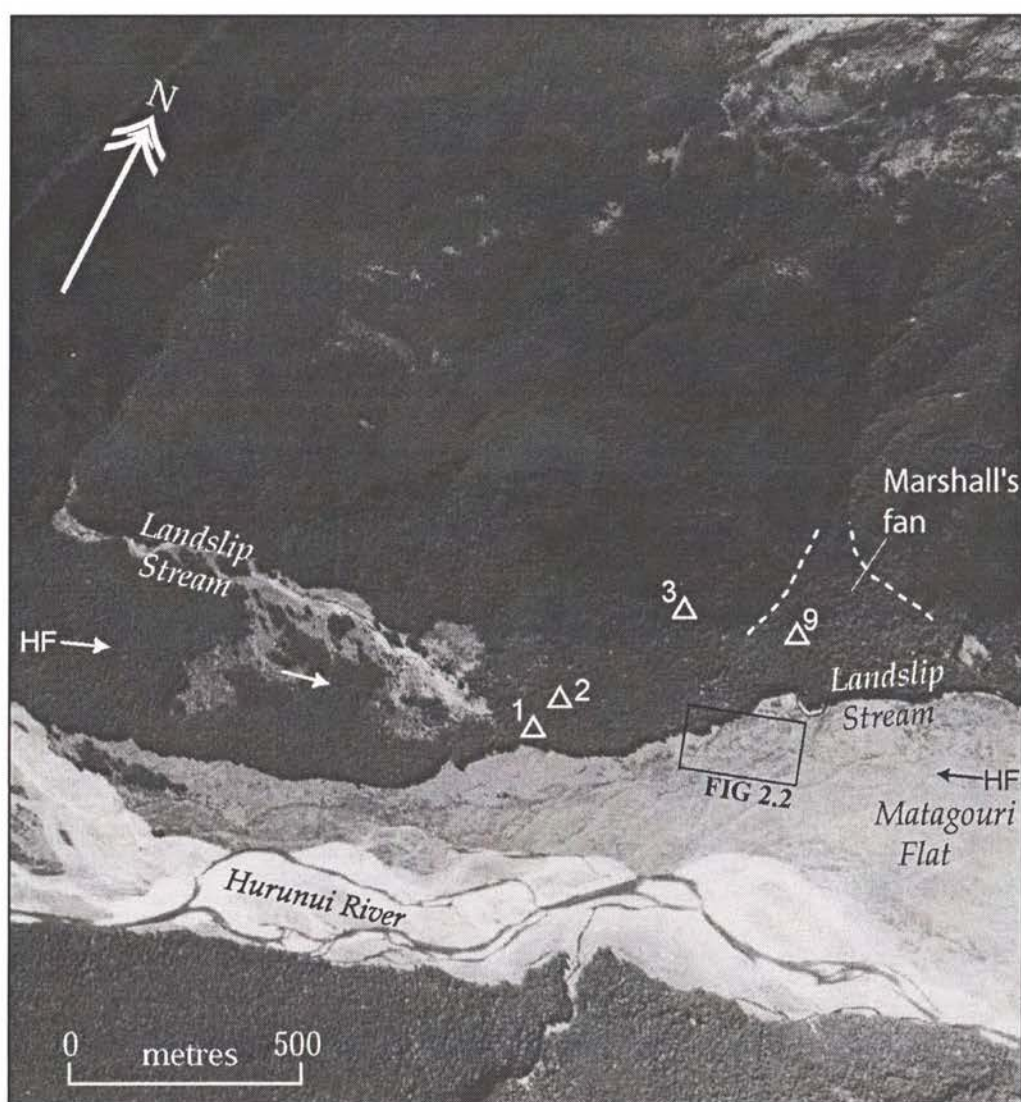


**Figure 4.1.** Aerial photograph and interpretation of geomorphic features between Landslip Stream and Matagouri Flat, upper Hurunui valley. Arrows show the general location of the trace of the Hope Fault (HF). Open triangles identify the 4 westernmost tree plots. The box shows the location of the trench site at Matagouri Flat.

scarp (RB5; RB6) appear to have been tilted at some point in their growth history (Fig. 3.2). RB6 has an obvious secondary crown where a branch has grown straight upward from the tilted trunk of the tree, presumably as a response to the tilting.

The age structure of the 17 dated trees is shown in Fig 4.2a and is as follows. No trees at the plot were younger than 100 years or older than 300 years, though two undated trees (RB2/RB6) had diameters of 90-95 cm. The median and modal tree diameters were c. 60 and 50-60 cm respectively. There is a strong modal age peak at 120-160 rings (years) and smaller modal peaks at 200-220 and 240-280 years. The implications of these peaks in the data of each individual plot will be discussed in Chapter 5.

Tilted trees, such as RB6, that are at least 233 yr old could be used as event indicators, i.e. the tree was stressed at some intermediate point in its growth history.

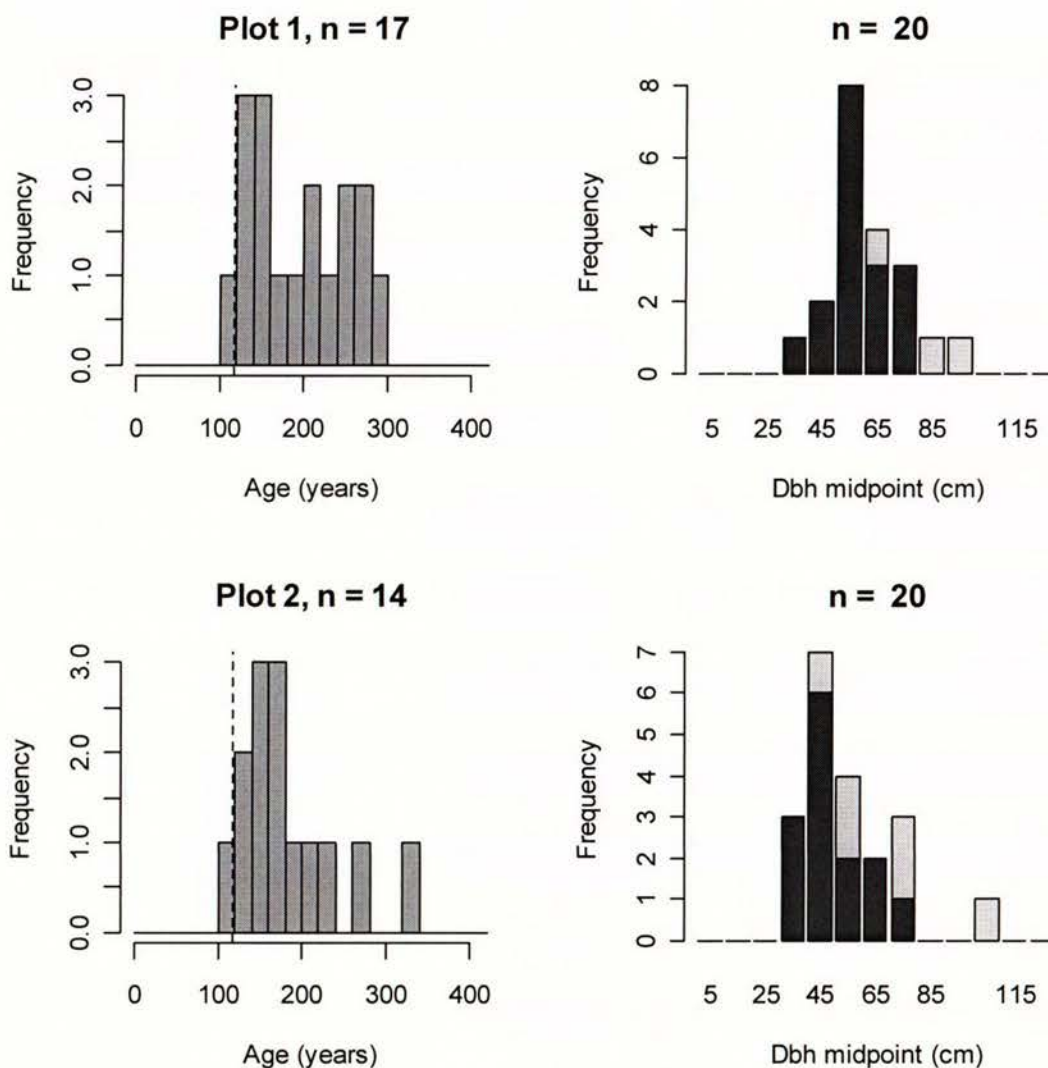


**Figure 4.2.** Age and Size structure for **A.** Plot 1 (above), and **B.** Plot 2 (below). n = the number of dated or measured trees. The dashed vertical line is placed at AD 1888.



### 4.1.3 Plot 3

Plot 3 is sited at grid reference L32/299348 on the range front of the fault c. 400 m north of Plots 1 and 2 (Figs. 4.1, 4.4). Plot 3 was immediately recognised in the field as having a different size structure and substrate to the surrounding forest.

The trees in this plot were growing on a small (c. 500 m<sup>2</sup>), hummocky and bouldery rockslide deposit. The sampled area covers about half of the area of the deposit (Fig. 4.4). The rockslide originates c. 10 m above the deposit itself, suggesting that the transport distance was very short, and the deposit did not spill out far from the range front or spread onto the valley floor. Trees outside the plot on the range front were not cored but appear to be consistently larger than those in Plot 3.

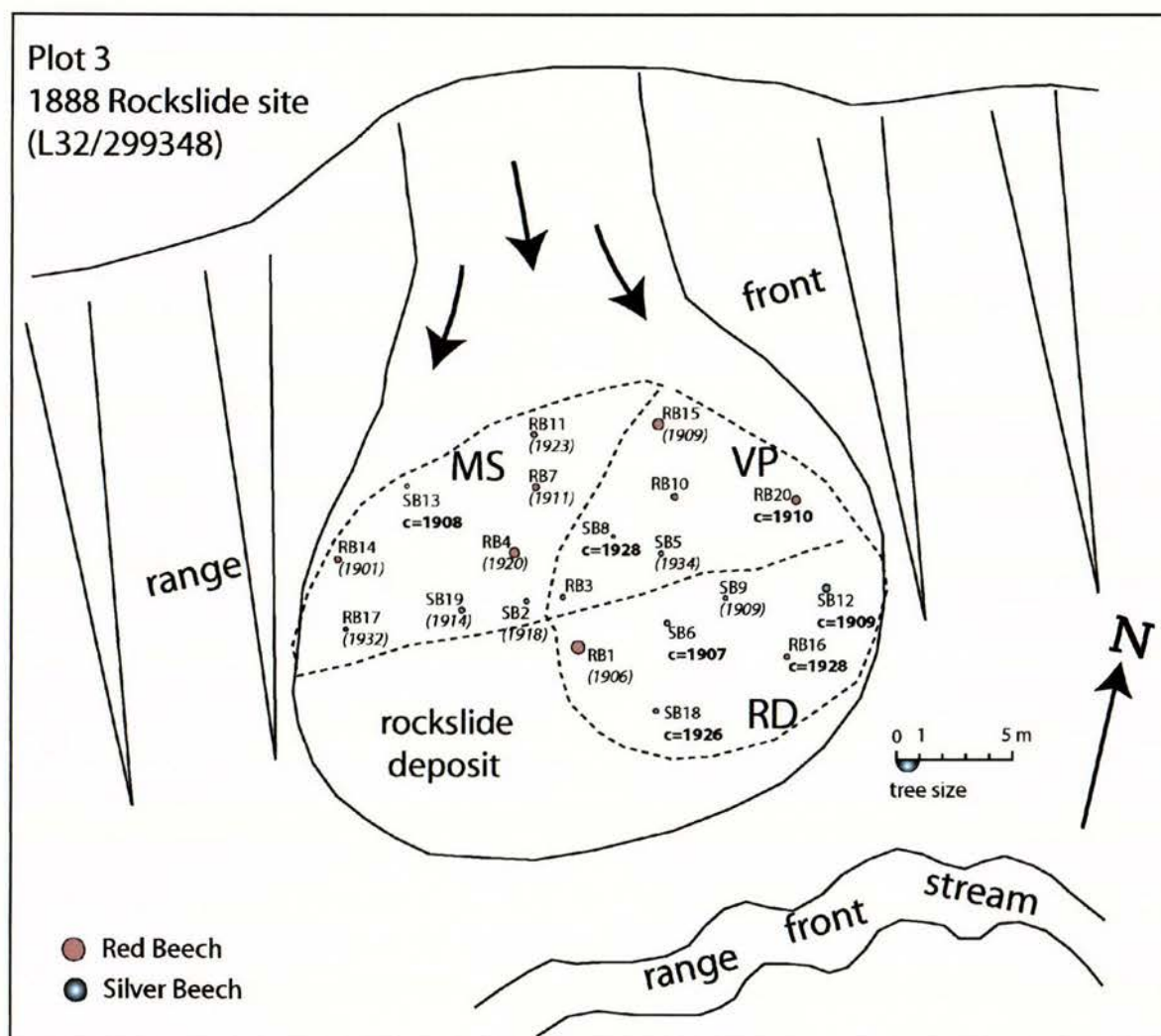


**Figure 4.4.** Sketch map of Plot 3 (roughly to scale). Trees are mapped according to their size, species and position. AD calendar ages when trees reached borer height are shown below the tree I.D.'s, e.g. c=1753 is a core that intercepted the tree centre, while ages in parentheses are 'good Arc' ages.

The 20 trees cored at this site had diameters up to c. 57 cm only. The modal size peak for 11 trees was sharp at 20-30 cm in diameter. The age structure of this site has the classic signature of a 'cohort' that has re-colonised the landscape following a significant forest event. At the bi-decadal level, the first tree appears 100-120 (rings) yr ago, followed by an intense colonisation spike; 12 of the 18 dated trees reached borer height 80-100 yr ago (Fig. 4.5a).

The peak age distribution shows an asymmetric tail at its younger end. There are no dated trees on Plot 3 older than 104 rings (yr) or younger than 71 rings. As will be discussed later in Section 6, we interpret this plot as having a single mode that we relate directly with the 1888 North Canterbury earthquake. Plot 3 has therefore been named the 1888 Rockslide site (Fig. 4.4). This is probably a reasonable assumption based on the colonisation of a deposit produced probably as a result of strong shaking from the c. M7.2 event. Later, we discuss this site in considering growth rates and the offset of tree colonisation ages following a major forest damage event.

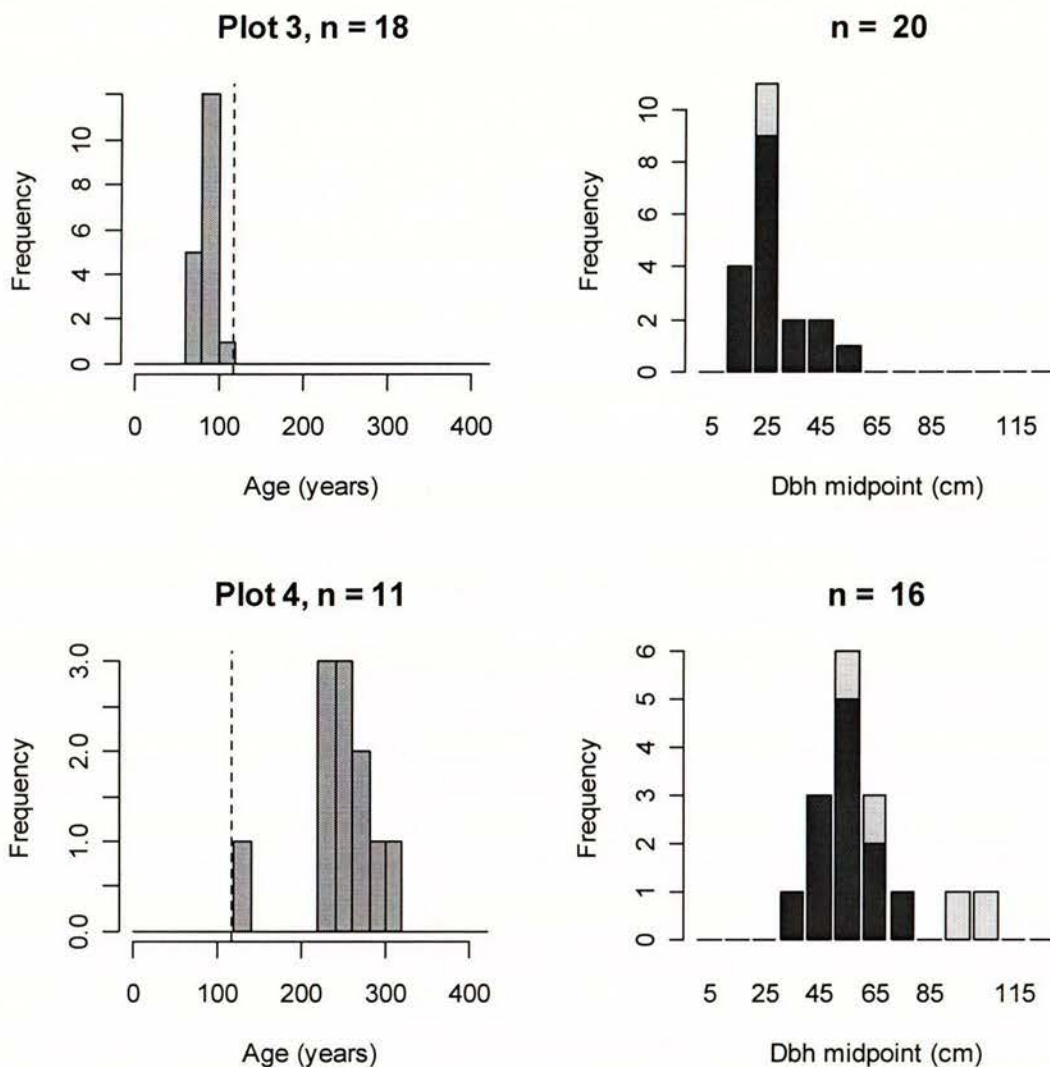


**Figure 4.5.** Age and Size structure for **A.** Plot 3 (above), and **B.** Plot 4 (below). n = the number of dated or measured trees. The dashed vertical line is placed at AD 1888.

#### 4.1.4 Plot 4

Plot 4 was sited at grid reference L32/328360 near the apex of a large fan on the range front above The Park (Figs. 4.1, 4.6). The site was chosen as the fan catchment headwaters exhibited signs of landslide scars high up on the range front that would provide source material for the alluvial fan below. Plot 4 was established immediately east of the main fan channel and adjacent to a minor inactive distributary fan channel (Fig. 4.6).

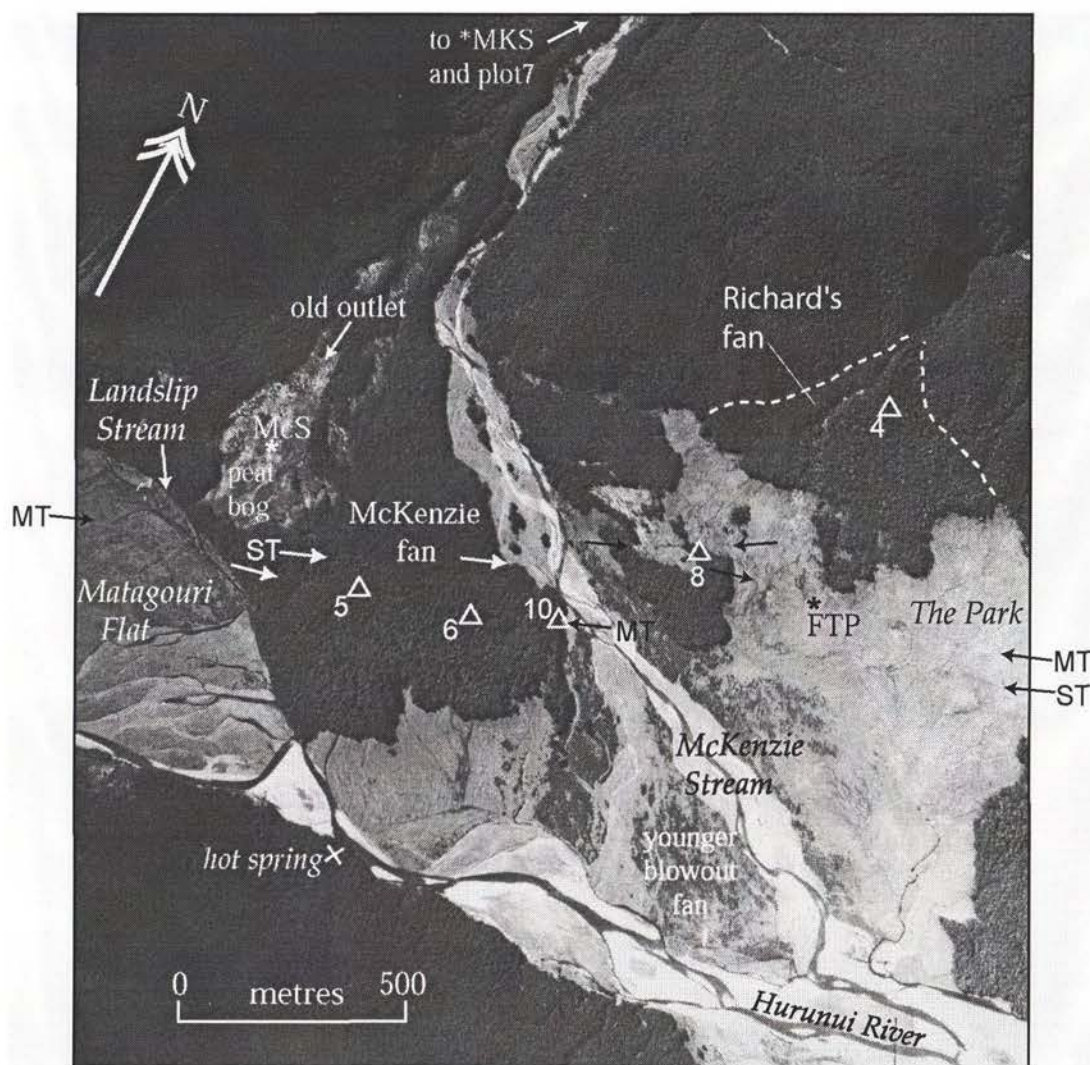


**Figure 4.6.** Aerial photograph and interpretation of the McKenzie fan area, upper Hurunui valley. Traces of the Hope Fault are shown by arrows from Matagouri Flat to The Park. Tree sample plots are marked on the photo by open triangles.

Sixteen Red and Silver Beech trees were cored in a 10 m radius about RB1 (Fig. 4.7). The size distribution of these trees shows a single mode and median at c. 50-60 cm diameter (Fig. 15b). Two large 95-105 cm trees in the plot were cored. The size distribution was mirrored by the age distribution. The oldest dated tree at the site (SB16) gave an age of 309 rings, thus the minimum age of that fan surface at Plot 4 must be at least 309 yr. The two largest trees on the fan did not yield ages, but must surely be in excess of 300 yr in age, implying that the fan has not had significant influxes of sediment in this area for at least this length of time. Eleven of the 16 trees yielded ages. Six of these trees clustered between 236-268 rings (yr) (Appendix 4), perhaps suggesting that a significant sedimentation or shaking event occurred on the fan prior to this time.

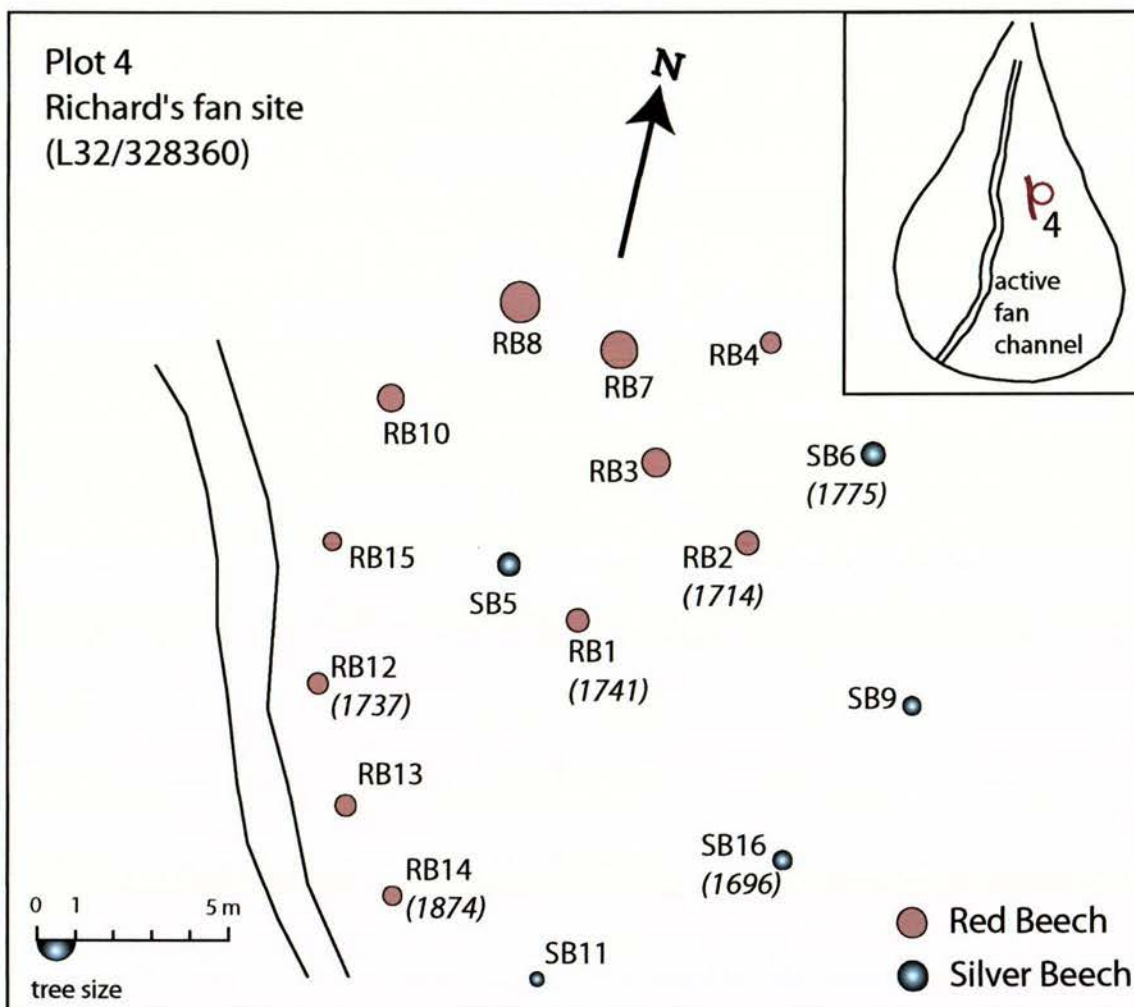


**Figure 4.7** Sketch map of Plot 4 (roughly to scale). Trees are mapped according to their size, species and position. See the Inset and Figure 4.6 for location of Plot 4 on the range front. AD calendar ages when trees reached borer height are shown below the tree I.D.'s, i.e. ages in parentheses are 'good Arc' ages, e.g. (1676). Other minimum ages from Short cores are not shown here (see Appendix 3).

The tree age distribution shows a distinct gap in tree colonisation between 140-220 rings. Indeed, we have cored and dated only one tree younger than 222 rings at this site. Therefore, there is no evidence on this part of this fan for an 1888 earthquake signal. In general, there is a rather old tree population on this fan, with a punctuated period of new tree growth c. 260 rings ago, i.e. from c. AD 1745. Whatever that event was, it cleared c. 50 percent of the trees in the forest at around time at this location. The older trees that survived this event are significantly 'buttressed' (RB7/RB8) or twisted (RB10).

The data also suggest that, if there were younger faulting or strong shaking events, e.g. 1888, that such a site, randomly selected and only 400 m from the Hope Fault on a mountain front fan, then there is no signal of any events in the last 260 years. It is possible that the signal showed at this tree plot is of strong shaking (or related sediment release) from a large earthquake such as the AD 1717 Alpine Fault earthquake that occurred c. 288 yr before our project.

#### 4.1.5 Plot 5

Plot 5 was a fault scarp site along a stable section of the old McKenzie fan (Langridge & Berryman, 2005) at grid reference L32/318349 (Fig. 4.6). The plot was centred about tree RB1 (Fig. 4.8). The scarp at Plot 5 was straight and has a height of c. 2.5 m. All 20 Red and Silver Beech trees were sampled from within 10 m of the upthrown edge of the scarp, or were growing on the edge of the scarp itself.

The McKenzie fan surface has a radiocarbon age of c.  $2331 \pm 55$  C-14 yr BP (2179-2467 cal yr BP) (Langridge & Berryman 2005). This age will be discussed further in relation to Plot 6. A soil profile investigated near this plot in the previous year suggested a relative soil age for the fan surface, of "a few thousand years" (see Appendix 1). This interpretation is considered to be consistent with the age defined by the radiocarbon age above

The oldest dated tree on the fault scarp (SB10) had 368 rings. Two larger trees on the scarp, SB12 (92 cm diameter) and RB5 (124 cm), could be even older than those dated trees (Fig 4.10b). All of the other 18 trees at Plot 5 yielded ages. The size distribution of all trees is dominated by trees 30-40 cm, and also arguably 20-30 cm in diameter.

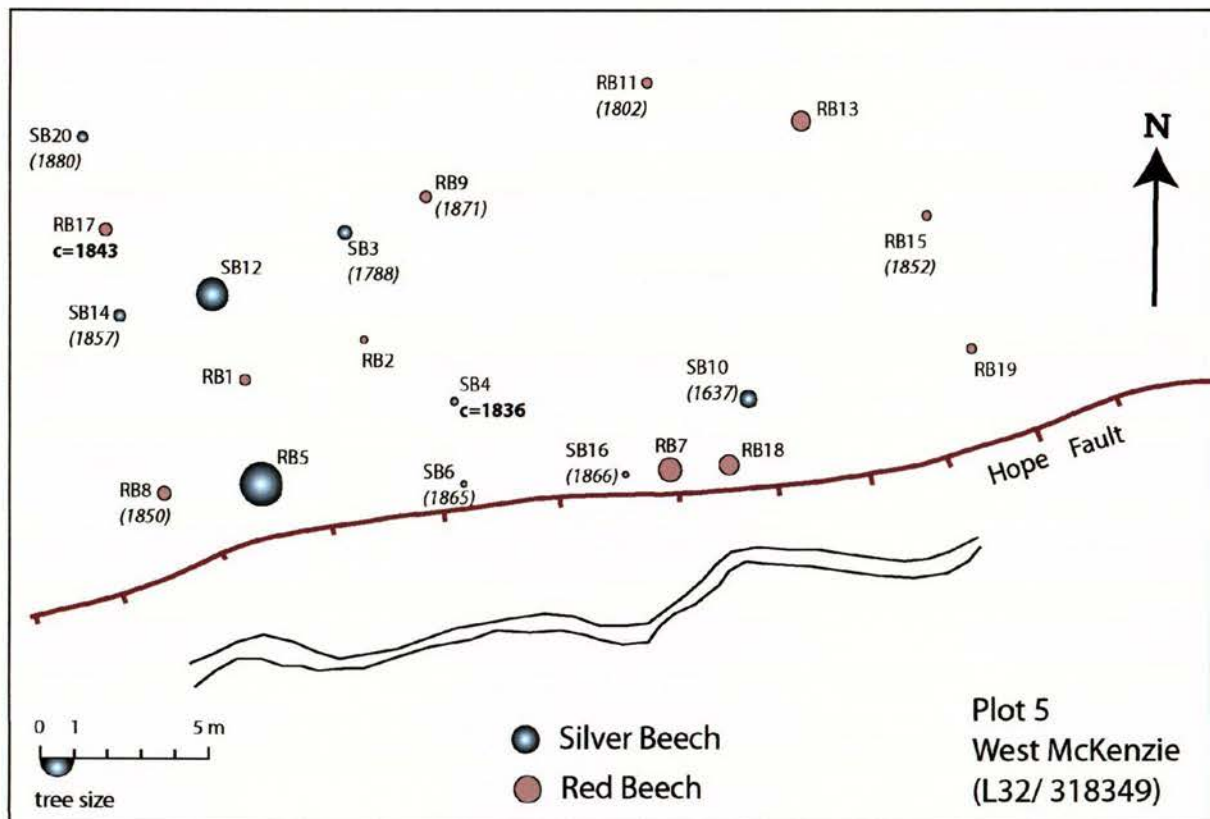


**Figure 4.8** Sketch map of Plot 5 (roughly to scale). Trees are mapped according to their size, species and location. AD calendar ages when trees reached borer height are shown below the tree I.D.'s, i.e., c=1753 is a core that intercepted the tree centre, while ages in parentheses, e.g. (1676) are 'Good Arc' ages. Other minimum ages from 'Short' cores are not shown here (see Appendix 3).



**Figure 4.9.** Photographs from Plot 5 on the scarp of the Hope Fault across McKenzie fan. **A.** Peter Almond cores tree SB3. **B.** the top of RB5 which had been crowned at some time in its past.

The age distribution has several interesting features. First, there are no dated trees in this plot that have <125 or between 257-365 rings. In other words for two century-long periods, there was no rejuvenation of the forest at this site. Second, between these two stable periods there are two modal peaks of tree ages: one at 200-240 rings, and another at 120-160 rings. These two modes and their tails probably account for all but the oldest three trees on the scarp and upthrown block.

There is some evidence at the plot for deformation of older trees, e.g. the largest tree RB5 was crowned (Fig. 4.9b), but has reshot, and toppling, e.g. SB12 has a perched root system, implying it grew over a fallen tree. Stress indicators are likely to be present in the ring records of the oldest trees.

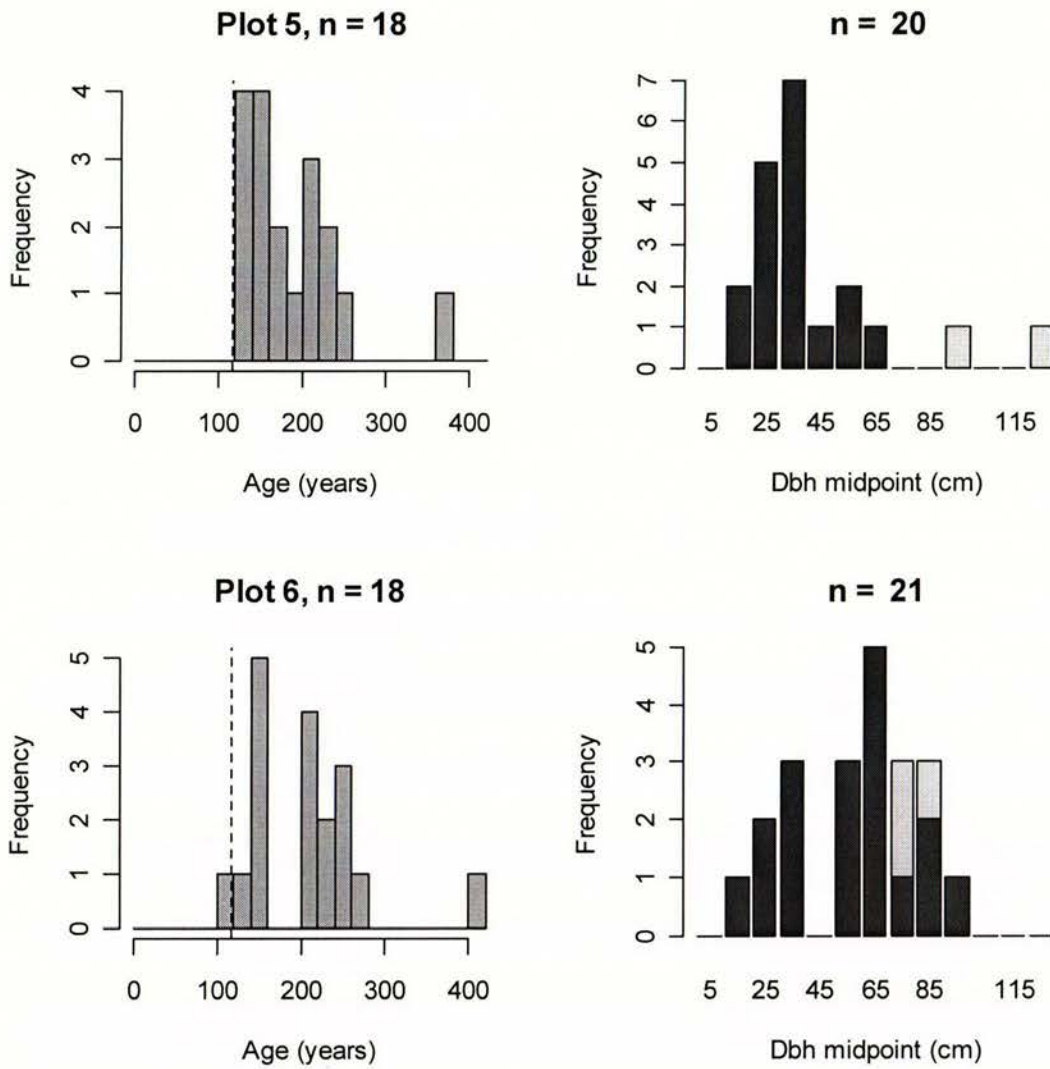


**Figure 4.10.** Age and Size structure for **A.** Plot 5 (above), and **B.** Plot 6 (below). n = the number of dated or measured trees. The dashed vertical line is placed at AD 1888.

#### 4.1.6 Plot 6

Plot 6 was located c. 350 m east of Plot 5 along the same fault scarp described previously at L32/321351 (Fig. 4.6). A 1 m deep soil pit was excavated at this site in a clear area between large trees on the upthrown block of the fault (Figs. 4.11, 4.12 a). The stratigraphy in the pit consists of a forest soil formed on c. 80 cm of silt. The silt overlies coarse, sub-rounded sandy gravels consistent with its relationship to the McKenzie fan complex (Fig. 2.1). The interpretation of relative age from analysis of the soil profile suggests an age of at least c. 1600 yr and perhaps 2000-5000 yr for this current surface (see Appendix 1).

A surficial abandoned channel in the upthrown block (Fig. 4.11) has been correlated with a displaced riser on the downthrown block, giving a dextral displacement of c. 9.5 m, or up to  $21 \pm 2$  m on a second abandoned channel just to the west. The vertical scarp height at Plot 6 is up to c. 1.8 m (Langridge & Berryman, 2005). Test auguring of the silt cover thickness around this plot suggests that the silt drapes a paleo-surface on the upthrown and downthrown sides of the fault scarp that is thickest to the east, e.g. near the soil pit, and thins to a cover of c. 10-20 cm to the west. The inflection of this silt thickness cover is fairly linear on both sides of the fault and suggests a dextral displacement of c.  $12 \pm 2$  m. This is comparable to the 9.5 m displacement of the surficial channel and riser.

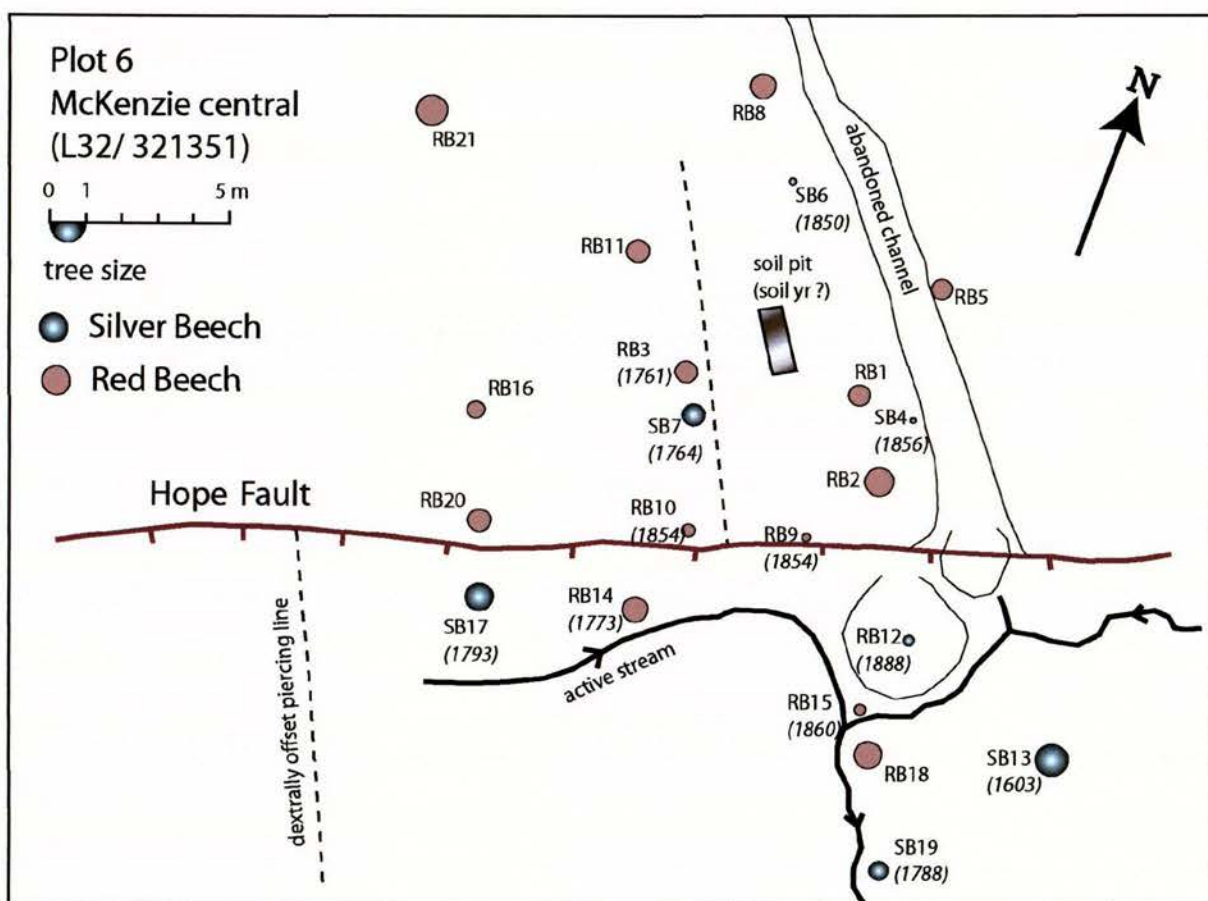


**Figure 4.11.** Sketch map of Plot 6 (not to scale). Trees are mapped according to their size, species and location. AD calendar ages when trees reached borer height are shown below the tree I.D.'s, i.e., ages in parentheses are 'good Arc' ages, e.g. (1876). Other minimum ages from Short cores are not shown here (see Appendix 3).



**Figure 4.12.** Photographs of Plot 6 on the scarp of the Hope Fault across McKenzie fan. **A.** Soil pit Hope 05-02 with OSL sample cavity in sidewall (see Appendix 1). **B.** looking east at the fresh form of the fault scarp. Vicente Perez is standing to the right of tree RB10.

A large sediment block was sampled from the wall of the soil pit at Plot 6. The block was submitted to the VUW Luminescence Laboratory. The sample was expected to provide an

age that could be compared to the relative soil development in the profile and/or the radiocarbon age acquired from fan sediments upvalley (Table 1). The sample age was  $17,200 \pm 2000$  yr BP. This age did not fit with the glacial history of this site (under ice at that time) (Suggate 1965); the geomorphology and age of the fan emanating from McKenzie Stream; or the soil developed in the silt cover at the site. The most reasonable age of the fan construct is still that reported by Langridge & Berryman (2005) at c. 2180-2470 cal yr BP. This age is more consistent with the observations from a soil profile at the western end and the soil exposed in the pit at Plot 6 in the central part of the McKenzie fan complex.

The oldest tree dated at this plot was SB13 on the downthrown side of the fault (Fig. 4.11). This very large Silver Beech had 402 rings, which possibly provides a minimum age for the soil exposed in the pit on the upthrown block. This is the largest dated tree in the whole study. Its age probably tells us that many of the undated trees that are too big or have rotten middles are up to or around 400 years in age.

Twenty-one Red and Silver Beech trees were sampled at Plot 6, and 18 of these trees yielded ring ages. Ten of the trees are growing on the upthrown surface of the fault, six are growing on the upthrown and downthrown edges of the sharp c. 1 m wide scarp (Fig. 4.12b), and five are growing on the downthrown side of the fault scarp. Three clear modes are observed in the size distribution of these trees, i.e. an 80-90 cm mode; a 60-70 cm mode; and a 30-40 cm diameter mode. These size modes correspond with the following three age modes in the dataset of Plot 6: a 145-55 ring mode; a 201-217 ring mode; and a 238-244 ring mode. These three modes could correspond to forest tree fall events at three distinct time periods.

Other features of the age distribution at Plot 6 include a lack of young trees with <117 rings; a lack of trees with 155-200 rings and a lack of dated trees older than 267 rings. This feature of the data suggests that there are periods of stability along the fault scarp ranging from 50-120 years when the canopy is established and stable, not allowing any young trees to emerge from the forest floor.

#### 4.1.7 Plot 7

Plot 7 is situated on a sidevalley fan adjacent to McKenzie Stream at grid reference L32/320375, c. 2 km upstream of (north of) the fault trace and fan (Figs. 1.3, 4.6). It is farther away from the trace of the fault than any other site. The plot is situated on a small alluvial fan that grades onto a low alluvial terrace surface of McKenzie Stream. The fan is lobate and has a central incised channel that probably carries water only at flood times (Figs. 4.13, 4.14a). In the walls of that channel a weakly developed forest soil can be recognised. The tree at the plot centre (RB1) roots into the soil and gravel at this level. However, a younger 20 cm thick gravel sheet buries the soil and the basal portion of the tree RB1 (see Profile on Figs. 4.13 & Fig. 4.14b). This gravel sheet has also aggraded around other trees, but generally thins downslope and to the sides of the fan. No beech seedlings have begun to grow on this upper gravel surface, in part because the tree canopy has not been sufficiently impacted by that event.

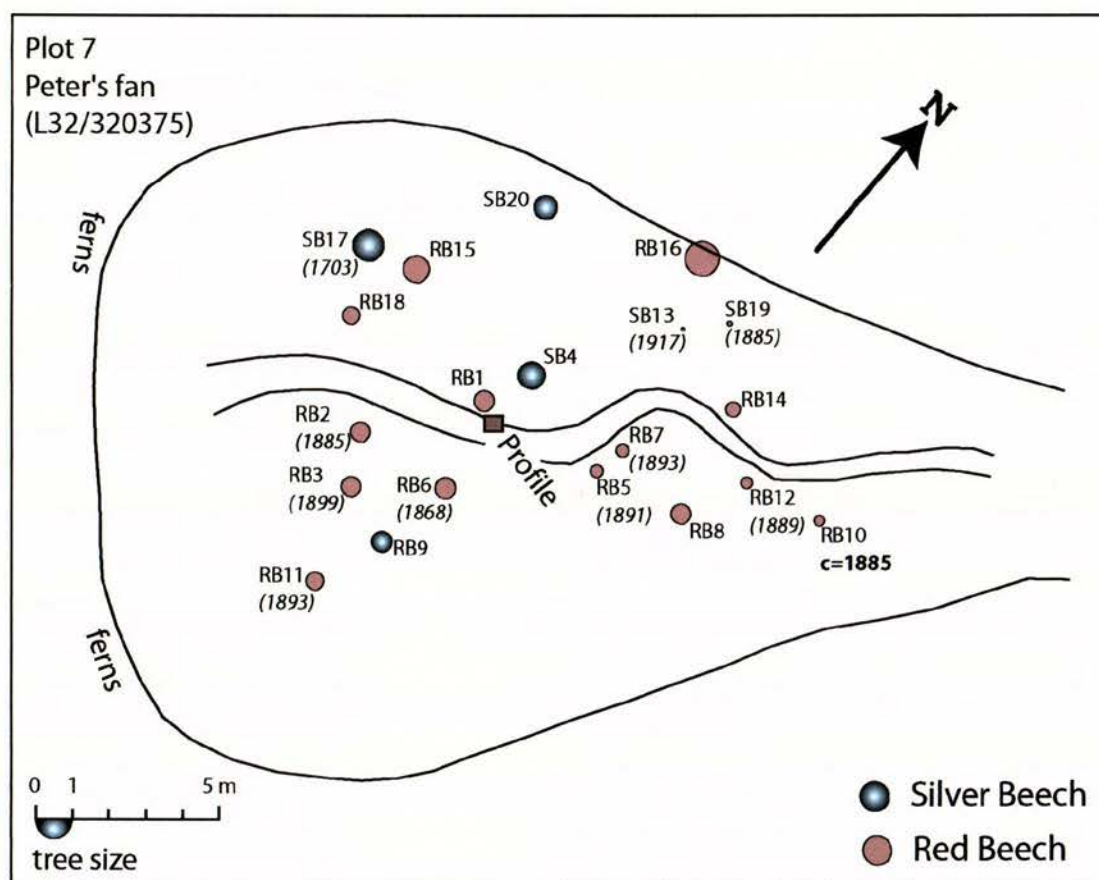


**Figure 4.13.** Sketch map of Plot 7 in the upper McKenzie Stream catchment (roughly to scale). Trees are mapped according to their size, species and location. An immature buried soil seen in profile in the channel wall is shown in Figure 4.14b. AD calendar ages when trees reached borer height are shown below the tree I.D.'s. Other minimum ages from Short cores are not shown here (see Appendix 3).

Twenty Red and Silver Beech trees were sampled on this fan and its fringes; 18 of which yielded tree ring dates. The oldest dated tree at the site (SB17) had 302 rings, which provides a minimum age for early fan deposition and the alluvial terrace surface here. One larger tree (RB16; 97 cm diameter) was undatable, but probably exceeds 300 yr in age (Fig. 4.14a).

The size distribution of trees at Plot 7 is apparently multimodal, with peaks in tree size at 10-20 cm, 30-40 cm, 50-60 cm and 70-80 cm. On inspection of the age distribution there is one

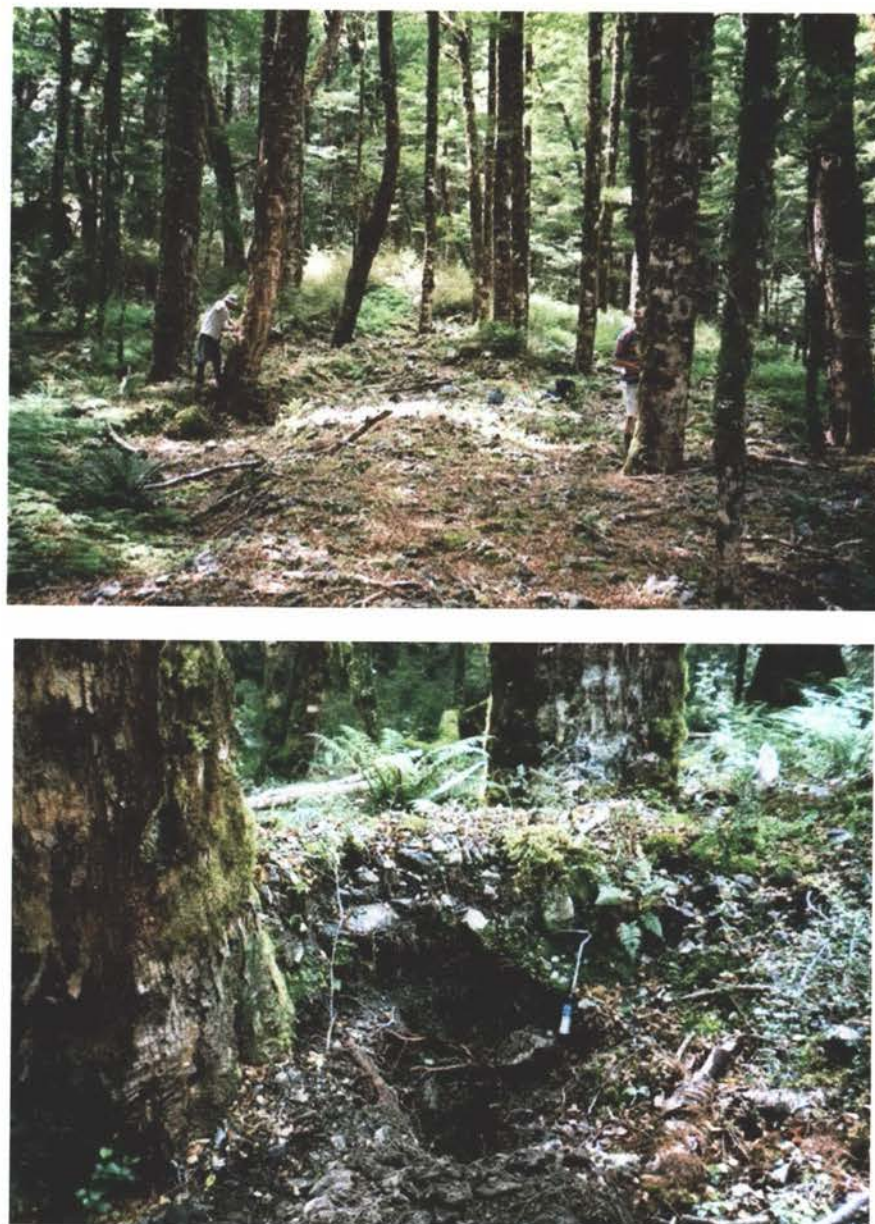


**Figure 4.14.** Photographs from Plot 7, upper McKenzie Stream. **A.** general view looking up the axis of the small fan of Plot 7. Vicente is coring tree RB1 and Marshall tree RB2. **B.** Fan profile exposed in the channel. Gravel is aggraded against tree RB1 that was established on an older fan gravel.

exceptional mode and perhaps a second, minor mode. The primary mode contains >50 percent of the dated trees at the site and peaks at 106-120 rings. The minor modal peak occurs at 220-229 rings. The primary modal peak has the same form as that seen at Plot 3 (Fig. 4.15a). However, care needs to be exhibited in interpreting this prominent mode as an 1888 earthquake shaking signal, as that event occurred 117 yr prior to our study. RB7, the tree clearly founded in a soil buried by the most recent gravel pulse has a tree ring count of 90, so may have grown on a gravel surface that stabilised (forming a soil) after 1888.

Alternatively, this fan is reactivated by other processes in the high country, independent of strong shaking events along the Hope Fault. An alternative means of a new cohort of trees due to the 1888 event at this site could have occurred by the following process: (i) there was an understory of small trees growing at or around borer height (c. 1.3 m) when the 1888 event occurred; (ii) strong shaking and subsequent gravel aggradation removed many of the bigger, older trees on the fan; and (ii) the understory trees became 'bolters' and grew quickly

up, through and beyond the borer height range to establish themselves as the new canopy on the fan. The argument is plausible, but probably unrealistic if the 1888 event caused significant fan gravel to be deposited at this site.

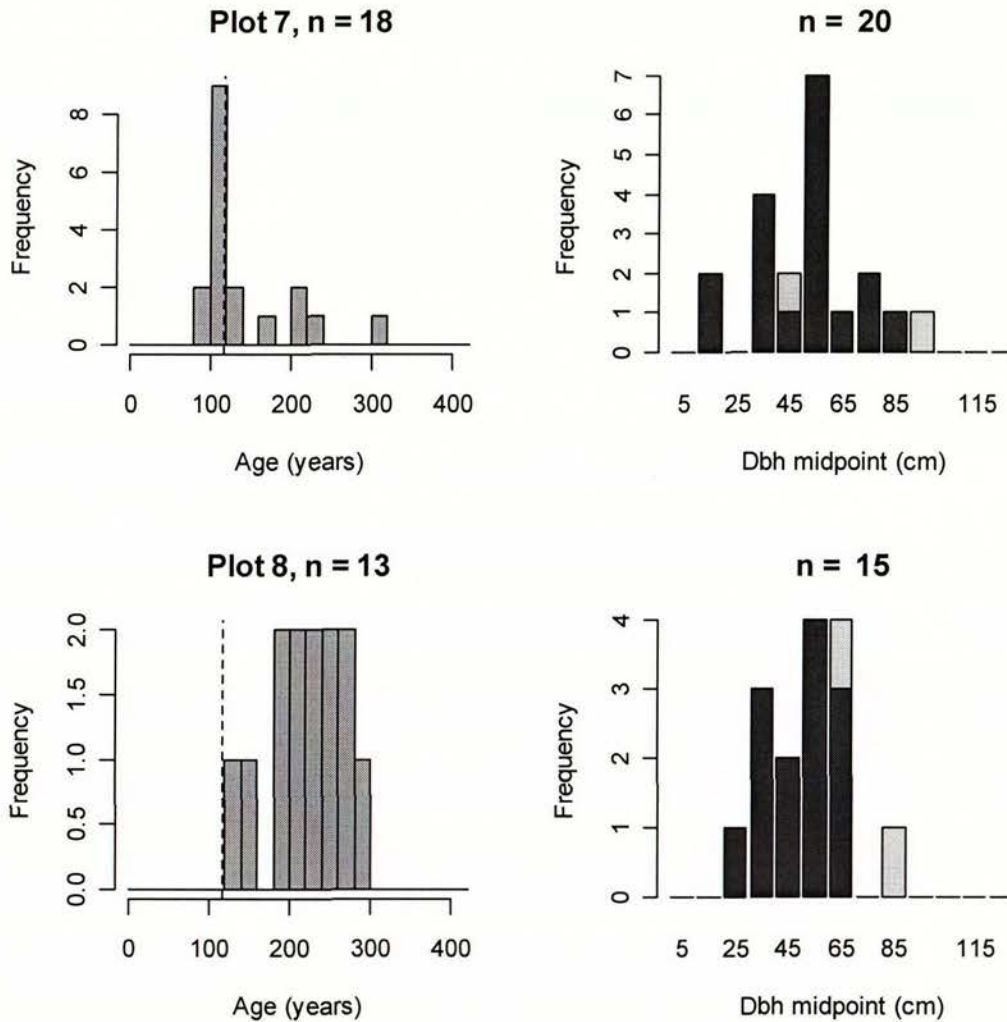


**Figure 4.15.** Age and Size structure for **A.** Plot 7 (above), and **B.** Plot 8 (below). n = the number of dated or measured trees. The dashed vertical line is placed at AD 1888.

#### 4.1.8 Plot 8

Plot 8 is situated east of the current true left bank of McKenzie Stream at grid reference L32/328354. Here, the Hope Fault crosses a remnant of the old McKenzie fan (see Figs. 2.1, 4.6). The site has a south-facing scarp of c. 1.5 m height adjacent to a stream, which is deflected dextrally by c. 6 m. A linear trough at the back of the plot is considered to be a secondary trace (Fig. 4.16).

The oldest dated tree at this site has 295 rings, which is the minimum age for the faulted surfaces here. Fifteen beech trees were sampled at this site. One tree (MB13), growing along the linear trough, is a Mountain Beech (*N. Solandri*) (Fig. 4.17a). The remaining Red and Silver Beech have been sampled predominantly on the downthrown side of the fault scarp. RB14 and RB15 are growing on the upper edge of the fault scarp, while RB1, SB12 and RB11 are growing on the fault scarp (Fig. 4.17b).

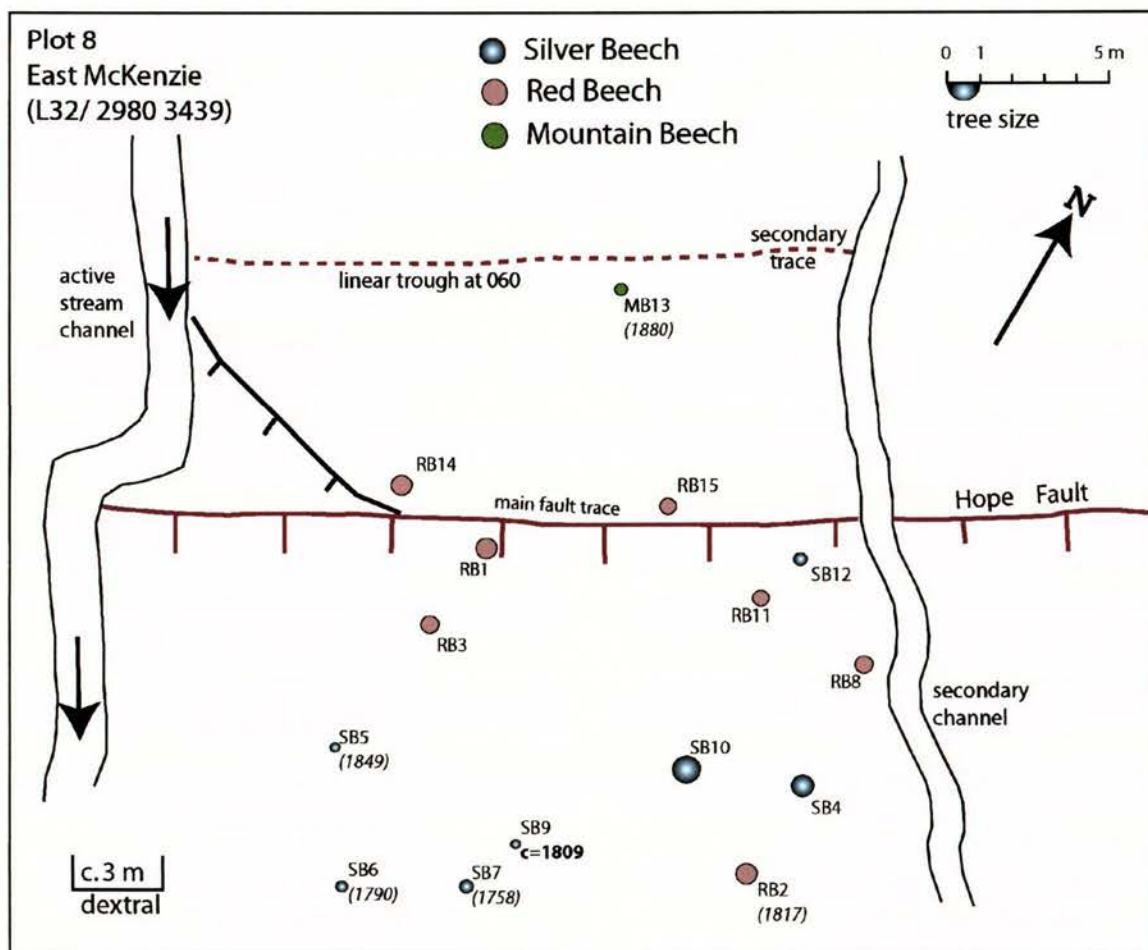


**Figure 4.16.** Sketch map of Plot 8 (roughly to scale). Trees are mapped according to their size, species and location. AD calendar ages when trees reached borer height are shown below the tree I.D.'s, e.g. c=1753 is a core that intercepted the tree centre, while ages in parentheses are 'good Arc' ages. Other minimum ages from Short cores are not shown here (see Appendix 3).

Thirteen of the 15 trees yielded tree ring ages. The size distribution of all 15 trees appears to show a bimodal distribution with peaks at 30-40 cm and 50-70 cm diameter (Fig. 4.15b). However, the age distribution of the site shows no distinct signal, with two trees growing anew at the site in five consecutive bi-decadal periods, i.e. 180-200 rings through 260-280 rings. The origin of such a distribution adjacent to the fault is uncertain at this time, but may include earthquake and windthrow effects.



**Figure 4.17.** Photographs of Plot 8, eastern McKenzie Stream. **A.** View looking SW across the secondary fault trough, with tree MB13 in the midground. **B.** Fault scarp in background with tree RB11 in foreground.

Two other features of the age distribution at Plot 8 are clear. First, only two trees (MB13 and SB5) have colonised this site in the last 188 yr (rings). Second, although two of the biggest trees remain undated, there are no dated trees older than c. 300 years.

Two of the dated trees (SB12, RB14) have perched root systems and both yield similar ages: 238 and 234 rings respectively. This suggests these are both 'nursery trees' that took advantage of open canopy due to treefall.

Another possibility for this flat distribution is that the tree age results may include a significant amount of uncertainty from cores with Bad Arcs or Short Cores, giving minimum ages.

#### 4.1.9 Plot 9

Plot 9, known as Marshall's fan, was an alluvial fan site at grid reference L32/307351, along the apron of the range front north of Matagouri Flat (Figs. 2.1, 4.1). Marshall's fan is a medium-sized range front fan relating to a catchment that extends c. 1 km back into the range, i.e. the fan has a significant, but local source area. Plot 9 was sited on a currently inactive part of the fan complex; the main channel currently sweeps around its west side (Figure 4.18). The fan here has a chaotic network of channels and a large number of big fallen trees and rotten stumps.

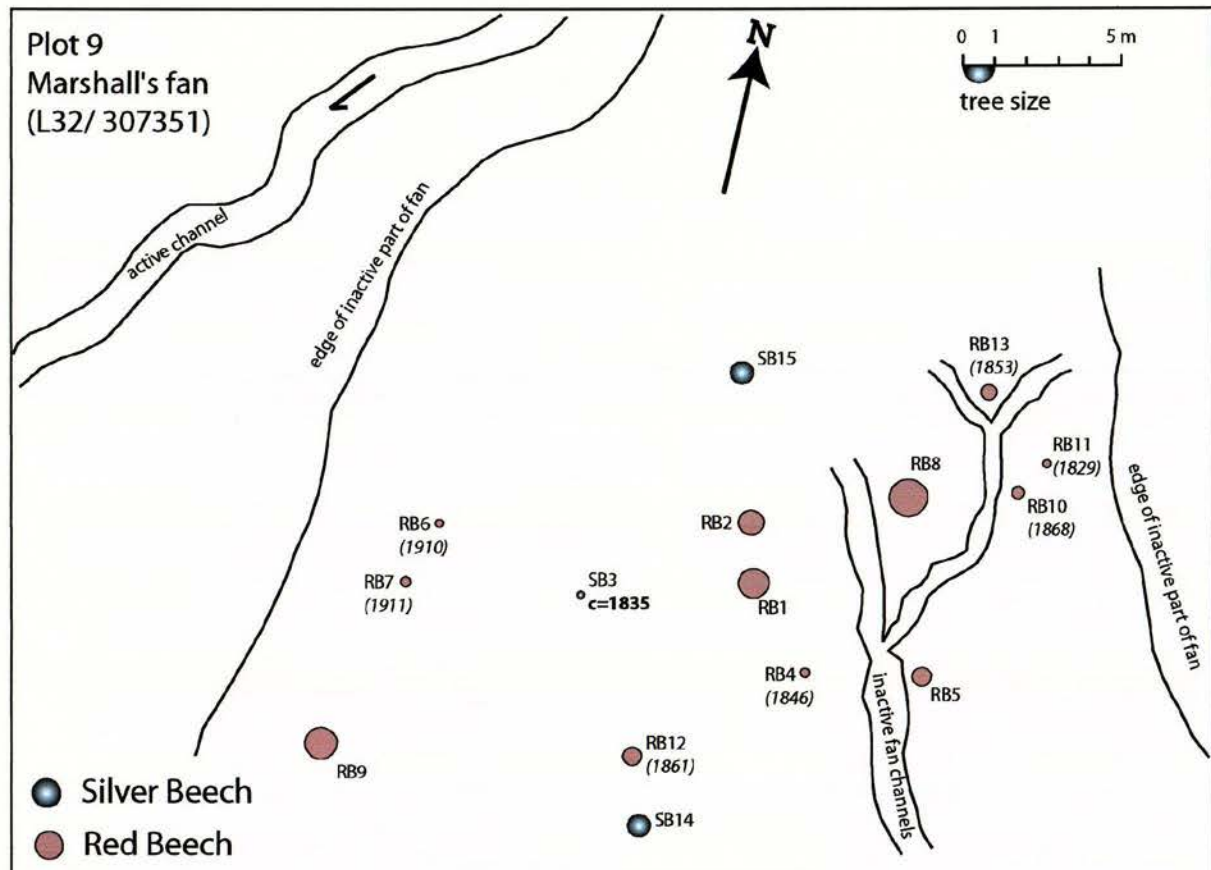


**Figure 4.18.** Sketch map of Plot 9 (roughly to scale). Trees are mapped according to their size, species and location. AD calendar ages when trees reached borer height are shown below the tree I.D.'s, e.g. c=1753 is a core that intercepted the tree centre, while ages in parentheses are 'good Arc' ages. Other minimum ages from Short cores are not shown here (see Appendix 3).

Fifteen Red and Silver Beech trees were cored at this site. In terms of size distribution these trees are possibly the most variable in size, with a bimodal preference toward 20-30 cm and 70-80 cm diameter trees (Fig. 4.19a). The mixed nature of the forest was identified in the field. The oldest dated tree at the site (SB14) has 338 rings, which provides a minimum age for the inactive part of Marshall's fan at this locality. Three larger trees remain undated, but are probably at least as old as SB14. In all, 11 of the 15 trees yielded tree ring ages. There are two clear modal peaks in the age distribution of Plot 9 trees. The younger peak (of two trees only) is at 94-95 years (rings). This peak potentially carries an 1888 earthquake signal as the regrowth of trees on the fan here is coincident with the cohort at nearby Plot 3. The larger modal peak is centred on 140-160 rings. This is a common feature of the range front fan sites that will be discussed in the next Chapter.

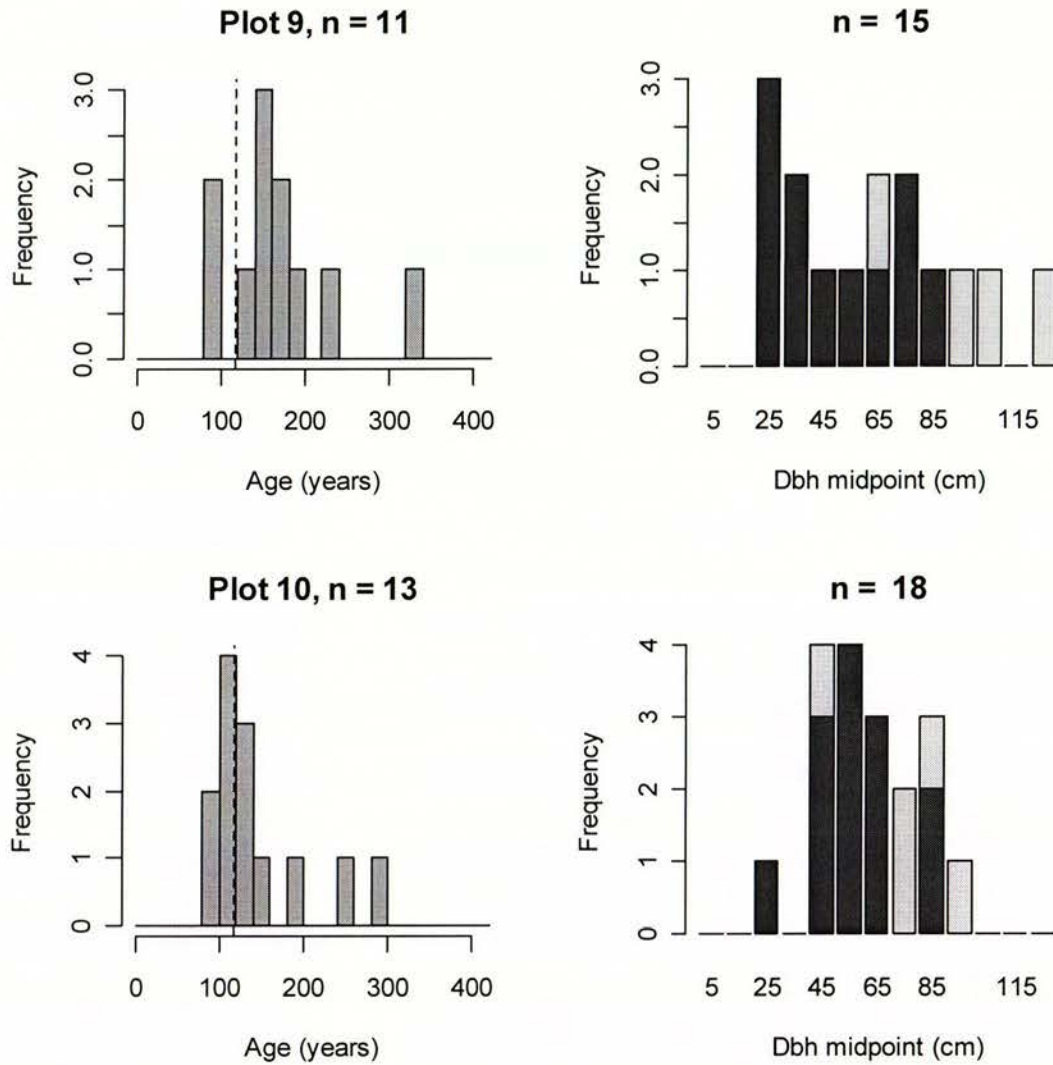


**Figure 4.19.** Age and Size structure for **A.** Plot 9 (above), and **B.** Plot 10 (below). n = the number of dated or measured trees. The dashed vertical line is placed at AD 1888.

#### 4.1.10 Plot 10

Plot 10 is situated on an alluvial terrace adjacent to the entrenched active channel of McKenzie Stream at grid reference L32/323351 (Figs. 2.1, 4.6). The terrace is flat and has no scarp even though it is c. 200 m along-strike from the scarp at Plot 6 (Fig. 4.20). A minor active channel flows at the west edge of Plot 10. This does not appear to be dextrally displaced, though there is evidence for disruption (faulting?) of a lower silt contact in the walls of the gully. The terrace surface is formed in a 1.5 m thick section of sandy silt. A soil is forming in the silt, and the minimum age on this soil based on the oldest tree at the plot is >299 rings (SB2). The soil is less well developed (in appearance) compared to that observed in the soil pit at Plot 6.

Eighteen trees were cored on this surface. There are two distinct modal size peaks amongst this date: one at 50-60 cm diameter, the other at 80-90 cm diameter (Fig. 4.19b). The age distribution from the 13 dated trees at the site shows a prominent peak centred at 102-115 years. There are not enough dated trees from this site to recognise any older peaks. If the four large undated trees had yielded ages, they would likely map out an older peak in the range 240-300 years. Interestingly, again there are no sampled trees <83 rings old, which suggests there have been no significant events at this plot throughout most or all of the 20<sup>th</sup> Century to have affected the canopy here.

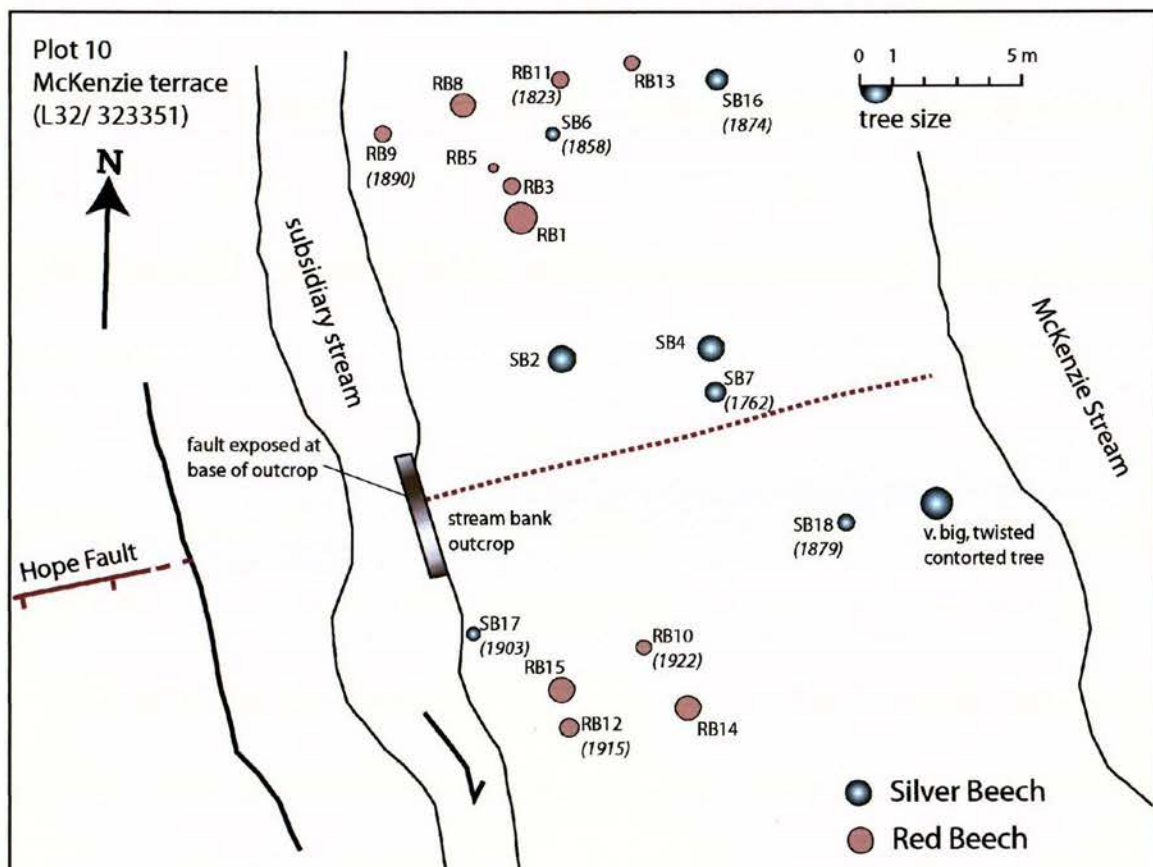


**Figure 4.20.** Sketch map of Plot 10 (roughly to scale). Trees are mapped according to their size, species and location. AD calendar ages when trees reached borer height are shown below the tree I.D.'s, i.e., ages in parentheses are 'good Arc' ages. Other minimum ages from Short cores are not shown here (see Appendix 3).

The nature of the sharp cohort peak for Plot 10 is arguably similar to that for Plot 7. The distribution is surprisingly clustered about the dashed line in Figure 4.19b, which is placed at

the time of the 1888 North Canterbury earthquake. That is, Plot 10 is clearly founded on a surface that has existed for at least 300 years. Trees have come and gone from this surface. At the time of the 1888 event, it is possible that a number of pre-existing 'bolters' took advantage of holes in the canopy to either shoot up past or beyond the average borer height. Thus, when such a young cohort peak straddles the dashed line on a stable surface, we believe that this may offer an 1888 earthquake signal at that site, e.g. Plots 7 and 10.



**Figure 4.21.** Photographs from Plot 10, McKenzie Stream. **A.** view looking at outcrop of sandy silt in exposure in subsidiary stream channel of McKenzie Stream. **B.** view to the south across the terrace surface with contorted tree RB10 in foreground.

## 4.2 Plots 11-14

Plots 11 through 14 were accessed via the eastern end of the Lake Sumner Forest Park through Glynn Wye Station. A 4-wheel drive access road on the south bank of the Hope River allows access to Hope-Kiwi Lodge (Fig. 4.22). From there, Plots 11-14 were accessed on foot using the Dept. of Conservation track that generally follows the Hope Fault, to Three Mile Stream Hut. The hut was used as a base to access Plots 12 and 13, while Plots 11 and 14 were closer to the Hope-Kiwi Lodge. Trees cored in 2002 along this part of the fault trace form part of Plot Ø (Fig. 4.22).

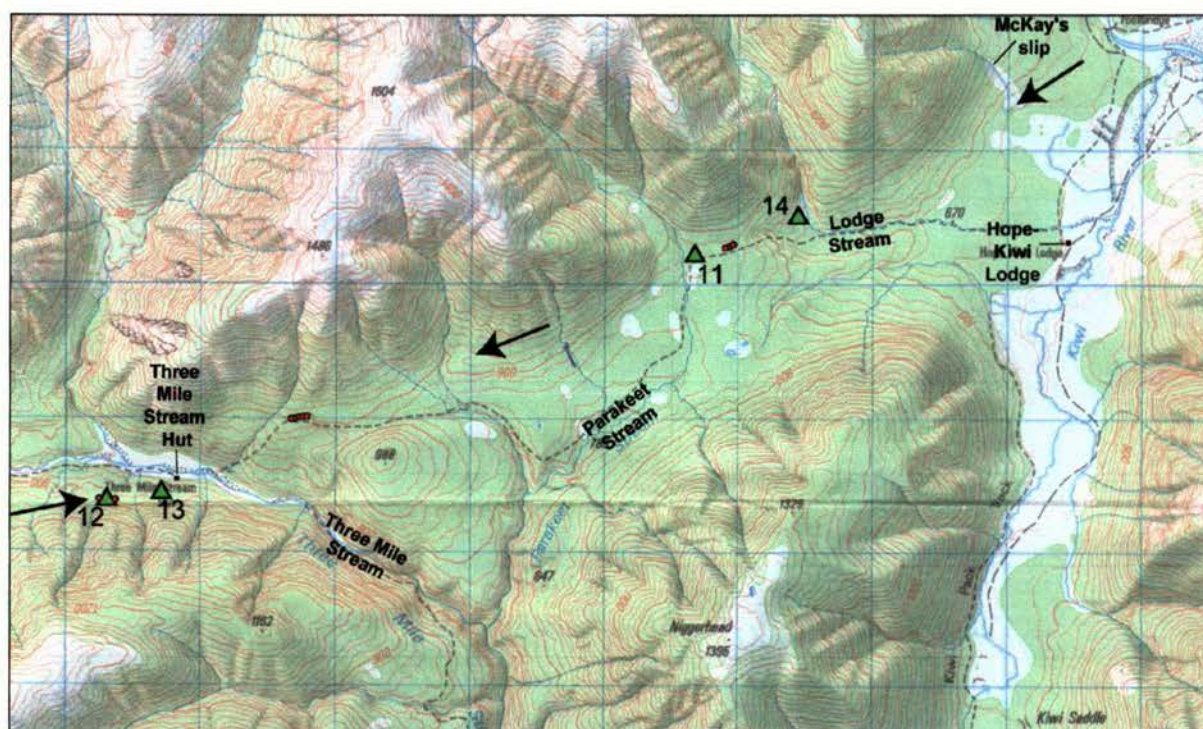


**Figure 4.22.** Location map of the four eastern tree plots (green triangles) in the study area. Trees are mapped according to their size, species and position. Red circles show the location of trees along the fault scarp cored in 2002, i.e. parts of Plot Ø. Black arrows point to distinct scarp localities along the Hope Fault, e.g. an uphill-facing scarp exists below McKay's slip (top right).

For plots 11-14, we set out to:

- (i) test the forest age structure along this portion of the Hope Fault;
- (ii) use this area as a comparison to Plots 1-10 accessed from the Lake Sumner Road and within a 2 km radius of the Hope Fault at McKenzie fan; and
- (iii) study this eastern part of the study area as it was significantly closer to the area involved in surface faulting related to the 1888 North Canterbury earthquake.

#### 4.2.1 Plot 11

Plot 11 is a fault scarp site just beyond the saddle separating Lodge Stream from Parakeet Stream at grid reference L32/448403 (Fig. 4.22). We have called this the Parakeet Saddle site, due to its location near the main branch of Parakeet Stream. Here, a steep uphill-facing scarp has formed and progressively deflected the drainage toward Parakeet Stream. One of the interesting features of this site is the predominance of Mountain Beech (*N. Solandri*) which accounts for 14 of the 17 trees sampled, and the absence of Red Beech, in keeping with this higher elevation locality (c. 865 m ASL) (Fig. 4.23).

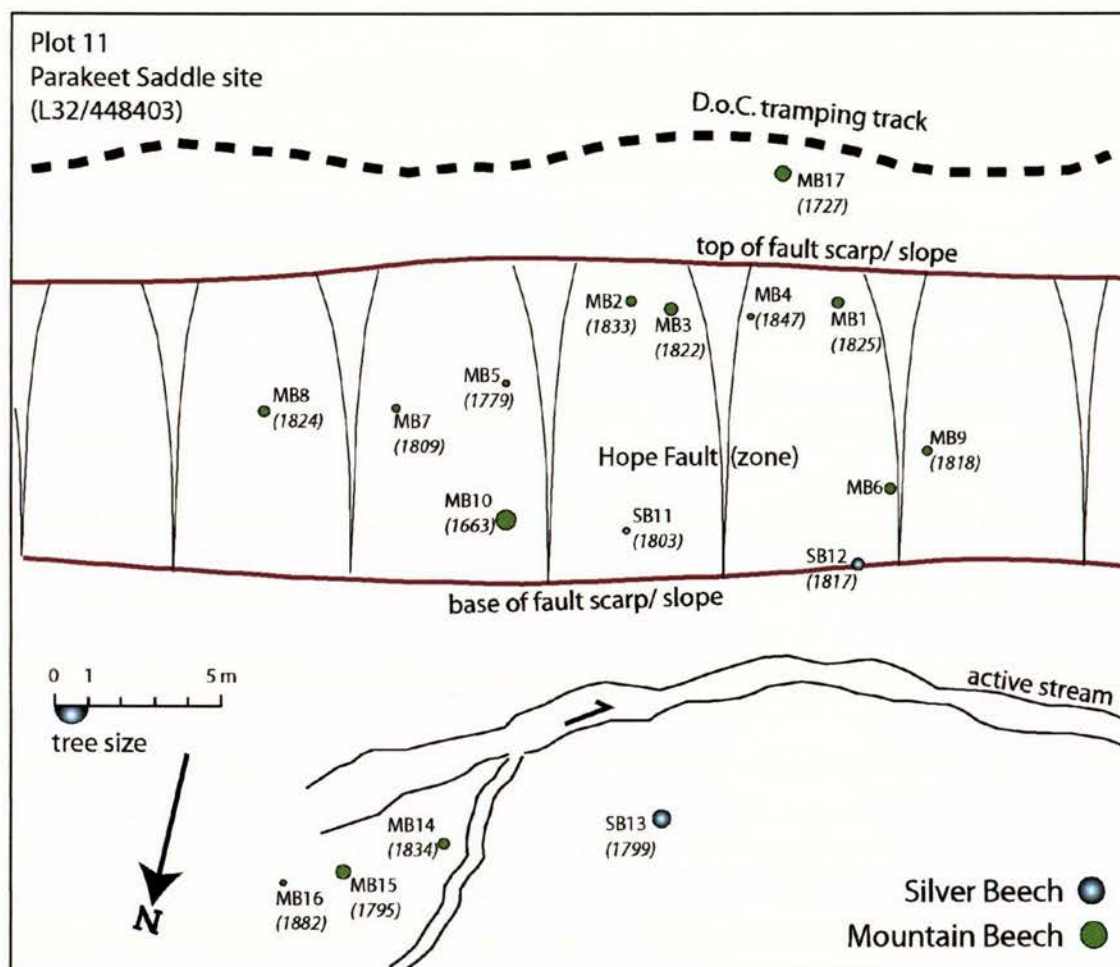


**Figure 4.23.** Sketch map of Plot 11. The site at c. 865 m ASL is dominated by Mountain Beech. Trees are mapped according to their size, species and location. AD calendar ages when trees reached borer height are shown below the tree I.D.'s, i.e., ages in parentheses are 'good Arc' ages, e.g. (1878). Other minimum ages from Short cores are not shown here (see Appendix 3).

The oldest tree ring age at the site is 342 yr (MB10). Twelve of the trees were growing directly on the broad scarp slope at Plot 11 and four others were growing opposite, near the stream banks. All 17 trees cored yielded ages (Fig. 4.24a). There was one major size mode at the site of 30-40 cm diameter. In correspondence with this mode, there was one single strong modal peak in the age distribution centred at 180-200 rings. This peak, though broad, has the form of a cohort colonisation. It is possible that due to the higher elevation or generally slower average growth rate of Mountain Beech c.f. Red or Silver Beech, that the establishment time to corer height may have been somewhat longer at this locality.

No trees that we sampled had colonised the site in the last 120 years. Therefore, even

though this plot is on the scarp of the Hope Fault and within 2-3 km of the known end of the 1888 surface rupture near Hope-Kiwi Lodge, there is no signal in the forest assemblage of a damaging event at that time.

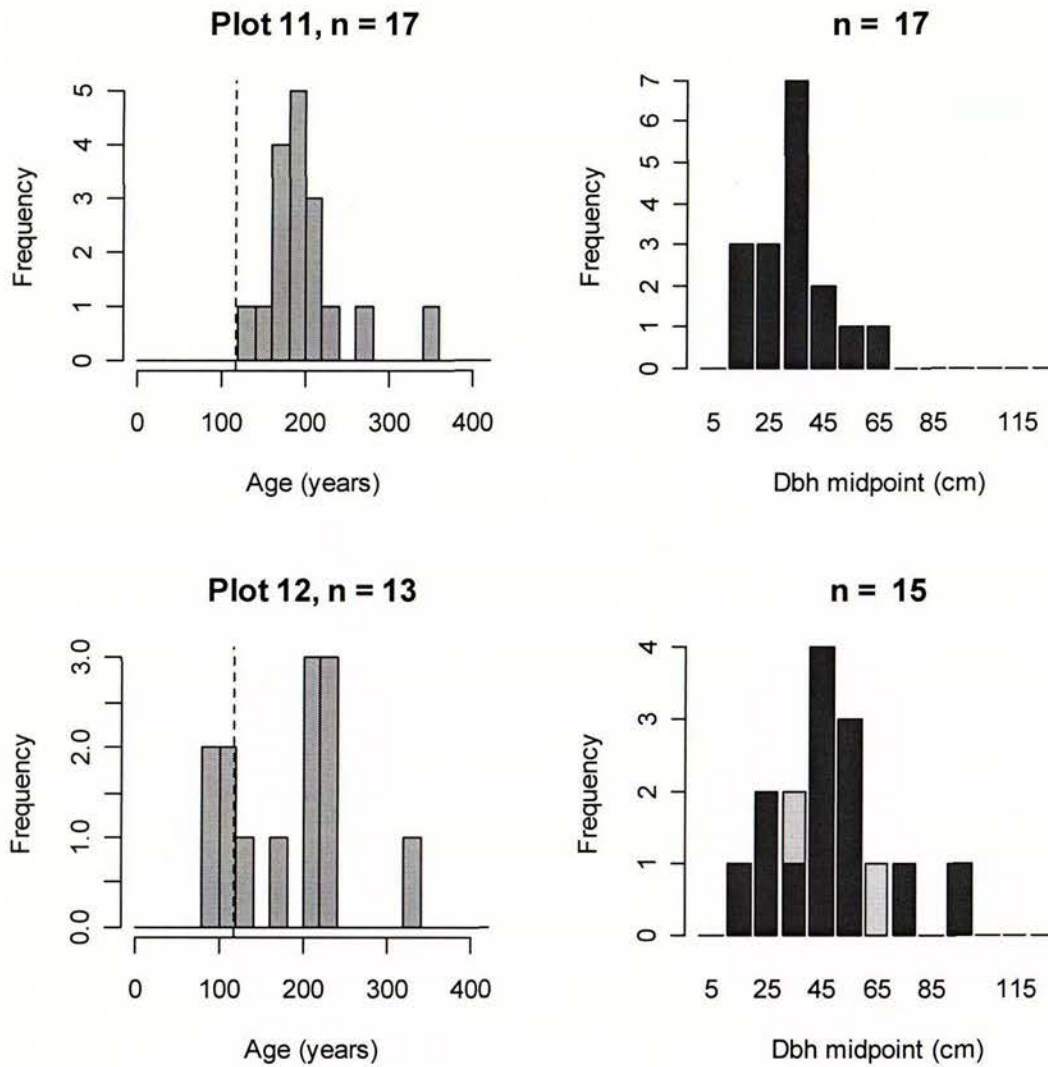


**Figure 4.24.** Age and Size structure for **A.** Plot 11 (above), and **B.** Plot 12 (below). n = the number of dated or measured trees. The dashed vertical line is placed at AD 1888.

#### 4.2.2 Plot 12

Plot 12 is known as the Fallen Beech site and was located c. 300 m west of Three Mile Stream Hut at grid reference L32/403384 (Fig. 4.22). At this site a large Red Beech (diameter c. 88 cm) had been previously growing at the toe of a rangefront scarp along the Hope Fault. The beech tree had fallen perpendicular to the scarp and an active stream about 15 m west of the tree. A thick debris flood deposit was deposited by the stream and at its eastern edge had banked up against the fallen beech tree (Fig. 4.25). Groundwater flow through the debris flow had prevented the fallen tree from decomposing.

We sampled the outside of the tree for radiocarbon dating purposes to estimate how long it was since the tree fell, but had not rotted. The "fallen beech" yielded a radiocarbon age of  $50 \pm 30$  yr BP. The calibrated age intervals for this date are AD 1690-1730, 1810-1860, 1870-1920 and 1950-1960 (Table 1). The preferred age of the tree fall will be discussed later with respect to the ages of standing trees at the plot. We also attempted to core the fallen beech in 2002 and 2005 for both a ring count of its age, and to later attempt a radiocarbon "wiggle match" experiment to more precisely date the tree's death. Our tree cores were badly oriented for the purposes of gaining a good ring count from DB1.

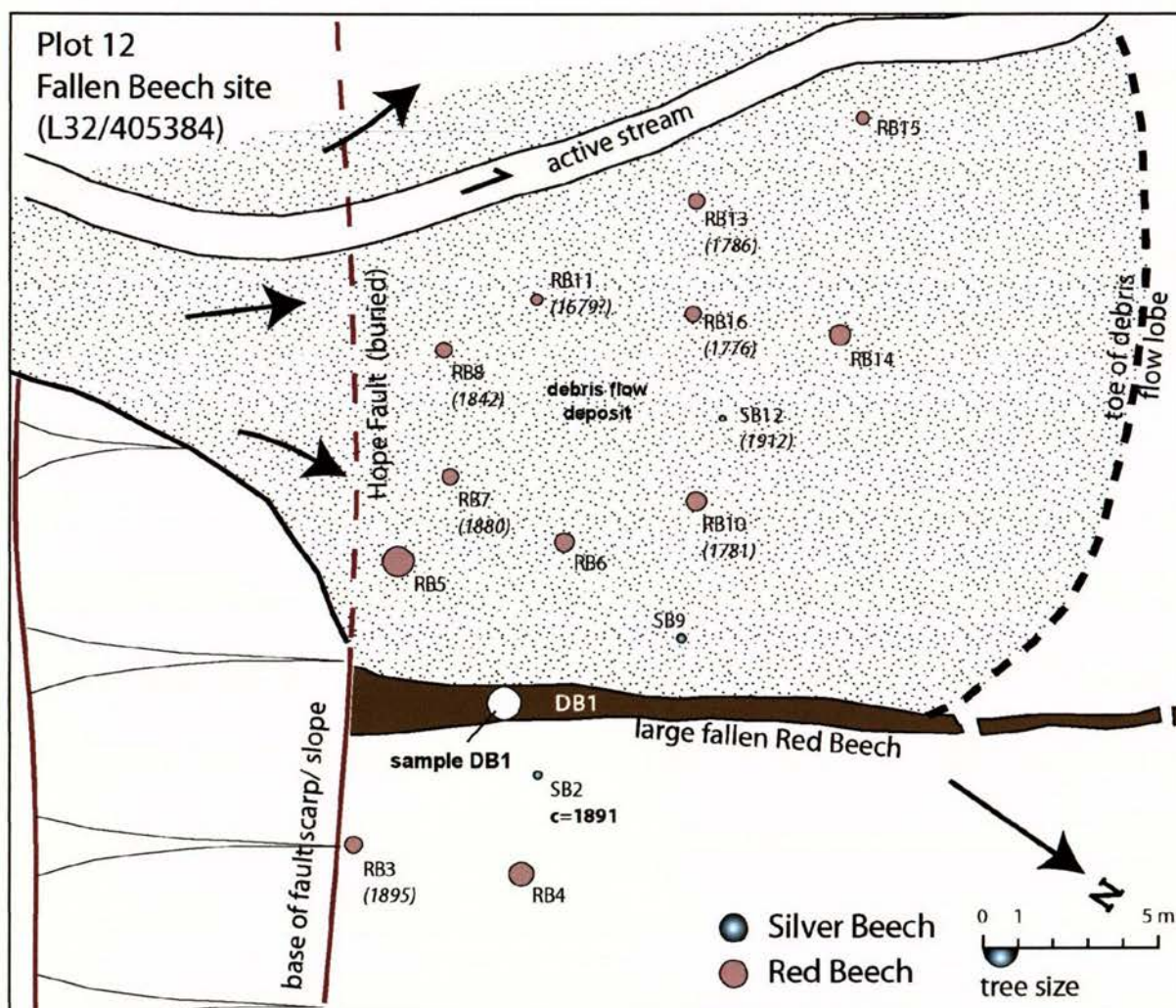


**Figure 4.25** Sketch map of Plot 12 (drawn to scale). Trees are mapped according to their size, species and location. AD calendar ages when trees reached borer height are shown below the tree I.D.'s, e.g. c=1753 is a core that intercepted the tree centre, while ages in parentheses are 'good Arc' ages, e.g. (1779). Other minimum ages from Short cores are not shown here (see Appendix 3).

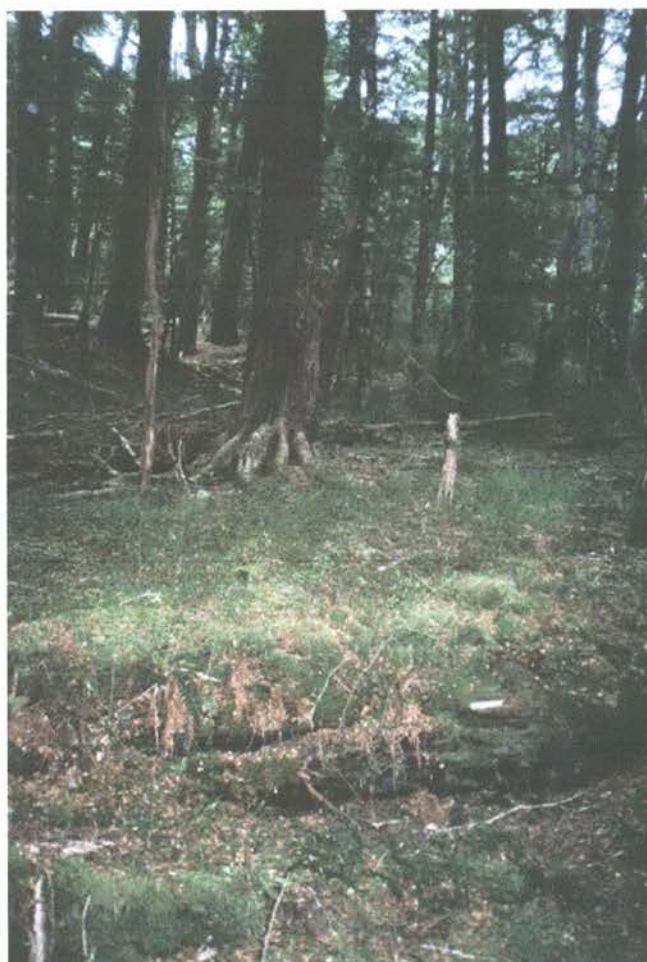


**Figure 4.26** Photograph from Plot 12. The Dead Beech (DB1) is lying in the foreground, with a debris deposit filling up the space adjacent to it. A number of trees such as RB5 (standing in midground) are useful for dating the debris fan surface.

However, a rather simpler method for obtaining a minimum age on the treefall is to core the trees living on the debris flow deposit. We sampled 15 trees at the site, 12 of which were growing on the debris deposit (Fig. 4.24b). One significant peak exists in the size population of the site, corresponding to a tree size of 40-50 cm diameter (five of the trees were between 47-52 cm diameter). This peak in size broadly corresponds to trees with an older age peak of 213-229 rings (ago).

A second, smaller modal peak of four trees covers the range 80-120 rings (actually five trees range from 93-125 rings). A minor peak in size distribution occurred at 20-30 cm diameter. This peak may postdate the 1888 earthquake event. Since c. 93 rings (yr) ago, the debris flood site at Plot 12 has remained stable, i.e. there were no young trees recognised in the understory. The canopy that had developed since the formation of the debris flood deposit must have been damaged around this time, i.e. some young trees were probably knocked down during the 1888 event. The oldest tree date at the site was from RB11. This was an estimated ring count of 326 rings, which was later discounted as inaccurate. The oldest true ring count came from RB16, with 229 rings. This is quite possibly the first tree to colonise the debris flood deposit. This tree and five others colonised the deposit between 213-229 "rings" ago (i.e.  $\geq$ AD 1776), implying that this is the window of time before which the fallen beech tree fell and the debris flood deposit was impounded behind it (Fig. 4.26). Later, we will discuss how these data argue for a large earthquake in the mid-1760's.

### 4.2.3 Plot 13

Plot 13 is a rangefront fan site adjacent to Three Mile Stream Hut at grid reference L32/407385 (Fig. 4.22). The active trace of the Hope Fault was not clear near Plot 13, but was possibly eroded, buried by fan debris, or consisted of a small scarp due to pure lateral movement. However, it was likely to be nearby, having been located at Plot 12 and at the hut toilet. The hypothetical test for Plot 13 was that this fan apron should be reactivated following a large surface-rupturing earthquake and/or there would be significant treefall/reorganisation of the forest canopy, due to extreme ground motions adjacent to the fault.

Seventeen Red and Silver Beech trees were sampled on the gently sloping apron surface in an area of roughly 150 m<sup>2</sup> centred on tree RB1 (Fig. 4.27). The size distribution at the site shows two distinct peaks in tree diameter. The larger tree size peak is at 70-80 cm. The smaller tree size peak covers the size range 30-50 cm diameter, with clusters of three trees sampled at 35-37 cm and 47-54 cm diameter (Fig. 4.28a).

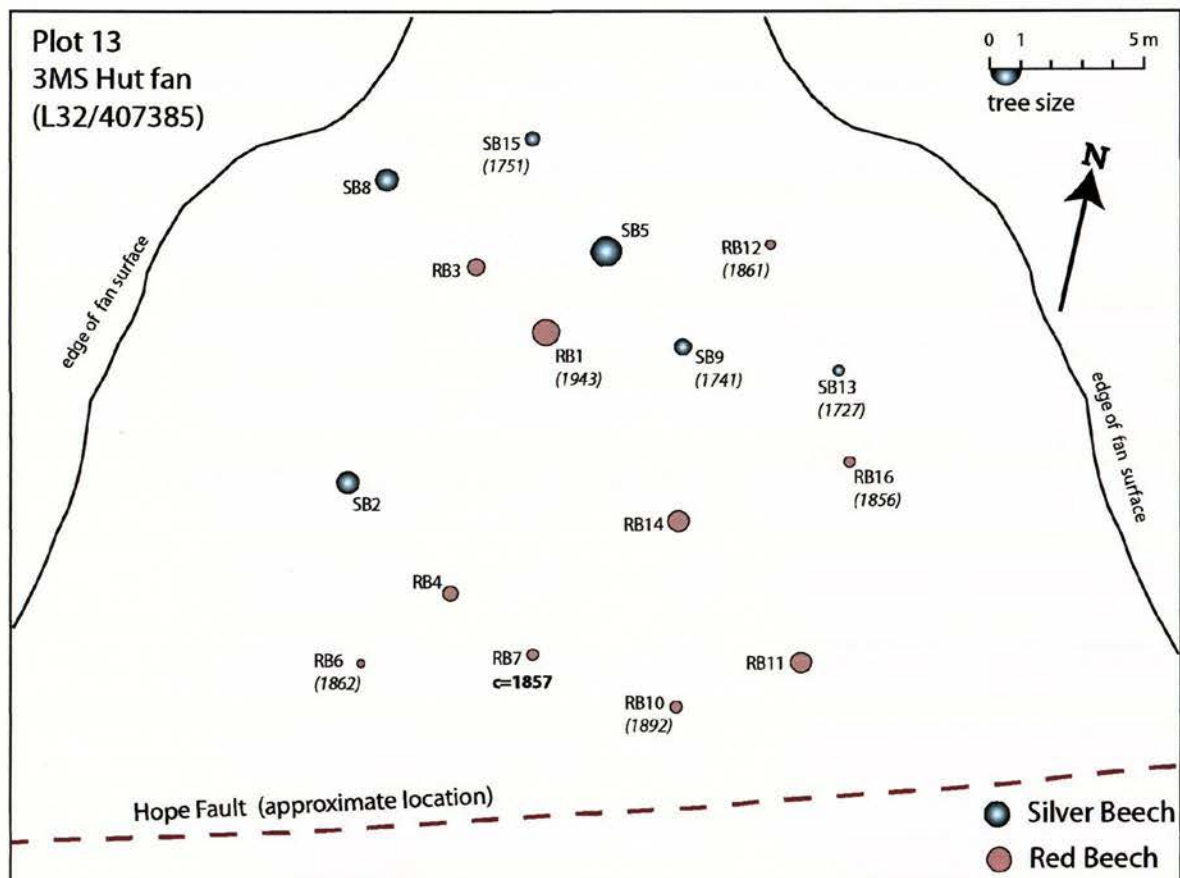


**Figure 4.27.** Sketch map of Plot 13 (roughly to scale). Trees are mapped according to their size, species and location. AD calendar ages when trees reached borer height are shown below the tree I.D.'s, e.g. c=1753 is a core that intercepted the tree centre, while ages in parentheses are 'good Arc' ages. Other minimum ages from Short cores are not shown here (see Appendix 3).

The age distribution is dominated by a modal peak at 143-149 rings. Smaller peaks of two trees exist at ages beyond 220 rings (years). Peaks of two trees depend strongly on the bi-decadal bin size used for the histogram in Figure 4.28a.

A better approach to understanding the cluster of 5 trees between 220-280 rings is to look at the age of each one. These trees have ring ages of 224, 233, 254, 264, and 278 rings (before 2005). In this case, there is no clear pattern of tree age clustering that could lead to

the designation of an event age(s).

In between the peaks in the distribution there are distinct periods of non-colonisation (stability) at Plot 13, such as the periods between 0-62, 187-224 and 278-352 rings. This record implies there have been punctuated events in the forest structure impacting a generally stable site over time.

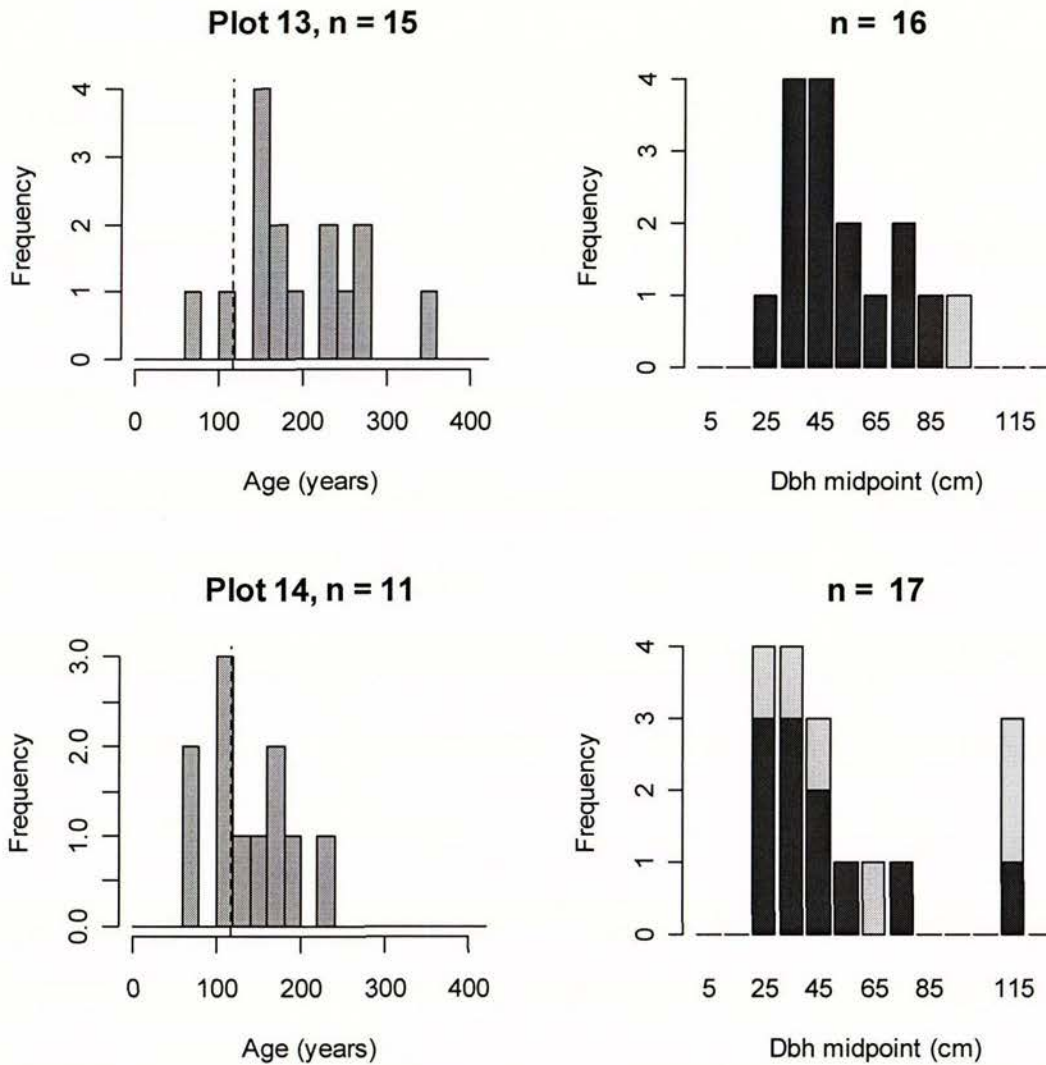


**Figure 4.28.** Age and Size structure for **A.** Plot 13 (above), and **B.** Plot 14 (below). n = the number of dated or measured trees. The dashed vertical line is placed at AD 1888.

#### 4.2.4 Plot 14

The Lodge Stream site (Plot 14) was located on a series of small remnant terraces and terrace risers adjacent to the hillslope rangefront of the Hope Fault at grid reference L32/455405 (Fig. 4.22). Lodge Stream, described in Langridge & Berryman (2005) emanates from the range and crosses the fault at this location and continues toward Hope-Kiwi Lodge. On the opposite bank, the fault trace climbs and forms a "rift zone" (uphill-facing scarp).

Plot 14 consists of a series of young, but progressively older alluvial terrace surfaces set against the rangefront of the Hope Fault at Lodge Stream (Fig. 4.29). A steep riser (R1) separates the plot from an infrequently active back channel of Lodge Stream. A point bar deposit above this back channel is covered by cobble-sized clasts with red lichen coverings. Growth of these lichen on rocks can occur within as little as c. 5 yr in a West Coast setting. The active channel of Lodge Stream is immediately east of the point bar and back channel.

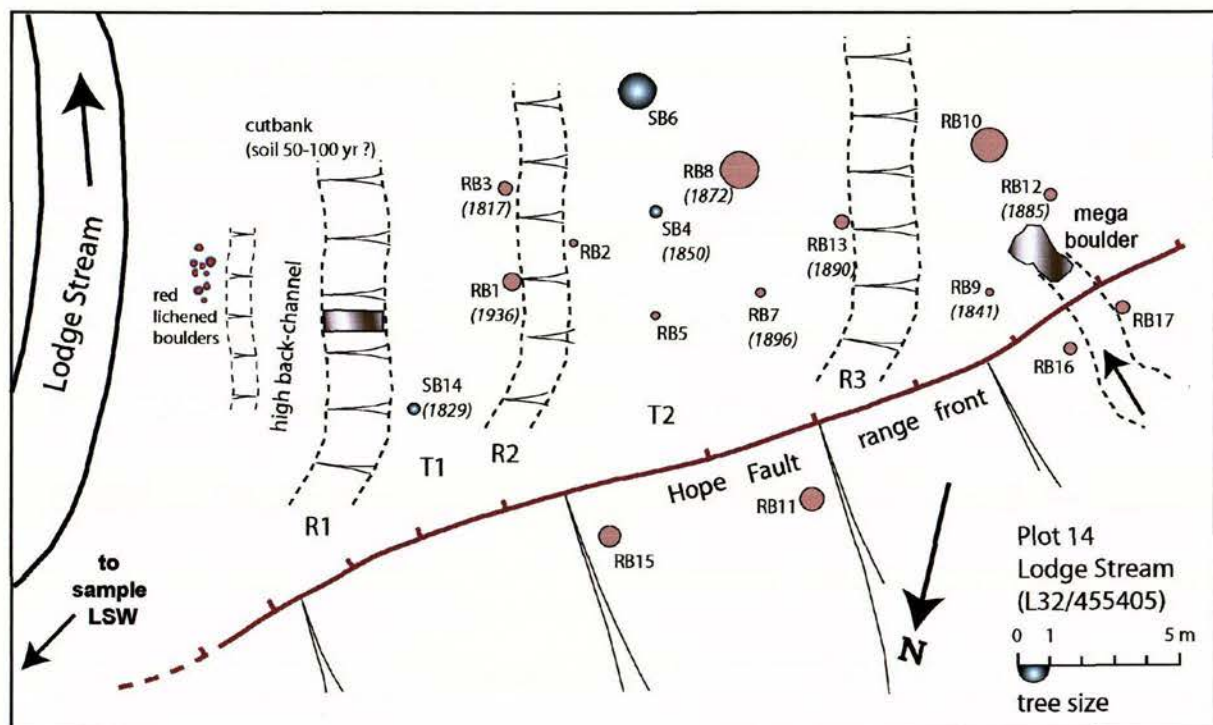


**Figure 4.29.** Sketch map of Plot 14 at Lodge Stream (roughly to scale). This site consists of a series of narrow terrace remnants and risers. Trees are mapped according to their size, species and location. AD calendar ages when trees reached borer height are shown below the tree I.D.'s, i.e. ages in parentheses are 'good Arc' ages, e.g. (1832). Other minimum ages from Short cores are not shown here (see Appendix 3).

In all, 17 trees were sampled at Plot 14. Modal peaks in size distribution occurred at 110-120 cm diameter (3 very large trees), 24-29 cm (4), 37-40 cm (4) and 43-47 cm diameter (3 trees). The age distribution of the site is also multi-modal with peaks at 65-69, 109-120 and 160-180 rings. The ages are not distributed according to the risers, terraces or hillslope, i.e. the dated trees do not directly correlate with the increasing age of surfaces from R1 through to T3, or of the age of the hillslope. However, we have been able to date the abandonment of T1 and recognise that very large but undated trees on T2 and T3 would probably be useful in dating those surfaces.

An exposure was cleared into the R1 cutbank to consider the age of the soil in the bank. From its weak development in comparison to other profiles we made an estimate of 100-200 yr of soil development only (Fig. 4.29). This is effectively an estimate of the age of T1, the c.

4 m wide terrace remnant above R1.

We sampled three trees growing on T1 of Plot 14. These trees should provide a minimum and more robust age for the abandonment of T1 and the cutting of R1, than provided by the soil profile in the stream bank. The oldest tree on T1 (RB3) had 188 rings. Terrace T1 was probably abandoned some time prior to AD 1817 (the age from RB3). Later, we will discuss what the offset age may be for the timing of that terrace abandonment and riser formation. Our estimate of soil development in the sandy silt on top of T1 is comparable to the tree age.

Two other riser/terrace pairs of similar height and width are included in Plot 14, i.e. R2/T2 and R3/T3. Surprisingly, though there were some very large undated trees on these surfaces, none of the dated trees were as old as tree RB3 on T1. The very large trees on T2 and T3 probably date to the abandonment of those surfaces. Tree SB6 is probably  $\geq 350$  years old. A very large ('van-sized') block of greywacke has fallen from the range front slope on the north side of the site onto terrace T3. This very large block had smashed downslope between RB16 and RB17, damaging both trees. Such a large block was likely mobilised during a strong shaking event. We had hoped to get good tree ages and may in future attempt to yield good tree damage ages from those trees.

The last surface from which we sampled trees at Plot 14 was the range front hillslope immediately above (north of) the flight of terraces. A minimum age of the hillslope, or perhaps stream incision against the hillslope, came from RB11 which had 224 rings.

Finally, Plot 14 may be unique in that it has 2 young trees that colonised the site as late as AD 1936 and 1940 (RB1 and RB2). It could be argued that their presence is evidence that shaking from the nearby rupture of the Poulter Fault in the 1929 Arthur's Pass earthquake was responsible for some forest clearance and alter re-colonisation of open canopy space at Plot 14.

### 4.3 Summary of the un-treated tree age dataset

In the preceding chapter we have presented site and tree data for all 14 tree plots in the study area along the Hurunui section of the Hope Fault. That data is summarised in Table 2, which presents the oldest tree age at a plot, the three most significant peaks in the dataset. Table 2 also highlights the most significant peak age at the site and the most significant tree diameter size.

It needs to be appreciated that the tree ring count data in this chapter has not undergone rigorous tests of uncertainty. Many of the ages presented in the graphs in Chapter 3, described in Chapter 4 and the data shown in Appendix 3 come from 'Short' Cores or cores with 'Bad Arcs' (see Section 5.1 for more detail). The ages from Short Cores tend to give minimum ages for trees in the study area. This probably means that many of the ages for the oldest tree at a site are likely minimum ages, i.e. the oldest tree is even older than what we could sample. In addition, much of the data spread toward younger ages for a given tree diameter (see Fig. 3.3) are caused by the inclusion of Short Core ages in the preceding chapters.

In the case of trees with Bad Arc ages, there is a considerable amount of uncertainty in the calculation of these tree ages. For these reasons the tree ages from Short and Bad Arc trees were left off the Plot maps and appear only in Appendix 3. In the next chapter the dataset will be subjected to an analysis of age uncertainty.

**Table 2.** Summary of tree colonisation peak ages at individual plots (\*un-treated data)

<i>Plot</i>	<i>Oldest tree age (AD)</i>	<i>Youngest (Y) peak ring age*</i>	<i>Intermediate (I) peak age*</i>	<i>Older (O) peak age*</i>	<i>Main peak at site (Y,I,O)</i>	<i>Major size peak at site (cm)</i>
1	≥ 1713	120-160	200-220	240-280	Y	50-60
2	≥ 1676	140-160	-	160-174	Y	40-50
3	= 1901	80-100	-	-	Y	20-30
4	≥ 1696	236-268	-	-	Y	50-60
5	≥ 1637	120-160	-	200-240	Y	30-40
6	≈ 1603	145-155	201-217	238-244	Y	60-70
7	≈ 1703	106-120	-	220-229	Y	50-60
8	≥ 1710	180-200	234-238	260-280	I	50-70
9	≈ 1667	94-95	-	140-160	O	20-30
10	≥ 1706	102-115	-	-	Y	40-60
11	= 1663	180-200	-	-	Y	30-40
12	= 1776	93-125	-	213-229	O	47-52
13	≥ 1653	143-149	220-240	260-280	Y	30-50
14	≥ 1781	60-80	109-120	160-180	I	20-40

## 5.0 UNCERTAINTY & INTERPRETATION OF TREE PLOTS

### 5.1 Uncertainty of tree ages

In Section 3.6 of this report we presented summary data for all of the trees sampled in the study (see Figs. 3.3, 3.4). The entire dataset, shown in Appendix 3, presents tree ages as exact calendar ages - for example, see the ages on each plot map (e.g. Fig. 3.1) – and does not consider the inherent uncertainties associated with many of the tree ages that are presented in Chapters 3 and 4. In this section, we present the results of the study in a different way where the uncertainty is considered and graphs shown below reflect not individual tree ages, but the likelihood that the population of trees sampled has a certain age distribution.

Measured tree cores fell into three classes: 1) those where the corer went through the centre of the tree (C=Centre); 2) those where the corer went close to the centre and arcs of tree rings near the centre were visible (A=Arcs); or 3) those that were either too short or too distant from the centre to determine a good age (S=Short). For Centre cores there is effectively no uncertainty in the estimated age at coring height because all rings were visible and could be counted. Therefore, these cores give the true tree age.

For Arc cores, the number of missing rings can be estimated by:

- a) using the curvature of the visible rings to estimate the distance from the core to the pith of the tree; and
- b) estimating the width of the missing rings (growth rate) near the centre and using the distance to the pith and growth rate to determine the number of missing rings (see Duncan, 1989). For Arc cores there is uncertainty in age estimates due to uncertainties associated with estimating the distance to the pith and growth rate in the missing portion. Moreover, these uncertainties are likely to be greater the larger the missing portion to be estimated. We aim to incorporate these uncertainties into our results.

The greatest source of uncertainty in age estimates for Arc cores is estimating the growth rate, as this can be highly variable among trees and within the same core. Growth rate near the pith of the tree can be very different from the growth rate further out if the conditions the tree was growing under change (due to overtopping neighbours, death of adjacent trees, suppression from neighbours etc)<sup>1</sup>.

For Short cores there are two major sources of uncertainty: estimating the distance to the pith and estimating the growth rate. Because both of these sources of uncertainty are likely to be important, and because we can't quantify the uncertainty associated with estimating distance to the pith, we did not use these cores in developing the age distributions in this chapter.

We used the following approach to incorporate uncertainty in growth rates into our age estimates for arc cores. First, for each arc core we estimated the distance to the pith based on the curvature of the rings (Duncan 1989). Second, for each species we compiled all the estimates of growth rate close to the tree centre (based on measurements of the 20

<sup>1</sup> Other variables that might affect growth rate across the study area are elevation, soil development, and local environmental (sun, rain, aspect, groundwater) conditions etc. These are not dealt with in this discussion.

innermost rings taken from each core). Given that we don't know the actual growth rate of a given core in the missing portion, and that growth rates are highly variable among trees and within a core, we assumed that the missing growth rate could take any value drawn from the

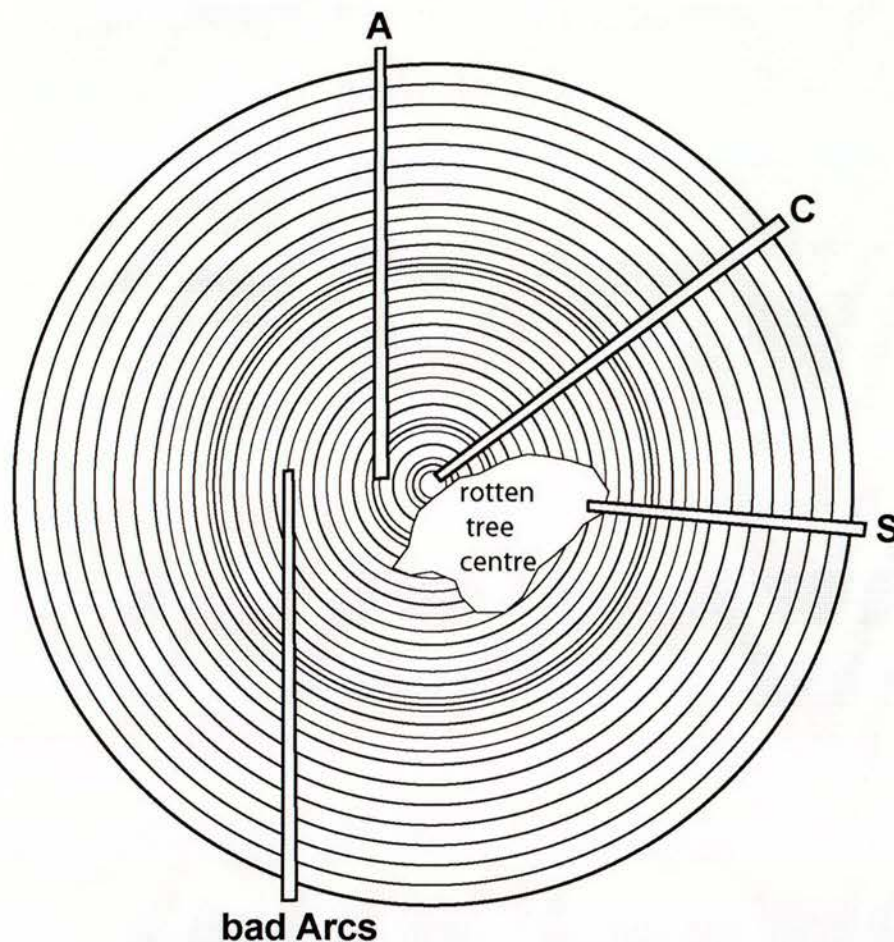


**Figure 5.1.** A consideration of uncertainty of tree age calculated from tree cores. C refers to a core that intercepted the centre; A has good arcs near the centre where the tree age can be estimated; S is too short to estimate the tree age well, due to encountering rotten heart wood; and bad Arcs refer to a poorly directed tree core where the ring curvature and distance to pith are too great.

distribution of actual growth rates compiled for a species. We obtained a distribution of the likely age of a tree with an Arc core by drawing at random and with replacement 10,000 values from the observed growth rate distribution and calculating 10,000 tree ages from those values. For trees with cores close to the pith, this distribution is tightly clustered as few missing rings need to be estimated. For trees further from the pith, the distribution is wider, reflecting greater uncertainty in the number of missing rings associated with the variation in growth rates.

For each tree, we normalised this distribution of ages (with Centre core trees having a value of 1 at the counted age) and then summed the normalised values to obtain a distribution of ages incorporating uncertainty in the age estimates.

## 5.2 Summary of tree core data incorporating uncertainty

The new distribution of all tree ages, taking uncertainty into consideration is shown in Figure 5.2a. Figure 5.2 also includes the 'untreated' graph of Figure 3.4a as a comparison. The general observation through comparison of the two graphs is that they are structurally similar, with multiple peaks at approximately the same tree ages. In detail, there are subtle differences that should be discussed. First, the new graph (Fig. 5.2a) utilises a bin size of 10 years, as opposed to 20 years, and with the bin centred on an odd number. This can have a surprising effect in terms of peak size and distribution.

Second, it is immediately clear that much of the data has been lost through our analysis of uncertainty. Of 207 trees that yielded ages in Chapter 3 and used throughout Chapter 4, only 144 of 207 of these trees (70 %) were Centre or Arc cores. In this 'Monte Carlo' style treatment of uncertainty, individual tree identities are lost. Therefore, it is impossible to see exactly where this 30 % of undatable trees come from, though it is likely that there is a falloff and spread in peak size for trees >200 yr. This means that many of those trees that were shown as older than 220 yr in Figure 5.2b were probably even older, as they can probably be viewed as minimum ages (i.e., many are from Short cores).

Third, as mentioned above, a similar set of peak ages comes out of the dataset. As the older peaks at 200-240 yr in Fig 5.2b have diminished, the relative frequency (height) of younger peaks has grown. In summary, there are only five peaks of note in the treated dataset. These are:

1. the peak centred at 85 years (rings), i.e. a range of 80-90 annular rings. This age is equivalent to an age to corer height of c. AD 1915-1925. This peak is sandwiched between two historical earthquakes of AD 1929 and 1888. The peak is certainly older than the Arthur's Pass earthquake of 1929. If this peak is related to a large earthquake event, it is more likely to represent an c. 32 yr setback from the 1888 earthquake, i.e. the peak time to corer height after the event is c. 32 yr. This issue will be discussed with respect to Plot 3 below in Chapter 5.
2. the shoulder peak centred at 105 yr which gives an age at corer height of AD 1900. This peak is also close in age to the timing of the 1888 event. The relevance of this peak with respect to that earthquake will be discussed below.
3. The most prominent peak in the dataset occurs from c. 130-150 rings (formerly 140-160 rings in Fig. 5.2b). This sharp peak implies a tree core date to corer height of AD 1855-1875<sup>2</sup>. Based on an estimated 10-30 yr time to corer height, this suggests that the event that caused this peak was historic, e.g. post-1840, or immediately pre-historical.
4. A minor peak centred at 185 rings to corer height, yielding a date to sample height of c. AD 1820. This peak is small but distinct, though not apparent in the 20 year binned plot of Fig. 5.2b. If this peak has a significant cause, e.g. seismic shaking, then it is a pre-historical event that occurred sometime near c. AD 1800.
5. A similar sized peak is centred at c. 235 rings to sample height, yielding a date to sample height of c. AD 1770. This peak is small but distinct and is apparent in the 20 yr binned plot of Fig. 5.2b. As is the case the previous peak, if this peak has a significant local to regional cause, e.g. seismic shaking, then it is a pre-historical event. The significance of this peak will be discussed below in relation to Plot 12.

<sup>2</sup> The tree core ages yielded are described as 'to borer height' ages, as the tree must have already reached the borer height for our sampler to core them.

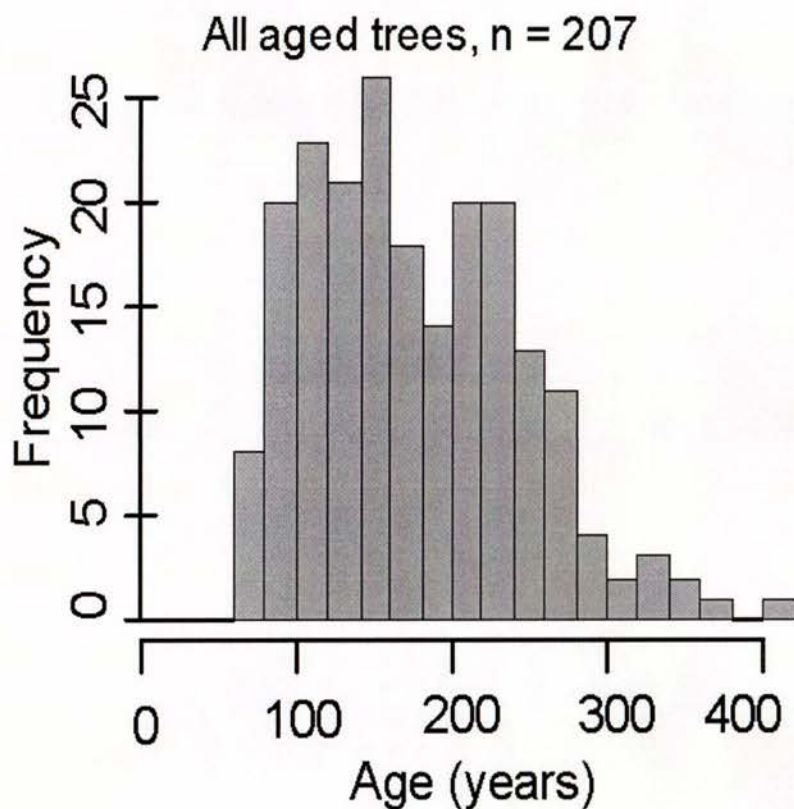
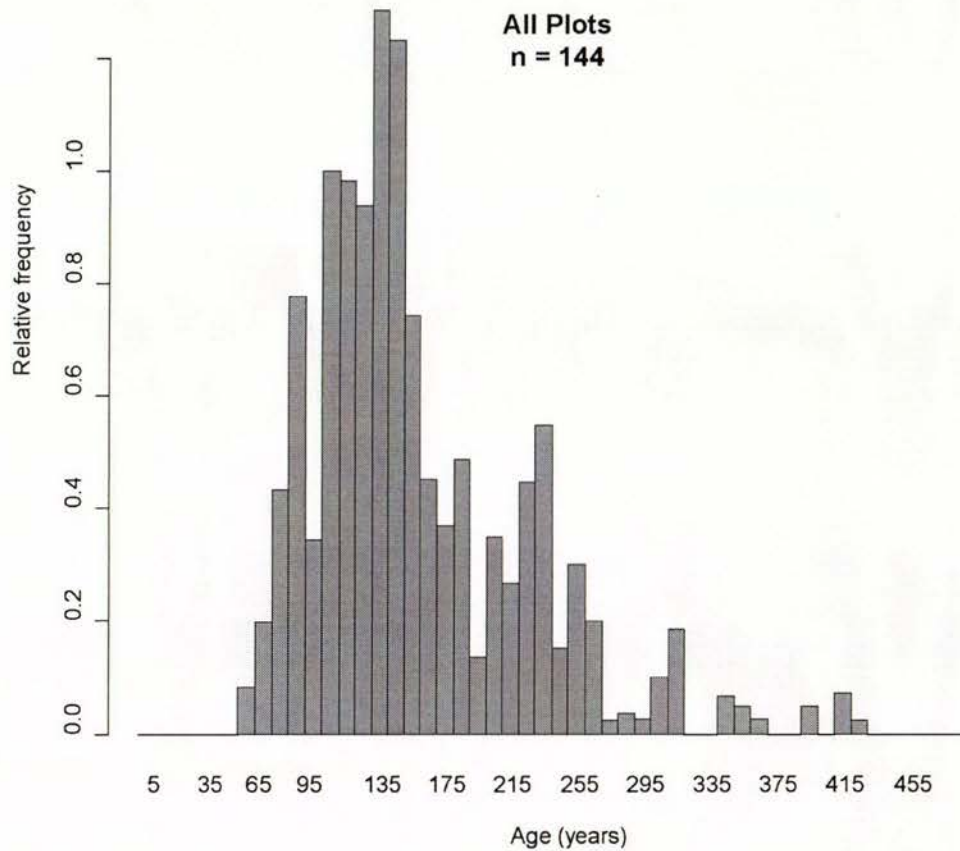


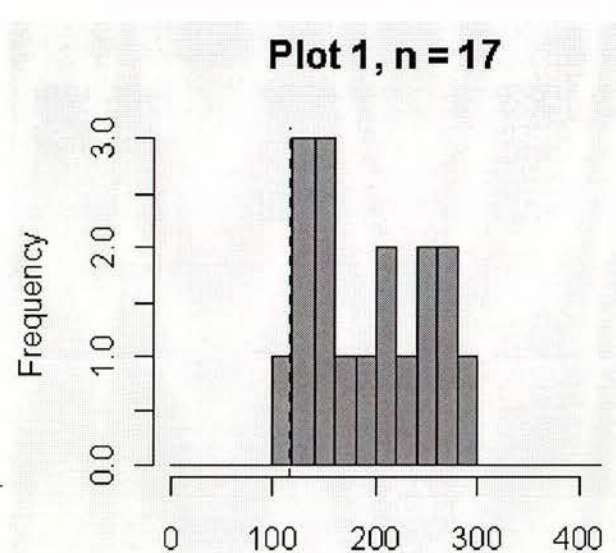
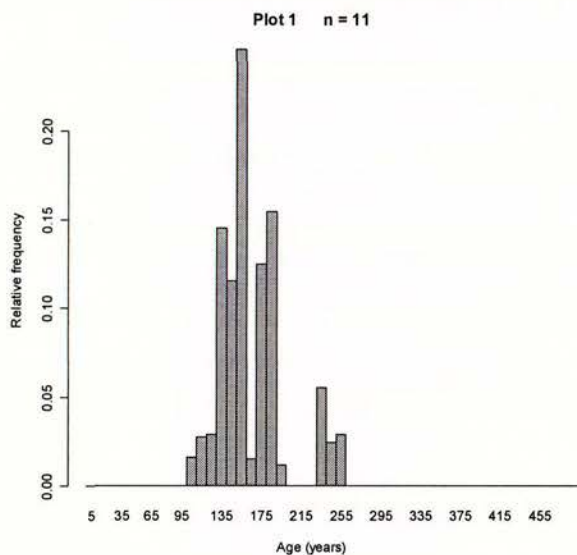
**Figure 5.2.** Histograms of age and size structure for all trees in the study. **A.** Decadal age structure for trees that were cored to their Centres or the had 'Good' Arcs. An uncertainty analysis has been applied to this set of  $n = 144$  cores. **B.** Bi-decadal age structure for all  $n = 207$  dated trees (as shown in Figure 3.4a), with no analysis of tree age uncertainty applied.

### 5.3 Incorporating uncertainty at the Plot level

In this section we will briefly discuss the effects of including the uncertainty of tree ages at the plot level. That is, we will compare the position and magnitude (frequency) of tree age peaks in the uncertainty treated and un-treated situations at each plot. In each case we will describe the peak distributions in the uncertainty-treated histograms first with the peak's age at corer height followed in brackets. Then we will compare the treated with the untreated peaks. The comparative histograms for the treated and untreated cases are presented side by side after a brief discussion of each plot below. For individual plots, we probably learn as much from the trees that were eliminated from the dataset due to uncertainty (cores too short, cores poorly directed), as those that remain. That is, a significant number of Short core trees must have been older than suggested by the 'untreated' dataset. The uncertainty treatment reduces the total number of dated trees from  $n=207$  to 144 (Fig. 5.2). Therefore, about 50 % of the tree data is lost from some plots, in which case the number of uncertainty-dated trees that remain is considerably diminished in less meaning. In reality, at the individual plot level, only the major peak is likely to have any significance, that being the most significant signal of forest change at any given plot.

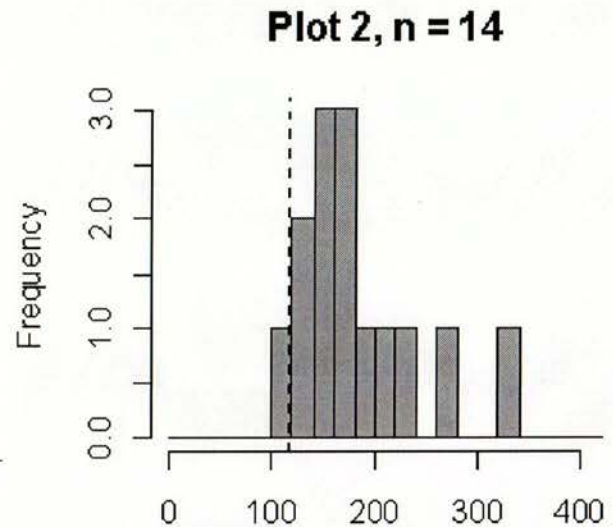
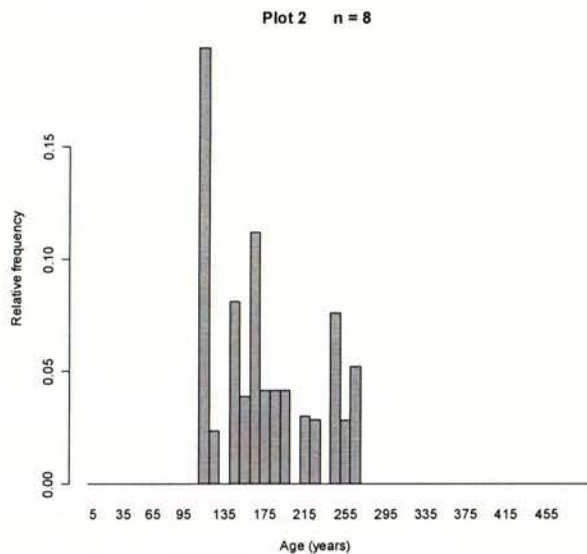
#### 5.3.1 Uncertainty-treated Plots 1-3

Plots 1-3 are the three westernmost plots in the study area. By applying the uncertainty process, Plot 1 (the Pilot scarp site; Fig. 3.1) lost 6 of its 17 'dated' trees. Plot 1 has a major peak at  $155 \pm 5$  rings (AD 1845-1855) (Table 2). There is an intermediate-sized, shoulder peak at  $135 \pm 5$  rings (AD 1865-1875). There is a second intermediate-sized peak at  $185 \pm 5$  rings (AD 1815-1825). A single tree (RB9) probably contributes to a minor peak at 230-240 yr (AD 1765-1775). This tree must be a remnant from an older forest or event. Four of the six trees that were dropped appear to have been older trees, possibly in the range 260-280 years.

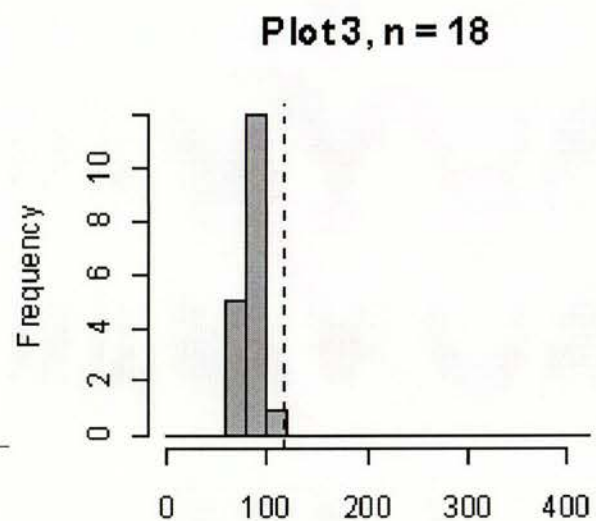
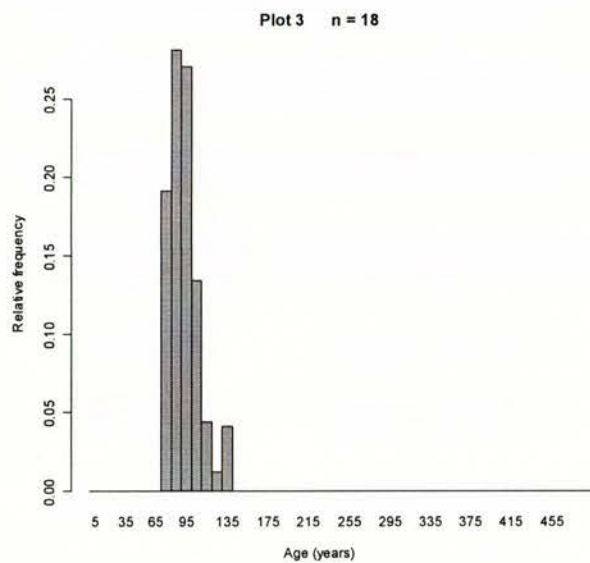


Plot 2 is the Landslip Stream toe site. The plot lost 6 of its 14 'dated' trees as a consequence of the uncertainty treatment (see histograms below). This loss of data has a radical effect on the peak distribution at Plot 2. The plot has its major peak at  $115 \pm 5$  rings (AD 1885-1895). There is an intermediate-sized, peak at  $165 \pm 5$  rings (AD 1835-1845). There is a smaller intermediate-sized peak at  $145 \pm 5$  rings (AD 1855-1865). A single tree (SB1) probably contributes to a minor peak at 240-250 yr (AD 1755-1765). This tree probably represents a single older, well characterised tree age. The new peak distributions do not entirely reflect

the size and probable age distribution of trees that we sampled at the site (Fig. 4.2). While the 2 oldest trees were probably eliminated from the 'untreated' population, so were 4 trees of probable age  $\geq 140-180$  rings. The major peak is probably reflective of our ability to hit Centre on smaller, younger trees.

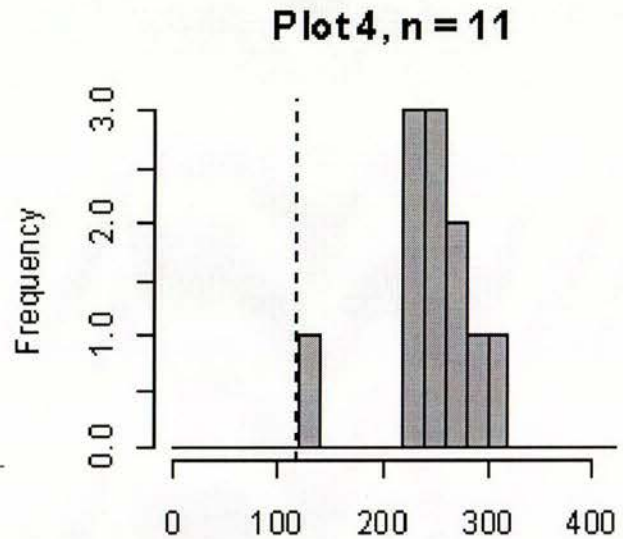
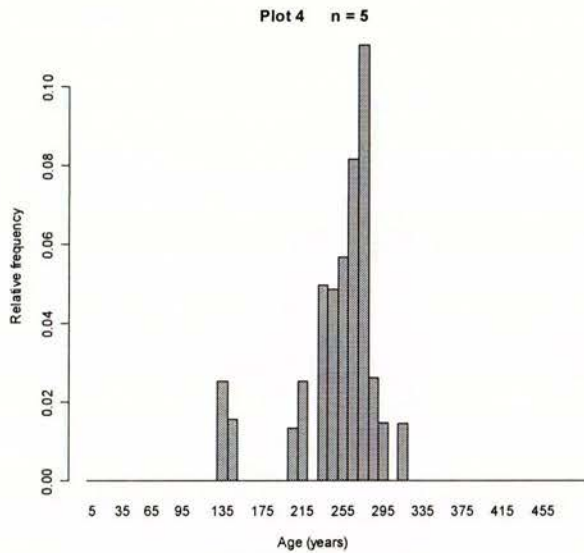


Plot 3 is the 1888 Rockslide site (Fig. 4.4). After the uncertainty process no trees were eliminated from the 'untreated' dataset of Plot 3 (18 of 18 trees). Predictably, Plot 3 has a major b-decadal peak at 80-100 rings (AD 1905-1925). It is difficult to break this peak into a distinct 10 yr peak as the probabilities in each are virtually identical. In addition, it is quite unlikely that any trees existed there (at corer height) before 110 rings ago (AD 1895). Clearly, this tree plot consists only of young trees of similar age. As described, we believe that this cohort of trees grew on a rockslide deposit that formed as a result of the 1888 North Canterbury earthquake. The peak is somewhat younger than expected cf. Figure 4.5, with a spike in trees reaching corer height 17-27 years after the 1888 earthquake.

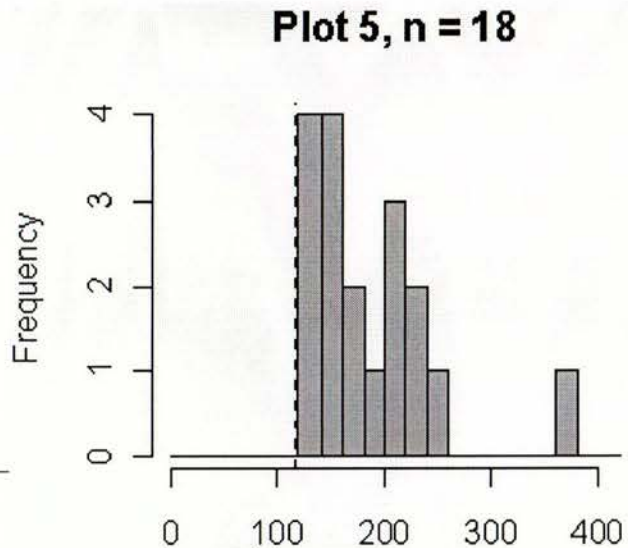
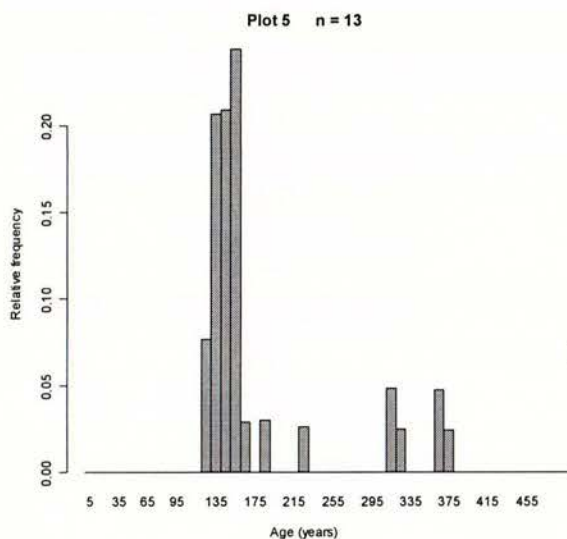


### 5.3.2 Uncertainty-treated Plots 4-6

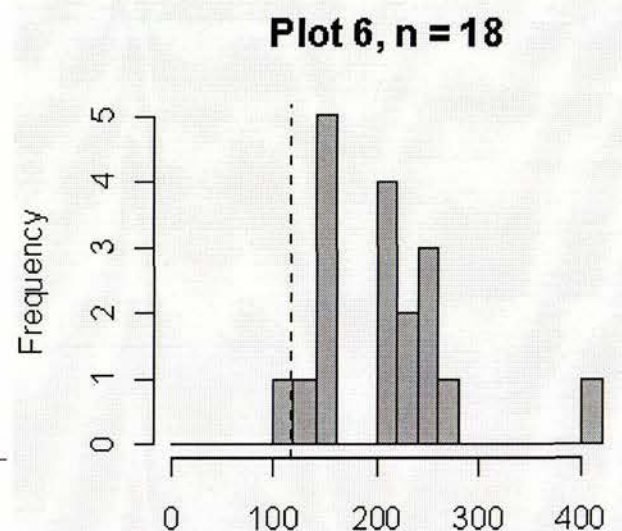
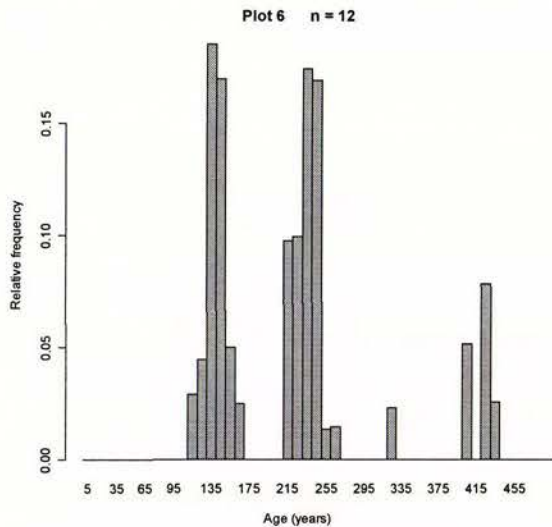
Plot 4 is Richard's fan site (Fig. 4.7). The data from Plot 4 was decimated by the uncertainty treatment with only 5 of 11 trees remaining with Centre of Arc tree ring distributions. The major peak in the treated Plot 4 dataset is at 270-280 rings (AD 1735-1745). It is apparent that the six trees lost from Figure 4.5 were either  $\geq 280$  rings or  $\geq 220-260$  rings. This site was located high on the range front above the fault trace on a fan. Clearly, this part of the fan had not been seriously rejuvenated or disturbed for over 200 years. This fact opens up the possibility that there may be a signal in specific parts of the study area from the last Alpine Fault earthquake, which occurred at c. AD 1717.



Plot 5 is the West McKenzie scarp site (Fig. 4.8). In the uncertainty-treated histogram, Plot 5 lost 5 of 13 trees from the un-treated dataset (see histograms below). Those 5 trees appear to have been lost from the 200-240 year part of the un-treated histogram, and were probably therefore, older than this. The major peak in the treated dataset occurs at 150-160 rings (AD 1835-1845). There may be a secondary shoulder peak at 130-140 rings (AD 1855-1865). There are no other significant peaks in the uncertainty-treated dataset for Plot 5.

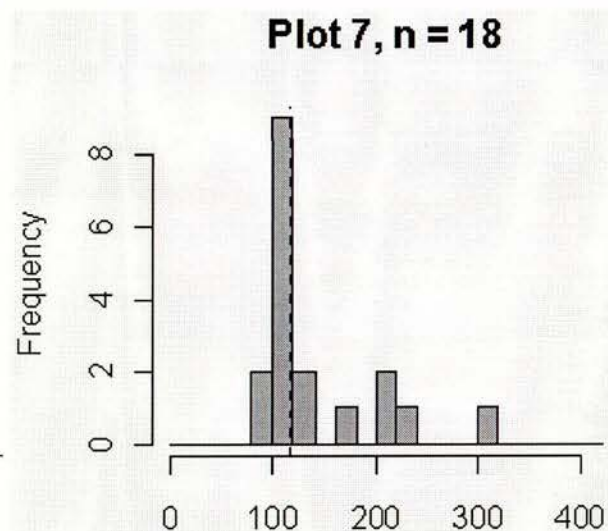
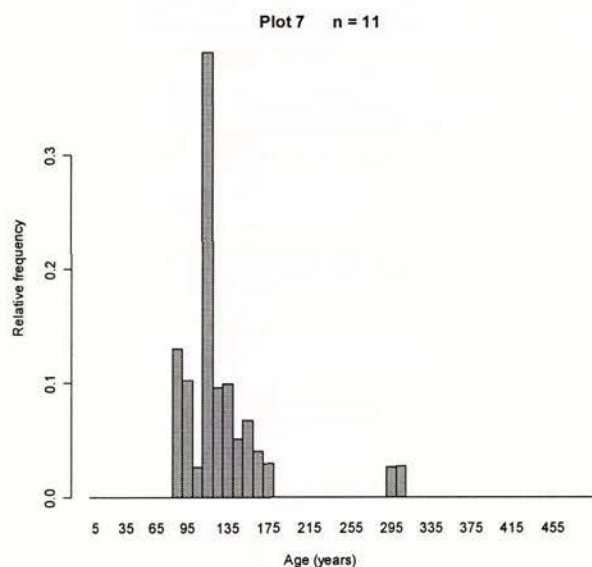


Plot 6 is the McKenzie Central scarp site (Fig. 4.11). In the uncertainty-treated histogram, Plot 6 lost one third of its dated trees (6 of 18) from the un-treated dataset. Most of those trees appear to have been lost from the 200-280 year part of the un-treated histogram and were probably therefore, older than suggested by the initial core ages shown in Chapter 4. Two intermediate-sized probability peaks occur at 130-150 rings (AD 1855-1875) and at 230-250 rings (AD 1755-1775). These peak positions somewhat mimic the distributions observed in the un-treated dataset (Fig. 4.10).

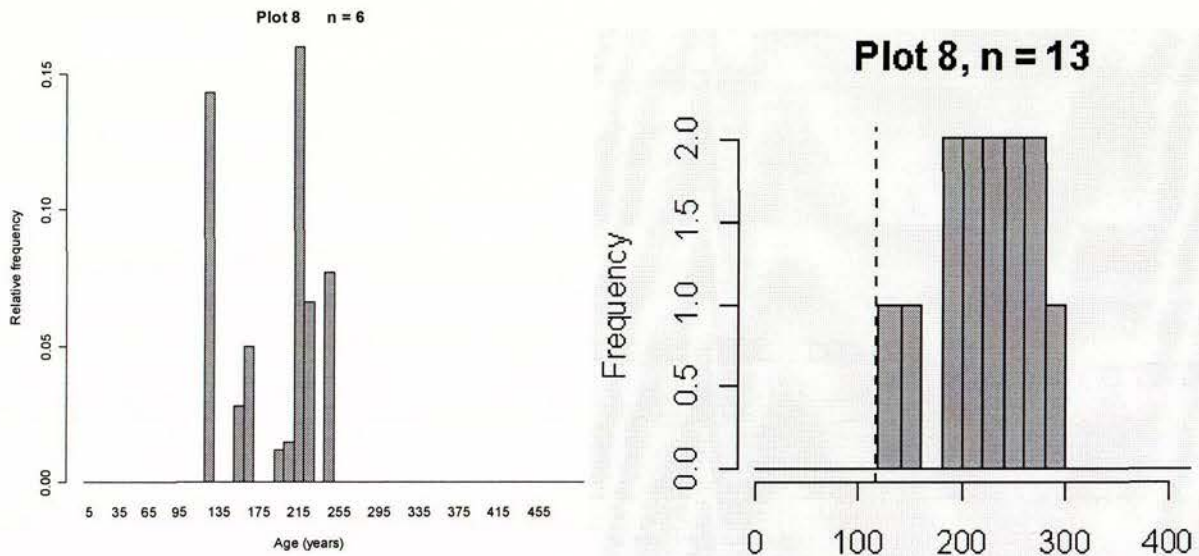


### 5.3.3 Uncertainty-treated Plots 7-10

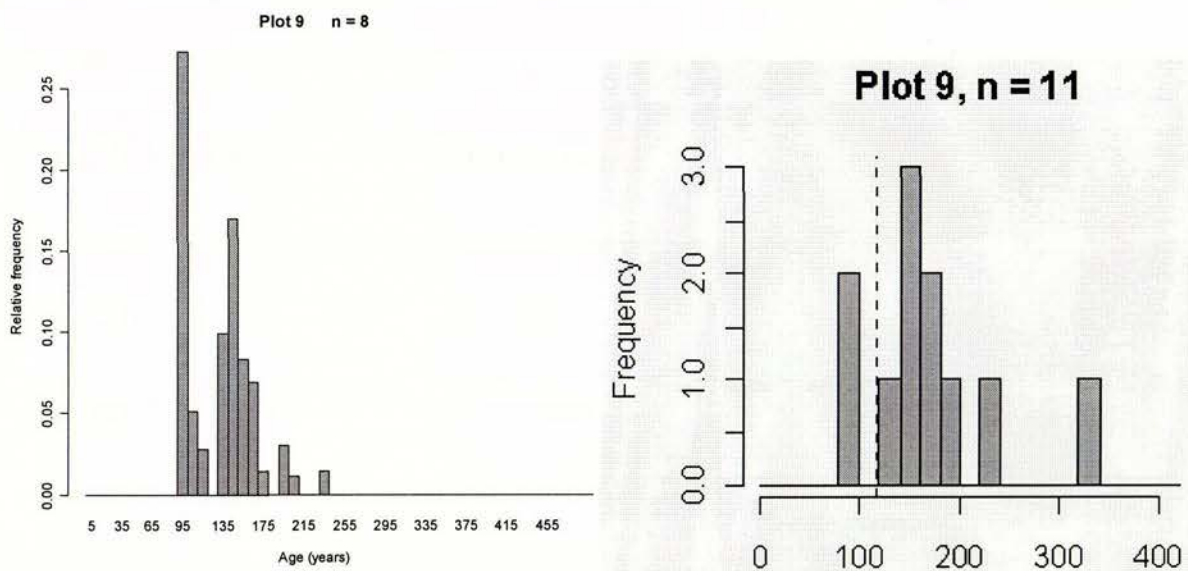
Plots 7-10 are all clustered in the McKenzie Stream and McKenzie fan area. In the case of Plot 7 (Peter's fan; Fig. 4.13), the treated and un-treated distributions are quite similar, despite the fact that 7 of 18 tree ages were eliminated after the uncertainty treatment (see histograms below). The major peak for Plot 7 still occurs at c. 110-120 rings (AD 1885-1895). A shoulder peak of younger tree age distribution occurs at 80-90 rings (AD 1915-1925). Clearly, there has been at least one young shaking and/or sedimentation event at this fan during the last c. 150 years or less. This fan may have been rejuvenated by sediment released as a consequence of the 1888 earthquake. Trees at this site may have been damaged or removed as a result of the consequent sediment influx.



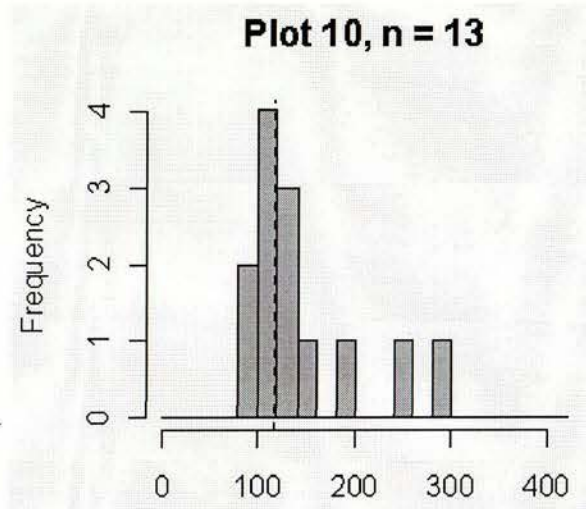
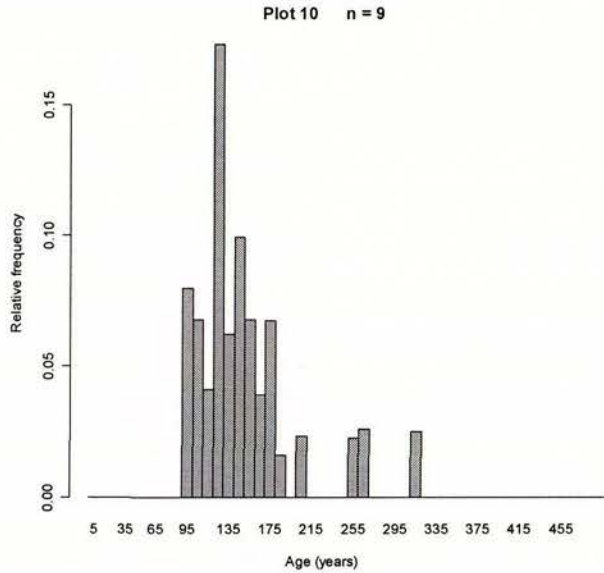
The dataset for Plot 8, the East McKenzie scarp site (Fig. 4.16), was severely reduced by the uncertainty treatment with only 6 of 13 trees remaining with Centre or Arc tree ring distributions. At Plot 8 one of the most dramatic differences between the treated and untreated datasets can be observed. In Figure 4.15, Plot 8 shows 5 consecutive 20 yr bins with 2 trees in each bar of the histogram. This is an even, unpunctuated distribution. After the uncertainty treatment there are two intermediate-sized peaks at 210-220 rings (AD 1785-1795) and at  $125 \pm 5$  rings (AD 1875-1885). A minor peak exists at  $245 \pm 5$  rings (AD 1755-1765). This probably represents a good age on one older tree. Considering that we originally cored 15 trees at this site, a single tree age is probably meaningless.



At Plot 9, Marshall's fan site (Fig. 4.18), eight of the original 11 trees that yielded ages were of Centre or Arc quality and remained in the dataset after the Uncertainty process. As a consequence, the shape of the distribution after the Uncertainty process is similar to the 'untreated' result (see histograms below). Perhaps the main difference is that the youngest peak of 80-100 yr in the 'untreated' data becomes the largest peak in the Uncertainty treated dataset. This major peak occurred at  $95 \pm 5$  rings (AD 1905-1915). This is also one of the distinctive decadal peaks for all 14 plots (see Fig. 5.2a) and perhaps suggests an offset in time from the 1888 earthquake event as the driver of this forest disturbance. The only other significant peak is an intermediate-sized peak at  $145 \pm 5$  rings (AD 1855-1865).

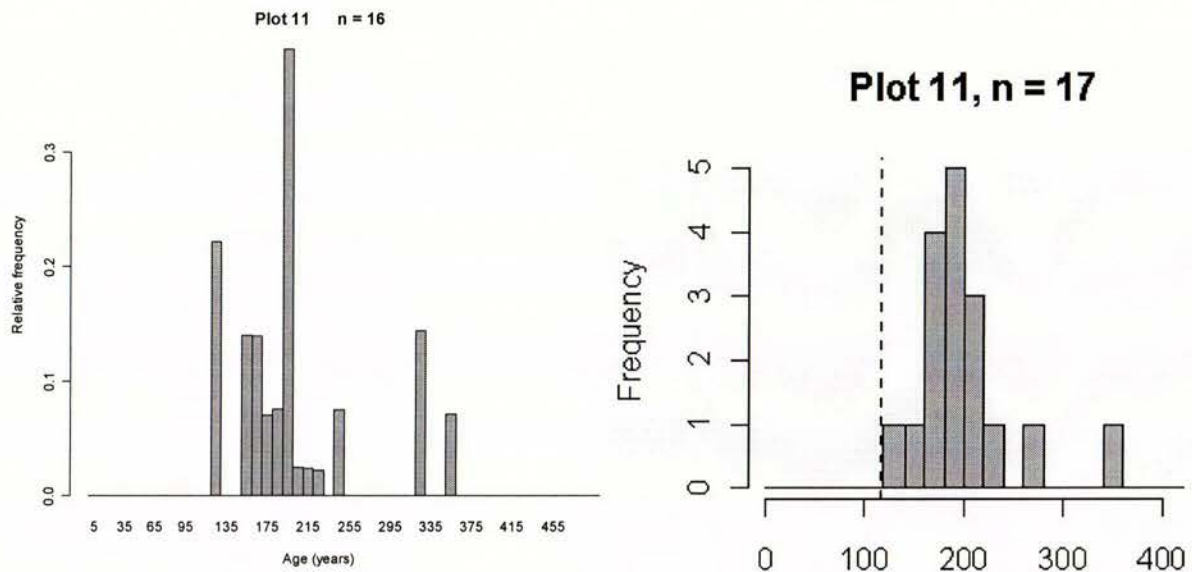


Plot 10 is the McKenzie Stream site (Fig. 4.20). At Plot 10, nine of the original 13 trees that yielded ages were of Centre or Arc quality and remained in the dataset after the Uncertainty process. As a consequence, the shape of the distribution after the Uncertainty process is again similar to the 'un-treated' result. The major peak at Plot 10 occurs at  $125 \pm 5$  rings (AD 1875-1885). There are several minor peaks at  $145 \pm 5$  rings (AD 1855-1865),  $95 \pm 5$  rings (AD 1905-1915), and at  $175 \pm 5$  rings (AD 1825-1835). Statistically, these minor peaks are probably of little relevance at an individual plot as they correspond to only 2 dated trees in each peak.

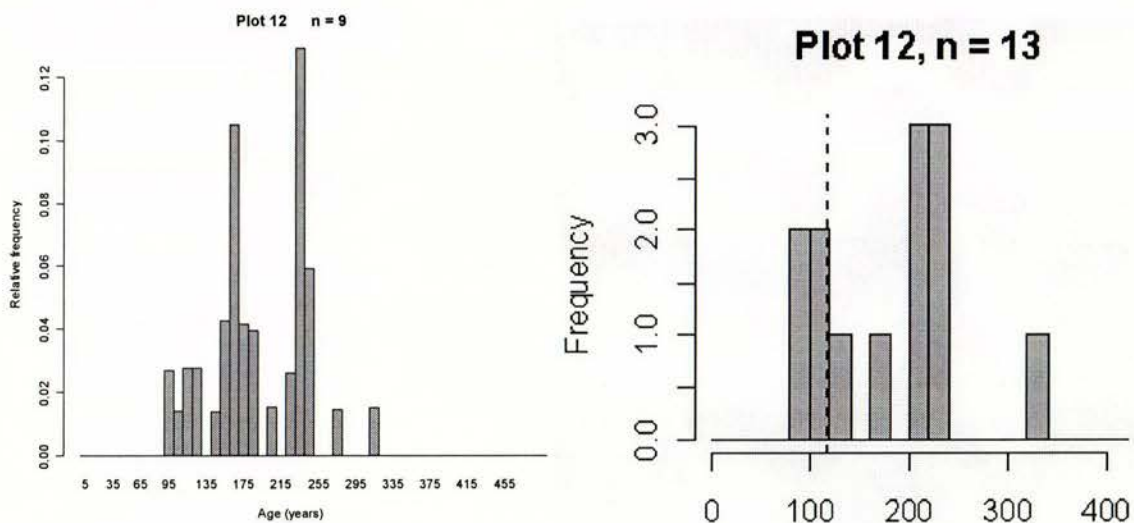


### 5.3.3 Uncertainty-treated Plots 11-14

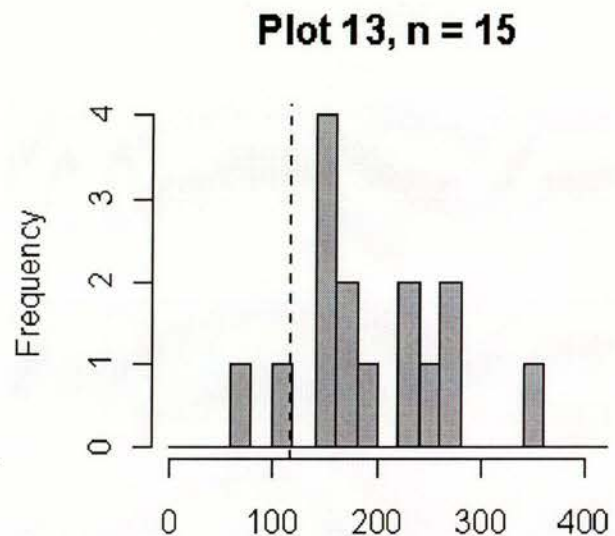
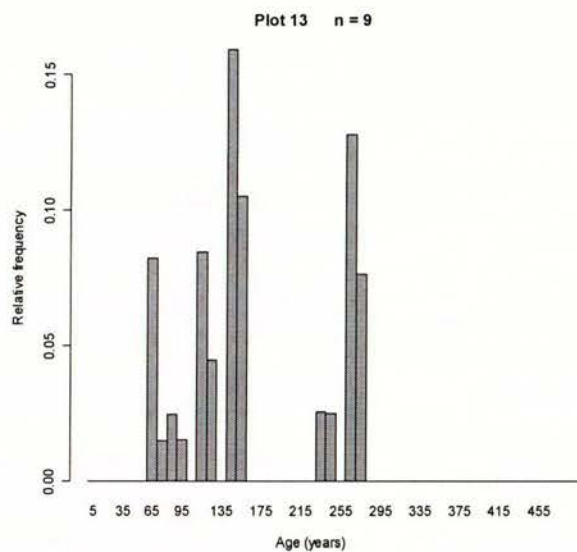
Plots 11-14 are the easternmost plots, being accessed via Glynn Wye Station and Hope-Kiwi Lodge. Plot 11 is the Parakeet Saddle site that was dominated by Mountain Beech (Fig. 4.23). Fifteen of the 16 trees at Plot 11 yielded Centre or Arc tree ages, therefore, the treated and 'untreated' distributions should be very similar. While the peaks are in the same age locations, the relative peak heights is affected by whether the tree age was a Centre or Arc age. The major peak at Plot 11 is at  $195 \pm 5$  rings (AD 1805-1815). The shoulder peaks related to this peak in Fig. 4.24a fall away to become minor. An intermediate sized peak exists at  $125 \pm 5$  rings (AD 1875-1885).



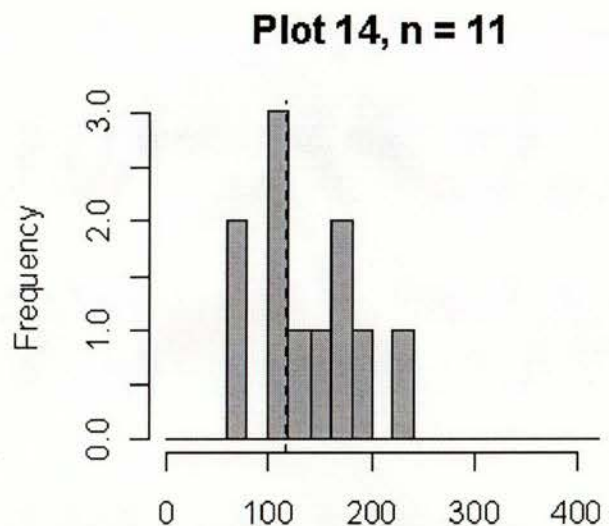
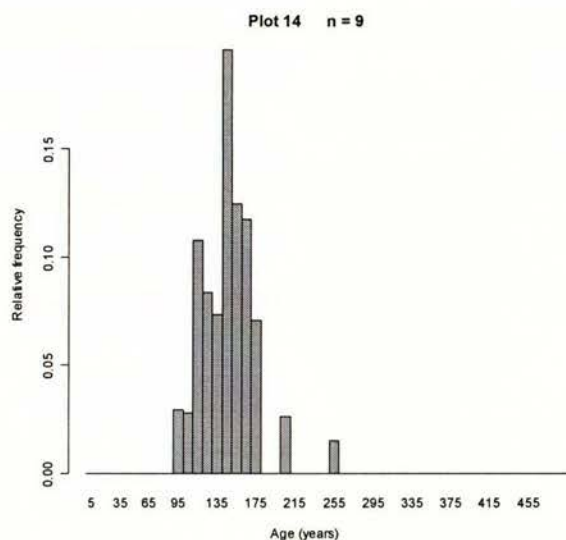
Plot 12 is the Fallen Beech site (Fig. 4.25). In the field, we described a sequence of events to create the cohort of trees growing on the young debris flow there. Four of the 13 trees from the 'un-treated' dataset were lost due to being Short or Bad cores. The major peak occurs at  $235 \pm 5$  rings (AD 1765-1775). This must be considered as the peak colonisation age for the cohort of trees that grew on the debris flow at Plot 12. There is in fact a very low probability that any trees were growing at corer height on this debris flow deposit before 250 rings ago (AD 1755). This point will be pursued further in Section 5.5.3. A second, intermediate-sized peak also exists for Plot 12. This peak is centred at  $165 \pm 5$  rings (AD 1835-1845) and suggests that there was a second pulse of tree colonisation on the debris flow, perhaps due to an event in the early 19<sup>th</sup> Century.



Plot 13 is the Three Mile Stream Hut fan site ( Fig. 4.27). By applying the uncertainty treatment to this plot we lost 6 of the 15 'un-treated' dates due to Short or Bad cores. The data from the remaining 9 trees yielded two intermediate-sized peaks at  $145 \pm 5$  rings (AD 1855-1865) and at  $265 \pm 5$  rings (AD 1735-1745). The former peak is common among several plots, while the latter is a significantly older peak of perhaps 3 'survivor' trees that have been growing on this fan since perhaps the time of the last Alpine Fault earthquake (c. AD 1717). Two minor peaks, that are probably due to single tree ages, appear at  $115 \pm 5$  rings (AD 1885-1895) and at  $65 \pm 5$  rings (AD 1925-1935). Interestingly, these two single trees could have perhaps grown up into the canopy as a consequence of treefall following the 1888 North Canterbury and 1929 Arthur's Pass earthquakes, respectively.



Plot 14, the Lodge Stream site (Fig. 4.29) had 11 'un-treated' tree ages prior to a consideration of uncertainties. Nine trees yielded Centre or Arc ages. The biggest peak from the 'untreated' results is not reproduced in the treated histogram. In this case, the highest peak is not in the 100-120 year range, but peaks at  $145 \pm 5$  rings (AD 1855-1865). This must be caused by a higher number of well characterised 'Arc' ages in this range. An intermediate-sized peak again exists at  $115 \pm 5$  rings (AD 1885-1895).



## 5.4 Summary of the uncertainty-treated dataset

In this chapter we have applied an uncertainty analysis to the tree data collectively and individually for all 14 tree plots in the study area. The entire dataset is summarised on Figure 5.2a and the results for each individual plot are summarised in Table 3, which presents the three most significant well-dated peaks at each plot.

In general the results from the uncertainty-treated and uncertainty-untreated datasets are similar, i.e. the same peaks in tree age are repeated from Table 2 to Table 3. However, there are subtle differences due to a number of factors. These include using a bi-decadal bin size vs. decadal, respectively.

**Table 3.** Summary of tree colonisation peak ages at individual plots (treated data)

<b>Plot</b>	<b>Youngest (Y) peak ring age</b>	<b>Intermediate (I) peak age</b>	<b>Older (O) peak age</b>	<b>Main peak at site (Y, I, O)</b>
<b>1</b>	130-140	<b>150-160</b>	180-190	I
<b>2</b>	<b>110-120</b>	140-150	160-170	Y
<b>3</b>	70-80	<b>80-90</b>	<b>90-100</b>	I + O
<b>4</b>	-	130-140	<b>270-280</b>	Y
<b>5</b>	120-130	<b>140-150</b>	-	I
<b>6</b>	<b>130-140</b>	<b>140-150</b>	<b>240-250</b>	all
<b>7</b>	80-90	<b>110-120</b>	-	I
<b>8</b>	120-130	<b>210-220</b>	240-250	I
<b>9</b>	<b>90-100</b>	140-150	-	Y
<b>10</b>	90-100	<b>120-130</b>	140-150	I
<b>11</b>	120-130	160-170	<b>190-200</b>	O
<b>12</b>	-	160-170	<b>230-240</b>	O
<b>13</b>	-	<b>140-150</b>	260-270	I
<b>14</b>	110-120	<b>140-150</b>	-	I

What is the significance of the Relative Frequency (height) of peaks at individual plots? To test the validity of the peaks shown in Table 3, we have applied a weighting system to the peak heights at each plot, such that, if the relative frequency is:

- >0.28, we award 7 points;
- 0.2-0.28, we award 5 points;
- >0.12-0.2, we award 3 points
- 0.1-0.12, we award 1 point.

Using this scheme, the peaks that receive the greatest points of course mimic the distribution shown in Figure 5.2a. Individually, the most important peak is at 140-150 rings (AD 1865-1855) which might suggest that a significant forest event occurred just prior to the European colonisation of New Zealand (i.e. post AD 1840).

One of the clearest conclusions of this type of analysis is that Plots 3, 7 and 11 stand out as both having a statistically large enough sample of dated trees (18, 11 and 16 respectively) and/or that sample has relatively low uncertainty values and therefore higher probability peaks. These three plots are discussed below, and are important as they have a significant signal and story.

## 5.5 Summary of the Uncertainty Treatment

We have considered the complete tree dataset in terms of the uncertainty of individual tree age results, and also for the case of each individual plot in the study.

The main points arising from our treatment of uncertainty are as follows:

- the peak positions and sizes are generally similar in the treated and 'un-treated' datasets
- The examination of uncertainty has been useful to indicate the accuracy of the results of the total tree dataset and the for individual tree plots. Many of the Short Cores and Bad Arc cores have been eliminated from the uncertainty treatment (n=207 dated trees in Chapter 3 are reduced to n=144).
- The Short cores provide only minimum ages for trees that, from their size, should be much older. The Bad Arc cores have the potential to give too much uncertainty.
- In the total tree data set, the absolute 'mass' of the data is useful for picking out significant trends in the data. For example, from the trees with Centre or Arc tree ages, there are significant peaks in tree age (at corer height)
- It is difficult to read a great deal into the individual peaks at individual plots. However, if we use a ranking system of points for peaks, then there are collectively significant probability peaks at  $95 \pm 5$  rings (AD 1905-1915),  $115 \pm 5$  rings (AD 1885-1895), and at  $145 \pm 5$  rings (AD 1855-1865).
- These are probably the most relevant peaks in the data and probably relate to significant impacting events in the forest. Rather than localised effects such as wind or storm damage, these events may be considered widespread 'regional' signals, such as forest damage caused by large earthquakes.
- All other individual plot peaks are site specific peaks, e.g. the 190-200 ring peak (AD 1805-1815) at Plot 11. This plot and its peak will be considered further below.

## 5.6 Similarity and Cluster Diagrams

In this section, we have used two methods to independently test the similarity of each of the plots to one another. This has been done in an unbiased way, in an effort to determine whether there are clusters of plots or of similar aged events at different times and in different areas along the fault within the study area. The following discussions were written before we decided to treat the possibility of uncertainty in the dataset. Some of the results therefore need to be treated with the caveat that we were not dealing with precise tree ages.

### 5.6.1 The Similarity Cluster Diagram

Figure 5.3 shows each numbered plot across the x-axis and height (a measure of how similar two plots are) on the y-axis. In Figure 5.4 a clear distinction is shown separating two clusters of similarity separating 6 plots from the other 8 (discussed below).

Plot 3 is most dissimilar to all other plots as it has a young uni-modal tree structure. We have already surmised that trees likely colonised this range-front rockslide deposit following the 1888 North Canterbury earthquake. Plot 3 is most alike to Plot 7, which has a strong cohort of young trees that may have 'bolted' around the time of the 1888 event, i.e. young trees that were already close to corer height at the time of the event. Plot 7 bears similarity to plots 10, 11, 12, and 14 that are generally toward the east end of the study area.

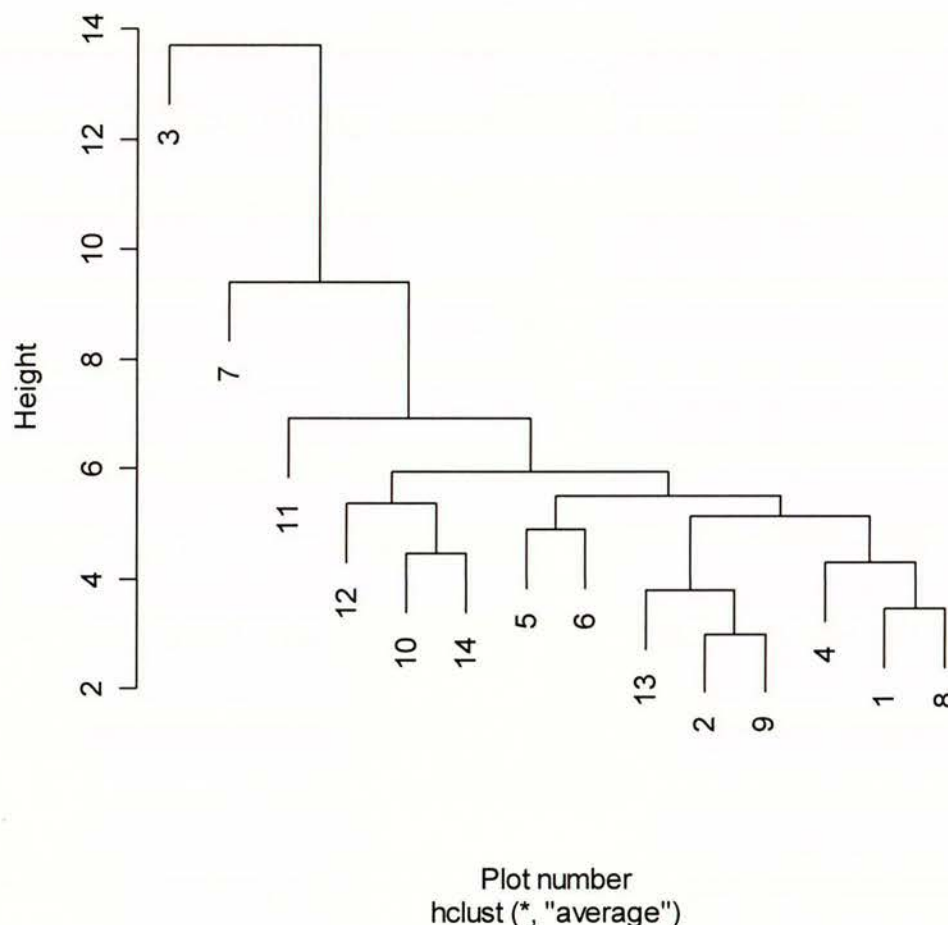


**Figure 5.3.** Similarity cluster diagram of all 14 plots in the study area. The y-axis (height) is a measure of how similar two plots are. Plots 3, 7, 11, 12, 10 and 14 are deemed to be relatively similar and clustered together, while the other 8 plots are deemed more similar to each other.

Plots 1, 2, 4, 5, 6, 8, 9 and 13 have been grouped together in the similarity plot (Fig. 5.3) and as Cluster 1 in Figure 5.4. Plots 5 and 6 are separated by several hundred metres along the fault scarp, and have very similar age character distributions. The similarity analysis has also clustered together Plots 2, 9 and 13. These three plots are all on alluvial fans adjacent to or on the range front of the Hope Fault. Reactivation of sedimentation on the fan or tree fall due to strong shaking may well have generated similar age distributions amongst these 3 plots (Fig. 5.4). In addition these three plots show some of the broadest histogram distributions across the study area, suggesting that pre-existing fan sites probably have a complex forest history.

## 5.6.2 The Plot Cluster Diagram

Figure 5.4 has taken the two significant plot-age structure groups and re-plotted the 'untreated' age data for the two clusters. In both clusters it is clear that: (i) there are peaks and troughs of tree establishment; (ii) younger peaks have more trees in their makeup and tend to have sharper peaks; (iii) older peaks tend to be broader and flatter. Cluster 1 contains plots 8, 1, 4, 9, 2, 13, 6 and 5 (see Fig. 5.3). These plots do not show a dendrochronological signal of the 1888 earthquake. However, they do show a distinct peak that precedes the 1888 event by some 20-40 years, or even earlier considering the offset time for the colonisation of new surfaces, or the shooting up of 'bolters' on pre-existing surfaces (discussed in Section 5.7).

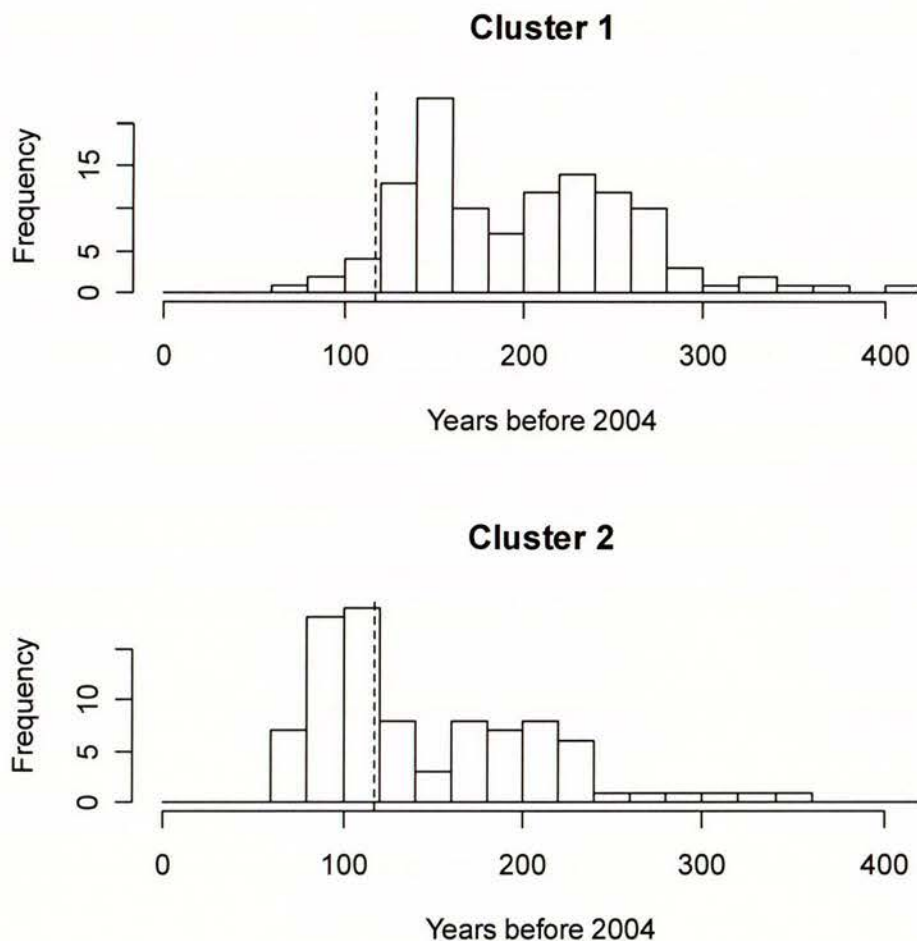


**Figure 5.4.** Cluster diagram of age distributions for the two distinct clusters devised from Figure 5.3. The dashed line identifies the year AD 1888.

Cluster 1 has an older 'smeared' peak that is centred at 220-240 rings (yr before 2005). This peak may actually hold more than 1 peak signal (event) within it. For example, this peak may de-cluster into a moderate peak at 220-240 yr and a small peak at 260-280 yr. However, in addition, it is clear that there are not enough data from older trees to define any re-colonisation before c. 300 yr (rings) ago.

Cluster 2 includes plots 14, 10, 12, 11, 7 and 3 (Figs. 5.3, 5.4). There are several interesting points that can be recognised from this cluster plot. It is interesting to consider what happens to Cluster 2 when Plot 3, the most 'unlike' plot in the study is removed. Then plots 7, 12 and 14 contribute to a young peak which is, in all likelihood, due to the 1888 event, as was the case for Plot 3. The peak shifts to the right (older) and straddles the dashed (1888) line. We believe that this is the signal of the 1888 earthquake on surfaces that were pre-existing at the time of the earthquake. At those locations, young trees were perhaps ready to take advantage of the canopy laid open by forest damage, and bolted upwards through the borer height, i.e. past c. 1.3-1.4 m height.

Cluster 2 exhibits an anti-peak (trough) of tree establishment over the same time interval (140-160 rings) that corresponds to a peak in the Cluster 1 plots (Fig. 5.4). The reason for these two clusters of plots being exactly out of 'synch' when they are in an overlapping geographical area cannot be speculated upon here.

Cluster 2 plots also show an older broad peak that is centred around 200 yr ago, that may again de-cluster into two distinct peaks. These separate peaks appear to be centred at c. 160-180 and 200-220 rings ago. About half of the trees in the broad peak come from Plot 11 (Parakeet Saddle). Removal of this plot confirms a small peak at 160-180 rings and a peak at 220-240 rings. The latter peak was also found in the Cluster 1 dataset. If re-colonisation of Mountain Beech at Plot 11 (865 m ASL) had taken twice as long as at other Red/ Silver Beech sites at lower elevations (generally 620-640 m ASL), i.e. c. 20 yr rather than 0 yr, then a peak in the Cluster 2 set may be shifted toward a similar peak at 220-240 yr in the Cluster 1 set. It is not possible to extract any peaks from the Cluster 2 set that are older than c. 220 yr. Some of these speculations need to be treated with the caveat that many trees in this age range have under-estimated ages due to Short or Bad Arc core ages.

## 5.7 Individual Age Offset Features at Plots

The following discussions were written before we decided to treat the possibility of uncertainty in the dataset. Some of the results therefore need to be treated with the caveat that we were not dealing with precise tree ages.

### 5.7.1 The significance of Plot 3

We have noted that the age structure of Plot 3 is both young and of any plot in this study it most resembles that of a colonising cohort of trees. That is, it has a very sharp, single asymmetric peak for both tree size and age in both the untreated (Fig 4.5a) and treated histograms. The deposit that the plot formed on was a fresh, bouldery rockslide and the trees growing on it have a significantly different size structure to the trees in the adjacent piece of bush on the stable part of the range front slopes. The age peak for the Plot 3 cohort ramps up suddenly and has an asymmetric younging tail. The modal peak is broadly 70-100 rings, in the uncertainty treated case, with the front of the peak at 90-100 rings (AD 1905-1915). The oldest cored tree growing on the rockslide reached borer height in 1901, and no larger or older trees existed at that height on the deposit prior to this date.

We have drawn the conclusion from the geomorphology of the site and these results, that the rockslide was formed as a consequence of the 1888 North Canterbury earthquake. We infer that very strong shaking of MM Intensity 7-8 (Cowan 1991; Hancox et al. 1997) in this area, loosed this small portion of the range front producing an open scar in the forest canopy above the blockslide. While other mechanisms for the rockslide are possible, such as an intense storm, we can rule out mechanisms like windthrow or other earthquakes, such as the 1929 Arthur's Pass earthquake (Berryman & Villamor 2004). Based on the assumption that Plot 3 was colonised following a blockslide in 1888 we can consider its age structure in greater detail. Three of the 18 dated trees reached borer height in AD 1909. Single trees reaching borer height preceded this peak in AD 1906-1908, and followed the first tree to reach borer height (the shooter) in 1901. Other single colonisers followed the 1909 peak in AD 1910, 1911 and 1914.

The dataset allows us the real possibility to test the rate of colonisation of a new Beech cohort in this setting, from a bouldery, remobilised substrate with a cleared out tree canopy. The data suggest that the 'bolter' tree could shoot up to borer height in a mere 13 years. The data also show that the peak of colonisation for this plot is some  $21 \pm 4$  yr after the 1888 earthquake. This value should be considered as a reasonable colonisation time for new geomorphic surfaces following unknown large forest damaging events in this area. This analysis also shows that the front (steeper) part of the cohort peak can be equated to the optimal colonisation time for a new forest site

### 5.7.2 The Significance of Plot 7

As shown by the Similarity Cluster diagram (Fig 5.3), of any site, Plot 3 is most similar to Plot 7. This discussion draws on this point to account for the age distribution of trees at Plot 7 and considers the possibility that the co-similar feature of these two plots is that they were greatly impacted by the 1888 earthquake. We know that the alluvial fan at Plot 7 was not first created in 1888 as probably was the case for Plot 3. There are considerably older trees at Plot 7. We consider here the possibility that the small fan at Plot 7 was rejuvenated as a consequence of that earthquake.

Several trees reached borer height at Plot 7 immediately after the 1888 earthquake age, i.e. at around AD 1889, 1893(2) 1894, and 1899. Based on our discussion above this would mean that it had taken a mere  $5 \pm 5$  yr after that event. In addition, three other trees at plot 7 were already at borer height in 1885 (RB2, RB10, SB19) three years before the earthquake.

For a fan like this that is pre-existing and largely inactive and infrequently rejuvenated or affected by storm sediment supply we invoke a special kind of tree colonisation. This is based on the possibility that there were several young Beech seedlings already established at this site, some of which were already at borer height (those with 120 rings) and others that were below borer height in 1888. This would effectively make the colonisation time at pre-existing fan sites a somewhat unbelievable  $5 \pm 8$  years, compared to  $21 \pm 4$  yr at Plot 3.

If this argument is viable then we have at this site a measure of how long it may take trees to be established on a pre-existing surface that had a tree cover. We are inferring that these trees quickly rose to fill the canopy that was evacuated by strong shaking and/or sediment supply (rejuvenation of the fan). However, other alternatives to this speculative hypothesis should be considered. For example, the fan at Plot 7 could have been rejuvenated by a storm/ sediment release event, or from some other nearby seismic sources. If this is the case, and we apply the 'new cohort' offset of  $21 \pm 4$  years from the previous section, then the

last significant event to affect the alluvial fan at Plot 7 was around c. AD 1864 or 1872. No such historically-timed earthquake or storm events in this time period are currently known to us.

### 5.7.3 The Significance of Plot 12

Plot 12 has a set of geomorphic conditions that might be explained by the occurrence of a past surface faulting event there. In section 4.22 we have described the relationship between the large fallen beech tree, the range front, fault trace and a debris flow deposit.

Three well-dated trees colonised the debris flow in c. AD 1776, 1781, and 1786. Three other Short core dates were of similar age to these results. We apply the control colonisation offset from Plot 3 ( $21 \pm 4$  yr) to these results and suggest that the cohort's trees to reach borer height, which was in AD  $1760 \pm 6$ . If we assume that the oldest daed tree on the debris flow (rb16) was a shooter which took c. 13 yr to reach borer height, then this yield a possible debris flow age of AD 1763. We infer that the debris flow and therefore the sediment release event that caused it (earthquake?) happened at c. AD 1760.

We can also use the power of stratigraphic succession to refine the radiocarbon age distribution for the date on DB1. The OxCal plot in Fig 5.5 illustrates what happens when we assume that the age of the debris flow is younger than the fallen tree and has a precise age of AD  $1760 \pm 6$  yr (it is inserted as an event with that age). The three younger calibration peaks are eliminated and the calibrated date for DB1 becomes AD 1690-1730.

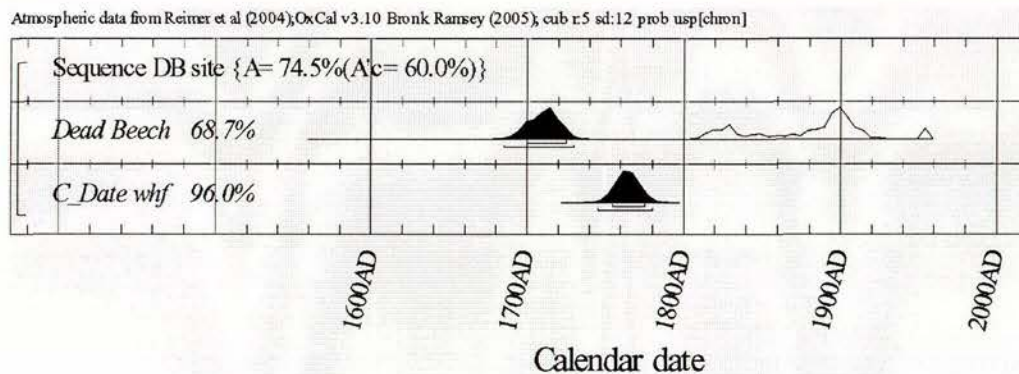


**Figure 5.5.** OxCal Sequence diagram showing the multi-peaked age distribution of the Fallen Beech tree. By inserting the colonisation of the debris flow as an event (C\_Date whf) then three of the four peaks are eliminated and the resultant age distribution of the tree is shown.

We have assumed that the earthquake, treefall of DB1 and arrival of the debris flow deposit are effectively coincident. However, there is an offset of possibly decades between the radiocarbon date (somewhere near the outside of DB1) and the estimate of the debris flow deposit. Therefore, there is some uncertainty as to the precise timing of the 'event' at Plot 12.

#### 5.7.4 The Significance of Plot 11

We begin a discussion of this plot by considering the site conditions, tree species and pre-existing trees at the Parakeet Saddle site. Plot 11 is sited on a steep, north facing scarp of the Hope Fault at c. 865 m ASL. Consequently, the predominant trees at the site are Mountain Beech (*N. Solandri*). We sampled most of the trees in an area that spanned from the top of the scarp, across the scarp, and over to a fault-guided stream at the base of the scarp. We have noted or state here that:

- i) The 'front' of a prominent cohort peak in the data set that has a mode of 180-200 rings;
- ii) The oldest tree has a borer height date of 342 rings.
- iii) Only one other tree has a borer height age of > AD 1779, when the main cohort peak at the plot begins from.
- iv) There is no signal of the 1888 earthquake at this site, despite it being near the location of the saddle alluded to by McKay (1890), at the western end of the 1888 surface faulting.

We note that for (ii) and (iii) that trees MB10 and MB17 are 'survivors' on the fault scarp of an event that decimated the forest here, probably after AD 1727, but well before AD 1779. At some time during the mid-18<sup>th</sup> century there were no trees growing on the area of the guided stream, and only 1 on the fault scarp, where we sampled. In this case, this plot effectively resembles a new or rejuvenated surface for colonising trees.

The first 5 trees to colonise the plot have borer height ages of AD 1779, 1795, 1799, 1803 and 1809. If we make the crude assumption that the forest-clearing event at this site could have been the same one that occurred at Plot 12, c. 5 km to the west, then:

- I) a large earthquake ruptured the fault at c. AD 1760  $\pm$  5 yr and is observed at both of these eastern plots:
- II) The first coloniser after this event (MB5) at Plot 11 was a 'shooter' and took c. 15 years to reach borer height.
- III) The four trees that follow map out an average borer height age of 1799  $\pm$  4 yr, giving an offset age from c.1760 of 39 yr.

These results overlook the 7 trees that followed this initial cohort from 1817-1834.

However, it is possible that at Plot 11, we are witnessing the effects of a slower tree growth rate at the higher elevation site and on the Mountain Beech species causing:

- A. a slower shoot-up time of c. 15 years for the first coloniser.
- B. A longer offset to the average colonisation age of c. 39 yr from the forest disturbance event age.
- C. A later, slow-colonising cohort (AD 1817-1834 trees) that peaks at c. 60 years after the forest disturbance event age.

Therefore, if these assumptions follow, we have observed three different rates of colonisation at three different sites that have different tree species, elevation (e.g. Plot 11; 39  $\pm$  8 yr), slope, substrate (e.g. Plot 3; 21  $\pm$  4 yr), canopy exposure, and sediment delivery (e.g. Plot 7; 8  $\pm$  5 yr).

### 5.7.5 The Significance of Troughs vs. Peaks in the Dataset

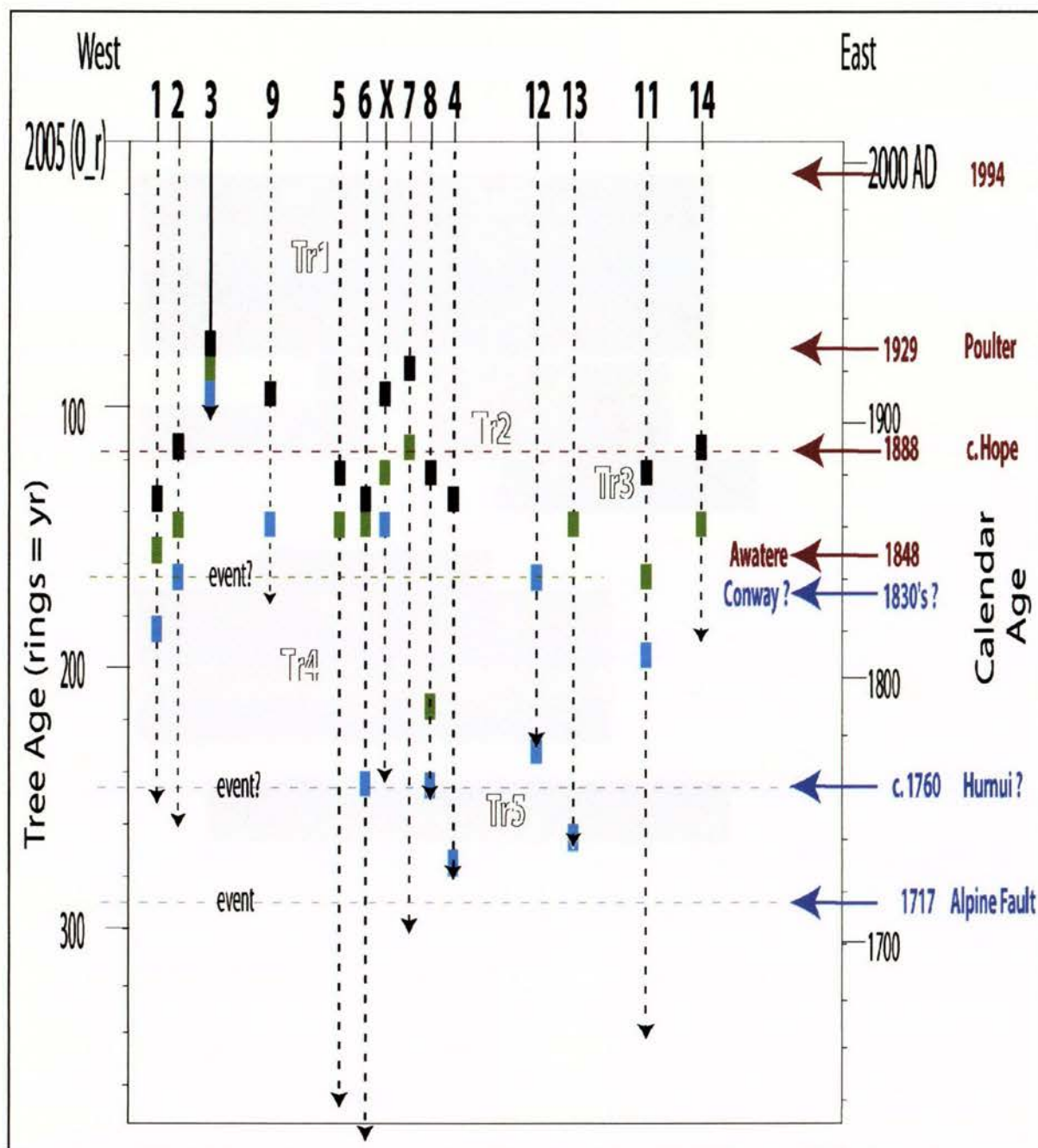
This project has focused on peaks or spikes in tree establishment. That is, we have been looking for signals of: (i) damage in the landscape that may be earthquake-related that have brought about subsequent tree colonisation on fresh geomorphic surfaces; or (ii) peaks in the tree population on established, more stable geomorphic surfaces, e.g. fault scarps, that point to times of strong shaking and/or fault rupture near a fault scarp. This study has not, so far, emphasised that there are significant periods of stability on established geomorphic surfaces that point to a lack of forest damage for long periods of time. These have already been discussed with regards to Plots 5 and 6 in Chapter 4. As well as peaks, these two plots have significant troughs in the tree population during portions of the 20<sup>th</sup>, 19<sup>th</sup> and 18<sup>th</sup> centuries.

Fig. 5.6 acts as an alternative summary plot to Figure 5.2 and as a catalyst for discussing the patterns of forest damage and re-establishment. These data are also summarised in Tables 2 & 3. In Figure 5.6, the tree plot data are expressed geographically from west to east on the x-axis and with time increasing on the y-axis. All tree plots have been projected onto the plane of the fault (x-axis), so that plots 7 and 4 are amongst the McKenzie fan plots (5, 6, 10 & 8). The long black dashed arrows show the oldest well-dated tree ages for each surface, thus providing a minimum age for the substrate of each plot. For plots 3 and 12 in particular, we believe that the surface age very closely precedes the age of the oldest tree on that surface. Coloured bars on Fig. 5.6 refer to peaks or clusters of well-dated tree ages at each plot. For example, black bars identify the youngest significant tree age peak; green, an intermediate aged peak (if present); and blue, the oldest tree age peak.

While other tree ages come from in between these peak bands, constructing Fig. 5.6 has allowed for the identification of the important geographic based peaks and troughs in the dataset. Five troughs in tree colonisation that represent times of forest stability have been recognised across the study area. These may broadly correspond to interseismic shaking intervals when the forest is not damaged by local earthquakes, or other events.

The greater part of the 20<sup>th</sup> Century represents the biggest trough in tree establishment throughout the forest we have investigated (Fig. 5.6). Only 7 well-dated trees (out of 144) are <80 rings old. i.e., trees dated that have reached borer height since 1925 (5 of those are at Plot 3). It may be that we overlooked a small number of thinner trees at each plot due to a bias toward dating bigger trees from older events. However, it is clear that there has been no significant event in the forest along the western Hope Fault since at least the time of the 1929 Arthur's Pass earthquake.

Perhaps only in the case of Plots 3 and 14 is there any potential signal of tree damage related to the most recent large shaking event in the area: the Poulter Fault rupture caused by the 1929 Arthur's Pass earthquake (Berryman & Villamor 2004). This is a surprising observation from an earthquake of M 7.1 on a fault that ruptured only c. 6-8 km away from many of the tree plots, and probably caused MM Intensity isoseismals of between VII-IX in the study area (Hancox et al. 1997). We consider there is a trough in tree colonisation across all other plots in the study area (Tr1 on Fig 5.6) from 1925 to possibly 1994, which was the time of the latter "Arthur's Pass earthquake". Tr1 post-dates the 1888 earthquake by c. 37 years. In other words, though we witnessed occurrences of recent treefall that must have been caused by wind or storm throw, there has been no widespread instability in most of the forest since the forest was rejuvenated as a result of the 1888 North Canterbury earthquake.



**Figure 5.6.** Space-time diagram of geographical location (western plots shown at right, eastern to left) versus the timing of major peaks and troughs in tree colonisation ages for the 'un-treated' dataset. X refers to Plot 10. The coloured bars represent the youngest (black), intermediate (green), and oldest colonisation age peaks at each tree plot (see Table 2). Troughs represent periods when little if any new tree colonisation was occurring, i.e. relative stability in the forest. Earthquake ages and fault segment ruptures are listed on the right side of the figure.

There are three equally surprising relationships in the data that we have related to the 1888 North Canterbury earthquake and its effects in the study area. These are:

- (i) we have found that only 6 of the 14 plots in the study area show any '1888' signal (Plots 2, 3, 9, 10, 7 and 14). The other 8 plots show no indication of any significant forest damage.
- (ii) at four of the '1888' plots, the '1888' signal is interpreted as a time when Beech seedlings at or near the borer height, 'bolted' up through that height.
- (iii) the six '1888' plots are spread geographically along the length of the study area. In addition, the plots that show no '1888' signal are as likely to be near the known mapped end of the 1888 rupture in the east, as those that are not. Thus, those sites that show no 1888 signal have a tendency to have a trough in tree

establishment ages that extends from the late 19<sup>th</sup> Century to the present, i.e. at these sites there have been no wholesale impacts on the forest for at least 120 years (Tr1 and Tr2 in Figure 5.6).

Trough 1 in particular, provides a very strong indicator that there has been little forest change during the last c. 80 years or more, and therefore that wholesale regional changes in the forest structure are possibly caused by seismic activity, as opposed to local effects such as storm or wind damage.

There are other troughs in the data set. First, at the 4 easternmost sites (Plots 11-14), there is a trough during the mid to late 19<sup>th</sup> Century. On Figure 5.6 we refer to this trough as Tr3 and it coincides with the 40 year gap between two well-known historic earthquakes: the 1848 Marlborough earthquake and the 1888 earthquake. No other large (>M 7) earthquakes occurred in the northeastern South Island during this period. As expected there is little to no forest re-colonisation at these sites during this period. Conversely, there is a strong forest recolonisation signal at many of the western plots at the time of Tr3 in the east. This may reflect a pre-1840 AD event that had a significant impact on forest in the area closer to the Main Divide than those plots in the east. In Figure 5.6, we infer that this event occurred at c. AD 1830. This is based on the idea that the peak colonisation of a site after an event should be offset by some amount, perhaps either  $21 \pm 4$  yr (as seen at Plot 3 from 1888 event) or as little as  $5 \pm 8$  yr (as seen from pre-existing sites). In addition, there are few known large earthquakes between AD 1830-1840 (see AD 1830 event in Grouden 1966) and no known events in this area in the decades immediately after AD 1840 (until 1888).

Tr4 is a pervasive trough in tree colonisation across most plots in the study area during the late 18<sup>th</sup> to early 19<sup>th</sup> centuries. We infer that there was a period lacking in forest re-colonisation between c. 165-225 rings ago (i.e. AD 1830-1780). If Tr4 post-dates a recolonisation following a major earthquake along the length of the Hope Fault, then it may be reasonable to assume that it has an offset similar to that shown by Tr1 following the 1888 earthquake at Plot 3. An offset of c.  $21 \pm 4$  yr would place such a large earthquake at c. AD 1760. This  $21 \pm 4$  yr window is characterised by tree colonisation at various other sites throughout the study area (see discussion on Plot 12).

There are few well-dated trees in the study area that predate the debris flow at Plot 12. However, Tr5 is shown in Figure 5.6 as a hypothesised trough in tree colonisation that post-dates the c. AD 1717 Alpine Fault earthquake. Strong shaking at that time probably caused collapse of part of the range front above Plot 4 (Richard's fan) and rejuvenation of the alluvial fan there.

## 5.8 Summary of Age Offset, Plot Similarity and Clustering Features

We have made a number of significant assumptions in reading and analysing the results of tree coring on a plot by plot basis. These assumptions have been driven by an attempt to understand the dataset, including the different ages of surfaces, the oldest trees on surfaces, elevation and species differences, and the knowledge that at least 1 historic earthquake (1888 and/or 1929) and pre-historic earthquakes (incl. AD 1717) could have impacted forest plots along the study area.

While some of these assumptions are reasonable, others may not be supportable by the amount of data presented from each plot. An important aspect of strengthening these assumptions has been to treat each plot as an 'earthquake geology' site, i.e. to map out the site geomorphology, relationship to slope or the fault, tree location and size, and tree species and elevation. This allows us to consider sites on or near the fault as locations of former surface rupture and/or very strong shaking.

While windthrow, localised storm and fires might have circular or non-aligned patterns of damage over local to wide areas, strong shaking damage related to earthquake fault rupture should show a rather unique pattern in the landscape or in tree damage and rejuvenation. If we consider the isoseismal patterns of shallow earthquakes they are known to be typically long and elliptical along and about the surface trace of the fault that is responsible for that large seismic event. Therefore, by developing a site strategy that has many sites spread along the length of the fault (c. 18 km), we may be able to observe whether there are small, localised circular and random damage patterns or long, elliptical co-temporal damage patterns.

We have made the following assumptions about a number of key plots. The selection of and resulting data from these plots has been somewhat serendipitous i.e., by selecting those sites we may have stumbled across some intrinsic signals, that we have developed into 'assumptions'. They are:

- (A) The substrate of Plot 3 formed as a result of strong shaking in 1888. The first coloniser (a shooter) reached borer height 13 yr after the event and the peak average time to borer height for colonisers was  $21 \pm 4$  yr.
- (B) Some pre-existing plots, like plots 7 and 10 have cohort peaks or trees that straddle the 1888 event. In this case a few pre-existing seedling Beeches became 'bolter' trees, i.e., they took advantage of tree fall and an open canopy to bolt up through and beyond the borer height. These sites show an offset age from the 1888 event of only  $5 \pm 8$  years;
- (C) The Fallen Beech site (Plot 12) has landscape change evidence consistent with a surface faulting earthquake that is inferred to be co-incident with the timing of a large tree fall and deposition of a debris flow deposit. This event occurred at c. AD 1760  $\pm$  5 yr.

Other plots have evidence that support these assumptions. While these assumptions might be considered biased or speculative, they follow the results of two un-biased discrimination tests shown by the similarity and cluster plots. For example, Fig.5.3 closely links plots 11 & 12. We have inferred that these two plots could have been affected by the same destructive event.

The similarity diagram separates out those plots that we assume have an 1888 signal (e.g.

Plots 3, 7, 10, 12 & 14) and their reasons for co-similarity are described within the assumptions A & B above.

The similarity diagram separates out the other plots (5, 6, 13, 2, 9, 4, 1 and 8) of Cluster 1 as being distinct from cluster 2 plots. Cluster 1 plots as shown in Figure 5.4 have:

(i) no 1888 earthquake signal; (ii) a mid 19<sup>th</sup> century signal (event related to assumption C); and (iii) an early 18<sup>th</sup> century signal.

In the case of the mid 19<sup>th</sup> Century signal it has been noted during Tree Growth suppression studies in the region at Craigeburn and Lewis Pass, that there is a decrease in Beech tree growth rate at around AD 1832 (current Lincoln Ph.D. student). The reason for this is not well understood, however, the western Hope Fault sites are placed geographically between the other two study areas. It is possible that there is a regional signal of an event at this time in the western Marlborough area. The only record of an historical earthquake at this time was a felt earthquake in Paihia (Northland). Paihia was one of the major European settlements in New Zealand at this time and occurs in an area of no active faults. It is c. 850 km north of our study area.

Finally, we infer that a peak in early 18<sup>th</sup> century, seen particularly well at Plot 4, was caused following moderately strong shaking from the last Alpine Fault earthquake in c. AD 1717. While we probably do not have enough old trees to understand what happened >270 years ago in this region, it is possible that the Alpine Fault has also been a significant agent of forest change in the western Hope area.

## 6.0 INTEGRATION OF LANDSCAPE, PALEOSEISMIC & TREE DATASETS

In Chapter 6, the objectives are to first bring together landscape observations (including landslide distribution) along the Hurunui valley with soil ages, radiocarbon ages and results from the Matagouri Flat trench to develop a landscape-derived model of surface faulting events along the Hurunui section of the Hope Fault (Fig. 6.1). Then, we will combine the landscape-derived and dendro-derived records (summarised in the previous sections) to create a surface rupture and inferred shaking record for the Hurunui section of the Hope Fault.

### 6.1 The penultimate faulting event

We have few indications of the amount of landscape change, forest damage or faulting related to the penultimate earthquake on the Hurunui section of the Hope Fault. Most of the data come from near the Matagouri Flat trench site. Data from the trench suggests that the penultimate faulting event occurred there after AD 1297-1425. This event probably caused 5-6 m of dextral displacement at Matagouri Flat, but typically less (c. 3.5 m) at McKenzie fan where there is a record of multiple displacements (Langridge & Berryman 2005). The western end of the Kakapo Fault projects toward the area between these two localities.

The penultimate faulting event is almost certainly not captured in the forest record unless the oldest trees dated in the forest (c. 400 yr old) colonised surfaces following an event at that time. These trees would have also had to survive through the most recent faulting event, other strong shaking events, fire, windthrow, storms and old age and still retain a completely coreable (unrotten) tree section. We dated only 1 tree that exceeded 400 yr in age, but attempted to date c. 14 other trees of similar size (>90 cm diameter) without luck. Therefore, without further insights, we conclude from the results at the Matagouri Flat trench, that the penultimate faulting event occurred after AD 1297-1425 (Fig. 6.1).

### 6.2 The most recent faulting event

Based on two radiocarbon dates in the upper Hurunui valley and faulting relationships in the trench, the timing of the most recent faulting event was since AD 1516-1655. At McKenzie swamp, a fragment of Red Beech buried within that swamp yielded a calendar age of AD 1516-1658. In the Matagouri Flat trench, the pebble gravels 2a or 3a (from which the date on MF4b is considered to equate to), have a calendar age of AD 1458-1655. Both of these ages pre-date the most recent event by an unknown amount. If this event was coincident with the timing of treefall for DB1 at Plot 12 ( $50 \pm 30$ , but "shaved" using OxCal to AD 1690-1730), then the most recent event was most likely during the 1700's.

Sample LSW from the outside of a log found in outcrop at Lodge Stream yielded a radiocarbon age of  $26 \pm 30$  yr. This age yields calendar calibrated ages in the ranges AD 1690-1730 (13.1%), 1810-1860 (10.2%), 1870-1920 (43.8%), and 1950-1960 (28.3%). The outcrop from which the log was extracted appeared to be faulted to above the level of the woody logs. This generates some interesting age restrictions on the faulting and age of the wood. First, we must assume from historic and stratigraphic observations that the faulting occurred in AD 1888 (McKay 1890; Langridge 2004; Hancox et al. 1997). Second, the deposit itself must be very young and was probably formed by the most recent faulting event for the Hurunui section of the Hope Fault. If the log died as a consequence of that event, then it must have occurred before 1888. We have again applied the concept of stratigraphic

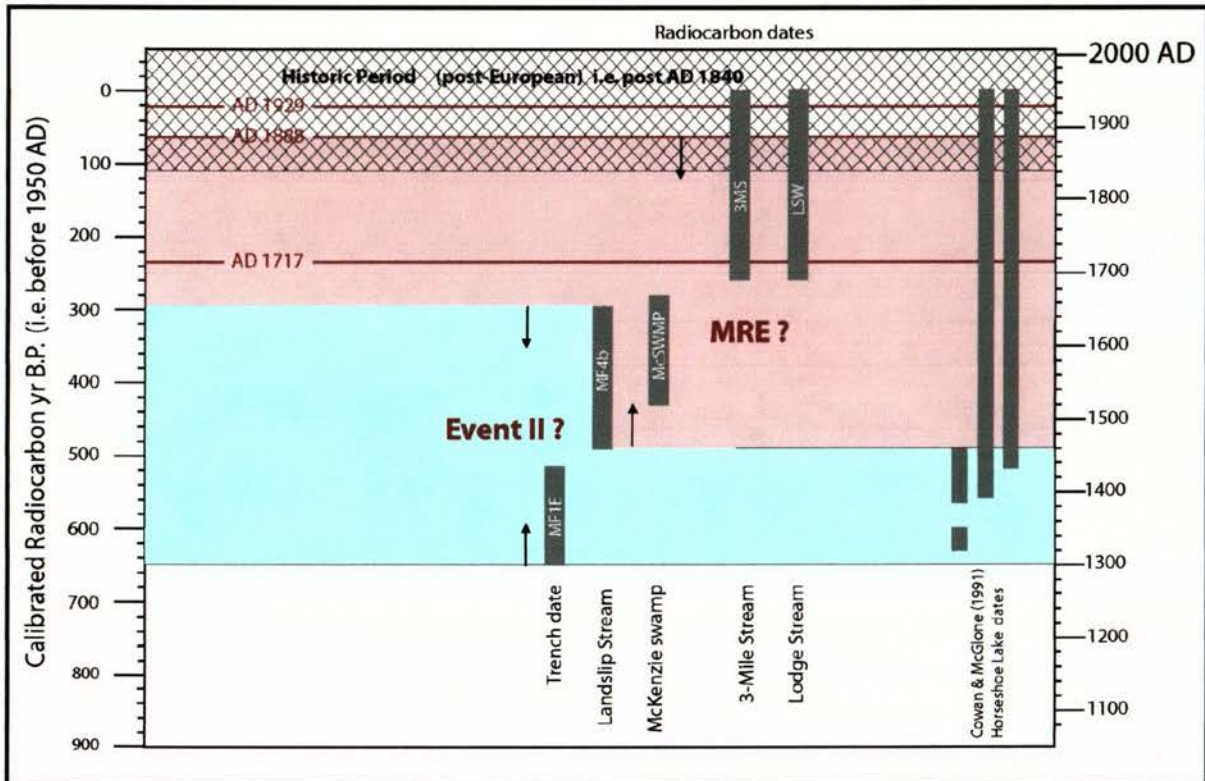


**Figure 6.1.** Summary diagram of paleoseismic data from trench and landscape dates. We infer in this plot that the 1888 North Canterbury earthquake was NOT the most recent event in the upper Hurunui.

ordering to this result using the OxCal program (Fig. 6.2). This argument eliminates a large part of the youngest distribution ranges for date LSW and re-weights the older peaks. This means it is more likely that the event which produced the debris fan was prior to AD 1888 and about equally likely that it occurred at the times of c. AD 1715±, 1830±, or 1885±.

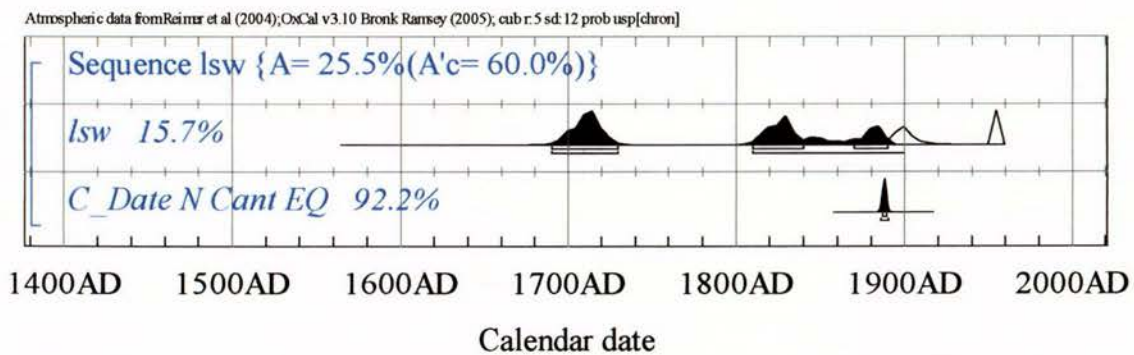


**Figure 6.2.** OxCal Sequence diagram showing the multi-peaked age distribution of the Lodge Stream log (lsw). By inserting the 1888 earthquake as a faulting event (C\_Date N Cant EQ) then the distribution is shifted and re-weighted to the left of AD 1888.

In summary, the combined data from four radiocarbon dates and a trench imply that the most recent faulting event occurred (at or) before AD 1888, but since c. AD 1460. The boundary zone between the western Hope Fault rupture (Hurunui section) and Hope River segment of the Hope Fault must be close to Lodge Stream, within the study area.

### 6.3 Integration of Landscape, Paleoseismic and Tree data

In this section we attempt to combine the results of the landscape, paleoseismic and dendrochronological studies to assess the age of the most recent seismic event(s) along the western part of the Hope Fault. The initial hypothesis of this research project - "did the western Hope Fault fail between AD 1717 and 1888" - will be put to the test here.

The dendrochronological data is generally limited to the last c. 270 years. This most recent period is also the time period over which the radiocarbon data is the weakest due to the problem of calibrating the age data over a flat portion of the Solar Radiation curve. In contrast, the radiocarbon age data is strongest over the period of 300-700 years ago.

Therefore, it is quite difficult to wed together the radiocarbon chronology with the dendrochronology. From the tree ring studies we can recognise that there are significant peaks in tree colonisation at around the beginning of the 20<sup>th</sup> Century, early 19<sup>th</sup> century and in the middle of the 18<sup>th</sup> Century. These peaks are all younger than the dates which best constrain the earthquake events in the trench at Matagouri Flat. We have stated that the most recent faulting event in the trench occurred before AD 1888, but since c. AD 1460. We entertained the possibility that a colluvial wedge that formed as a consequence of this event was re-faulted by a younger event. Thus, the trench record tells us that there have been 2 and possibly 3 earthquake ruptures between c. AD 1460-1888 (428 yr), while the dendro record tells us that there have been 2 and possibly 3 forest damaging (seismic shaking?) events during the period AD 1717-1888 (171 yr). These give simple recurrence ranges of 214-428 yr and 57-85 yr, respectively.

Clearly, there is a mismatch in the records provided by the two different techniques. If every peak in the dendro dataset was caused by an earthquake on that segment of the Hope Fault alone, then there would be many distinct earthquake displacements and we might expect another event to have occurred during the 20<sup>th</sup> century. Therefore, we have to entertain the possibility of multiple sources to produce the dendro record such as: multiple separate seismic sources, e.g. different sections of the Hope Fault, Alpine Fault and other nearby faults in the Marlborough Fault System; storm; windthrow; fire; or disease.

It is also difficult to test for many of these "natural" effects on the forest (i.e. windthrow, storm, disease). There is no evidence for fire, in the form of extensive young charcoal or charred stumps, having affected the forest during the last few hundred years. In addition, the forested areas that we studied had not been greatly modified by human activities. The upper Hurunui valley was a route used by Maori to travel across the Main Divide at Harper Pass to head into Pounamu country on the West Coast. It was also a favoured route for miners travelling to the West Coast goldfields during the 1860's and 1870's. For example, the name Matagouri Flat, was once called Wild Irishman's Flat and Landslip Stream was probably named around this time, as a reflection of the fresh nature of the landslip up on the range front above the stream.

We infer that the most significant regional agent of damage to the forest is likely to be seismic shaking and fault rupture (along the fault). We cannot completely rule out storm, windthrow or disease as agents of dynamic change in the forest. These may impact trees at the plot level. However, we attribute the strong cumulative signal that comes from the data as punctuated earthquake shaking damage.

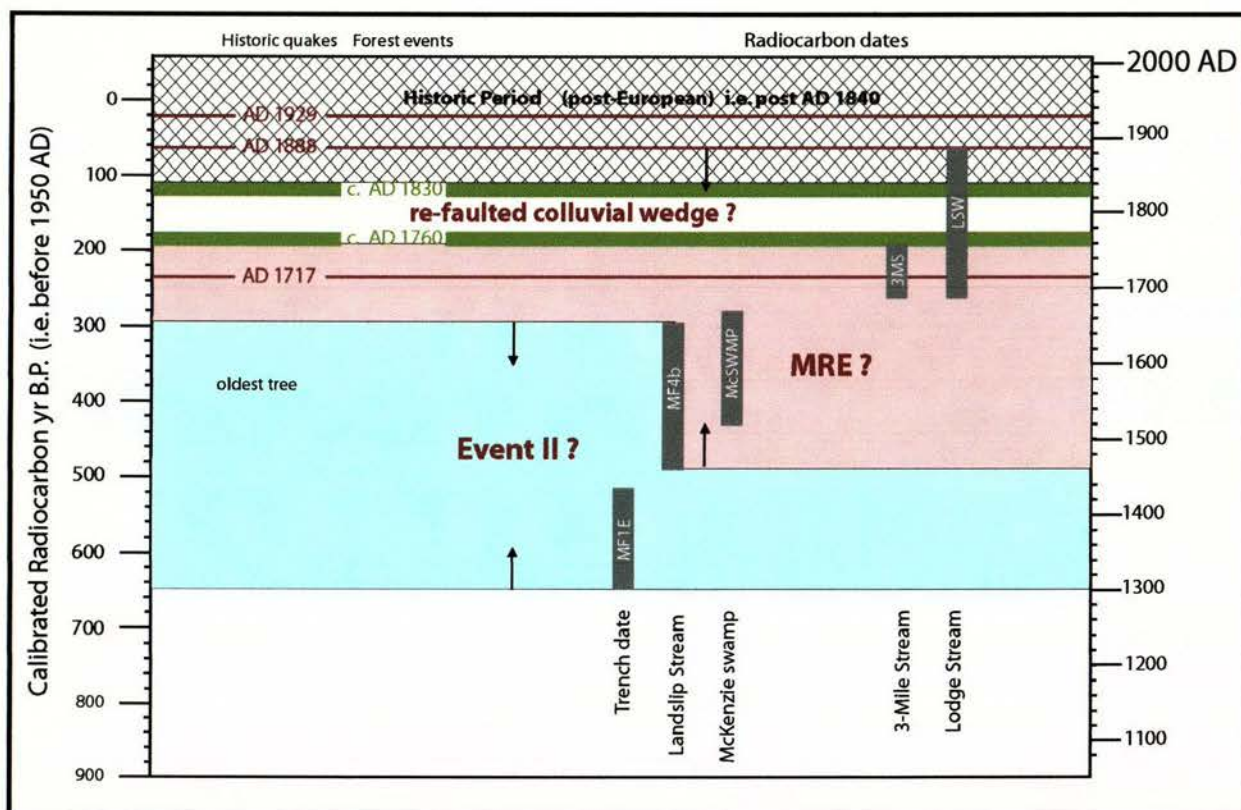


**Figure 6.3.** Summary diagram of paleoseismic data from trench and landscape dates combined with possible earthquake rupture ages from the record of tree recolonisation (green).

In the east of the study area we have recognised tree damage (Plots 11-14) and faulting (near Plot 14) related to the AD 1888 earthquake event. This earthquake generated strong shaking effects as far west as Plot 3, though we expect that the surface faulting extended as far west as near Plot 14 at Lodge Stream. Therefore, there are two possible candidates for a distinct surface faulting and strong motion event along the western (Hurunui) portion of the Hope Fault in recent times: at c. AD 1760  $\pm$  5 yr and/or at c. AD 1830.

Both of these ages are possible as they: (1) precede widespread colonisation of New Zealand by Europeans, i.e. if they had occurred at these times they would have probably been undocumented; (2) fit within the time window of the penultimate faulting event at the Matagouri Flat trench (and if the colluvial wedge was re-faulted then they are likely candidate ages); (3) fit a hypothesis of a sequential series of ruptures from the Alpine Fault toward the northeast, i.e. the seismic unzipping of *Aotearoa* (Langridge 2006).

Two accounts of pre-1840 earthquakes that are documented in Grouden's (1966) "Early New Zealand Earthquakes" that are intriguing are from AD 1773 and 1830. The former account is from the narrative of Captain Fumeaux, part of Captain Cook's party to New Zealand at that time. They recorded that on May 11, 1773 "we felt two severe shocks of an earthquake but received no kind of damage"...."p.m. abt 5, the people at the Tent felt two severe shocks of an earthquake". We can only speculate as to where this earthquake was and how big it may have been, though it appears that it was big enough for both the P and S waves to be felt at Motuara Island in the Marlborough Sounds where they were wintering over (Grouden 1966).

The second event described is in early 1830 in Paihia, Northland. An extract from a letter by Marianne Williams states that "Within these two months we have seen a comet and felt the shock of an earthquake". Again the source and size of this event is unknown. However, as

this part of New Zealand is rather aseismic, it could be assumed that this account relates to a large, distant earthquake event.

The data presented in this study are intriguing but not robust enough in nature to prove many of these remarks. Clearly, there are signals in the forest record that may correspond to surface faulting records that are displayed in the Matagouri Flat trench. The accuracy and precision of the two datasets is not robust enough to provide a positive match of actual events. In summary, there is a strong likelihood that one of the two forest recolonisation signals is related to rupture of the western part of the Hope Fault. In this case, our hypothesis has proved to be correct. However, it is possible that the most recent event was either: (1) before the most recent Alpine Fault event of c. AD 1717, or (2) actually part of the AD 1888 North Canterbury earthquake; though both of these possibilities are not our preferred option.

We cannot easily favour either of the two peak ages over the other; both have arguments that may be considered weak and flawed in certain ways. However, it is likely that the western Hope Fault ruptured at either around c. AD 1760  $\pm$  5 yr and/or around c. AD 1830.

## 6.5 The likelihood and frequency of strong shaking

The investigation of 14 tree plots along the western end of the Hope Fault has occurred at the same time as re-evaluations of the National Seismic Hazard model and Shake Models. In particular, for the area of the central South Island it is possible to view the probabilities of a combined level of shaking from multiple seismic sources for different periods of time, i.e., probabilistic periods of time, e.g. 10% in 50 yr. In Figure 6.4 we can see the best available current knowledge of shaking intensity for central South Island at the level of 10% in 15 yr. This probability roughly equates to the level of shaking in 150 years. This period of time is equivalent to the historic period, i.e. since widespread colonisation of New Zealand by Europeans. This 150-yr "Shake Map" should therefore be a useful comparison to the historic

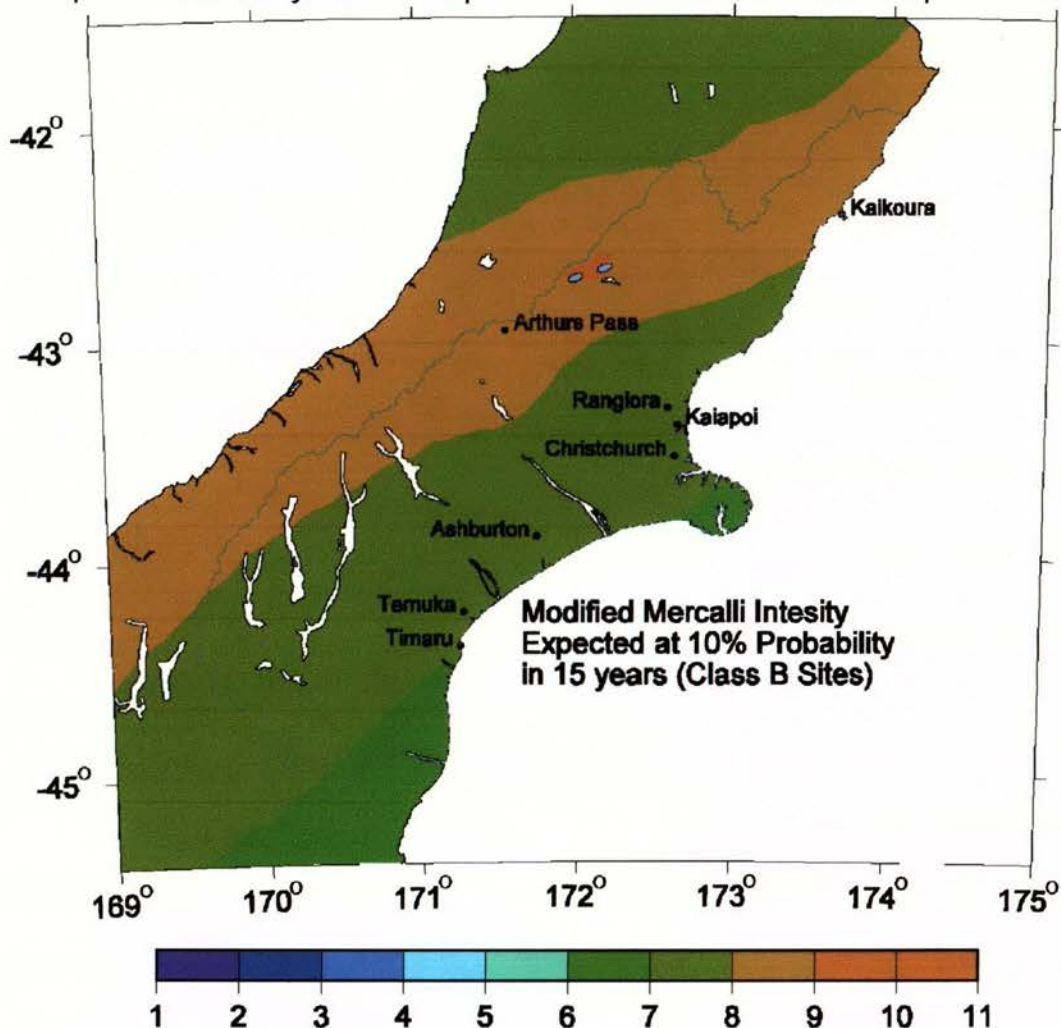


**Figure 6.4.** Cumulative Modified Mercalli Intensity plot for the central South Island developed from data in the National Seismic Hazard Model. This equates to a probability of a certain level of shaking in 150 yr. The two purple ovals (top centre) represent the western and eastern tree plot areas.

record of shaking. It is interesting to note that the entire zone surrounding the Alpine Fault, Main Divide and southern part of the Marlborough Fault System is in a zone of expected MM Intensity 8-9 over a 150 year interval (Fig 6.4). In addition, the two main areas of tree coring along the western Hope Fault occur in an area where the cumulative level of MM Intensity shaking over this period should be MM 9-10. Figure 6.5 tests this model with shaking intensity contours from the 1888 North Canterbury and 1929 Arthur's Pass earthquakes that caused very strong shaking in the upper Hurunui valley. In addition, we have added an

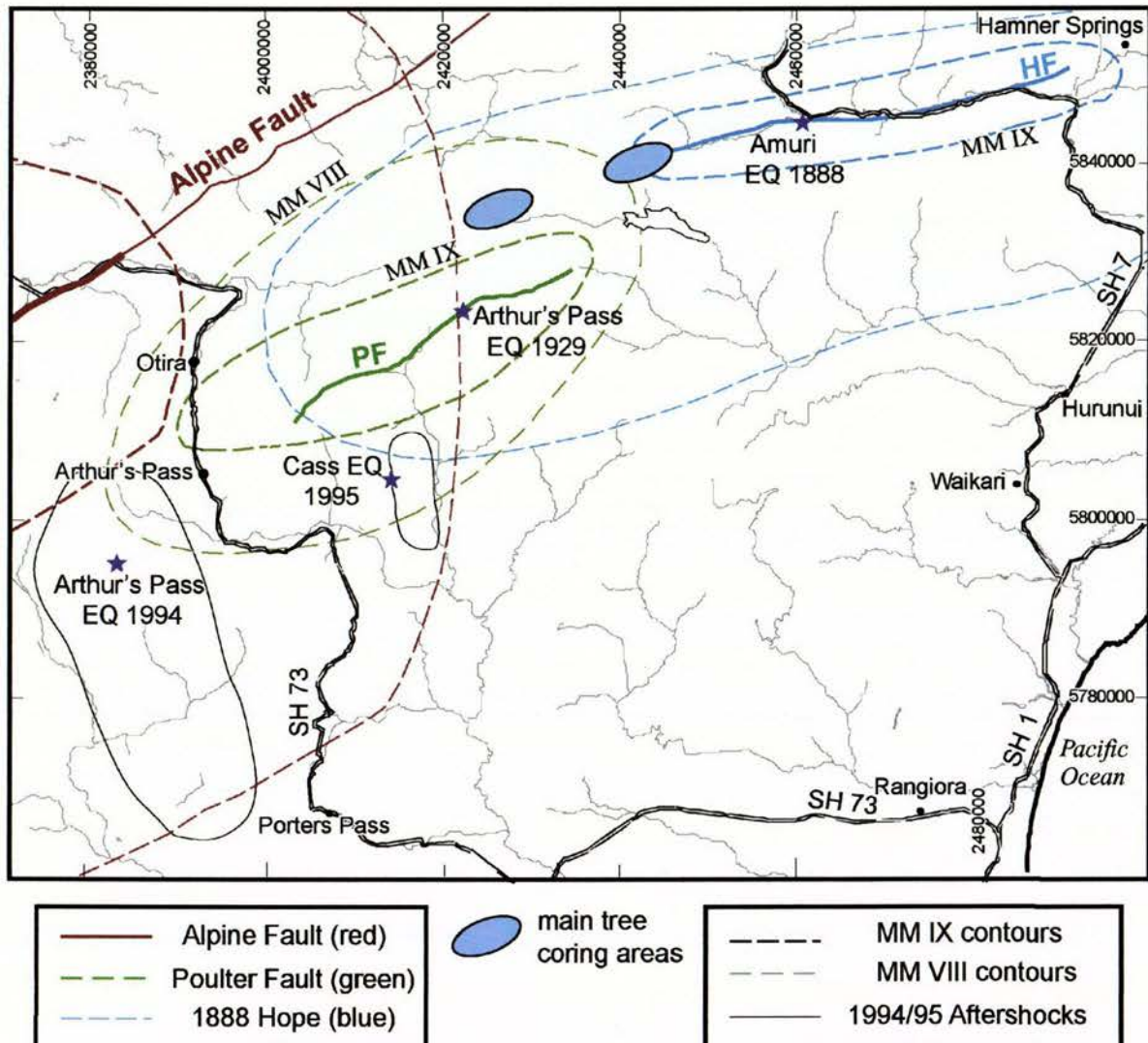


**Figure 6.5.** Modified Mercalli Intensity plot for the Alpine – Hope transition area, central South Island. The two blue ovals represent the western and eastern tree plots in the study area. Faults and their shaking contours are given the same colours, e.g. Poulter Fault and 1929 Arthur's Pass earthquake contours are green. The Hurunui section of the Hope Fault is not shown. The Alpine Fault contours are from an M 8.0 rupture scenario ending at Inchbonnie (see text).

Alpine Fault shaking scenario (Milford-Inchbonnie; Magnitude 8.0) and the aftershock patterns of the 1994 and 1995 earthquakes near Arthur's Pass. This map does not show the western end of the Hope Fault or Kelly Faults, which we have considered as obvious sources in the last 250 years.

In Figure 6.5 we have mapped out the MM IX and VIII contours for the 1888 and 1929 earthquakes. Our tree plot sites sit firmly in areas of MM VIII shaking from the 1888 earthquake and MM VII shaking from the 1929 Arthur's Pass earthquake (Hancox et al. 1997) and Alpine Fault scenario earthquake.

It is clear from Figure 6.5 that the forest in the study area can be hit by multiple seismic sources over short periods of time. If we consider the lifetime of the forest that we have dated in this area, i.e. c. 250 yr of forest, then it is likely that our sites will not only be hit by the Alpine Fault or an 1888 earthquake source, but also a Kelly Fault and western Hope Fault source (if distinct). Thus a 10% in 25 yr analysis of this area would probably place these western and eastern tree plot areas in area of MM Intensity 8-9 as suggested by Figure 6.4.

## 7.0 USING SYNTHETIC SEISMICITY TO MODEL FAULT INTERACTIONS

Deterministic computer models of seismicity can be used to generate very long catalogues of artificial earthquakes. The catalogues are complete and homogeneous, unlike the short, real world catalogues. Insofar as they capture the essential physics of faulting and fault interactions, statistical techniques can be used to answer various questions that could never be addressed otherwise. It is important to realise that the idea is not necessarily to reproduce some specific sequence of known events but to generate a catalogue that captures the overarching features of the seismicity as seen in statistics of event occurrence.

The results presented here are an extension to a previous study of “synthetic seismicity” of the Alpine-Marlborough fault network in the northern South Island (Robinson 2004). Since the details of the fault network are given in that reference, as well as a complete description of the synthetic seismicity computer programme (see also Robinson & Benites 1996, 2001) we describe these only briefly here. The resulting catalogue we analyse here is about twice as long as that in Robinson (2004), so the statistics of fault interaction are better constrained.

### 7.1 The Fault Network

The fault network consists of 36 segments of major faults in the region (Fig. 7.1). Most of the segments represent vertical faults, but some dipping faults are present as well. The main segment of the Alpine Fault dips at  $60^\circ$  to the SE. Segment end points are defined by changes in strike, surface disappearance, and junctions with other faults. All segments are further subdivided into cells of c.  $5 \times 5$  km. The long-term slip rates, and directions, are taken from geologic and paleoseismic studies.

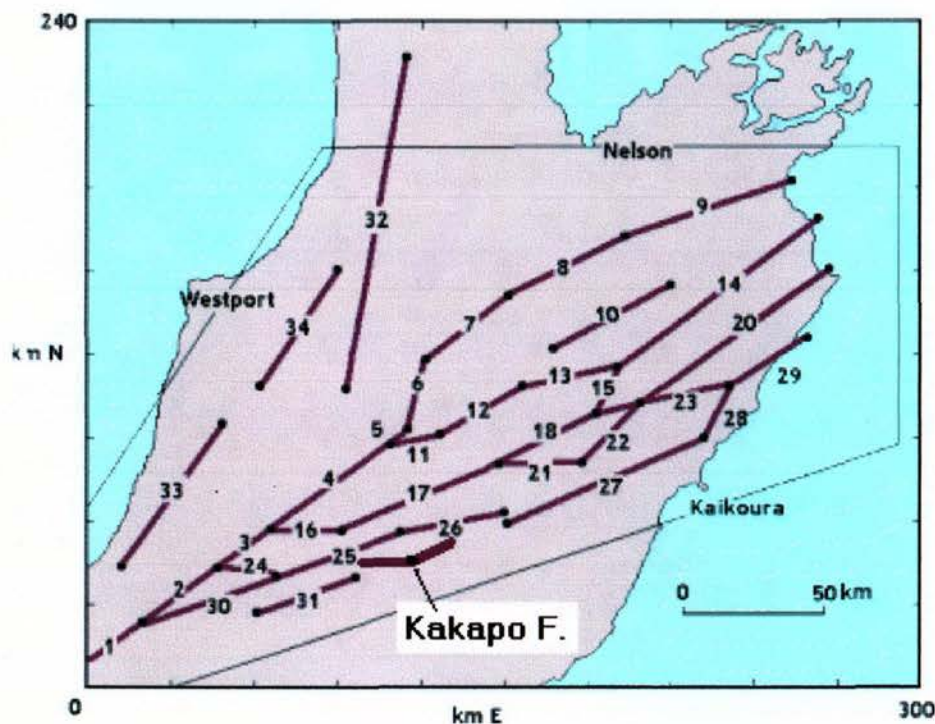


**Figure 7.1.** Major fault segments in the synthetic model. Segments 35 and 36, representing the Kakapo Fault, have been added to the fault network of Robinson (2004). The irregular box shows the region in which 3600 random small faults are distributed.

In addition, there are c. 3600 small faults distributed at random through the region. The strike and dip of these small faults are some small, random perturbation of the strike and dip of the nearest major fault segment. These small faults serve to “fill in the gaps” and create more of a mechanical continuum. The size distribution of the small faults is taken as that required to give a regional b-value of c. 1.0.

The network extension consists of adding two fault segments to represent the Kakapo Fault (Figure 7.1), and correcting an error in one fault’s geometry. The Kakapo Fault carries c. 6-6.8 mm/yr in dextral motion (Yang 1991), which is about 1/3 of the total slip rate for the Hope Fault (system) along this portion of its length (Langridge & Berryman 2005). The Kakapo Fault is in close proximity to the Hope Fault.

## 7.2 The Synthetic Seismicity Model

Several synthetic seismicity models have been developed in recent years (e.g., Ward 2000; Rundle et al. 2006). Our synthetic seismicity model differs from other models in that faults of any orientation and sense of slip are embedded in a 3-D elastic half-space, fault rupture is pseudo-dynamic, the cell size can be small enough that rupture histories can be used to generate strong-motion seismograms, and changes in pore pressure are included. Visco-elasticity can be added but that is not done in the present study. It has been shown that the model can reproduce the various slip features exhibited by real faults (Robinson & Benites 2001).

The model consists of these elements: 1: A geometric description of the faults, as given above; 2: a driving mechanism that loads the faults toward failure; 3: fault failure based on the Coulomb Failure Criterion; 4: static/dynamic frictional behaviour with healing; and 4) fault interactions via induced static stress changes and induced changes in pore pressure. The basic idea is that once one cell fails due to loading it may or may not induce slip on other cells due to induced changes in stress; the more cells involved the bigger the synthetic event. Thus the model is deterministic, not stochastic, once the initial conditions are specified.

Various model parameters are adjusted so that the model fault’s long-term displacement rates (and senses of slip) closely match the observed rates. Also, the regional b-value should be close to 1.0, and the characteristic events have the same amount of slip as observed. A further condition is that fault ruptures can jump across a fault offset of 0.5 km 50% of the time, as observed. These conditions are sufficient to closely constrain the free parameters, although much trial-and-error is needed to find the best values.

In the present model, the friction is a simple static/dynamic type, with healing after a few seconds, as described by Heaton (1990) and Somerville et al. (1999). Cells can fail more than once in a single event. The lack of any time dependence (except healing and pore pressure decay) means that most events such as aftershocks occur at the same time as the inducing event. A more realistic friction law would spread them out more in time. So in the model, immediately induced events should be considered as having their time uncertain by something like 3 years, a typical aftershock sequence duration.

In this study the driving mechanism is “transpression” in accord with plate convergence, with the rates of stress accumulation adjustable to result in the observed slip rates and directions. The model includes a “dynamic enhancement factor” that is intended to emulate the effect of

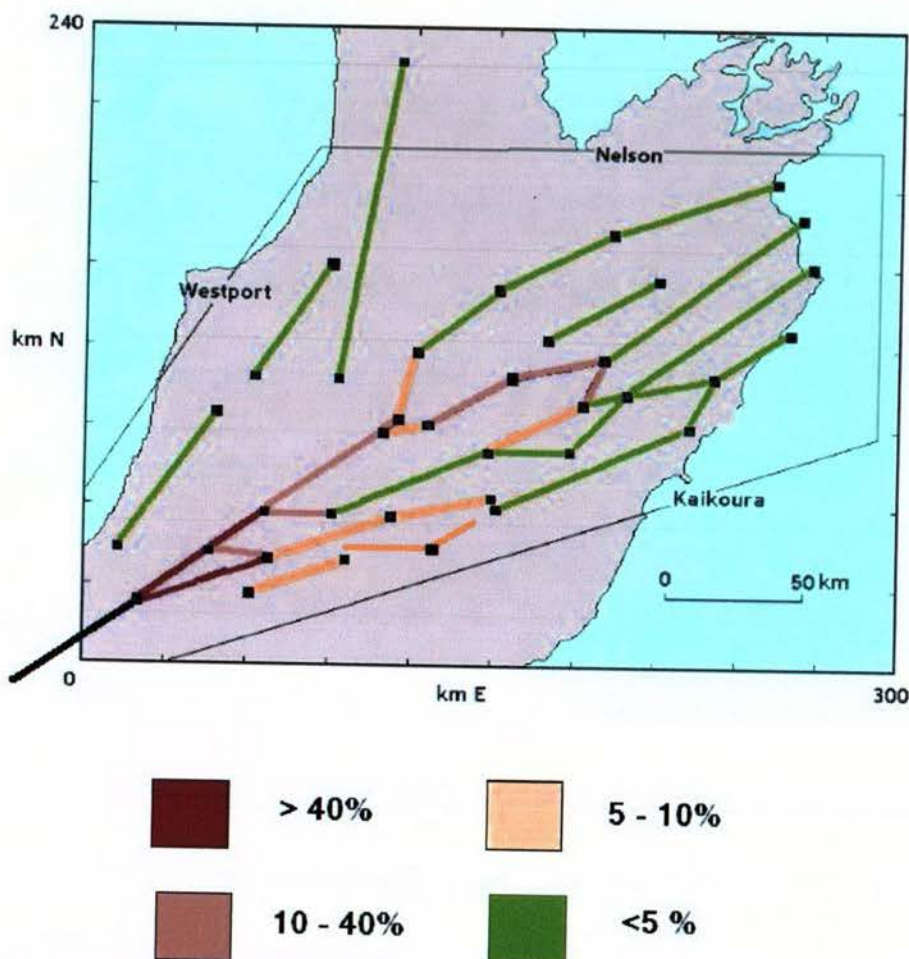


**Figure 7.2.** Probabilities of rupture on faults following the main segment of the Alpine Fault (black) triggering significant activity elsewhere (aside from on lots of small faults) within a period of 3 years.

dynamic rupture stress increases at the edge of a propagating crack. It operates only on cells immediately next to a slipping cell and for only a very short time. Its value was determined in previous studies (e.g., Robinson 2004) by requiring that a rupture be able to jump a fault offset of 0.5 km 50% of the time.

The initial parameters include the coefficient of dry friction for each cell (random between 0.7 and 0.8), a specified stress drop on failure (uniformly 15%), and a hydrostatic pore pressure. Initial cell stress levels are randomly set to between 80 and 90% of the failure level. A standard upper crust rigidity is used. Once the model run begins, there are two time scales. The first is long-term, in which the stresses are incremented in one time step to give failure on the cell closest to failure. Once the event starts, time is stepped in increments of 0.2 sec. Induced stress changes propagate at the S-wave velocity. This means that it is possible to extract a very detailed picture of the progress of a large rupture if required for other purposes.

### 7.3 Alpine – Hope Fault Interaction

In this study we consider a synthetic catalogue of 7,000,000 events, magnitude 4.8 to 8.2, representing c. 560,000 years. The fault network, of course, cannot evolve in time as would a real network. The long duration of the catalogue is just so that all modes of interaction are sampled many times. We note that because the initial conditions do not represent a stable network configuration, some catalogue time has to elapse before analysis can begin

(~10,000 years here). The duration of this initial transient state is evident in a b-value vs. time plot.

Once the initial transient period has passed, the regional b-value settles down to a value close to 1. Because of the model parameters (primarily stress drop and dynamic enhancement factor) most major segments behave in a “characteristic” way, i.e. a substantial fraction of events on the segment cascade into large, characteristic events (here taken as an event rupturing 90% or more of the cells on a segment). This behaviour is in accord with the “type B” faults in the US Geological Survey Seismic Hazard Map for California. It allows a fairly clear distinction between the characteristic events and lesser events on the same segment.

Figure 7.2 shows the probability of a large event on the ‘Cook’ segment of the Alpine Fault (Milford to Styx River in black) triggering a substantial event (magnitude 6.5 or more) on other segments in the model within three years. Remember that instantaneous triggering in the catalogue can be anything from 0 to 3 years. The most probable triggering scenarios, i.e., those with a probability of >40%, are for fault rupture to propagate: (i) onto the Kelly Fault; or (ii) further along the Alpine Fault, past the junctions with the Kelly Fault (at the Styx River) and Hope Fault (at the Taramakau River). This second example of high probability triggering is terminated at the junction between the Alpine and Clarence faults. Triggered rupture on the western part of the Hope Fault, east of Harper Pass within 3 yr of an Alpine Fault event is far less likely (5-10 %). However, if triggered activity on the Kelly Fault itself occurred following an Alpine Fault, then there is likely to be an elevated probability of continued along strike rupture through the Hope Fault system. We have not assessed this dynamic continuation.

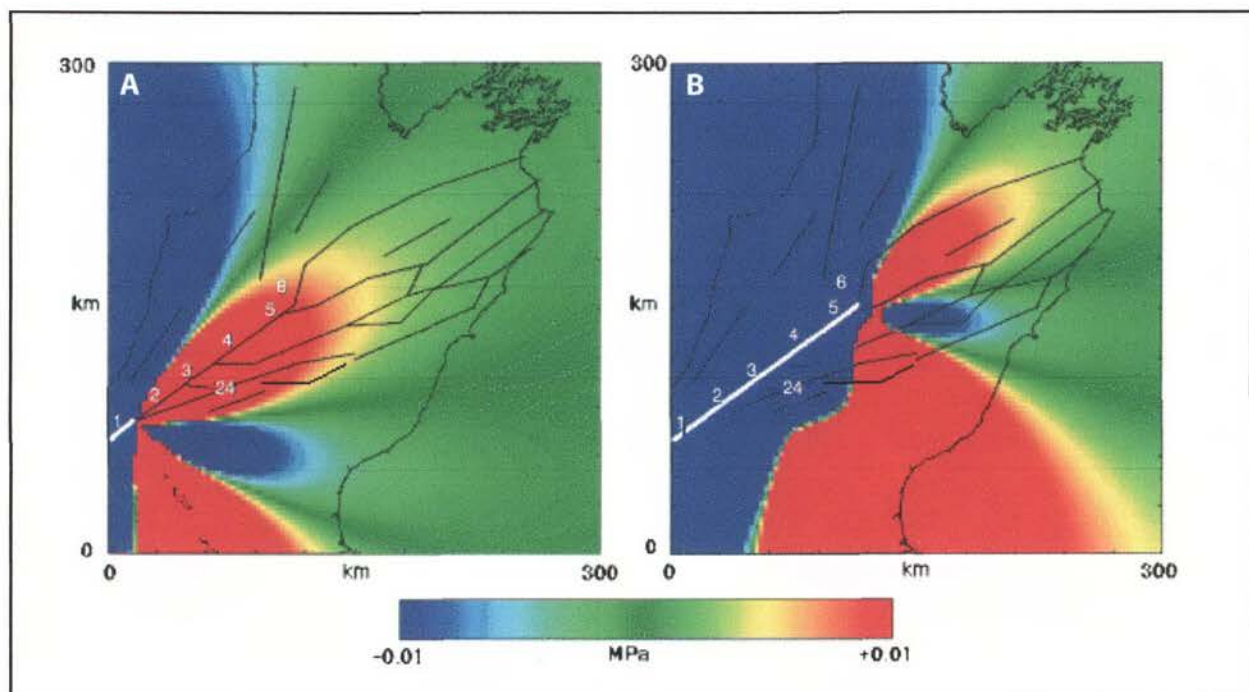


**Figure 7.3.** Changes in Coulomb Failure Stress on faults oriented like the western Hope Fault due to rupture on the Alpine Fault. A – If rupture stops at the Alpine-Hope juncture near the Styx River; B – If rupture continues along the Alpine Fault to the NW to the Maruia River.

These results can be examined more closely by looking at the changes in induced Coulomb Failure Stress placed on faults oriented like the Hope Fault following rupture of the Alpine Fault in Westland (Fig. 7.3) (Robinson, 2004). In the first example (Fig. 7.3a), the Alpine Fault rupture is terminated at its junction with the Kelly Fault near the Styx River. This yields a positive (red) change in Coulomb Stress across a wide region to the north and east of the fault termination, including a significant part of the western Marlborough Fault System. In particular, the Kelly and Hope Faults are favourably aligned to have significant increases in Coulomb Failure Stress as a result of a 'Cook' segment rupture of the Alpine Fault. In Figure 7.3b, a different Alpine Fault rupture scenario is posed, in which the rupture continues to the northeast to the junction of the Alpine and Awatere faults. In this case, parts of the Kelly Fault, western Hope Fault and western Clarence Fault nearest to the junction with the Alpine Fault become relatively de-stressed. At the same time, it appears that the Hope River (1888) segment of the Hope Fault and the Kakapo Fault have an elevated Coulomb Failure Stress.

#### 7.4 Summary

A new version of the Synthetic Seismicity of the Marlborough region has been developed that includes the Kakapo Fault and its relationship with the Hope Fault. There are two new model runs that have been made from the revised fault network. The first model run demonstrates that if the northeastern termination of the Alpine Fault occurs near the Styx River (junction with Kelly Fault), as suggested by arguments of slip rate transfer, then the likelihood of failure due to an elevated Coulomb Failure Stress (CFS) is high (>40 %) for the two sections of the Alpine Fault immediately to the northeast of that point, and the Kelly Fault. There is also an elevated CFS region over a large part of the western Marlborough Fault System under this scenario.

In contrast, the second model run shows that for a longer Alpine Fault rupture (northeast to the Maruia River area), that, within 3 years of such an event, there is an elevation in CFS toward the Awatere Fault and Hope River (1888) segment of the Hope Fault, but diminished CFS in the area of the Kelly and western Hope Faults.

This analysis shows that for a sequence of large earthquakes to have occurred along the western end of the Hope Fault system, including the Kelly Fault, then it is more likely that such a sequence would occur as a consequence of an Alpine Fault rupture that terminates near the Styx River area.

## 8.0 SUMMARY & CONCLUSIONS

Scientists from GNS Science, Lincoln University and Landcare have undertaken a four-pronged, EQC-funded research project to consider the timing of the most recent faulting event(s) on the western (Hurunui) section of the Hope Fault, South Island, and the implications of this result on the understanding of fault failure processes between the Alpine and Hope Faults. The four research tools we have applied are (i) geomorphic and soil age approaches to understanding landscape change; (ii) a traditional paleoseismic approach, e.g. excavating a trench; (iii) a dendrochronologic study of tree plots along and adjacent to the Hope Fault; and (iv) a reanalysis of synthetic seismicity to devise a Coulomb Failure Stress model for the western Marlborough region. We have also considered historic observations of the large 1888 and 1929 earthquakes in the area.

Geomorphic observations coupled with radiocarbon dates and soil age estimates show that all of the surfaces that we have investigated in this study are of late Holocene age (generally <2500 yr) and some may have developed as recently as AD 1888. Two soil pits and additional soil exposures studied in association with tree plots support this age range and give independent results for the antiquity of forest stands and forest soils. Radiocarbon dates on a fallen tree, swamp-drowned tree, and faulted log all give young ages (<300 yr) that confirm there have been recent major landscape events in the vicinity of the western Hope Fault that we generally attribute to large earthquakes. A hand-dug trench on Matagouri Flat provides evidence for at least two surface faulting events during the last c. 650 yr at that locality. The penultimate event was probably since AD 1297-1425; the most recent faulting event was probably since AD 1458-1655. Some sympathetic, dm-scale faulting may have occurred since then (1888?) to re-fault the uppermost colluvial wedge in the trench.

Chapter 3 of this report outlines how we developed a strategy for site selection of 14 dendrochronology (tree ring counting) plots along and adjacent to the Hope Fault in the study area. We also describe the methodology used for coring trees and preparing the cores for ring count analysis. We also broadly describe the two main geomorphic types of tree plots: fault scarp; and alluvial plots, and describe the general results of the entire tree ring dataset.

We cored over 250 Red, Silver and Mountain Beech trees at 14 plots in the study area. We achieved a set of untreated tree age results from 207 trees<sup>3</sup>. The oldest dated tree in the study area had 402 rings. In general terms, the results show that: (i) Red (*Nothofagus fusca*), Silver (*N. Menziesii*) and Mountain (*N. Solandri*) Beech have similar, though distinct average growth rates; (ii) plots in the forest have a typically young and even aged appearance; (iii) the entire tree age and size datasets show bi- to multimodal peaks; and (iv) there were only a handful of trees that yielded ages of >300 rings (yr) or <80 rings.

The plots were divided into a western group (Plots 1-10) accessed via Lakes Station, and an eastern group (Plots 11-14) accessed via Glynn Wye Station. At each plot a map shows the site geomorphology and layout of each tree with respect to landscape features, and other trees, marked by their species and size. Between 16 to 20 trees were cored at each plot to yield reasonable individual plot and total tree count statistics. Plots 1, 2 and 3 are the westernmost plots, being located near Landslip Stream on the fault scarp, toe of a fan and on a rangefront blockslide deposit, respectively. Plot 9 is a rangefront fan site near those three

<sup>3</sup> these ages do not consider the uncertainty of the age measurement on trees where the tree centre was not intercepted.

plots and the trench site at Matagouri Flat. Plots 5, 6, 8 and 10 were all situated along or across the scarp of the Hope Fault on the broad c. 2500 year old McKenzie fan. Plot 7 was situated on a sidevalley fan, c. 2 km upstream from the fault in the valley of McKenzie Stream. Plot 4 was another rangefront fan site above 'The Park'.

Plots 11-14 were accessed on foot from Hope-Kiwi Lodge. Plots 11 and 14 were at Parakeet Saddle and Lodge Stream, respectively, while plots 12 and 13 were situated near Three Mile Stream Hut at rangefront apron and fan localities. Discussions of the characteristics of each plot are reviewed in Chapter 4. The tree ages presented here have no age uncertainty attached to them. Therefore, the results presented there are biased toward minimum ages.

In Chapter 5, we have developed a more rigorous approach to uncertainty taking into consideration the actual quality of each tree core age. Tree ages were divided into (C)entre, (A)rc or (S)hort tree ring counts. Short core tree age results were eliminated from the dataset as minimum tree ages. In Chapter 5 we also scrutinised the results from individual plots in great detail to attempt to extract meaningful signals of forest damage or colonisation cohorts. The 14 plots have been separated into two similar clusters of plots based on the tree age structures they possess. Cluster 1 consists of Plots 8, 1, 4, 9, 2, 13, 6 and 5. Cluster 2 consists of Plots 14, 10, 12, 11, 7 and 3. In general, in a geographic sense there is a tendency for Cluster 1 plots to be in the west and for Cluster 2 to contain the eastern plots.

However, there is overlap of events along the length of the study area. Cluster 1 has tree establishment peaks in the mid 19<sup>th</sup>, mid 18<sup>th</sup> and early 18<sup>th</sup> centuries. There is no apparent forest signal at these plots for the 1888 earthquake. We infer that the three peaks relate to very strong shaking nearby, from surface rupture of the western Hope Fault; and possibly the c. AD 1717 rupture of the Alpine Fault. Troughs in the dataset are probably indicative of relative site stability in the forest for many decades at a time. In the absence of other widespread agents of forest change, we equate these troughs to inter-seismic shaking intervals. Using troughs and offset times for colonisation we present a possible large earthquake age in the mid-19<sup>th</sup> century of AD 1830 for the western plots.

Cluster 2 plots are characterised by a c. 100 ring peak and two smaller peaks at c. 180 and 220 rings (yr). There is apparently no mid-19<sup>th</sup> century peak at these plots. We have recognised that several plots provide control data on the rates of cohort colonisation and tree growth at sites varying in their tree ages, substrate age, elevation, location and tree species. Assumptions built from these data allow us to suggest that: (i) the c. 100 yr peak is a strong 1888 earthquake signal; (ii) the 220 yr peak corresponds to the mid-18<sup>th</sup> century peak observed at Cluster 1 plots. This event has been precisely dated at Plot 12, and occurred at c. AD 1760 ± 5 yr; (iii) the 180 yr peak is partially due to the long colonisation time for Mountain Beech trees at the high elevation Parakeet Saddle site, and may in fact correlate with the Plot 12 event.

By combining data from the Matagouri Flat trench with landscape indicators it appears that the penultimate faulting event caused 5-6 m of dextral displacement there and occurred after AD 1297-1425. This event is almost certainly not captured in the forest record unless the oldest trees dated in the forest (c. 400 yr old) colonised surfaces following an event at that time. Based on faulting and age relationships in the trench and nearby exposures, and the age of a sample from a swamp-drowned Red Beech, the most recent faulting event in the upper Hurunui valley occurred since AD 1516-1655. This may coincide with the death of the Red Beech (DB1) at Plot 12 (AD 1690-1730) and the faulted log LSW at Lodge Stream. The age derived for this event from the tree plot (12) where DB1 was found is c. AD 1760 ± 5

based on the age of the tree cohort that colonised a debris flow that has backed up against this tree. This is a candidate age for the most recent surface faulting event for the Hurunui section of the Hope Fault. If this indeed represents the 'Hurunui' rupture age then it comes some 48-58 years after the last Alpine Fault rupture event farther to the southwest.

Very strong shaking from a mid-19<sup>th</sup> century event probably caused forest damage that affected up to 8 of the 14 tree plots. Five of the tree plots show evidence of a strong shaking signal from the 1888 North Canterbury earthquake. We believe that the 1888 event is not well identified in the trench (perhaps as sympathetic slip?), nor in the landscape in the form of moderate to large landslips – for the upper Hurunui valley. Thus, we conclude that while there are signs of landscape and forest damage at sites and plots in the study area, that the 1888 surface faulting probably finished somewhere near the Hope-Kiwi Lodge, such as near the Lodge Stream site.

There are few to no indicators of forest or landscape damage resulting from the M 7.1 1929 Arthur's Pass earthquake which ruptured the Poulter Fault, a mere 6-8 km from the majority of our sites and plots. We have no clear explanation for the persistent mid-19<sup>th</sup> century peak in the tree ring dataset. While we would lean toward a seismic source, e.g. 1848 Marlborough or 1830's Conway segment rupture, both of these events should be too distant to have caused such obvious damage to the forest there. We propose a second candidate time for the rupture of the western Hope Fault, based on the predominance of a forest signal in the western plots at around AD 1830. We could speculate that this event was on another fault, such as the Kelly Fault.

A new model of the Synthetic Seismicity of the Marlborough region has been developed that includes the Kakapo Fault. The model shows that for a longer Alpine Fault rupture (NE to Maruia River), that, within 3 years of such an event, there an elevation in Coulomb Failure Stress (CFS) toward the Awatere Fault and Hope River segment of the Hope Fault, but diminished CFS in the area of the Kelly and western Hope Faults. However, if the northeastern termination of the Alpine Fault occurs near the Styx River (junction with Kelly Fault), then the likelihood of failure due to an elevated CFS is raised for the next sections of the Alpine Fault and the western ends of all of the Marlborough faults, including the Kelly and western Hope faults.

The data in this study suggest that the western Hope Fault ruptured some c. 50-115 yr after the Alpine Fault (c. AD 1717), followed later by the Hope River segment of the Hope Fault (another c. 50 yr later) in September 1888. Clearly, the process of stress triggering gives us a good indicator of the future patterns of faults likely to rupture. However, the time scales of several years (e.g. AD 1848 to 1855) to decades (e.g. AD 1717 to 1764 to 1888) suggest that a simple elastic CFS process may not be warranted for New Zealand faults at this time.

In summary, this project has identified that the most recent earthquake event along the Hurunui section of the Hope Fault occurred at either c. AD 1765 or c. 1832. These ages are consistent with data from a trench, from landscape observations including landslides in the ranges and is remarkably consistent with the data set of lichens growing on rockslides and rockfalls through out the Marlborough and Southern Alps regions.

There is little evidence that surface faulting from the 1888 North Canterbury earthquake extended farther west than that described by Alexander McKay (1890). The forest and landscape shows virtually no signal from the 1929 Arthur's Pass earthquake despite its proximity, and only patchy evidence of forest damage from the 1888 earthquake, particularly

in the west. Following this logic, the 1848 Marlborough and eastern Hope Fault ruptures (1830's ?) should have been too distant to have left their mark on the forest along the western Hope Fault. Consequently, we attribute the strong age signal pointing to a significant forest event, at particularly the western sites, in the mid-19<sup>th</sup> century to rupture of another nearby fault, perhaps the Kelly Fault. This also may explain why the forest along the western end of the Hope Fault shows about twice as many forest damage events as are expressed in the shallow trench at Matagouri Flat, i.e. the forest there is hit by multiple seismic sources. It is possible that spatially, the east and west-dominant signals in the forest record of the Hurunui section point toward rupture and shaking caused by the Hope River (1888 earthquake) section of the Hope Fault and Kelly Fault, respectively.

In contrast, there has been no significant forest damage event through the study area since the AD 1888 North Canterbury earthquake. Aside from a lack of damage from either large earthquakes in 1929, this is in keeping with the historic record which is generally lacking in large shallow earthquakes in the central South Island. Perhaps the most instructive conclusion of the dendrochronological part of this study is that the forest in the area was hit by multiple earthquake events between AD 1717 and 1888, and has not been significantly damaged since. The repeat time for strong shaking of MM VIII or greater along this part of the fault in the period since the 1717 Alpine Fault earthquake and including the 1994 Arthur's Pass earthquake is c. 60 yr, as is shown in probabilistic Mercalli Intensity maps.

The elapsed time since the most recent faulting event is at least c. 170 yr. This compares to an average published recurrence estimate of 310-490 yr for the Hurunui section of the Hope Fault. The trench dug at Matagouri Flat tells us that there have been 2 and possibly 3 earthquake ruptures between c. AD 1460-1888, while the forest record suggests that there have been 3 and possibly 4 major forest damaging (seismic shaking?) events during the period AD 1717-1888. These give simple recurrence ranges of 214-428 yr and 57-85 yr, respectively.

## 9.0 REFERENCES

- Anderson H, Webb T, Jackson JA 1993. Focal mechanisms of large earthquakes in the South Island of New Zealand: Implications for the accommodation of the Pacific-Australia Plate motion, *Geophysical Journal International* 115: 1032-1054.
- Barka A 1992. The North Anatolian fault zone. *Annales Tectonicae* 6: 164-195.
- Barka A., Akyuz HS, Sunal G, Çakir Z, Dikbas A, Yerli B, Altunel E, Armijo R, Meyer B, Chebalier JB, Rockwell T, Dolan JR, Hartleb R, Dawson T, Christofferson S, Tucker A, Fumal T, Langridge R, Stenner H, Lettis W, Bachhuber J, Page W The Surface Rupture and Slip Distribution of the 17 August 17 1999 Izmit earthquake, (M 7.4), North Anatolian Fault. *Bulletin of the Seismological Society of America, Special Volume on the Izmit Earthquake* 92: 43-60.
- Berryman K 1999. Upper plate Quaternary strain rates, kinematics and paleoseismology in the transition from Hikurangi subduction to Southern Alps collision, New Zealand, in: *Subduction to Strike-Slip Transitions on Plate Boundaries*. Geological Society of America Penrose Conference, Keynote Talks and Poster Abstracts, Puerto Plata, Dominican Republic.
- Berryman KR, Beanland S, Cooper AF, Cutten HN, Norris RJ, Wood PR 1992. The Alpine Fault, New Zealand: variation in Quaternary structural style and geomorphic expression. *Annales Tectonicae*, VI, 126-163.
- Berryman KR; Rattenbury M; Isaac M; Villamor P; Van Dissen R 2003. Active faulting and strain at the junction of the Alpine and Hope Faults, New Zealand. *Geological Society of New Zealand Miscellaneous Publication* 116A: 18.
- Berryman K, Villamor P 2004. Surface rupture of the Poulter Fault in the March 9, 1929 Arthur's Pass Earthquake, and re-definition of the Kakapo Fault, New Zealand *Journal of Geology and Geophysics* 47: 341-351
- Bibby, H. M. 1976: Crustal strain across the Marlborough Faults, New Zealand. *New Zealand Journal of Geology and Geophysics* 19: 407-25.
- Boume SJ; T Amadottir, J Beavan, DJ. Darby, PC. England, B Parsons, RI Walcott, PR Wood 1998. Crustal deformation of the Marlborough fault zone in the South Island of New Zealand: Geodetic constraints over the interval 1982-1994. *Journal of Geophysical Research*, 103, 30-147-30,165.
- Bull WB 2003. Lichenometry dating of coseismic changes to a New Zealand landslide complex. *Annals of Geophysics* 46: 1155-1168.
- Bull W, Brandon MT 1998. Lichen dating of earthquake-generated regional rockfall events, Southern Alps, New Zealand. *Geological Soc. of America Bulletin* 110: 60-84.

- Browne GH 1987: Geological comments on the Lake Sumner-Harper Pass area, Southern Alps. Immediate Report, New Zealand Geological Survey, Christchurch.
- Clayton L 1968. Late Pleistocene glaciations of the Waiiau Valleys, North Canterbury. *New Zealand Journal of Geology and Geophysics* 11: 753-767.
- Cowan HA 1989. An evaluation of the late Quaternary displacements and seismic hazard associated with the Hope and Kakapo faults, Amuri District, North Canterbury. Unpublished MSc Engineering Geology thesis, lodged in the Library, University of Canterbury. 239 p.
- Cowan HA 1991. The North Canterbury earthquake of September 1, 1888. *Journal of the Royal Society of New Zealand* 21: 1-12.
- Cowan HA, McGlone MS 1991. Late Holocene displacements and characteristic earthquakes on the Hope River segment of the Hope fault, New Zealand. *Journal of the Royal Society of New Zealand* 21: 373-384.
- DeMets C, Gordon RG, Argus DF, Stein S 1994. Effect of recent revisions to the geomagnetic reversal time scale on estimates of current plate motions. *Geophysical Research Letters* 21:2191-2194.
- Downs GL, Dowrick, DJ, Van Dissen RJ, Taber JJ, Hancox GT, Smith EGC 2001. The 1942 Wairarapa, New Zealand, earthquakes: analysis of observational and instrumental data. *Bulletin of the New Zealand Society for Earthquake Engineering*, 34(2): 125-157.
- Duncan RP 1989. An evaluation of errors in tree age estimates based on increment cores in kahikatea (*Dacrycarpus dacrydioides*). *New Zealand Natural Sciences* 16: 31-37).
- Freund R 1971. The Hope Fault: A strike-slip fault in New Zealand. *New Zealand Geological Survey Bulletin* 86, 49 p.
- Hancox GT, Perrin ND, Dellow GD 1997. Earthquake-induced landsliding in New Zealand and implications for the MM Intensity and Seismic Hazard Assessment. GNS Science Client Report 43601B.
- Hancox GT, Perrin ND, Dellow GD 2002. Recent studies of historical earthquake-induced landsliding, ground damage, and MM intensity in New Zealand. *Bulletin of the New Zealand Society for Earthquake Engineering*, 35(2): 59-95
- Heaton T 1990. Evidence for and implications of self-healing pulses of slip in earthquake ruptures. *Physics of the Earth and Planetary Interiors* 64, 1-20.

- Holt WE, Haines AJ 1995. The kinematics of northern South Island, New Zealand, determined from geologic strain rates. *J. Geophysical Research* 100: 17,991-18010.
- Knuepfer PLK 1992. Temporal variations in latest Quaternary slip across the Australian-Pacific plate boundary, northeastern South Island, New Zealand. *Tectonics* 11: 449-464.
- Langridge RM 2004. How is tectonic slip partitioned from the Alpine Fault to the Marlborough Fault System? – Results from a FRST Post-Doctoral Fellowship, GNS Science Science Report 2004/32. 18 p.
- Langridge RM 2006. Historic and Pre-Historic uNZipping of the New Zealand Plate Boundary. 100<sup>th</sup> Anniversary Earthquake Conference. Commemorating the 1906 San Francisco Earthquake. SSA Publication.
- Langridge RM, Stenner HD, Fumal TE, Christofferson SA, Rockwell TK, Hartleb R, Bachhuber J, Barka AA 2002. Geometry, slip distribution, and kinematics of Surface rupture on the Sakarya fault segment during the August 17, 1999 Izmit earthquake. *Bulletin of the Seismological Society of America* 92: 107-125.
- Langridge RM, Berryman KR 2005. Morphology and slip rate of the Hurunui section of the Hope Fault, South Island, New Zealand. *New Zealand Journal of Geology and Geophysics* 48: 43-57.
- Langridge RM, Campbell J, Pettinga J, Hill N, Pere V, Estrada B, Berryman K 2003. Paleoseismology and Slip Rate of the Conway Segment of the Hope Fault at Greenburn Stream, South Island, New Zealand. *Annals of Geophysics* 46: 1119-1139.
- Lettis W, J Bachhuber, R Witter, C Brankman, CE Randolph, A Barka, WD Page, and A Kaya, 2002. Influence of Releasing Step-overs on Surface Rupture and Fault Segmentation: Examples from the 17<sup>th</sup> August, 1999 Izmit Earthquake on the North Anatolian Fault, Turkey. *Bulletin of the Seismological Society of America* 92: 19-43.
- McCormac FG; Palmer JG; Xiong L; Pilcher, JR; Brown, D; Hoper, ST.; Hogg, AG; Higham, TFG.; Baillie, M 1998: Variations of radiocarbon in tree rings: Southern hemisphere offset preliminary results. *Radiocarbon* 40: 1153-1159.
- McKay A 1890. On the earthquakes of September 1888, in the Amuri and Marlborough Districts of the South Island. N. Z. Geological Survey Report of Geological Explorations 20: 1-16.
- Nathan S; Rattenbury MR, Suggate RP (compilers) 2002: Geology of the Greymouth area., Institute of Geological and Nuclear Sciences 1: 250 000 geological map 12. 1

- sheet + 65 p. Lower Hutt, New Zealand: Institute of Geological and Nuclear Sciences.
- Perrin ND, Hancox GT 1992. Landslide dammed lakes in New Zealand – Preliminary studies on their distribution, causes and effects. In, Landslides, Bell (ed.). Balkema, Rotterdam.
- Pettinga, JR; Chamberlain CG.; Yetton, MD; Van Dissen, RJ; Downes G 1998: Earthquake Source Identification and Characterisation: Stage 1 (Part A) Earthquake Hazard and Risk Assessment Study'. Canterbury Regional Council CRC Publication No. U98/10: 121 pages and 6 Appendices.
- Pettinga J.R; Yetton MD; Van Dissen R.J.; Downes G 2001. Earthquake Source Characterisation for the Canterbury Region, South Island, New Zealand. Bulletin of the New Zealand Society for Earthquake Engineering 34: 282-317.
- Pope JG 1994. Secondary structures, Holocene displacements and paleoseismicity of the Conway segment of the Hope fault, Greenburn Stream to Sawyers Creek. Unpublished BSc (Hons) project. Geological Sciences Library, University of Canterbury, Christchurch, New Zealand.
- Reyners M; H Cowan 1993. The transition from subduction to continental collision: crustal structure in the North Canterbury region, New Zealand. Geophysical Journal International 115: 1124-1136.
- Robinson R 2004. Potential Earthquake Triggering in A Complex Fault Network: The Northern South Island, New Zealand. Geophysical Journal International 159: 734-748.
- Robinson R, Benites R 1996. Synthetic Seismicity Models for the Wellington Region, New Zealand: Implications for the Temporal Distribution of Large Events", Journal of Geophysical Research 101: 27,833-27,845.
- Robinson R, Benites R 2001. Upgrading a synthetic seismicity model for more realistic fault ruptures. Geophysical Research Letters 28: 1843-1846.
- Robinson R, McGinty, P 2000. The enigma of the Arthur's Pass, New Zealand, earthquake, 2: The aftershock distribution and its relation to the regional and induced stress fields. Journal of Geophysical Research, 105: 16,139-16,150.
- Rundle J. et al., 2006. Virtual California: Fault model, friction parameters, and applications. Pure and Applied Geophysics, 163, 1819-1846.
- Schwartz DP., Sibson, RH (editors) 1989: Proceedings of Conference XLV; A workshop on Fault segmentation and controls of rupture initiation and termination. U. S. Geological Survey *Open File Report*, OF 89-0315, Palm Springs, CA, USA.
- Somerville P et al. 1999. Characterizing crustal earthquake slip models for the prediction of strong ground motion. Seismological Research Letters 70: 59-80.

- Stein RS, Barka AA, Dietrich JH 1997. Progressive failure on the North Anatolian fault since 1939 by earthquake stress triggering. *Geophysical J. Intl.* 128: 594-604.
- Suggate RP 1965. Late Pleistocene geology of the northern part of the South Island, New Zealand. *New Zealand Geological Survey Bulletin 77*. NZ Dept. of Scientific and Industrial Research, Wellington, New Zealand, 91 p..
- Van Dissen R, Yeats RS 1991. Hope fault, Jordan thrust, and uplift of the Seaward Kaikoura Range, New Zealand. *Geology* 19: 393-396.
- Ward S 2000. San Francisco Bay area earthquake simulations: A step toward a standard physical earthquake model. *Bulletin of the Seismological Soc of America* 90: 370-386.
- Wells A, Duncan RP, Stewart GH 2001. Forest dynamics in Westland, New Zealand: the importance of large, infrequent earthquake-induced disturbance. *Journal of Ecology* 89: 1006-1018.
- Wells A, Yetton MD, Duncan RP, Stewart GH 1999. Prehistoric dates of the most recent Alpine fault earthquakes, New Zealand. *Geology* 27: 995-998.
- Whitehouse IE, Griffiths GA 1983. Frequency and hazard of large rock avalanches in the central Southern Alps, New Zealand. *Geology* 11: 331-334.
- Yang, J. S. 1991: The Kakapo Fault – a major active dextral fault in the central North Canterbury –Buller regions of New Zealand. *New Zealand Journal of Geology and Geophysics.* 34, 137-143.
- Yetton MD, Wells A, Traylen NJ 1998. The probability and consequences of the next Alpine Fault earthquake. EQC Research Report 95/193.

## 10.0 ACKNOWLEDGEMENTS

Primarily, the authors wish to thank the Earthquake Commission for the vision to fund this project, to investigate the critical link between the highest slip rate and seismic hazard areas of South Island. We also wish to acknowledge Mr. Ted Phipps (Lakes Station), Michael Cox (Glynn Wye Station), and the Department of Conservation (Mr. Wayne King) for permission to access their lands and undertake geologic studies. Some of the initial studies in this project were funded by the Foundation for Science, Research and Technology under the FRST Post-Doctoral Fellowship scheme (# CO5903) and through GNS Science FRST funding sources (Active Faults Transitional).

This work could not have been achieved without the enthusiastic help of Vasso Mouslopoulou (Greece; VUW) Marshall Smith (Lincoln) and Vicente Perez (UAG, Grenada) in the field. Marshall Smith undertook all of the lab preparation and analysis of the tree cores, and for this we are very grateful. We also wish to thank Graham Hancox and Kelvin Berryman for GNS Internal review of this report and for their help and interest during this project.

## APPENDICES

### APPENDIX 1 – Soil Profile Descriptions

#### **Geomorphic, Soil and Forest Age Evidence for Hope Fault Rupture Events 25-27 February 2004**

##### ***Party members:***

Peter Almond, Soil and Physical Sciences Group, Lincoln University;  
Rob Langridge, GNS Science,  
Richard Duncan, Ecology and Entomology Group; Lincoln University

##### ***Introduction***

The intention of the visit was to assess the efficacy of using tree ring ages and soil development indices to interpret the rupture history and slip rate of the Hope Fault in the north branch of the Hurunui River. Trees established on or near the fault trace since the last rupture, or trees disturbed by the last rupture should record the timing of the event in their annual growth rings. Estimates of the age of a geomorphic surface based on the degree of development of soils, and the displacements of geomorphic features on that surface can be used to calculate a slip rate.

##### ***Valley Floor Fans***

##### **Site 1: - Hope 1 (26 February)**

###### Description:

The trace of the Hope fault followed in a westerly direction from an earlier trenching site on the western end of Matagouri Flat (Langridge) passes into a stand of beech forest where it shows approximately 1 m of vertical throw, upthrown to the south. The estimate of throw may well be a minimum owing to possible sediment accumulation on the footwall. Above the fault scarp, prominent windthrow mounds comprising stones and boulders have been colonised by red and silver beech trees (Plate 1). These trees were cored for age estimates (dbh c. 60 cm). Some larger trees growing on the scarp are tilted and show regrowth of canopy branches in adjustment to the tilting. These trees were cored as well. A soil pit (Hope 1) was excavated on the upthrown site of the fault to provide an estimate of the age of the geomorphic surface, which is part of the surface of the fan of Landslip Stream. The degree of development of the soil, which shows incipient podzolisation, suggests an age of a few thousands of years, perhaps 1500 to 4000 years.



**Plate 1.** Red Beech growing on bouldery windthrow mounds above the Hope Fault trace at Hope 1 site



**Plate 2.** Hope 1 soil pit

## Site 2: Hope 2 (25 February)

### Description:

Hope 2 (Plate 3) is an exposure in the bank of Landslip Stream near its confluence with the Hurunui River. The exposure shows a composite Brown Soil representing something in the order of a few thousand years of soil development and sedimentation. The site is covered by red and silver beech forest.



Plate 3. Hope 2 soil exposure

## Site 3 Hope 5 (27 February)

### Description:

A c. 1.8 m thick stream bank section under mixed mountain, silver and red beech forest on the southern margin of the Park exposes multiple buried soils (Plate 4). The upper most is a well developed podsol. The lower most soil is a well developed Brown soil. The soil units in between are relatively weakly developed. The combined period of soil development and sedimentation is estimated to span at least 6000 year

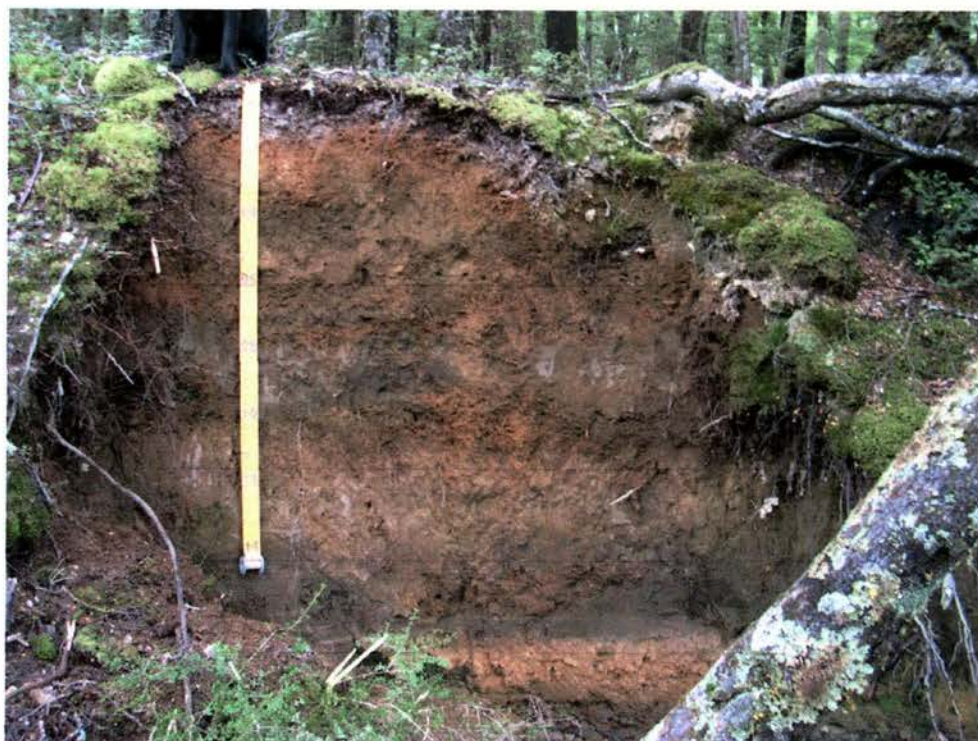


Plate 4. Hope 5 soil exposure

### ***Valley Floor Bog***

#### **McKenzie Bog (informal name)**

##### Description:

A sphagnum and rush bog has formed on the western side of the fan of the McKenzie Stream near the fan apex, apparently as a result of disruption of surface drainage due to one or more displacements on the Hope Fault. The extension of sphagnum into the forest at the margins of the bog suggests that the water table is rising and the bog is extending. The peat is very fluid and fibrous, indicating a weakly decomposed status. At three sites cored by hand auger (Bog 1, Bog 2 and Bog 3, Fig.1) the peat was no deeper than 1.2 m. A small piece of wood from a submerged (red beech?) log was retrieved from the Bog 3 site and will be submitted for radiocarbon dating.

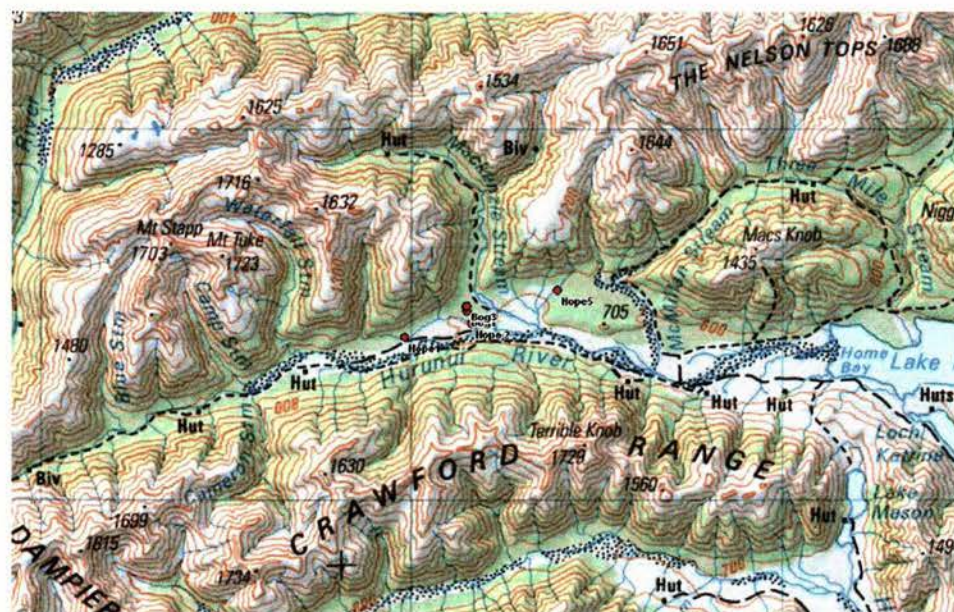
##### ***Summary***

The soil stratigraphy and degree of development of soils on fans in the valley floor of the Hurunui River upstream of Lake Sumner suggest relative stability of these landforms. The exposures examined in detail indicate no deposition or episodic deposition of thin sedimentary units since as early as mid-Holocene. cursory examination of other exposures suggests there are also parts of these fans that have received significant deposition more recently. Poorly developed Brown soils on toes of fans indicate a period of hundreds of years since deposition. In general soils of the flood plain are weakly

developed (Recent) soils, indicating recent and probably frequent inundation and sedimentation.

A bog on the fan of McKenzie Stream appears to have formed relatively recently as a result of disruption of surface and perhaps subsurface drainage by fault displacement. A radiocarbon date from a log buried by peat (submission R. Langridge) will provide a minimum age for the inception of the bog and help constrain the timing of fault rupture events.

### Site Locations (Figure 1)



Soil Name:  
 Profile code: Hope 1  
 NZ Soil Classification: Typic Orthic Podzol  
 NZ Gentic Classification:  
 USDA Soil Taxonomy:  
 Survey: Hope Fault  
 Region:  
 Location: On the fan of Landslip Stream, true right north branch of the Hurunui River  
 Map Reference: NZMS 260  
 Mean Annual Rainfall:  
 Landform: Valley Landform Genesis: Fan  
 Microrelief: Pit and mound Aspect:  
 Profile drainage: Well Land use:  
 Date described: 26/2/2004 Author(s): PCA  
 Parent material: Greywacke alluvium Parent rock:



L,F,H	0 - 5 cm	.
AE	5 - 11 cm	2.5Y 4/1 (dark grey to dark greyish brown); moderate medium nutty structure; gradual smooth boundary.
E	11 - 21 cm	moderately stony silt loam; 5Y 5/1 (grey); strong medium blocky structure; many discontinuous 7.5YR 2.5/1 humus/oxide coatings; many medium and fine roots; many slightly weathered rounded stones.; Note: Clasts have bleached surfaces, and a c. 1 mm thick weathering rind. Ectomycorrhizae common.
Bf	21 - 21.2 cm	7.5YR 3/3 (dark brown); weakly cemented; sharp wavy boundary.
Bw	21 - 36 cm	very gravelly, stony, bouldery silt loam; 10YR 5/4 (yellowish brown); moderate very fine and fine blocky structure; common discontinuous 10YR 5/6 (yellowish brown) oxide coatings; many unweathered rounded gravels to boulders; clear boundary; Note: Clasts make up c. 60 % of the soil.
Bs	36 - 48 cm	slightly bouldery, stony gravelly sandy loam; 7.5YR 3/3 (dark brown); strong coarse granular structure; few prominent 7.5YR 3/3 (dark brown) oxide coatings; unweathered rounded gravels and stones, few boulders; clear boundary.
BC	48 - 78 cm	slightly bouldery, stony, gravelly coarse sand; 2.5Y 4/1 (dark grey to dark greyish brown) and 10YR 4/3; weak coarse granular and single grains

Soil Name:

Profile code: Hope 1

B

structure; few patchy 10YR 4/4 (dark yellowish brown) oxide coatings; gradual boundary.

C

78 - 80 cm

slightly bouldery, stony, gravelly coarse sand; 2.5Y 4/1 (dark grey to dark greyish brown); loose soil strength, single grains.

Soil Name:  
 Profile code: Hope 5  
 NZ Soil Classification: Typic Orthic Podzol  
 NZ Gentic Classification:  
 USDA Soil Taxonomy:  
 Survey: Hope Fault  
 Region:  
 Location: In beech forest immediately south of the Park, upper Hurunui River, north branch  
 Map Reference: NZMS 260 2433895 5835675  
 Mean Annual Rainfall:  
 Landform: Valley  
 Landform Genesis:  
 Microrelief:  
 Aspect:  
 Profile drainage:  
 Date described: 27/2/2004  
 Parent material:  
 Land use:  
 Author(s): PCA  
 Parent rock:



L,F,H	0 - 5 cm	.
E	5 - 15 cm	very gravelly silt loam; 10YR 7/1 (light grey); rounded gravels..
Bs	15 - 22 cm	slightly gravelly silt loam; 7.5YR 4/6; .
2Bw	22 - 30 cm	silt loam; 10YR 5/4 (yellowish brown); strong medium nutty structure; .
2bA1	30 - 45 cm	silt loam; 2.5Y 5/2; moderate medium nutty structure; .
2bA2	45 - 60 cm	sandy loam; 2.5Y 5/2; .
3bCf	60 - 78 cm	moderately fine gravelly sandy loam; .

Soil Name:  
Profile code: Hope 5

4bC	78 - 100 cm	sandy loam; .
5b2Bw	100 - 135 cm	silt loam; 2.5Y 5/3 (greyish brown to light olive brown); moderate medium prismatic structure; 10YR 4/2 (dark greyish brown) oxide coatings; .
6b2BC	135 - 152 cm	sandy loam; weak prismatic structure; few oxide coatings; .
7b2Cf	152 - 164 cm	slightly stony fine gravel; ; Note: Oxide coatings on clasts.
8b3A/C	164 - 172 cm	sandy loam; .
9b3Bw	172 - 190 cm	gravelly silty clay loam; 10YR 5/6 (yellowish brown); moderate medium blocky structure; .
10C	190 - 200 cm	; Note: Cemented fan gravel.

**Profile code: Hope05-2**

Survey: Hope Fault  
 Region: North Canterbury  
 Location: Hurunui Valley adjacent to Hope Fault on McKenzie Fan

Grid Reference: NZMS 260 243 2088 283 5036

Date described: 30/1/2005

Authors: PCA, MS

Site notes: Soil pit dug on the upthrown side of the Hope Fault.



L	0 - 2 cm	.
F,H	2 - 4.5 cm	7.5YR 5/2 (brown); clear smooth boundary.
A	4.5 - 6 cm	10YR 4/2 (dark greyish brown); weak soil strength, semi-deformable failure, weak medium nutty structure; clear wavy boundary.
Er	6 - 14 cm	silt loam; 10YR 6/1 (light grey to grey); common coarse distinct 10YR 4/6 (dark yellowish brown) mottles; moderately firm soil strength, brittle failure, moderate medium blocky structure; sharp wavy boundary.
Bfm	14 - 14.1 cm	sharp wavy boundary; Note: Thin moderately cemented iron pan.
Bw	14.1 - 23 cm	silt loam; 10YR 5/4 (yellowish brown); slightly firm soil strength, brittle failure, moderate medium blocky structure; gradual boundary.
BC	23 - 42 cm	sandy loam; 5Y 4/2 (olive grey); slightly firm soil strength, brittle failure, weak coarse blocky structure; few faint clay coatings; gradual boundary; Note: Coatings on ped faces 2.5Y 6/3.
C	42 - 80 cm	sandy loam; 5Y 4/1 (dark grey); slightly firm soil strength, brittle failure, massive; abrupt wavy boundary.
2C(s)	80 - 115 cm	bouldery, stony, gravelly coarse sand; (yellowish brown) moderately coherent soil strength, single grains; ; Note: Boulders and stones subround, gravels angular, 10YR 5/6 coatings on clasts..

Comment (from PA): Extrapolating from the data I presented in the Inchbonnie report, given the soil has an E horizon, it has to be older than 1.6 kyr. I'd be putting my money on a 2-5 ka soil

## APPENDIX 2 – Trench Unit Descriptions and Radiocarbon samples

### Unit Descriptions for Matagouri Flat trench

- 1a – medium brown soil unit (topsoil) formed at current ground surface, with root mat of grasses penetrating to c. 8 cm depth
- 1b – darker, organic soil form in dark, medium sand below the topsoil (proper). Could be part of the same soil
- 2a – rounded pebble gravel, with a dirty brown sand matrix. Likely to be in the B-horizon zone of the current soil.
- 2b - re-oriented gravel as colluvium, includes more soil and sand than adjacent gravel
- 3a – weakly bedded cobble gravelly sand, clasts up to 15 cm, but typically 1-3 c, in matrix of coarse sand to fine gravel. Matrix supported, clasts sub-angular to sub-rounded. Quite well sorted on upthrown side, fining upward sequence
- 3b – pseudo-imbricated pebble gravel grades to fine gravel. Cobble rich channel gravel with sub-angular to sub-rounded clasts of greywacke, clast supported.
- 3c – well sorted fine gravel, clasts < 1cm, filling base of channel form
- 4a – beige-brown, massive silty fine sand to fine sandy silt with some clay
- 4b – silty, medium to coarse sand lenses within unit 3a. A well sorted fine gravel is included on downthrown side
- 5a – light brown sandy silt to silty fine sand
- 5b – well sorted coarse sand grading laterally to a grey brown silty medium sand
- 6 – pebble to cobble gravel, sub-angular to sub-rounded and bladed clasts, clast supported. Matrix is coarse sand. Interpretation: Coarse angular channel gravel.

### Radiocarbon material sampled from Matagouri Flat trench

- MF1E – organic sample, fine material, possibly grassy roots found in East wall of trench Within (at the top of) Paleosol unit 5a.
- MF2W – similar looking sample from about the same level in the trench on the West wall. However, it is mapped as coming from just above the Paleosol at the base of Unit 4a. Even more rooty looking than MF1E.

## APPENDIX 3 – Tree site data

**Plot 0 Cores taken by Rob and Vasso in 2002**

Tree I.D.	corer	Circumf	Diameter r (cm)	# cores	quality	Comment	# of rings	R Age (AD)
<u>trees 1-3 at L32/380380 =Plot -1</u>								
RB1	VnR	440	140.08	70.04	1	core length 32 cm, tree photo'd in <i>large buttressed tree on edge of scarp</i>		
RB2	VnR	291	92.65	46.32	1	core length 33.5 cm, 1st 3 cm gai <i>same spot</i>		
RB3	VnR		0.00	0.00	1	big tree at base of scarp <i>overstepped spot</i>		
<u>trees at new Plot 12 site</u>								
RB4	VnR		92.00	46.00	1	33 cm core, looks like Red Beech <i>fallen tree called DB1</i>		
RB5	VnR	290	92.33	46.16	1	31 cm core = Plot 12_RB5 (diam. <i>tree photo'd in 2001 on DF deposit</i> )		
RB6	VnR	177	56.35	28.18	1	37.5 cm core= Plot 12_RB6 (diam <i>on debris flow as is 5</i> )	<b>c. 257 ??</b>	1745
<u>big scarp site between Lodge Pass and 3-Mile Stream =Plot 0 (L32/417390)</u>								
RB7	VnR	213	67.81	33.91	1	26 cm long core into flatter Sth fa <i>grow. at top of 1/2 scarp above stream</i>		
RB8	VnR	308	98.06	49.03	1	37 cm core <i>20-25 m high tree</i>		
RB9	VnR	275	87.55	43.78	1	29 cm core; photo in FZ <i>tree on fault line, sc. is scalloped</i>		
RB10	VnR	253	80.55	40.27	1	25 cm core, well buttressed tree <i>black barked RB on edge of 5 m scarp</i>		
RB11	VnR	285	90.74	45.37	1	incomplete core <i>x</i>		
<u>adjacent to new Plot 11 site at Lodge Pass</u>								
MB12	VnR	185	58.90	29.45	1	32 cm core into 25 m high MB <i>40 m W of clearing so near Plot 11</i>	<b>c. 257 ??</b>	1745
MB13	VnR	244	77.68	38.84	1	20 cm core, corer rejected from fi <i>biggest tree on scarp in sight, 10 m W of 12</i>		
MB14	VnR	147	46.80	23.40	1	28.5 cm core <i>3/4 way up scarp on old trail to E</i>	<b>c. 257 ??</b>	1745
<u>Greenburn Stream trench site (O31/</u>								
RB15	VnR	287	91.37	45.69	1	33 cm core, 15 m from fault <i>largest tree on faulted surface</i>		
K17	VnR	147	46.80	23.40	1	no corer penetration <i>Kanuka growing on fault rupture</i>		

**Plot 1 - original scarp site between Matagouri Flat and Landslip Stream (L32/298344); tr 2/2004 and 26/01/2005**

Tree I.D.	corer	Circumf	Diameter r (cm)	# cores	quality	Comment	# of rings	R Age (AD)
RB1	R		68	34	1	<i>no (C)entre</i>	>251	>1753
RB2	R		95	47.5	1	<i>no (C)entre</i>	>169	>1835
RB3	R		60	30	1	<i>(A)rca</i>	190	1814
RB4	R		65	32.5	1	<i>A</i>	265	1739
RB5	R		47	23.5	1	<i>A</i>	232	1772
RB6	R		90	45	1	<i>no (C)entre</i>	231	1773
RB7.2	R		67	33.5	2	<i>no (C)entre</i>	272	1732
RB8	R		70	35	1	<i>no (C)entre, rotten middle</i>	164	1840
RB9	R		62	31	1	<i>C</i>	251	1753
SB1.2	R		38	19	2	<i>A</i>	251	1753

*all in Italics sampled in 2004*

					12			
RB10	V	230	73.22509	36.61254	3	not a great tree, maybe some (A) tree on scarp, could be repeat of R	210	1795
RB11	R	156	49.66571	24.83286	2	rotten middle tree on scarp	292	1713
RB12	M	186	59.21681	29.6084	2	can see A on 2nd one tree on scarp	230	1775
RB13	V	229	72.90672	36.45336	2	1st one can't see C but long core, ditto 2nd	272	1733
RB14	R	129	41.06972	20.53486	1	A visible, short core	137	1868
RB15	M	248	78.95575	39.47787	1	long, but end of barrel	202	1803
SB16		184	58.58007	29.29004	2	2 good cores next to each other	137	1868
RB17		177	56.35148	28.17574	2		108	1897
SB18		179	56.98822	28.49411	1		131	1874
RB19		159	50.62082	25.31041	2	2 good cores	159	1846
RB20		158	50.30245	25.15123	1	A to C on 1st; 2nd one was drop on surface above scarp	150	1855

#### Plot 2

Tree I.D.	corer	Circumf	Diameter	r (cm)	# cores	quality	Comment	# of rings	R Age (AD)
SB1	R	198	63.04	31.52	2	1st good; 2nd is better - near (C)entre		261	1744
RB2	M	149	47.44	23.72	2		2 m from gravel channel	188	1817
RB3	V	157	49.98	24.99		1st rotten in inner 1/3			
SB4	R	177	56.35	28.18	0	tree is growing in active gravel bed & looks sick			
RB5	R	117	37.25	18.62	2	on sm. mound 1 m from active gravel channel		168	1837
RB6	R	123	39.16	19.58	1	on prominent buttress 1.5 m from active gravel channel		173	1832
SB7	M	168	53.49	26.74	1	good core			
RB8	V	160	50.94	25.47	1	Arcs (A) seen		139	1866
RB9	R	135	42.98	21.49	1	A seen		160	1845
SB10	R	250	79.59	39.8	1	rotten middle	big twisted and leaning SB		
RB11		123	39.16	19.58	1	with C	on mound in creek	221	1784
SB12	V	335	106.65	53.33	2	2nd core into smaller bole with D= v. large SB big canopy, on surf 6 m from gravel fan			
RB13	M	246	78.32	39.16	1	rotten middle with worm? at end			
SB14	R	130	41.39	20.69	1	C		125	1880
RB15	M	158	50.3	25.15	1	good core		174	1831
RB16	R	234	74.5	37.25	1	straight rings - MIN age		149	1856
RB17	M	135	42.98	21.49	2	lost 1 one, hit C on 2nd		216	1789
SB18	V	208	66.22	33.11	1			329	1676
SB19	R	126	40.11	20.06	2	2nd one close to C		117	1888
RB20	M	134	42.66	21.33	2	A to C on 1st; 2nd one was dropped so a bit mixed		144	1861

Plot 3		25							
Tree I.D.	corer	Circumf	Diameter r (cm)	# cores	quality	Comment	# of rings	R Age (AD)	
RB1	R	180	57.31	28.65	2	(A)rcs on 1st; A on 2nd	v big RB, fast growth	99 1906	
SB2	M	67	21.33	10.67	1	Arcs (A) seen	87 1918		
RB3	V	66	21.01	10.51	1	C			
RB4	M	132	42.02	21.01	1	good A	RB at edge of bench	85 1920	
SB5	V	67	21.33	10.67	2	1st one A?; 2nd one crumbly end	71 1934		
SB6	R	80	25.47	12.73	2	1st has some A	98 1907		
RB7	M	90	28.65	14.33	1	tight A, maybe (C)entre	94 1911		
SB8	V	48	15.28	7.64	1	C	78 1927		
SB9	R	60	19.10	9.55	2	2nd one close to C	both in same tube	96 1909	
RB10	V	91	28.97	14.49	1	C			
RB11	M	85	27.06	13.53	1	tight A, maybe (C)entre	larger of two boles	82 1923	
SB12	R	104	33.11	16.56	1	2nd one had C	on steep slope near base of slide	96 1909	
SB13	M	60	19.10	9.55	1	C	97 1908		
RB14	M	90	28.65	14.33	1	A, just off C	104 1901		
RB15	V	146	46.48	23.24	2	1st hasd wide A; 2nd one A close	1st core was into non-buttress	96 1909	
RB16	R	75	23.88	11.94	2	2nd one hit C	77 1928		
RB17	M	56	17.83	8.91	2	1st one wide A; 2nd one tight A	bigger live bole of 2; 2nd one got di	73 1932	
SB18	R	66	21.01	10.51	2	1st one has A	2 cores in one tube	79 1926	
SB19	M	80	25.47	12.73	1	A close to C	91 1914		
RB20	V	114	36.29	18.15	1	C hit again	95 1910		

Plot 4		28							
Tree I.D.	corer	Circumf	Diameter r (cm)	# cores	quality	Comment	# of rings	R Age (AD)	
RB1	V	185	58.90	29.45	2	1st rotten centre; 2nd looks like A of C	264 1741		
RB2	M	195	62.08	31.04	2	2 long cores with prob no (A)rcs or C	291 1714		
RB3	M	237	75.45	37.73	1	1 long core but prob no A = MIN age	245 1760		
RB4	M,RL	169	53.80	26.90	2	1st one may have A; 2nd ditto (R)	slightly rotten core	236 1769	
SB5	V	185	58.90	29.45	2	1st got broken lost 4 mm, straight rings			
SB6	M	195	62.08	31.04	1	A seen in long core, just off C	230 1775		
RB7	V	300	95.51	47.76	2	both had straight rings no visible	Circumference Includes buttressing		
RB8	V	330	105.06	52.53	1	1 shot, some A close to C	Circumference Includes buttressing		
SB9	M	149	47.44	23.72	1	A visible right at very end	222 1783		
RB10		220	70.04	35.02	2	2 long cores from same spot on t	bit twisted tr		
SB11		117	37.25	18.62	2	2 short bad cores	on edge of channel cut into deris fa	257 1748	

RB12	168	53.49	26.74	1 good, some A	12, 13, 14 are 3 trees on falling edge	268	1737
RB13	176	56.03	28.02	1 one long core, mushy in middle	debris flow	257	1748
RB14	158	50.30	25.15	2 dud tree		131	1874
RB15	150	47.76	23.88	1 big enough?		605?	
SB16	155	49.35	24.67	1 maybe C		309	1696

**Plot 5**

24

Tree I.D.	corer	Circumf	Diameter	r (cm)	# cores	quality	Comment	# of rings	R Age (AD)
RB1	M	96	30.56	15.28	1	v good (A)rcs	med-aged coloniser grow. Into can	213	1792
RB2	V	70	22.29	11.14	1	(C)entre	smallish RB in canopy space	142	1863
SB3	P	125	39.80	19.90	1	2nd one with A	1 photo (GR 1750 4909)	217	1788
SB4	V	70	22.29	11.14	1	C just		169	1836
RB5	M	389	123.85	61.92		both cores mush and in same tub	this is the big RB that got crowned, 2 PH		
SB6	V	55	17.51	8.76	1	C again	tree looks <100 yr, near edge of sc	140	1865
RB7	V	213	67.81	33.91	2	1st bad, 2nd maybe A	big RB on verge of scarp, 1 PH	238	1767
RB8	M	122	38.84	19.42	1	A on 2nd attempt	coloniser next to RB5	155	1850
RB9	P	105	33.43	16.71	1	C	(GR 1753 4905)	134	1871
SB10	V	153	48.71	24.36	3	1st, 3rd cores bad; 2nd core had	broad A	368	1637
RB11	P	94	29.93	14.96	2	2nd one hit C	(1755 4901)	203	1802
SB12	M	290	92.33	46.16	2	both cores had muchy ends	giant SB w/ preched root system ex-log		
RB13	P	176	56.03	28.02	2	2nd core hit C	(1766 4898)	257	1748
SB14	M	106	33.75	16.87	1	good A	v spread out buttressed roots	148	1857
RB15	P	84	26.74	13.37	2	1st core no A, 2nd one hit C	(1756 4897)	153	1852
SB16	V	55	17.51	8.76	1	hit C	small SB on verge of scarp	139	1866
RB17	M	115	36.61	18.31	1	v good A, prob C	spread out roots on forest floor	162	1843
RB18	V	178	56.67	28.33	2	1st core straights; 2nd core good	med RB on scarp verge next to RB	224	1781
RB19	P	89	28.33	14.17	2	4th attempt was good but not sur	near edge of subdued part of sc	199	1806
SB20	M	95	30.25	15.12	1	C visible	c. 100 yr, 15 m from scarp (furthesi	125	1880

## Plot 6

28

Tree I.D.	corer	Circumf	Diameter r (cm)	# cores	quality	Comment	# of rings	R Age (AD)
RB1	M	193	61.45	30.72	1 possible (A)rcs in long core	med RB grow. on mound on edge c	243	1762
RB2	V	262	83.41	41.71	1 long core with A ?	tree on corner off scarp and aband.	267	1738
RB3	P	201	63.99	32.00	2 both cores had broad A		244	1761
SB4	M	56	17.83	8.91	1 C	sm. SB growing in abandoned ch (	149	1856
RB5	M	187	59.54	29.77	2 both cores give MIN but 2nd better	RB on edge of A.C.	213	1792
SB6	V	66	21.01	10.51	2 1st core had A, better than 2nd	small SB next to A.C.	155	1850
SB7	P	204	64.95	32.47	2 1st one OK A, 2nd one no better	growing 3 m from scarp	241	1764
RB8	V	229	72.91	36.45	1 long core with good A	looks like growing on mound, former log		
RB9	M	76	24.20	12.10	2 1st had A, 2nd one poss. (C)centre	SB growing on verge of scarp	151	1854
RB10	P	121	38.52	19.26	2 1st one end may hav flipped; 2nd	tree right on verge of scarp	151	1854
RB11	V	209	66.54	33.27	2 both had weal rotten centre MIN		238	1767
RB12	M	96	30.56	15.28	1 good A	RB on debris mound at base of sca	117	1888
SB13	M	291	92.65	46.32	1 long core, A poss. C	on sm mound on DT side of fault	402	1603
RB14	P	231	73.54	36.77	2 ?	on DT side above sm hollow, sl. Le	232	1773
RB15	M	103	32.79	16.40	1 C	on DT side of fault, on sm mound	145	1860
RB16	V	159	50.62	25.31	1 has A within 1 cm of C	growing on mound poss. Ex-root pl	201	1804
SB17	P	252	80.23	40.11	1 broad A	just on DT side of fault scarp	212	1793
RB18	M	247	78.64	39.32	1 soft in middle MIN age	growing on DT side just above ch and WT		
SB19	M	168	53.49	26.74	1 softish centre but moved on and l	8 m from scarp on DT side above c	217	1788
RB20	P	208	66.22	33.11	2 2nd one had A poss C	c. 100 yr, 15 m from scarp (furthesi	129	1876
RB21	V	281	89.46	44.73	2 2nd one OK A	broad sinuous root system on sm mound		

## Plot 7

31

Tree I.D.	corer	Circumf	Diameter r (cm)	# cores	quality	Comment	# of rings	R Age (AD)
RB1	V	181	57.62	28.81	2 1st OK (A)rcs; 2nd ?	next to gravel/soil exposure	90	1915
RB2	M	175	55.71	27.86	1 good A	top of roots just showing	120	1885
RB3	M	175	55.71	27.86	2 both had broad A	(GR 2432007; 5537402)	106	1899
SB4	V	240	76.41	38.20	1 long core but not good A = MIN a	weird 4 boled tree, rotten centre?	229	1776
RB5	V	117	37.25	18.62	2 both had O.K. Arcs	(GR 2431990; 5537415)	114	1891
RB6	M	188	59.85	29.93	1 had O.K. Arcs	(GR 2431992; 5537402)	137	1868
RB7	V	115	36.61	18.31	1 good A	big RB on verge of scarp, 1 PH	112	1893
RB8	V	177	56.35	28.18	?	had bow/ incline in tree growth	162	1843
RB9	M	182	57.94	28.97	1 good A	(GR 2431998; 5537399)	111	1894
RB10	V	96	30.56	15.28	1 C visible	(GR 2432004; 5537418)	120	1885

RB11	M	160	50.94	25.47	1	good A	(GR 2431989; 5537397)	112	1893
RB12	V	105	33.43	16.71	1	v good A, close to C	(GR 2432003; 5537421)	116	1889
SB13	RL	32	10.19	5.09		?, maybe no cores	(GR 2432004; 5537432)	88	1917
RB14	V	132	42.02	21.01	1	good A, maybe C	(GR 2432010; 5537419)		
RB15	M	238	75.77	37.89	1	straight rings MIN age	big tree	203	1802
RB16	V	305	97.10	48.55	2	1st one only straights, 2nd ?	(GR 2432005; 5537409)		
SB17	P	275	87.55	43.78	2	both only straights, prob. no A, MI	(GR 2431988; 5537424)	302	1703
RB18	M	156	49.67	24.83	2	both cores A, maybe C	(GR 2431985; 5537422)	132	1873
SB19	V	43	13.69	6.84	2	both have OK A, both in same str	this tree and 13 on most recent sur	120	1885
SB20	V	211	67.18	33.59	2	1st one broad A; 2nd one v good	big bend in tree at 2 m height toward	220	1785

**Plot 8**

26

Tree I.D.	corer	Circumf	Diameter r (cm)	# cores	quality	Comment	# of rings	R	Age (AD)
RB1	V	211	67.18	33.59	3	all three are rotten, kept 1			
RB2	RL	211	67.18	33.59	2	1st one straight, 2nd one v good	DT side, 5 m from scarp	188	1817
RB3	V	180	57.31	28.65		2nd one longer, but no A?	growing at foot of scarp	278	1727
SB4	RL	218	69.40	34.70	2	1st short and rotten, 2nd long, rotten		251	1754
SB5	V	95	30.25	15.12	1	good A	young SB growing in space	156	1849
SB6	V	112	35.66	17.83	1	very close to C	young SB growing in space	215	1790
SB7	V	134	42.66	21.33	1	good A, near C	sl. Bigger SB than 5,6	247	1758
RB8	RL	179	56.99	28.49	1	2nd one long but prob no A	RB at toe of scarp	264	1741
SB9	V	94	29.93	14.96	2	1st one C, 2nd one maybe A		196	1809
SB10	V	269	85.64	42.82	2	both are short with rotten middle,	2nd bole on tree damaged /snapped off		
RB11	RL	162	51.58	25.79	1	good A, maybe C	tree growing on scarp	216	1789
SB12	RL	129	41.07	20.53	2	1st rotten in middle, 2nd worse	growing 1/2 way up scarp with perc	228	1777
MB13	V	122	38.84	19.42	1	C maybe	growing on edge of 2ndary trace	125	1880
RB14	V	202	64.31	32.16	2	1st one bad, 2nd one better	on top of scarp, perched roots, 3m	234	1771
RB15	RL	165	52.53	26.27	1	went thru rotten bit and hit C	tree near the top of main scarp	295	1710

**Plot 9**

22

Tree I.D.	corer	Circumf	Diameter r (cm)	# cores	quality	Comment	# of rings	R	Age (AD)
RB1	M	308	98.05794	49.03	1	long core ut MIN age			
RB2	V	259	82.45782	41.23	1	long core ut MIN age		195	1810
SB3	V	74	23.55938	11.78	1	C		170	1835
RB4	M	97	30.88188	15.44	1	C		159	1846
RB5	M	194	61.76377	30.88	1				

RB6	V	83	26.42471	13.21	1	multiple (A)rcs, maybe C or 2 centres	95	1910
RB7	V	103	32.7921	16.40	1	C	94	1911
RB8	M	389	123.8459	61.92	1	long core MIN age <i>sl. perched and buttressed</i>		
RB9	V	328	104.4253	52.21	2	1st one rotten, 2nd one ?		
RB10	M	128	40.75135	20.38	1	good A	137	1868
RB11	M	85	27.06145	13.53	2	both had rotten centre <i>both in same tube</i>	176	1829
RB12	V	190	60.49029	30.25	2	1st broad A, 2nd are long, good A	144	1861
RB13	M	161	51.25756	25.63	1	good A	152	1853
SB14	V	228	72.58835	36.29	1	long core, no A	338	1667
SB15	M	230	73.22509	36.61	1	some A, not great	226	1779

Plot 10

18

Tree I.D.	corer	Circumf	Diameter	r (cm)	# cores	quality	Comment	# of rings	R Age (AD)
RB1	M	311	99.01	49.51	1	long core straight (R)ings			
SB2	V	269	85.64	42.82	1	long core with beginnings of (A)rcs		299	1706
RB3	M	168	53.49	26.74	1	too dark to tell		109	1896
SB4	V	259	82.46	41.23	1	A, maybe (C)entre, long core		103	1902
RB5	M	90	28.65	14.33	1	inclined tree, hit C		139	1866
SB6	M	136	43.30	21.65	1	went further in and hit C <i>funny kink in botom of tree</i>		147	1858
SB7	V	200	63.67	31.84	2	1st one broad A, 2nd one maybe C		243	1762
RB8	M	244	77.68	38.84	1	OK A			
RB9	M	167	53.17	26.58	2	good A		115	1890
RB10	V	151	48.07	24.04	1	v good A, maybe C <i>tree has flowered out, may have lo:</i>		83	1922
RB11	M	170	54.12	27.06	2	good A, maybe C		182	1823
RB12	V	189	60.17	30.09	2	v good A, maybe C		90	1915
RB13	M	151	48.07	24.04	1	1st one poor A, mushy Centre			
RB14	V	249	79.27	39.64		long core, no A			
RB15	V	255	81.18	40.59		<i>inclined tree with 3 upper boles</i>			
SB16	M	209	66.54	33.27	1	straight R		131	1874
SB17	M	132	42.02	21.01	2	broad A on both <i>growing next to cutbank</i>		102	1903
SB18	V	163	51.89	25.95	1	good A maybe C <i>slight curve in tree</i>		126	1879

Plot 11				21			
Tree I.D.	corer	Circumf	Diameter r (cm)	# cores	quality	Comment	# of rings R Age (AD)
MB1	M	106	33.75	16.87	1	good (A)rcs, complex (C)entre	multi-buttressed 180 1825
MB2	V	97	30.88	15.44	2	1st one broad A, 2nd one good m	near top of scarp 172 1833
MB3	V	123	39.16	19.58	2		toward top of scarp 183 1822
MB4	M	58	18.47	9.23	1	OK (A)rcs, close to C	sl. Inclined growth at base of scarp 158 1847
MB5	V	65	20.69	10.35	1	v good A, close to C	226 1779
MB6	M	105	33.43	16.71	2	prob C, but was complex	2 cores in tube, rotten in centre? 176 1829
MB7	V	79	25.15	12.58	1	prob C	inclined growth form out of scarp 196 1809
MB8	V	103	32.79	16.40	1	looks like near C	181 1824
MB9	M	90	28.65	14.33	1	v close to C	inclined style of growth 187 1818
MB10	V	193	61.45	30.72	2	1st one broad A, 2nd similar	growing near foot of scarp 342 1663
SB11	M	61	19.42	9.71	1	v good A, prob near C	202 1803
SB12	M	116	36.93	18.47	1	v good A	near toe of s., just above terrace 188 1817
SB13	M	174	55.40	27.70	2	2 cores, goodish A on both	growing on stream terrace 206 1799
MB14	V	104	33.11	16.56	1	v good A	on flat, v between two streamlets 171 1834
MB15	V	139	44.25	22.13	2	broad on both, 2nd one better	prob MB 210 1795
MB16	V	57	18.15	9.07		this and 15 are growing above 14 on mini-spur	123 1882
MB17	M	147	46.80	23.40	2	both have broad A, 2nd one wavy	growing right next to track 278 1727

Plot 12				23			
Tree I.D.	corer	Circumf	Diameter r (cm)	# cores	quality	Comment	# of rings R Age (AD)
Dead RB1	M		88.00	44.00	2	maybe (A)rcs in 1st one	big log that forms dam to debris lobe
RB2	V	79	25.15	12.58	1	C	on bottom side of DB1 114 1891
RB3	V	162	51.58	25.79	2	both with broad A	growing on hillslope edge down fro. 110 1895
RB4	M	226	71.95	35.98	2	1st one straight rings, 2nd one rol	phlanged buttressed tree down fro. 216 1789
RB5	V	285	90.74	45.37	1	long core, poss A near end	on debris flow, cored previously 223 1782
RB6	M	178	56.67	28.33	1	O.K. Arcs	on debris flow, cored previously 213 1792
RB7	V	150	47.76	23.88	1	O.K. Arcs	further up debris cone 125 1880
RB8	V	148	47.12	23.56		1st one O.K. A	even further up DF 163 1842
SB9	M	89	28.33	14.17	1	v good A	above fallen DB1
RB10	V	183	58.26	29.13	1	good A close to C	above fallen DB1 224 1781
RB11	M	108	34.38	17.19	1	good A	326 1679
SB12	M	55	17.51	8.76	1	v good A	trees 11-16 are all on the debris co
RB13	M	148	47.12	23.56	1	good A	surface, boys moving up it 93 1912
RB14	V	197	62.72	31.36	1	v long core MIN age	219 1786

?_B15	V	123	39.16	19.58	1	long core throuh C area		
RB16	V	147	46.80	23.40	1		229	1776

**Plot 13**

18

Tree I.D.	corer	Circumf	Diameter r (cm)	# cores	quality	Comment	# of rings	R Age (AD)
RB1	V	287	88.00	44.00	1	short core = MIN <i>rotten on inside, damaged tree</i>	62	1943
SB2	M	228	72.59	36.29	1	long core, poss some A or C near end	352	1653
RB3	RL	177	56.35	28.18	2	1st one rotten toward the centre	224	1781
RB4	M	156	49.67	24.83	1	O.K. (A)rcs		
SB5	V	310	98.69	49.35	2	2nd is longer than 1st and shows A		
RB6	M	81	25.79	12.89	1	v good A	143	1862
RB7	M	116	36.93	18.47	1	(C)entre	148	1857
SB8	RL	136	43.30	21.65	2	both prob missed C <i>check radius oint for A</i>	233	1772
SB9	V	171	54.44	27.22	1	prob C	264	1741
RB10	M	126	40.11	20.06	1	v good A, but complex C	113	1892
RB11	M	213	67.81	33.91	1	v long core, no A	187	1818
RB12	V	96	30.56	15.28	1	good A	144	1861
SB13	V	113	35.98	17.99	1	good A	278	1727
RB14	M	222	70.68	35.34	1	long core = MIN age, poss A at <i>entirely warped tree grow. by channel</i>	178	1827
SB15	RL	149	47.44	23.72	1	O.K. A, near C	254	1751
RB16	V	112	35.66	17.83	1	good A	149	1856

**Plot 14**

19

Tree I.D.	corer	Circumf	Diameter r (cm)	# cores	quality	Comment	# of rings	R Age (AD)
RB1	M	179	56.99	28.49	2	2nd one broad (A)rcs at end, 1st <i>grown on edge of (T)errace 2</i>	69	1936
RB2	V	77	24.51	12.26	1	good A, near C <i>just above (Rs)er2</i>	65	1940
RB3	M	138	43.94	21.97	1	v good A, close to C <i>growing on edge of Rs2</i>	188	1817
SB4	V	118	37.57	18.78		OK (A)rcs, close to C <i>on T2</i>	155	1850
RB5	M	84	26.74	13.37		v good A, close to C <i>on T2</i>		
RB6	RL	365	116.21	58.10		got core stuck insode corer <i>v big tree on T2</i>		
RB7	M	91	28.97	14.49	1	good A <i>grow. near back of T3</i>	109	1896
RB8	V	373	118.75	59.38	1	v long but no A <i>on T2</i>	133	1872
RB9	M	77	24.51	12.26	1	good A <i>grow. near back of T3</i>	164	1841
RB10	V	352	112.07	56.03	1	<i>grow.on T3</i>		
RB11	M	239	76.09	38.05	1	v long core poss. Some A <i>leaning tree on hillslope</i>	224	1781
RB12	V	124	39.48	19.74	1	good A <i>on T3</i>	120	1885

RB13	V	148	47.12	23.56	1	broad A	<i>on edge of R3</i>	115	1890
SB14	V	120	38.20	19.10	1	good A	<i>growing on T1</i>	176	1829
RB15	M	214	68.13	34.07	1	long cores, no A visible	<i>growing on hillslope</i>		
RB16	V	125	39.80	19.90	1	long core, good A, poss C	<i>16 n 17 survived but were sterred</i>		
RB17	V	135	42.98	21.49	1	has A, maybe C	<i>by fall of 2m boulder that fell onto T3</i>		

15

65% *N. fusca* (173 trees); 28% *N. menziesii* (74); 7% *N. solanderi* cl.(18)

38.1% Vicente(102); 36.6% Marshall (98); 10.8% Richard (29); 7.0 % Rob (13); 4.9% Peter (13); 2.6% Vasso (7)

# cores #VALUE!



[www.gns.cri.nz](http://www.gns.cri.nz)

#### Principal Location

1 Fairway Drive  
Avalon  
Lower Hutt 5010  
PO Box 30368  
Lower Hutt 5040  
New Zealand  
T +64-4-570 1444  
F +64-4-570 4600

#### Other Locations

Dunedin Research Centre  
764 Cumberland Street  
Dunedin 9016  
Private Bag 1930  
Dunedin 9054  
New Zealand  
T +64-3-477 4050  
F +64-3-477 5232

Wairakei Research Centre  
114 Karetoto Road, Wairakei  
Taupo 3377  
Private Bag 2000  
Taupo 3352  
New Zealand  
T +64-7-374 8211  
F +64-7-374 8199

National Isotope Centre  
30 Gracefield Road, Gracefield  
Lower Hutt 5010  
PO Box 31312  
Lower Hutt 5040  
New Zealand  
T +64-4-570 1444  
F +64-4-570 4657